ภาคผนวก ก.

ก.1 รายชื่อบทความและบทความที่ได้รับการตอบรับเพื่อตีพิมพ์ในวารสารวิชาการระดับนานาชาติที่มี Impact Factor

1. P. Chindaprasirt, C. Jaturapitakkul, W. Chalee, U. Ratanasak*. Comparative study on the characteristics of fly ash and bottom ash geopolymers, Waste Management, 29 (2009), 539-543. (IF 2.208)
2. P. Chindaprasirt, C. Jaturapitakkul, U. Ratanasak*. Influence of fineness of rice husk ash and additives on the properties of lightweight aggregate, Fuel, 88 (2009), 158-162. (IF 2.536)
3. W. Chalee, C. Jaturapitakkul*, P. Chindaprasirt. Predicting the chloride penetration of fly ash concrete in seawater, Marine Structures, 22 (2009), 341-353. (IF 0.615)
4. W. Chalee, C. Jaturapitakkul*. Effects of W/B ratios and fly ash finenesses on chloride diffusion coefficient of concrete in marine environment, Materials and Structures, 42 (2009), 505-514. (IF 0.892)
5. W. Tangchirapat, C. Jaturapitakkul*, P. Chindaprasirt. Use of palm oil fuel ash as a supplementary cementitious material for producing high-strength concrete, Construction and Building Materials, 23 (2009), 2641-2646. (IF 0.947).
6. W. Tangchirapat, C. Jaturapitakkul*, K. Kiattikomol. Compressive strength and expansion of blended cement mortar containing palm oil fuel ash, Journal of Materials in Civil Engineering, Technical Note, 21 (2009), 426-431. (IF 0.526)
7. N. Chusilp, C. Jaturapitakkul*, K. Kiattikomol. Utilization of bagasse ash as a pozzolanic material in concrete, Construction and Building Materials, 23 (2009), 3352-3358. (IF 0.947)
8. N. Chusilp, C. Jaturapitakkul*, K. Kiattikomol. Effects of LOI of ground bagasse ash on the compressive strength and sulfate resistance of mortars, Construction and Building Materials, 23 (2009), 3523-3531. (IF 0.947)
9. W. Chalee, P. Ausapanit , C. Jaturapitakkul*. Utilization of fly ash concrete in marine environment for long term design life analysis, Materials & Design, 31 (2010), 1242-1249. (IF 1.107).
10. S. Songpiriyakij*, T. Kubprasit, C. Jaturapitakkul, P. Chindaprasirt. Compressive strength and degree of reaction of biomass-fly ash –based geopolymer, Construction and Building Materials, 24 (2010), 236-240. (IF 0.947)

11. T. Cheewaket, C. Jaturapitakkul, W. Chalee*. Long term performance of chloride binding capacity in fly ash concrete in a marine environment, Construction and Building Materials, 24 (2010), 1352-1357. (IF 0.947)

12. W. Tangchirapat, R. Buranasing, C. Jaturapitakkul*. Use of high fineness of fly ash to improve properties of recycled aggregate concrete, Journal of Materials in Civil Engineering ASCE, 22, No. 6 (2010), 565-571.(IF 0.526).

13. J. Wongpa, K. Kiattikomol, C. Jaturapitakkul*, P. Chindaprasirt. Compressive strength, modulus of elasticity, and water permeability of inorganic polymer concrete, Materials & Design, 31 (2010), 4748-4754. (IF 1.107).

14. Vanchai Sata*, Chai Jaturapitakkul, Chaiyanunt Rattanashotinunt. Compressive Strength and heat evolution of concrete containing palm oil fuel ash, Journal of Materials in Civil Engineering ASCE. (accepted) (IF 0.526).

15. Nattapong Makaratat, Chai Jaturapitakkul*, Thanapol Laosamathikul. Effects of calcium carbide residue-fly ash binder on mechanical properties of concrete, Journal of Materials in Civil Engineering ASCE. (accepted) (IF 0.526).

ก.2 เอกสารการยื่นขอจดสิทธิบัตร

เอกสารคำขอจดสิทธิบัตร ที่ 100100038 เรื่อง **"กรรมวิธีการผลิตวัสดุประสานสำหรับผลิตคอนกรีตซึ่งมีกำลังสูง มีความร้อนต่ำ และมีความทนทานสูง"** ซึ่งอยู่ระหว่างการพิจารณาของกรมทรัพย์สินทางปัญญา

1. P. Chindaprasirt, C. Jaturapitakkul, W. Chalee, U. Ratanasak. Comparative study on the characteristics of fly ash and bottom ash geopolymers, Waste Management, 29 (2009), 539-543. (IF 2.208)

Waste Management 29 (2009) 539–543

Contents lists available at ScienceDirect

Waste Management

journal homepage: www.elsevier.com/locate/wasman

Comparative study on the characteristics of fly ash and bottom ash geopolymers

Prinya Chindaprasirt [a], Chai Jaturapitakkul [b], Wichian Chalee [c], Ubolluk Rattanasak [d,*]

[a] Department of Civil Engineering, Faculty of Engineering, Khon Kaen University, Khon Kaen 40002, Thailand
[b] Department of Civil Engineering, Faculty of Engineering, King Mongkut's University of Technology Thonburi, Bangkok 10140, Thailand
[c] Department of Civil Engineering, Faculty of Engineering, Burapha University, Chonburi 20131, Thailand
[d] Department of Chemistry, Faculty of Science, Burapha University, Chonburi 20131, Thailand

ARTICLE INFO

Article history:
Accepted 11 June 2008
Available online 19 August 2008

ABSTRACT

This research was conducted to compare geopolymers made from fly ash and ground bottom ash. Sodium hydroxide (NaOH) and sodium silicate (Na_2SiO_3) solutions were used as activators. A mass ratio of 1.5 Na_2SiO_3/NaOH and three concentrations of NaOH (5, 10, and 15 M) were used; the geopolymers were cured at 65 °C for 48 h. A Fourier transform infrared spectrometer (FT-IR), differential scanning calorimeter (DSC), and scanning electron microscope (SEM) were used on the geopolymer pastes. Geopolymer mortars were also prepared in order to investigate compressive strength. The results show that both fly ash and bottom ash can be utilized as source materials for the production of geopolymers. The properties of the geopolymers are dependent on source materials and the NaOH concentration. Fly ash is more reactive and produces a higher degree of geopolymerization in comparison with bottom ash. The moderate NaOH concentration of 10 M is found to be suitable and gives fly ash and bottom ash geopolymer mortars with compressive strengths of 35 and 18 MPa.

1. Introduction

Every year, there is an increase in consumption of fossil fuels to produce energy. Coal is mainly used to generate the steam for industrial operation and electricity generation. Consequently, coal ash is obtained as a waste product that needs to be disposed of in an environmentally friendly way. However, because of the large quantity produced, most types of ash, including fly and bottom ash, are disposed of in landfills. This disposal process leads to environmental and other problems.

In Thailand, the annual output of fly ash and bottom ash from large and small power plants totals about 4.0 million tons. Approximately 1.8 million tons of fly ash is used as a pozzolanic material in the concrete industry. The partial replacement of Portland cement with fly ash reduces the heat of hydration and improves the workability and durability of the concrete. However, the level of fly ash replacement is normally restricted to less than 40% of Portland cement (Mehta, 1998).

Bottom ash, in contrast, does not possess the same enhanced workability. However, the chemical constituents of these two materials are very similar, with the main difference being particle shape and size. Bottom ash is larger in size and very irregular, containing pores and cavities. Ground to a proper fineness, bottom ash can be used as a pozzolan that produces relatively high strength concrete (Jaturapitakkul and Cheerarot, 2003). Since fly ash is not yet completely used, a very large amount of bottom ash is still discarded.

Manufacturing of Portland cement is an energy intensive process that releases a very large amount of greenhouse gas (Maholtra, 2002). Therefore, the use of pozzolans to replace part of Portland cement is receiving a lot of attention. Other efforts have also been made to develop alternative cementitious materials. One promising finding is the use of an alumino-silicate material called "geopolymer". Since fly ash contains a large amount of silica and alumina, it is a suitable source material for making geopolymers (Lee and Van Deventer, 2002). The fly ash geopolymer is prepared by incorporating high alkaline solution and sodium silicate and is activated with temperature curing. The polycondensation reaction provides an alumino-silicate cementitious compound. Apart from fly ash, other materials, such as calcined kaolinite and burnt clay, can also be used as source materials. Bottom ash, which has similar chemical ingredients as fly ash, should also be used to produce geopolymers. The bottom ash, however, may need some grinding to improve its reactivity.

The utilization of coal ash in the production of geopolymers offers an alternative cementitious material. Therefore, this research focuses on the physical and chemical structures of coal ash geopolymer. Original fly ash and ground bottom ash were used to prepare geopolymers by mixing with sodium hydroxide and sodium

* Corresponding author. Tel.: +66 38103066; fax: +66 38393494.
E-mail address: ubolluk@buu.ac.th (U. Rattanasak).

0956-053X/$ - see front matter © 2008 Elsevier Ltd. All rights reserved.
doi:10.1016/j.wasman.2008.06.023

silicate solutions. Mix proportions varied in order to analyze their effects on strength and other material properties.

2. Materials and methods

2.1. Materials

Fly ash and bottom ash from Mae Moh power plant in the north of Thailand were used in this research. Bottom ash was ground to a similar particle size as fly ash. Table 1 shows the significant chemical composition of coal ash using X-ray fluorescence (XRF). XRD patterns of fly ash and bottom ash displayed in Fig. 1 show that fly ash contained a higher content of amorphous phase particles compared to the bottom ash. The crystalline phases are predominantly quartz and mullite. Sodium hydroxide solution (NaOH) at 5, 10, and 15 M concentration and sodium silicate solution (Na_2SiO_3) with Na_2O 9% and SiO_2 30% by weight were used. The viscosities of 5, 10, and 15 M NaOH solutions were 3.9, 9.3, and 14.3 cps (centipoises), respectively. The sodium silicate solution's viscosity was higher at 60.6 cps.

2.2. Mixing procedure for the geopolymer paste

Coal ash was mixed with NaOH solution for 10 min to allow the leaching of ions. Sodium silicate solution was then added to the mixture and mixed until uniform, usually about 60 s. The mass ratio of Na_2SiO_3/NaOH of 1.5 was used. The mix proportions are tabulated in Table 2. Compositions of geopolymers in mole ratios are shown in Table 3. After mixing, paste specimens were molded into 25 mm diameter × 25 mm height plastic containers. They were then cured at 65 °C for 48 h, based on previous work done on fly ash (Chindaprasirt et al., 2007). FT-IR, Differential Scanning Calorimetry (DSC), XRD and EDX analyses were performed on the hardened sample.

Table 1
Chemical composition and physical properties of coal ash

Composition (%)	Fly ash (FA)	Ground bottom ash (BT)
SiO_2	38.7	38.8
Al_2O_3	20.8	21.3
FeO_3	15.3	12.1
CaO	16.6	16.5
Na_2O	1.3	1.0
TiO_2	0.5	0.8
MgO	1.3	1.7
K_2O	2.1	2.5
SO_3	2.6	2.4
LOI	0.8	2.9
Retained on sieve no. 325 (% by weight)	32	29

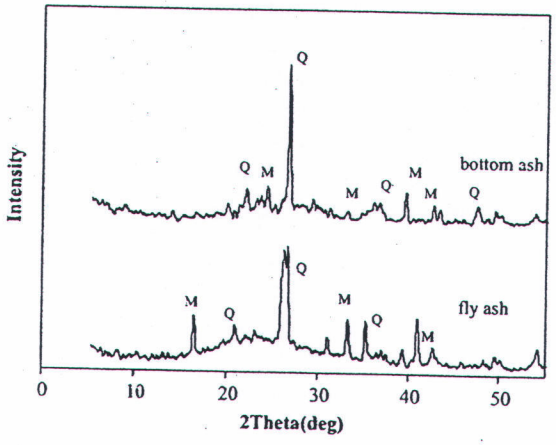

Fig. 1. XRD patterns of fly ash and bottom ash. Q = quartz, M = mullite.

Table 2
Mix proportion of coal ash geopolymer paste

Materials	Mix proportion (% by weight)
Fly ash or bottom ash	60
NaOH (5, 10, and 15 M)	16
Na_2SiO_3	24

Table 3
Composition of geopolymers prepared from fly ash and bottom ash

Sample	NaOH (M)	Mole ratio			
		Na_2O/SiO_2	SiO_2/Al_2O_3	H_2O/Na_2O	Na_2O/Al_2O_3
FA5	5	0.15	4.14	19.95	0.64
FA10	10	0.21	4.14	13.33	0.89
FA15	15	0.26	4.14	10.40	1.08
BT5	5	0.15	4.05	19.95	0.62
BT10	10	0.21	4.05	13.33	0.87
BT15	15	0.26	4.05	10.40	1.05

2.3. Mixing procedure and tests of the geopolymer mortar

When making the mortar, sand was added to the paste mixture at a sand-to-coal ash ratio of 2:1 (by weight) and mixed for another two 2 min. The mixture was then cast into 50 mm^3 molds in accordance with ASTM C109 and covered with cling film to avoid moisture evaporation during heat curing. The mixture was subsequently cured in an oven at 65 °C for 48 h to complete the geopolymerization. After that, the specimens were cooled to room temperature and tested for strength. The results are reported as an average of three samples.

3. Results and discussion

3.1. IR spectra

FT-IR was used to study the geopolymerization of the paste. The distinct band near 460 cm^{-1} can be ascribed to the O–Si–O bending mode (Barbosa et al., 2000; Günzler and Gremlich, 2002). The Si–O–Si stretching vibration was detected at the wave number range of 1200–950 cm^{-1}. The Si–O–Si stretching vibration was more prominent than the O–Si–O bending mode. It is, therefore, logical to use the Si–O–Si vibration to indicate the degree of geopolymerization.

The results of the IR spectra are shown in Fig. 2a and b. The significant broad bands are located at approximately 3450 cm^{-1} and 1650–1600 cm^{-1} for O–H stretching and O–H bending, respectively. Si–O–Si position is shifted to the right position or lower frequency compared with the original ash, implying a chemical change in the matrix. The band at 1460 cm^{-1} represents the sodium carbonate resulting from the carbonation (Barbosa et al., 2000).

The peak areas and peak heights are frequently used in quantitative assessment of the reaction. The ratios of peak area of Si–O–Si stretching vibration (AS) are tabulated in Table 3. For the fly ash system, the AS is relatively low. The AS of the geopolymer paste increases with an increase in the concentration of sodium hydroxide (up to 10 M). At a higher concentration of 15 M NaOH, the AS of paste is still high (Table 4). The AS ratios of the 5, 10, and 15 M NaOH paste to that of the fly ash are 1.43, 4.53, and 3.61, respectively. This suggests that a relatively high degree of geopolymerization is obtained with the use of 10 M NaOH. At a low concentration, the geopolymerization is low, due to the low con-

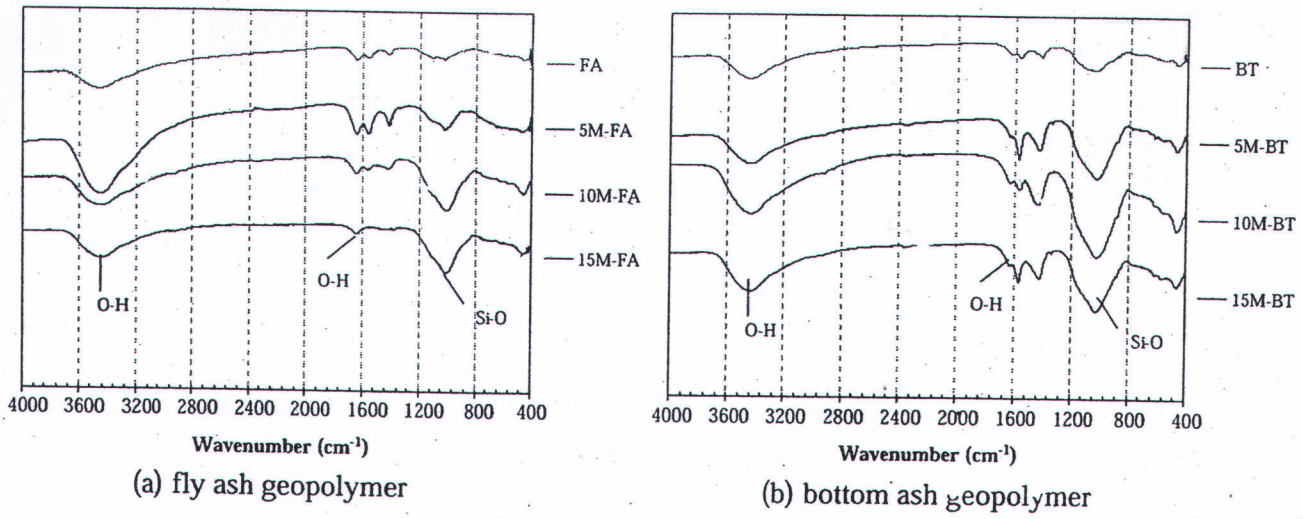

Fig. 2. FT-IR spectra of fly ash and bottom ash geopolymers.

Table 4
Inverted peak area and AS ratio from IR spectra of pastes at Si–O–Si stretching vibration

Sample	NaOH (M)	Location of Si–O–Si (cm^{-1})	AS ratio	Peak height ratio
Fly ash particles	–	1016	1	1
1	5	1016	1.43	1.74
2	10	1001	4.53	4.14
3	15	1008	3.61	3.93
Bottom ash particles	–	1023	1	1
4	5	1023	3.23	2.75
5	10	1016	4.56	3.82
6	15	1020	3.11	2.38

centration of base and, hence, less leaching of silica and alumina from the source material. At the high concentration of 15 M NaOH, although the concentration of base is high, the matrix becomes very stiff, as the viscosity of the 15 M NaOH is 14.3 cps in comparison to the 9.3 cps of the 10 M NaOH. The high viscosity hinders the leaching of the silica and alumina, resulting in a lesser degree of geopolymerization as compared to that of the 10 M NaOH paste. The peak height also gives similar indications of the degree of geopolymerization. For the bottom ash system, the results are similar to those of the fly ash system. The 10 M NaOH paste also gives a high degree of polymerization. The bottom ash pastes behave in a similar manner to the fly ash pastes as they contain similar amounts of silica and alumina and come from the same source.

3.2. Differential Scanning Calorimetry (DSC)

Differential scanning calorimetry was used to measure a number of characteristic properties of the geopolymer pastes. Using this technique, it is possible to observe exothermic and endothermic events, as well as glass transition temperatures (T_g). The range of investigation is between −30 and 100 °C. The results of the DSC thermograms (exothermal up) of the fly ash, ground bottom ash, and geopolymer mixed with 10 M NaOH are shown in Fig. 3. The DSC thermograms of fly ash and bottom ash are relatively straight, indicating no sign of reaction. The thermograms of coal ash geopolymers show several peaks, indicating some degree of geopolymerization. A significant peak representing the melting point of water is observed in all geopolymer samples at 0 °C (Phair et al., 2003). The exothermal peaks found in the fly ash geopolymer at the temperature of approximately 20 °C reflect the glass transition

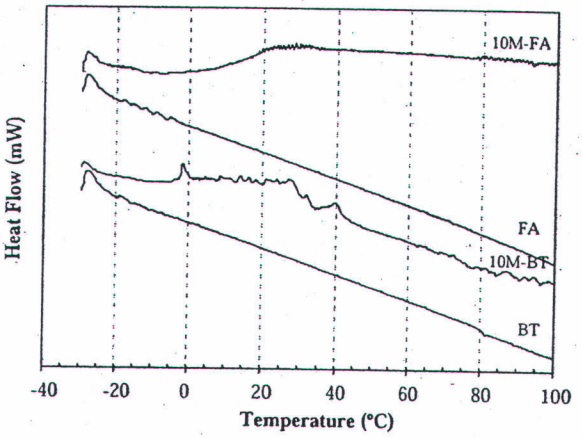

Fig. 3. DSC thermogram of geopolymer pastes using 10 M NaOH.

temperature (T_g). The bottom ash geopolymer reveals several small peaks in the temperature range of 10–40 °C. The peaks at this range of temperature can be attributed to the crystallization temperature (T_c), at which an amorphous solid could become less viscous and obtain enough freedom of motion to spontaneously arrange into a crystalline form. This transition from amorphous solid to crystalline solid is an exothermic process, and it results in a peak in the DSC signal (Dean, 1995).

Within the temperature range of 30–100 °C, the slope of the DSC thermogram for the fly ash geopolymer is relatively flat as compared to that of the bottom ash geopolymer. This indicates a difference in the degree of geopolymerization of the two geopolymers. For the bottom ash geopolymer, although the DSC thermogram at this range contains several distinct peaks, the slope of the thermogram is about the same as that of the base material (i.e., bottom ash). This suggests a low degree of geopolymerization of the bottom ash geopolymer. The slope of the fly ash geopolymer, however, is significantly different from that of fly ash, indicating a higher degree of geopolymerization.

3.3. Microstructure

The typical SEM-EDX of hardened fly ash geopolymer is shown in Fig. 4. The paste shows unreacted and/or partially reacted grains

of fly ash and a continuous mass of alumino-silicate. A large proportion of fly ash still does not completely react, especially the large particles. Although the matrix is continuous and relatively dense, voids and cracks are easily observed. This would limit the binding capacity and strength of the geopolymer. For the bottom ash geopolymer, as shown in Fig. 5, the paste also shows a continuous mass of alumino-silicate with unreacted and/or partially reacted grains of irregular coal ash particles. The irregular particles are porous and would thus exert a negative influence on the strength of the geopolymer.

The results of the EDX analyses of the fly ash and bottom ash geopolymers are also shown in Figs. 4 and 5. The major elements are Si and Al, with some Na and Ca also present. The presence of Ca is from the source materials as the fly ash and bottom ash both contain large amounts of CaO. The ratios of Si/Al for the fly ash and bottom ash geopolymers are significantly different. The ratio of Si/Al for the fly ash geopolymer is 3.0, and the same ratio for the bottom ash geopolymer is much higher at 6.0. This indicates that the leaching of alumina in the fly ash geopolymer matrix is better than that in the bottom ash matrix. The higher ratio of Si/Al results in geopolymers with lower strength and higher elasticity (Fletcher et al., 2005).

3.4. Compressive strength

Fig. 6 shows the compressive strength of geopolymer mortars when heat cured at 65 °C for 48 h. The fly ash geopolymer mortar gives a higher compressive strength in comparison to the bottom ash geopolymer. The results also indicate that the use of a low NaOH concentration of 5 M gives geopolymer mortars with relatively low strength. For the fly ash geopolymer, the use of 5 M NaOH gives a mortar with a moderate strength of 24 MPa. Higher strengths of 35 and 33 MPa are obtained with the use of 10 M and 15 M NaOH. The compressive strength results are consistent with the results of the FT-IR, thermograph, and SEM.

For the bottom ash, the compressive strengths of mortars are lower than those of the fly ash geopolymer. The strengths of 5, 10, and 15 M geopolymer mortars are 10, 14, and 18 MPa, respectively. The degree of polymerization of the bottom ash geopolymer is lower than that of the fly ash polymer, as suggested by the thermograph. The dissolution of bottom ash in the NaOH solution would be lower than that of the fly ash. Bottom ash thus requires a higher concentration of NaOH for the dissolving of alumina and silica and for geopolymerization. The fact that a large number of

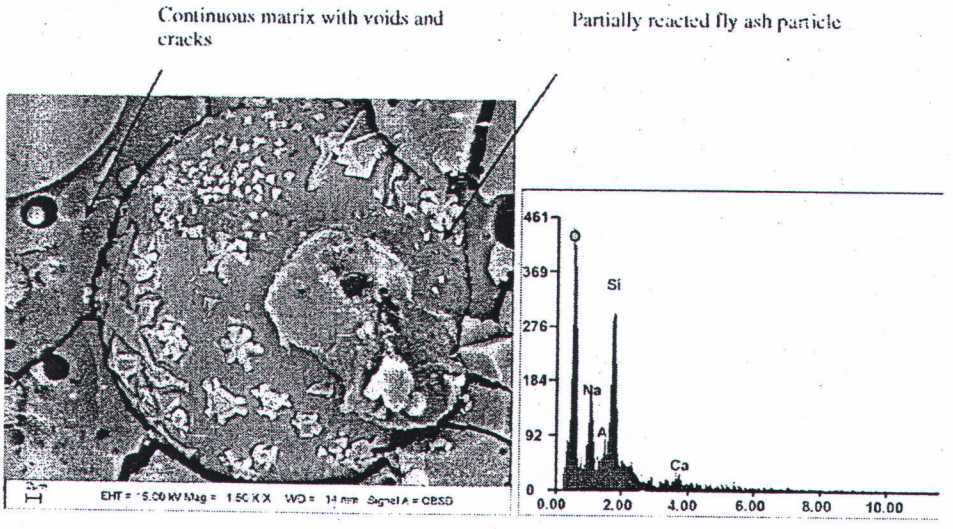

Fig. 4. SEM-EDX analysis of fly ash geopolymer.

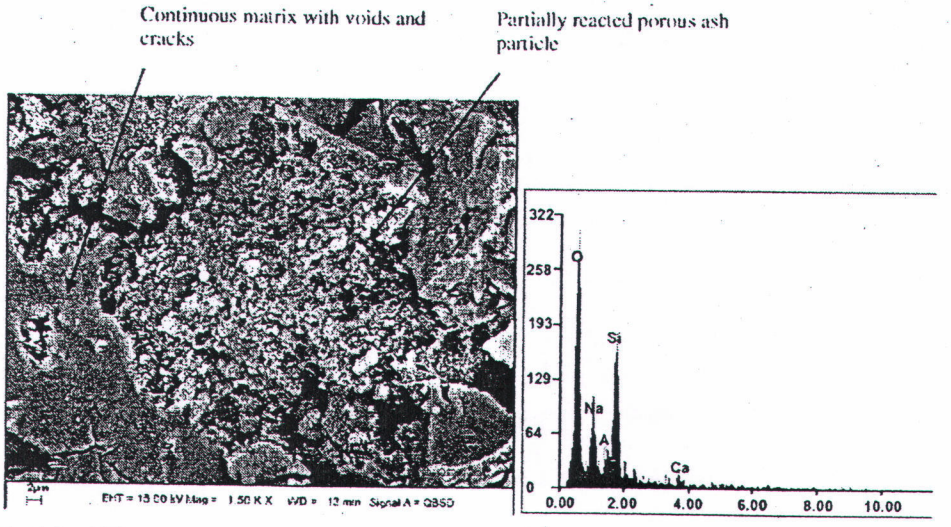

Fig. 5. SEM-EDX analysis of bottom ash geopolymer.

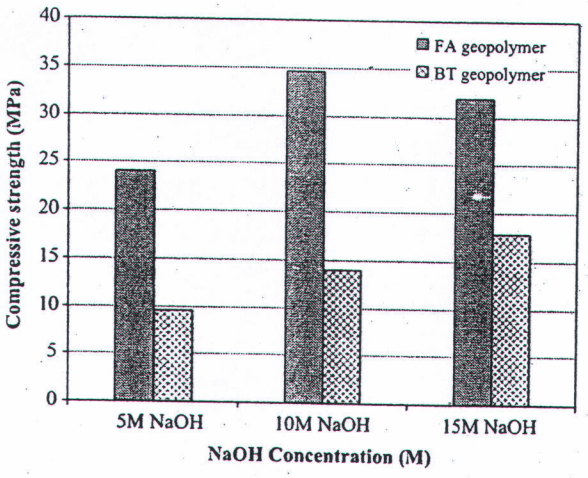

Fig. 6. Compressive strength of geopolymer mortars.

the bottom ash particles are porous also contributes to the lower mortar strength.

The analysis of geopolymer paste characteristics and microstructure, using FT-IR, DSC thermographs, and SEM, reinforces the importance of a physical property, i.e., the compressive strength of geopolymer mortars.

4. Conclusions

Fly ash and ground bottom ash are suitable source materials for producing geopolymers. The results of the FT-IR, DSC thermogram, SEM, and XRD analyses indicate that fly ash is more reactive than bottom ash and gives a higher degree of geopolymerization. The compressive strength of the fly ash geopolymer mortar is reasonably high at 35 MPa, and it is significantly higher than the 18 MPa of the bottom ash geopolymer mortar. The strength of a geopolymer is also dependent on NaOH concentration. The optimum NaOH concentration of 10 M is suitable for both ash materials.

Acknowledgments

The authors gratefully acknowledge the financial support from the Thailand Research Fund (TRF) under TRF New Researcher Scholar Contact No. MRG4980145, TRF Senior Research Scholar Contact no. RTA5080020, and the Commission on Higher Education, Ministry of Education, Thailand. Appreciation is also extended to PERCH-CIC Program.

References

Barbosa, V., MacKenzie, K., Thaumaturgo, C., 2000. Synthesis and characterisation of materials based on inorganic polymers of alumina and silica: sodium polysialate polymer. International Journal of Inorganic Materials 2, 309–317.

Chindaprasirt, P., Chareerat, T., Sirivivananon., V., 2007. Workability and strength of coarse high calcium fly ash geopolymer. Cement and Concrete Composites 29, 224–229.

Dean, J.A., 1995. The Analytical Chemistry Handbook. McGraw Hill, Inc., New York, USA.

Fletcher, R.A., Mackenzie, K.J.D., Nicholson, C.L., Shimada, S., 2005. The composition rang of aluminosilicate geopolymers. Journal of the European Ceramic Society 25, 1471–1477.

Günzler, H., Gremlich, H., 2002. IR Spectroscopy: An Introduction. Wiley-VCH Verlag GmbH, Germany.

Jaturapitakkul, C., Cheerarot, R., 2003. Development of bottom ash as pozzolanic material. Journal of Materials in Civil Engineering 15, 48–53.

Lee, W.K.W., Van Deventer, J.S.J., 2002. Structure reorganisation of class F fly ash in alkaline silicate solutions. Colloids and Surfaces A: Physicochemistry Engineering Aspects 211, 49–66.

Maholtra, V.M., 2002. Introduction: Sustainable development and concrete technology. ACI Concrete International 24, 22–23.

Mehta, P.K., 1998. Role of pozzolanic and cementitious by-products in sustainable development of the concrete industry. In: Sixth CANMET/ACI/JCI Conference: Fly Ash, Silica Fume, Slag and Natural Pozzolans in Concrete, Bangkok, Thailand.

Phair, J.W., Smith, J.D., Van Deventer, J.S.J., 2003. Characteristics of aluminosilicate hydrogels related to commercial 'Geopolymer'. Materials Letters 57, 4356–4367.

2. P. Chindaprasirt, C. Jaturapitakkul, U. Ratanasak. Influence of fineness of rice husk ash and additives on the properties of lightweight aggregate, Fuel, 88 (2009), 158-162. (IF 2.536)

Fuel 88 (2009) 158–162

Contents lists available at ScienceDirect

Fuel

journal homepage: www.elsevier.com/locate/fuel

Influence of fineness of rice husk ash and additives on the properties of lightweight aggregate

P. Chindaprasirt [a], C. Jaturapitakkul [b], U. Rattanasak [c,*]

[a] Department of Civil Engineering, Faculty of Engineering, Khon Kaen University, Khon Kaen 40002, Thailand
[b] Department of Civil Engineering, Faculty of Engineering, King Mongkut's University of Technology Thonburi, Bangkok 10140, Thailand
[c] Department of Chemistry, Faculty of Sciences, Burapha University, Chonburi 20131, Thailand

ARTICLE INFO

Article history:
Received 14 December 2007
Received in revised form 17 April 2008
Accepted 28 July 2008
Available online 21 August 2008

Keywords:
Lightweight aggregate
Rice husk ash
Sodium hydroxide
Solubility
Disintegration

ABSTRACT

In this paper, the preparation of lightweight aggregate (LWA) from rice husk ash (RHA) obtained from a biomass power plant was studied. As-received and ground RHAs were mixed with sodium hydroxide solution (NaOH) and cured to obtain the hardened sodium silicate paste. The samples were then crushed and heated to form LWA. The LWA was tested for acid and base solubility and for disintegration in boiling water. The results showed that ground RHA–LWA gave better performances in terms of expansion, solubility, and disintegration than the as-received RHA–LWA. However, the disintegration of LWA in boiling water was the main problem. It was found that the incorporation of 2–7% boric acid by weight of RHA alleviated this problem and no sign of disintegration was observed. The density of LWA of 0.20–0.40 g/cm^3 was achieved.

1. Introduction

Rice husk is an agricultural by-product and the annual output is approximately 5 million tons in Thailand alone. It consists of about 40% cellulose, 30% lignin group and 20% silica and hence its ash contains a large amount of silica [1,2]. It is used as an energy source for biomass power plants, rice mills and brick factories. When burnt, rice husk ash (RHA) with approximately one-fifth of the original weight is obtained as a by-product. RHA contains over 80% of silica and small proportion of impurities such as K_2O, Na_2O and Fe_2O_3 [2,3]. The silica exists in amorphous and crystalline forms depending on the temperature and duration of burning. Amorphous silica is obtained by burning rice husk at temperature lower than 700 °C [4]. For higher burning temperature, some crystalline silica is formed and to produce amorphous silica, the burning duration needs to be shortened [5]. The specific gravity of RHA is around 2.0–2.3 depending on the burning temperatures [6]. The cellular nature of the rice husk gives the cellular porous structure of the RHA texture. The RHA is, therefore, bulky and the transportation could pose some problems.

The commercial uses of RHA are in the silica extraction process [7,8], pozzolanic material [1,3,9] and other applications such as soil improvement. The silica from RHA can be extracted economically with sodium hydroxide solution at 100 °C to obtain a soluble salt in the form of sodium silicate [7]. The reactive RHA produced from proper burning and grinding can also be used for partial replacement of Portland cement. The concrete containing RHA is of good quality with reduced porosity, and improved resistance to sulphate attack and chloride penetration [9,10]. With the problem of handling and transportation, a large amount of RHA is, however, treated as waste and disposed at landfill site. Therefore, an increase in the utilization of RHA has enormous potential for waste management and value added commercial applications.

Lightweight aggregate (LWA) is an alternative way to utilize this by-product. The production of LWA is done by pelletizing the powder and expanding the sintered aggregate at high temperature of 900–1300 °C [11,12]. The expansion mechanism of sintered LWA is a dynamic balance process of the expanded gas escaping from the pellet and the inhibiting effect of liquid viscosity [13]. This interaction results in the expansion of sintered raw material. In some cases, foaming agent is added to improve the expansion [14]. This method is widely used as it is convenient, but the process is not environmental friendly as it consumes high energy.

The sodium silicate pellets can also be used to make LWA as it possesses the expansive property [15]. The sodium silicate can be obtained from the reaction of RHA and NaOH. Low temperature used in the expansion process is expected owing to the thermal expansion property of sodium silicate when heated in comparison to the fusion method. The stability of this RHA–LWA after soaking in water and other solutions could pose some problems owing primarily to the high porosity and weak pore structure of RHA.

* Corresponding author. Tel.: +66 38 103 066; fax: +66 38 393 494.
E-mail address: ubolluk@buu.ac.th (U. Rattanasak).

0016-2361/$ - see front matter © 2008 Elsevier Ltd. All rights reserved.
doi:10.1016/j.fuel.2008.07.024

The incorporation of boric compound significantly reduces the melting point and lowers the transformation temperature. This renders the effective control of the morphology and phase purity of the particles [16]. Boric acid (H_3BO_3) is the most common compound and is generally used as an additive to improve the stability and setting of powdery particles at high temperature [17,18]. As temperature increases above 170 °C, H_3BO_3 decomposes to metaboric acid (HBO_2) which further decomposes to boron oxide (B_2O_3) at higher temperature. In the formation of various calcium-aluminate phases, the addition of H_3BO_3 as a flux drastically reduces the heating temperature from 1700 to 1300 °C [18]. Calcium oxide (CaO) is another common additive which is widely used in mortar and plaster to increase the rate of hardening and to improve the adhesion [19]. In addition, CaO is also used to reduce the melting temperature of slag in a similar manner to boric acid [20].

This paper, therefore, explores an alternative method for the production of expanded aggregate from RHA. The method is based on alkaline solubility of silica in RHA. It is more environmental friendly than the current fusion method. The influence of the additives, i.e. boric acid and calcium oxide on the stability of the LWA is also studied.

2. Materials and methods

2.1. Materials

Rice husk ash from biomass power plant in the central part of Thailand and sodium hydroxide (NaOH) pellet were used. NaOH pellet was dissolved in water to obtain NaOH solution at concentrations of 10, 15 and 25 M. Three types of ash viz., as-received rice husk ash (A-RHA), ground medium fineness rice husk ash (M-RHA) with 12% retained on sieve No. 325, and ground fine rice husk ash (F-RHA) with 5% retained on sieve No. 325 were used. Analytical grade boric acid (H_3BO_3) and calcium oxide (CaO) were used as additives to solve the problem of disintegration in boiling water. The chemical composition of the RHA is shown in Table 1.

2.2. LWA preparation

The RHA, NaOH solution and H_3BO_3 (or CaO) were thoroughly mixed in the mixer for 5 min to form uniform paste. The mixture was then placed in the 100 × 100 × 10 mm^3 mould and cured for 24 h. The curing temperatures of 85, 100 and 115 °C were used. The hardened pastes were then crushed and passed through sieve No. 4 (4.75 mm opening) and retained on sieve No. 10 (2 mm opening). They were, then, put in the oven at 350, 500 and 650 °C for 30 min for expansion. The percentage retained on sieve No. 4 of the LWA was measured to indicate the degree of expansion. In addition, the bulk density, gradation, fineness modulus, solubility and the boiling tests were performed. The experiment parameters for LWA are summarized in Table 2.

2.2.1. Mixes for LWA with various finenesses of RHA

The mixes with different finenesses of RHA are shown in Table 3. The NaOH with the concentration of 10 M was used. The A-RHA requires a larger amount of NaOH to obtain the paste with similar consistency. Therefore, the RHA:NaOH ratio of 1:1 was used for A-RHA and the ratio of 1:2.5 was used for M-RHA and F-RHA.

Table 1
Chemical composition of RHA%

SiO_2	Al_2O_3	CaO	Fe_2O_3	MgO	K_2O	LOI
87.46	2.53	0.78	0.40	1.58	4.73	2.52

Table 2
Experiment parameters and tested properties

(a) Experiment parameters
1. Fineness of RHA: A-RHA, M-RHA, F-RHA
2. RHA:NaOH ratio: 1:2.5, 1:1
3. Curing temperature (°C): 85, 100, 115
4. Expansion temperature (°C): 350, 500, 650
5. Boric acid content (% by weight of RHA): 2, 4, 7, 10
6. Calcium oxide content (% by weight of RHA): 4, 10
7. NaOH concentrations (M): 10, 15, 20
(b) Tested properties
1. Degree of expansion
2. Bulk density
3. Time to disintegrate in boiling water
4. Solubility in acid and base
5. Crushing resistance
6. Water absorption
7. Gradation and fineness modulus

Table 3
Physical properties of LWA prepared with various fineness RHA

RHA	RHA:NaOH ratio	Expansion (%)	Bulk density (g/cm^3)	Time to disintegrate (min)	Solubility
A-RHA	1:2.5	15	0.30	1	Yes
M-RHA	1:1	22	0.32	10	No
F-RHA	1:1	29	0.28	12	No

2.2.2. Study on curing and expansion temperatures

In this series, the M-RHA was selected based on the result of the test of Section 2.2.1. Pastes were prepared using 10 M NaOH with RHA:NaOH ratio of 1:1. The curing temperatures were varied at 85, 100 and 115 °C. The crushed samples were left to expand in the oven at different temperatures of 350, 500 and 650 °C for 30 min.

2.2.3. Mixes with CaO and H_3BO_3

The 10 M NaOH and M-RHA:NaOH ratio of 1:1 were used for the preparation of LWA. Four H_3BO_3 contents of 2%, 4%, 7% and 10% by weight of RHA and two CaO contents of 4% and 10% by weight of RHA were investigated. Based on the result of Section 2.2.2, 115 °C was selected to cure the paste and the temperature of 500 °C was used for the expansion.

2.2.4. Mixes for various concentrations of NaOH solution

For comparison purpose, 10, 15 and 20 M NaOH were used to prepare the LWA using M-RHA:NaOH ratio of 1:1, with 4% and 10% of H_3BO_3. Sample was cured at 115 °C for 24 h and then left to expand at 500 °C for 30 min.

2.3. Tests of LWA

LWA was tested for bulk density, solubility in 12 M HCl acid and 20 M NaOH base solutions, disintegration in boiling water by soaking in boiling water for 60 min, crushing resistance, water absorption and gradation. The bulk density of the LWA was tested in accordance with BS EN 1305 [21]. The acid and base solution test was adapted from the procedure described in ASTM C114 [22]. The boiling test was applied from the procedure described in BS EN 1367 method of the boiling test for "Sonnenbrand" basalt [23]. The crushing resistance, the water absorption and the gradation of the LWA were tested in accordance with BS 1305. The tested properties of LWA are summarized in Table 2. In addition, the microstructure of the fractured samples was microscopically examined with scanning electron microscope (SEM).

3. Results and discussion

3.1. Effects of fineness of RHA

The results of degree of expansion, bulk density and disintegration in boiling water of LWA with various finenesses of RHA are shown in Table 3. There was a tendency that the larger expansion was found with the increase in the fineness of RHA. The expansions of the LWA made from A-RHA, M-RHA, and F-RHA were 15%, 22% and 29%, respectively. The bulk density of LWA was fairly low between 0.28 and 0.32 g/cm^3 and not affected by the fineness of RHA. The low bulk density is one of the very important properties of LWA. The other important property is the stability.

The result of disintegration in boiling water shown in Table 3 indicated that the stability of the LWA increased with the increase in fineness of RHA. The grinding of RHA increased its fineness and reactivity [3–5] and hence produced a stronger paste as compared with the as-received RHA as shown in Fig. 1. The RHA grains were easily detected. The LWA showed non-uniform texture of the RHA agglomeration and appeared as weak porous aggregate leading to disintegration in boiling water. LWAs prepared from M-RHA and F-RHA showed no sign of solubility in acid and base, and prolonged the time to disintegration in boiling water. M-RHA was, therefore, selected to further study the properties of LWA because of the economy and the practicality.

3.2. Properties of LWA from M-RHA

3.2.1. Effect of curing and expansion temperatures

The results of bulk density and time to disintegration of LWA prepared at various curing and expansion temperatures are shown in Table 4. The curing temperatures of 85 and 100 °C for 24 h were not sufficient to accelerate the paste stiffening and resulted in unhardened pastes which were not suitable for further process. The use of high temperature of 115 °C for 24 h resulted in hardened paste. At this temperature, rice husk ash reacted with sodium hydroxide solution to form the sodium silicate [7] as described in the following equation:

$$2NaOH + SiO_2\ (\text{from RHA}) \xrightarrow{\text{heat}} Na_2SiO_3 + H_2O + \text{insoluble material}.$$

The hardened sodium silicate and ash mixtures were then crushed and left to expand at high temperature. The temperature for expansion affected the properties of LWA. At low temperature of 350 °C, the LWA expansion was low leading to a relatively high bulk density of 0.42 g/cm^3. The use of higher temperatures of 500 and 650 °C resulted in lighter and stronger aggregate as reflected by the low bulk density of 0.32 and 0.31 g/cm^3. The time to disintegration was also improved to 10 min comparing to 7 min of that using 350 °C expansion temperature. Rapid heating caused the aggregate to expand owing to the high coefficient of thermal expansion of sodium silicate [15]. The sodium silicate mixture melted at approximately 500 °C which corresponded to its deformation temperature [15]. The texture of the LWA before expansion is shown in Fig. 2. The particle of RHA and a small amount of needle-like particles were readily detected. After heating at 500 °C (Fig. 3), the texture of the LWA was quite homogenous with some pores. The needle-like particles disappeared owing to the melting and expansion of sodium silicate. The improved homogeneity and reduced porosity led to the higher resistance of aggregate against disintegration in boiling water.

Table 4
Bulk density and time to disintegration of LWA prepared at various curing and expansion temperatures

Sample	Curing temperature (°C)	Bulk density (g/cm^3)			Time to disintegrate (min)		
		Expansion temperature			Expansion temperature		
		350 °C	500 °C	650 °C	350 °C	500 °C	650 °C
1	85	N/A	N/A	N/A	N/A	N/A	N/A
2	100	N/A	N/A	N/A	N/A	N/A	N/A
3	115	0.42	0.32	0.31	7	10	10

3.2.2. Effects of CaO and H_3BO_3 on disintegration in boiling water

The incorporation of H_3BO_3 and CaO was to promote the binding capacity of the paste and, hence, more stable pastes should be obtained. It was found that the use of H_3BO_3 resulted in significant improvement on the disintegration. The results of the tests are shown in Table 5. The addition of 2–7% of H_3BO_3 in the mixture with 10 M NaOH solved this problem because no sign of disintegration was observed. Since there was a non-bridging oxygen in a sodium silicate structure, addition of H_3BO_3 resulted in BO_4 tetrahedral in the sodium silicate matrix and enabled the oxygen to bridge again resulting in a more stable structure. In other words, the structure tended to be solidified as H_3BO_3 was used [17]. However, excessive use of H_3BO_3 had an adverse effect on the disintegration.

In contrast, the use of CaO only slightly improved the stability of the LWA in terms of the disintegration in boiling water. CaO reacted with silica to form calcium silicate with low bulk density

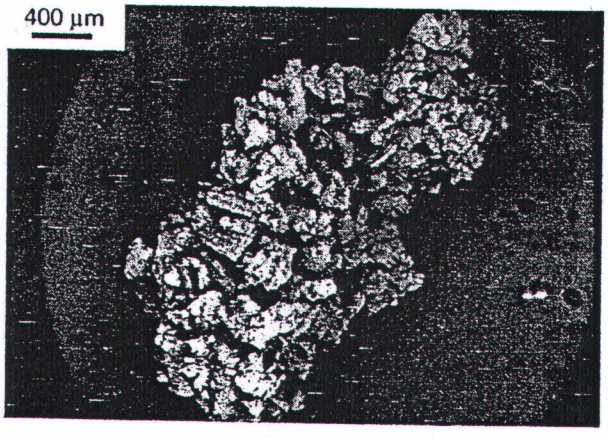

Fig. 1. SEM of LWA (A-RHA, 10 M NaOH, curing temperature 115 °C, expansion temperature 500 °C).

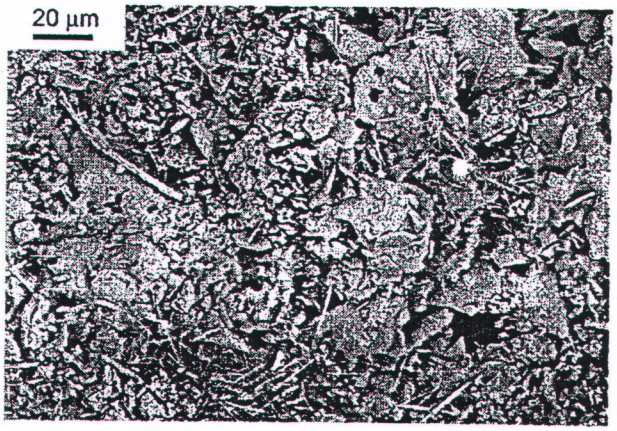

Fig. 2. SEM of hardened M-RHA paste (10 M NaOH, 2% boric acid, curing temperature 115 °C, before expansion).

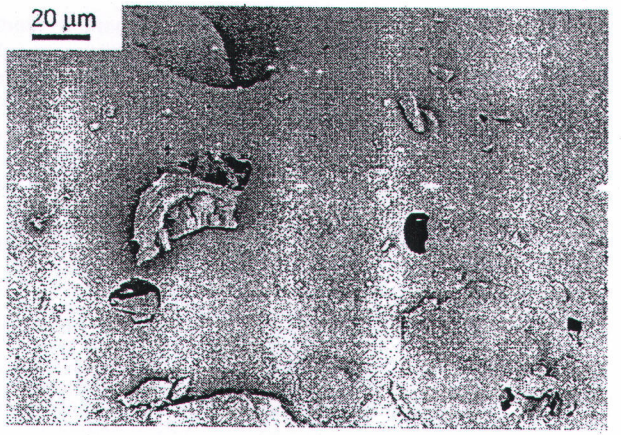

Fig. 3. SEM of LWA (M-RHA and 10 M NaOH, 2% boric acid, curing temperature 115 °C, expansion temperature 500 °C).

Table 5
Physical properties of M-RHA–LWA with 10 M NaOH, H_3BO_3 and CaO

RHA (g)	NaOH (g)	H_3BO_3 (g)	CaO (g)	Expansion (%)	Bulk density (g/cm^3)	Solubility	Time to disintegrate
100	100	–	–	22	0.32	No	10 min
100	100	2	–	28	0.37	No	None in 60 min
100	100	4	–	45	0.19	No	None in 60 min
100	100	7	–	43	0.25	No	None in 60 min
100	100	10	–	35	0.36	No	20 min
100	100	–	4	29	0.34	No	8 min
100	100	–	10	8	0.51	No	20 min

and high physical water absorption property [19]. Matrix with calcium silicate was, therefore, easily damaged in boiling water.

3.2.3. Effects of concentration of NaOH on disintegration in boiling water

The results of the effects of NaOH on disintegration in boiling water shown in Table 6 indicated that only the use of 10 M NaOH with 4% H_3BO_3 resulted in no disintegration in boiling water. For the 15 and 20 M NaOH, the problem of disintegration still persisted. The LWA made from 10 M NaOH with 4% of H_3BO_3 showed high bulk density as compared with those of 15 and 20 M NaOH. These concentrations also resulted in larger expansion as measured by percentage retained on sieve No. 4 in comparison to that using 10 M NaOH. With high NaOH concentrations of 15 and 20 M, the viscosity of the mixtures increased and the solubility and mobility of the system were reduced. For lower concentration of 10 M NaOH, the absorption and interaction between the NaOH solution and RHA particles were better than those with the higher NaOH concentration. Disintegration was, therefore, dependent on alkali solution concentrations and additives added.

3.3. Basic properties and application of LWA

M-RHA mixed with 4% of boric acid and 10 M NaOH was prepared for testing of physical properties of LWA. The gradation as shown in Fig. 4 presented that the particles sizes of LWA were mainly between 2.4 and 4.7 mm with the fineness modulus of 5.1. Its crushing resistance was 3.2 N/mm^2. Its low crushing resistance and bulk density suggest the use for lightweight concrete panels or blocks for thermal insulation and noise absorption and/

Table 6
Physical properties of LWA prepared with various NaOH concentrations

NaOH (M)	RHA (g)	NaOH (g)	H_3BO_3 (g)	Expansion (%)	Bulk density (g/cm^3)	Solubility	Time to disintegrate
10	100	100	–	22	0.32	No	10 min
	100	100	4	45	0.19	No	None in 60 min
	100	100	10	35	0.36	No	20 min
15	100	100	–	36	0.18	No	4 min
	100	100	4	56	0.07	No	15 min
	100	100	10	35	0.28	No	6 min
20	100	100	–	42	0.12	No	3 min
	100	100	4	61	0.10	No	4 min
	100	100	10	48	0.21	No	4 min

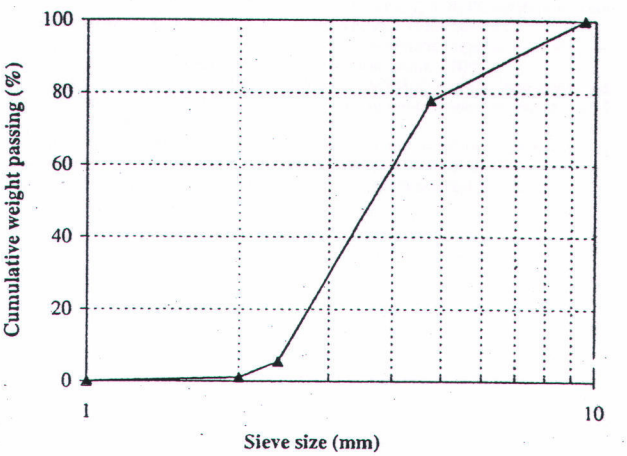

Fig. 4. Gradation of LWA (M-RHA, 10 M NaOH, 2% boric acid, curing temperature 115 °C, expansion temperature 500 °C).

or fire protection. The water absorption of the LWA was 64%. The high porosity and absorption capability together with the insolubility in acid and base make the LWA suitable for use as an absorbent for a wide variety of liquids. Once absorbed, the liquid is retained by LWA allowing easy handling and disposal. Also with its low density, LWA concrete is a viable solution for reducing loading on the structure of the building. Although, LWA is more expensive to produce than gravel or crushed stone aggregates, the reduced overall weight of the structure leads to overall saving [24]. The cost of this RHA–LWA should be less than that obtained from the fusion method as it consumes less energy.

4. Conclusion

Rice husk ash has the potential for making light weight aggregate with low bulk density of 0.20–0.40 g/cm^3. The properties of LWA are enhanced with the increase in fineness of RHA. The RHAs with 12% and 5% retained on sieve No. 325 give better LWA than the as-received RHA. The process involves the reaction of RHA with 10 M sodium hydroxide solution at 115 °C for 24 h to form the sodium silicate and the expansion of crushed hardened sodium silicate and ash mixture at 500 °C. The stability of the LWA is obtained by incorporating 2–7% boric acid by weight of RHA in the mixture.

Acknowledgements

The authors gratefully acknowledge the financial supports from the Thailand Research Fund (TRF) under TRF Senior Research

Scholar Contact No. RTA5080020 and the Commission on Higher Education, Ministry of Education, Thailand. Appreciation is also extended to the Thai PERCH-CIC Program.

References

[1] Mehta, PK. The chemistry and technology of cements made from rice husk ash. In: UNIDO/ESCAP/RCTT workshop on production of cement-like materials from agro-wastes, Peshawar, Pakistan; 1979. p. 113–22.
[2] Real C, Alcala MD, Criado JM. Preparation of silica from rice husks. J Am Ceram Soc 1996;79:2012–6.
[3] Stroeven P, Bui DD, Sabuni E. Ash of vegetable waste used for economics production of low to high strength hydraulic binders. Fuel 1999;78:153–9.
[4] Della VP, Kuhn I, Hotza D. Rice husk ash as an alternative source for active silica production. Mater Lett 2002;57:818–21.
[5] De Silva A. Current stage of research on reactivity of rice husk ash cement. Master of Engineering Thesis. Asian Institute of Technology. Thailand. 1980.
[6] Ibrahim DM, Helmy M. Crystal growth of rice husk ash silica. Thermochem Acta 1981;45:79–85.
[7] Kalapathy U, Proctor A, Shutz J. A simple method for production of pure silica from rice hull ash. Bioresour Technol 2000;73:257–62.
[8] Della VP, Kühn I, Hotza D. Rice husk ash as an alternate source for active silica production. Mater Lett 2002;57:818–21.
[9] Chindaprasirt P, Kanchanda P, Sathonsaowaphak A, Cao HT. Sulfate resistance of blended cements containing fly ash and rice husk ash. Constr Build Mater 2007;21:1356–61.
[10] Chindaprasirt P, Rukzon S, Sirivivatnanon V. Resistance to chloride penetration of blended Portland cement mortar containing palm oil fuel ash, rice husk ash and fly ash. Constr Build Mater 2008;22:932–8.
[11] Harikrishnan KI, Ramamurthy K. Influence of pelletization process on the properties of fly ash aggregates. Waste Manage 2006;26:846–52.
[12] Adeli V, Cheeseman CR, Doel A, Beattie A, Boccaccini AR. Comparison of rapid and slow sintered pulverised fuel ash. Fuel 2008;87:187–95.
[13] Guo YS, Ding JT, Kimura K, Li MW, Song PJ, Huang MJ. Comparison of properties of high performance lightweight aggregate and normal lightweight aggregate. J Concrete (China) 2000;6:22–6.
[14] Ducman V, Mladenovič A, Šuput JS. Lightweight aggregate based on waste and its alkali-silica reactivity. Cement Concrete Res 2002;32:223–6.
[15] Shermer HF. Thermal expansion of binary alkali silicate glasses. j Res Nat Bureau Stand 1956;57:97–101.
[16] Jung DS, Hong SK, Lee HJ. Effect of boric acid flux on the characteristics of (CeTb)$MgAl_{11}O_{19}$ phosphor particles prepared by spray pyrolysis. J Alloys Compd 2005;389:309–14.
[17] Kim KD, Choi KY, Yang JW. Formation of spherical hollow silica particles from sodium silicate solution by ultrasonic spray pyrolysis method. Colloids Surf A – Physicochem Eng Aspects 2005;254:193–8.
[18] Haranath D, Sharma P, Chander H, Ali A, Bhalla N, Halder SK. Role of boric acid in synthesis and tailoring the properties of calcium aluminate phosphor. Mater Chem Phys 2007;101:163–9.
[19] Taylor HFW. Cement chemistry. 2nd ed. Thomas Telford; 1997.
[20] Kurzon D, Elliott L, Wang SM, Wall T, Novak F, Lucas J, et al. Dissolution of lime into synthetic coal ash slags. Fuel Process Technol 1998;56:45–53.
[21] British Standard Institute. BS EN 1305: Lightweight aggregate – Part 1: lightweight aggregates for concrete, mortar and grout; 2002.
[22] American Society for Testing and Material. ASTM C 114-03: Standard test methods for chemical analysis of hydraulic cement. Annual Book of ASTM Standards; 2003.
[23] British Standards. BS EN 1367: Test for thermal and weathering properties of aggregates – Part 3: boiling test for "Sonnenbrand" basalt; 2001.
[24] Mindess S, Young JF, Darwin D. Concrete. 2nd ed. Prentice-Hall; 2003.

3. W. Chalee, C. Jaturapitakkul, P. Chindaprasirt. Predicting the chloride penetration of fly ash concrete in seawater, Marine Structures, 22 (2009), 341-353. (IF 0.615)

Marine Structures 22 (2009) 341–353

Contents lists available at ScienceDirect

Marine Structures

journal homepage: www.elsevier.com/locate/marstruc

Review

Predicting the chloride penetration of fly ash concrete in seawater

W. Chalee [a], C. Jaturapitakkul [b,*], P. Chindaprasirt [c]

[a] Department of Civil Engineering, Faculty of Engineering, Burapha University(BUU), Chonburi 20131, Thailand
[b] Department of Civil Engineering, Faculty of Engineering, King Mongkut's University of Technology Thonburi (KMUTT), Bangkok 10140, Thailand
[c] Department of Civil Engineering, Faculty of Engineering, Khon Kaen University(KKU), Khon Kaen 40000, Thailand

ARTICLE INFO

Article history:
Received 16 March 2008
Received in revised form 24 November 2008
Accepted 5 December 2008

Keywords:
Chloride diffusion
Corrosion
Fly ash
Prediction
Seawater

ABSTRACT

In this study, a model for predicting chloride penetration in fly ash concrete under long-term exposure in a marine environment is developed. The empirical model was based on 2-, 3-, 4-, and 5-year investigation of concretes in a marine site. Regression analysis of the data was carried out by applying Fick's second law of diffusion to generate an empirical formula for predicting chloride concentration in concrete. The model uses the water to binder (W/B) ratio, fly ash content, distance from the concrete surface, and exposure time. Model validation revealed that the predicted chloride concentration levels were within a ±25% error margin ($R^2 = 0.91 - 0.99$) in the samples used to develop the model. The model was also verified using data from previous laboratory and field studies. Most predicted chloride concentration levels were within a ±30% margin of error from field samples. The model also predicted the strong effect of fly ash and W/B ratio on reducing chloride diffusion in concrete. Results clearly indicated that a high volume fly ash replacement (up to 50% by weight of binder) and a low W/B ratio will yield good chloride resistance in concrete under long-term exposure in a marine environment.

1. Introduction

New methods for designing more durable reinforced concrete structures are now required to minimize maintenance costs. By determining the causes of damage and providing appropriate

* Corresponding author. Tel.: +66 2 470 9131; fax: +66 2 427 9063.
E-mail address: chai.jat@kmutt.ac.th (C. Jaturapitakkul).

0951-8339/$ – see front matter © 2008 Elsevier Ltd. All rights reserved.
doi:10.1016/j.marstruc.2008.12.001

protection, designers will be able to create marine concrete structures with a long service life at minimal construction cost. However, concrete is destroyed by a complex combination of chemical and physical processes [1], and data from laboratory tests are insufficient to predict long-term behavior. Thus, long-term data of actual on-site marine concrete structures are needed for design and construction. Normally, the concrete is an excellent corrosion protection for reinforcing steel, but exposure to various environmental conditions during its service life may accelerate the destruction process. One well-known cause of steel corrosion in concrete is chloride. Many factors govern chloride ingress into concrete, including the type of cementitious material, water to binder (W/B) ratio, curing time, exposure period, and other physical factors. Generally, the rate of chloride ingress into concrete depends on the chloride diffusion coefficient, which varies with the length of exposure. Therefore, studies on the long-term performance of chloride ingress into concrete should incorporate the changing chloride diffusion coefficient during the exposure period.

Many studies have predicted the chloride profile in concrete over long-term exposure based on a constant chloride diffusion coefficient [2,3]. However, the chloride diffusion coefficient changes during the exposure period, decreasing with an increased length of exposure [4,5]. Thus, an appropriate prediction of a chloride diffusion profile must consider changes in the chloride diffusion coefficient over time. Moreover, the chloride diffusion profile should be based on data obtained from marine sites to represent actual concrete structures. If the chloride diffusion profile of fly ash concrete under long-term exposure in an actual marine environment can be calculated, this should reveal the behavior of chloride ingress into concrete. In turn, the results can be used to design more durable reinforced concrete structures.

2. Experimental program

2.1. Materials and specimens

The concrete mixtures were composed of ordinary Portland cement type I (ASTM C 150), class F fly ash (ASTM C 618) from Thailand ($SiO_2 + Al_2O_3 + Fe_2O_3 = 79.45\%$) with a 30-μm median particle size, graded sand, and crushed limestone with a maximum size of 19 mm. The chemical properties of fly ash and Portland cement type I are presented in Table 1. Concrete cube specimens sized $200 \times 200 \times 200\ mm^3$ were prepared and the specimens were cast using fly ash to replace Portland cement type I at 0, 15, 25, 35, and 50% by weight of binder. W/B ratios were set at 0.45, 0.55, and 0.65. Table 2 lists all concrete mix proportions and compressive strength at 28 days. After casting for 24 h, all concrete specimens were removed from the molds and then cured in water for 27 days; they were then transferred to a tidal zone marine site in Chonburi Province in the Gulf of Thailand (see Fig. 1). The air temperature at this site ranges from 25 °C to 35 °C, and the concrete specimens were exposed to two

Table 1
Chemical composition of Portland cement type I and fly ash.

Chemical composition (%)	Cement type I	Fly ash (FA)
Silicon dioxide, SiO_2	20.80	44.95
Aluminum oxide, Al_2O_3	5.50	23.70
Iron oxide, Fe_2O_3	3.16	10.80
Calcium oxide, CaO	64.97	13.80
Magnesium oxide, MgO	1.06	3.47
Sodium oxide, Na_2O	0.08	0.07
Potassium oxide, K_2O	0.55	2.38
Sulfur trioxide, SO_3	2.96	1.31
Loss on ignition, LOI	2.89	0.52
Tricalcium silicate, C_3S	56.50	–
Dicalcium silicate, C_2S	17.01	–
Tricalcium aluminate, C_3A	9.23	–
Tetracalcium aluminoferrite, C_4AF	9.62	–

Fig. 1. Concrete specimens in seawater, Chonburi Province, Thailand.

wet–dry cycles of seawater daily. Chloride and sulfate compositions in the seawater ranged from 16,000 to 18,000 ppm and from 2200 to 2600 ppm, respectively.

2.2. Experimental investigation for chloride content

After exposure to seawater for 2, 3, 4, and 5 years, concrete specimens were dry-cored to obtain a core sample 50 mm in diameter. Cores were sliced from the top surface to produce slides with a 10 mm thickness, and each slide was ground into small powdery particles. Nitric acid was added to 10 g of the ground concrete powder and the mixture was heated on a hot plate for 3 min; this process ensures the digestion of chloride from the concrete powder sample. The sample was allowed to cool and then filtered to obtain the solution state. Auto-titration equipment was used to test this filtrate for chloride content, which determined the total chloride content of the concrete in accordance with ASTM C1152 [6]. Chloride content was plotted against the distance from the top surface of the concrete to present the chloride diffusion profile in concrete.

3. Model formulation

In this study the experimental data were used to generate a model for predicting the chloride diffusion profile of concrete in a marine environment by applying Fick's second law [7] as shown in Eq. (1):

$$\frac{\partial C}{\partial t} = D_c \frac{\partial^2 c}{\partial x^2} \tag{1}$$

The chloride diffusion model in this study was developed based on the experimental data gathered from the practice site. Controlling all parameters that affect the chloride diffusion of concrete in a field site (e.g., temperature, humidity, abrasion–erosion damage) is difficult, and thus some studies have suggested simulating a chloride diffusion profile by fitting Fick's second law, which can be used efficiently on data obtained at a field site [4,8]. Since this equation provides the best fit with the behavior of a chloride diffusion profile, it is concluded that Eq. (1) is appropriate when developing a chloride diffusion model based on an actual field environment.

As discussed above, a model for predicting a chloride penetration profile over long-term exposure must incorporate the changing chloride diffusion coefficient (D_c) over time. Since a change in D_c at any time has a considerable effect on the penetration rate of chloride in marine concrete [9], predictions of

such a long-term chloride penetration profile must incorporate a time-dependent D_c into Fick's second law. According to Mangat and Limbachiya [5], the relationship between D_c and exposure time can be approximated by an empirical relationship in the form of an inverse exponential function. The principle of this relationship can be applied to generate Eq. (2):

$$D_c = (t)^{-\beta} \tag{2}$$

Substituting D_c into Eq. (1),

$$\frac{\partial C}{\partial t} = t^{-\beta}\frac{\partial^2 c}{\partial x^2} \tag{3}$$

a general solution for Eq. (3) can be given as

$$C_{x,t} = C_0\left[1 - \mathrm{erf}\left(\frac{x}{2\sqrt{\frac{t^{(1-\beta)}}{(1-\beta)}}}\right)\right]. \tag{4}$$

In Eq. (4), concrete exposure time (t) is in units of seconds. When this equation is used for long-term prediction, the exposure time should be converted into units of years. With this alteration, Eq. (4) becomes Eq. (5):

$$C_{x,t} = C_0\left[1 - \mathrm{erf}\left(\frac{x}{2\sqrt{\frac{(31{,}536{,}000t)^{(1-\beta)}}{(1-\beta)}}}\right)\right], \tag{5}$$

where $C_{x,t}$ = total chloride concentration (% by weight of binder) at position x and exposure time t, t = exposure time (years), x = distance from the concrete surface (mm), C_0 = chloride concentration at the concrete surface (% by weight of binder) at exposure time t, β = empirical coefficient, erf = error function.

In Eq. (5), $C_{x,t}$ is determined by evaluating the β and C_0 values using the best fit of chloride penetration profile curves. Fig. 2 shows how Eq. (5) provides the best fit to experimental data for a chloride penetration profile of concrete with a W/B ratio of 0.65 obtained from the actual marine site. Regression analysis yielded the empirical coefficient (β) and the chloride concentration at concrete surface (C_0) for concrete with W/B ratios of 0.65 at 2-, 3-, 4-, and 5-year exposures to the tidal zone of marine environment in Thailand. Using the same procedure, β and C_0 of the other concrete mixtures ($W/B = 0.45$ and 0.55) at a given exposure time can be determined, as shown in Tables 2 and 3, respectively. Table 3 shows that β values for a specific mix proportion do not change with time, so a prediction of β can be interpolated in terms of fly ash replacement and the W/B ratio by plotting β values against fly ash content. Therefore, β values can be generated using Eq. (6):

$$\beta = \delta(F) + \phi \tag{6}$$

where δ and φ are the empirical coefficients in terms of the W/B ratio obtained from the regression technique shown below:

$$\delta = -0.0015(W/B) + 0.0034 \tag{7}$$

$$\phi = -0.175(W/B) + 0.840 \tag{8}$$

Substituting Eqs. (7) and (8) into Eq. (6),

$$\beta = [-0.0015(W/B) + 0.0034]\,(F) + [-0.175(W/B) + 0.840] \tag{9}$$

where F = fly ash replacement (%), W/B = water to binder ratio.

Equation (9) can be used to calculate the value of β for fly ash replacement up to 50% by weight of binder and W/B ratios ranging from 0.45 to 0.65.

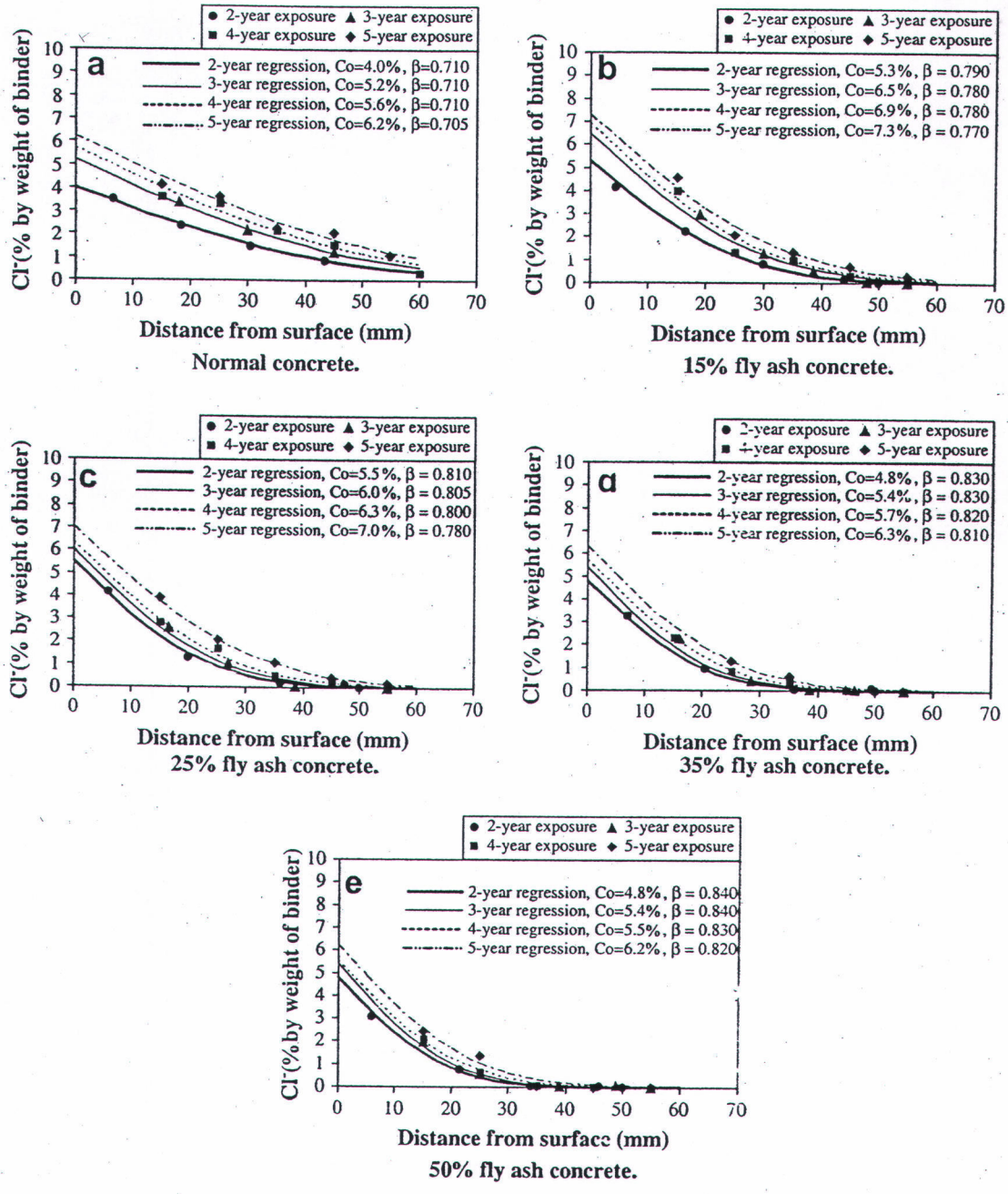

Fig. 2. Chloride penetration profiles for concrete with *W/B* ratio of 0.65 at 2-, 3-, 4-, and 5-year exposures in a tidal zone of marine environment in Thailand.

Table 4 lists chloride concentrations at the concrete surface (C_o), which are used to generate the model for predicting C_o over long-term exposure. In this model, C_o values are not related to fly ash replacement, so it is decided to generate the predictive function in terms of exposure time (t) and the *W/B* ratio. The average C_o values with *W/B* ratios of 0.45, 0.55, and 0.65 at 2-, 3-, 4-, and 5-year exposure periods was generated by plotting the average C_o versus exposure time (see Fig. 3), and expressed this as a logarithm function:

$$C_o = \alpha \ln(t) + \gamma \tag{10}$$

where α and γ are empirical coefficients in terms of the *W/B* ratio obtained from a regression analysis of the empirical data as shown below:

Table 2
Concrete mixture proportions and compressive strength at 28 days.

Mix	Concrete mixture proportions (kg/m³)					W/B ratio	Compressive strength at 28 days (MPa)
	Cement	Fly ash	Fine aggregate	Coarse aggregate	Water		
I45	478	–	639	1024	215	0.45	50.4
I45FA15	406	72	639	1024	215	0.45	47.4
I45FA25	359	119	639	990	215	0.45	45.2
I45FA35	311	167	639	977	215	0.45	45.0
I45FA50	239	239	639	957	215	0.45	33.8
I55	478	–	639	971	262	0.55	37.0
I55FA15	406	72	639	948	262	0.55	32.0
I55FA25	359	119	639	933	262	0.55	30.3
I55FA35	311	167	639	918	262	0.55	32.7
I55FA50	239	239	639	897	262	0.55	20.9
I65	478	–	639	922	311	0.65	29.0
I65FA15	406	72	639	898	311	0.65	19.9
I65FA25	359	119	639	881	311	0.65	21.0
I65FA35	311	167	639	864	311	0.65	22.9
I65FA50	239	239	639	840	311	0.65	16.6

$$\alpha = -0.379(W/B) + 2.064 \tag{11}$$

$$\gamma = 4.078(W/B) + 1.011 \tag{12}$$

Substituting Eqs. (11) and (12) into Eq. (10),

$$C_o = [-0.379(W/B) + 2.064]\ln(t) + [4.078(W/B) + 1.011], \tag{13}$$

where C_o = chloride concentration at the concrete surface at time t (% by weight of binder), t = exposure time (years), W/B = water to binder ratio.

Equation (13) can predict the chloride concentration at the concrete surface (C_o) for W/B ratios ranging from 0.45 to 0.65 and for exposure to a marine environment beyond 2 years. Thus, chloride concentration can be predicted over a long-term exposure to a marine environment by substituting β from Eq. (9) and C_o from Eq. (13) into Eq. (5).

The model [Eq. (5)] was developed based on experimental data collected from the marine test site and from regression analyses. The chloride concentration in fly ash concrete is a function of several

Table 3
Empirical coefficient β.

Mix no.	Empirical coefficient, β				Average β
	2-year exposure	3-year exposure	4-year exposure	5-year exposure	
I45	0.769	0.760	0.755	0.740	0.756
I45FA15	0.83	0.820	0.820	0.810	0.820
I45FA25	0.835	0.835	0.830	0.825	0.831
I45FA35	0.835	0.840	0.840	0.840	0.839
I45FA50	0.930	0.920	0.890	0.880	0.905
I55	0.750	0.735	0.735	0.735	0.739
I55FA15	0.820	0.795	0.790	0.790	0.799
I55FA25	0.830	0.820	0.815	0.800	0.816
I55FA35	0.835	0.830	0.820	0.800	0.821
I55FA50	0.910	0.920	0.900	0.890	0.905
I65	0.710	0.710	0.710	0.705	0.709
I65FA15	0.790	0.780	0.780	0.770	0.780
I65FA25	0.810	0.805	0.800	0.780	0.799
I65FA35	0.830	0.830	0.820	0.810	0.823
I65FA50	0.840	0.840	0.830	0.820	0.833

Table 4
Chloride concentration at concrete surface (C_o).

Mix no.	Chloride concentration at concrete surface, C_o (% by weight of binder)				Average C_o (% by weight of binder)			
	2-year exposure	3-year exposure	4-year exposure	5-year exposure	2-year exposure	3-year exposure	4-year exposure	5-year exposure
I45	3.5	5.0	5.5	6.4	4.2	4.8	5.2	6.0
I45FA15	4.8	5.5	5.8	6.3				
I45FA25	4.6	5.1	5.7	6.5				
I45FA35	4.1	4.3	4.5	5.5				
I45FA50	4.0	4.3	4.7	5.4				
I55	4.0	4.7	5.0	6.0	4.6	5.4	5.8	6.4
I55FA15	4.6	5.6	6.0	6.8				
I55FA25	5.2	5.4	5.5	6.3				
I55FA35	4.8	5.5	6.0	6.4				
I55FA50	4.6	5.6	6.4	6.6				
I65	4.0	5.2	5.6	6.2	4.9	5.7	6.0	6.6
I65FA15	5.3	6.5	6.9	7.3				
I65FA25	5.5	6.0	6.3	7.0				
I65FA35	4.8	5.4	5.7	6.3				
I65FA50	4.8	5.4	5.5	6.2				

parameters, including distance from the concrete surface (x), the W/B ratio, exposure time (t), and fly ash replacement (F). The model can predict the chloride concentration in fly ash concrete at any depth and at any exposure time within a marine environment. The environmental conditions are considered in the two wet–dry cycles of seawater daily, air temperature ranges from 25 °C to 35 °C, chloride and sulfate compositions in the seawater ranged from 16,000 to 18,000 ppm and from 2200 to 2600 ppm, respectively. However, the model has a limited application because it only uses one-dimensional chloride dispersion. The model was constructed using chloride penetration profiles obtained from dry-cored concrete cube specimens, and thus one-dimensional chloride ingress from the outer surface to the inner concrete yields good results.

4. Model validation

4.1. Comparison to experimental data

The empirical model was validated by using experimental data collected from samples in the Thai marine environment. Fig. 4 presents the predicted curves of chloride penetration profiles derived from

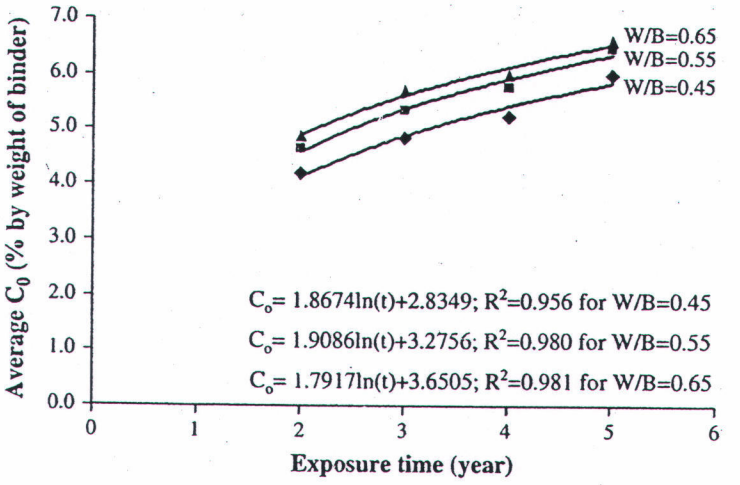

Fig. 3. Relationships between the average chloride concentration at the concrete surface and exposure time in a tidal zone of marine environment in Thailand.

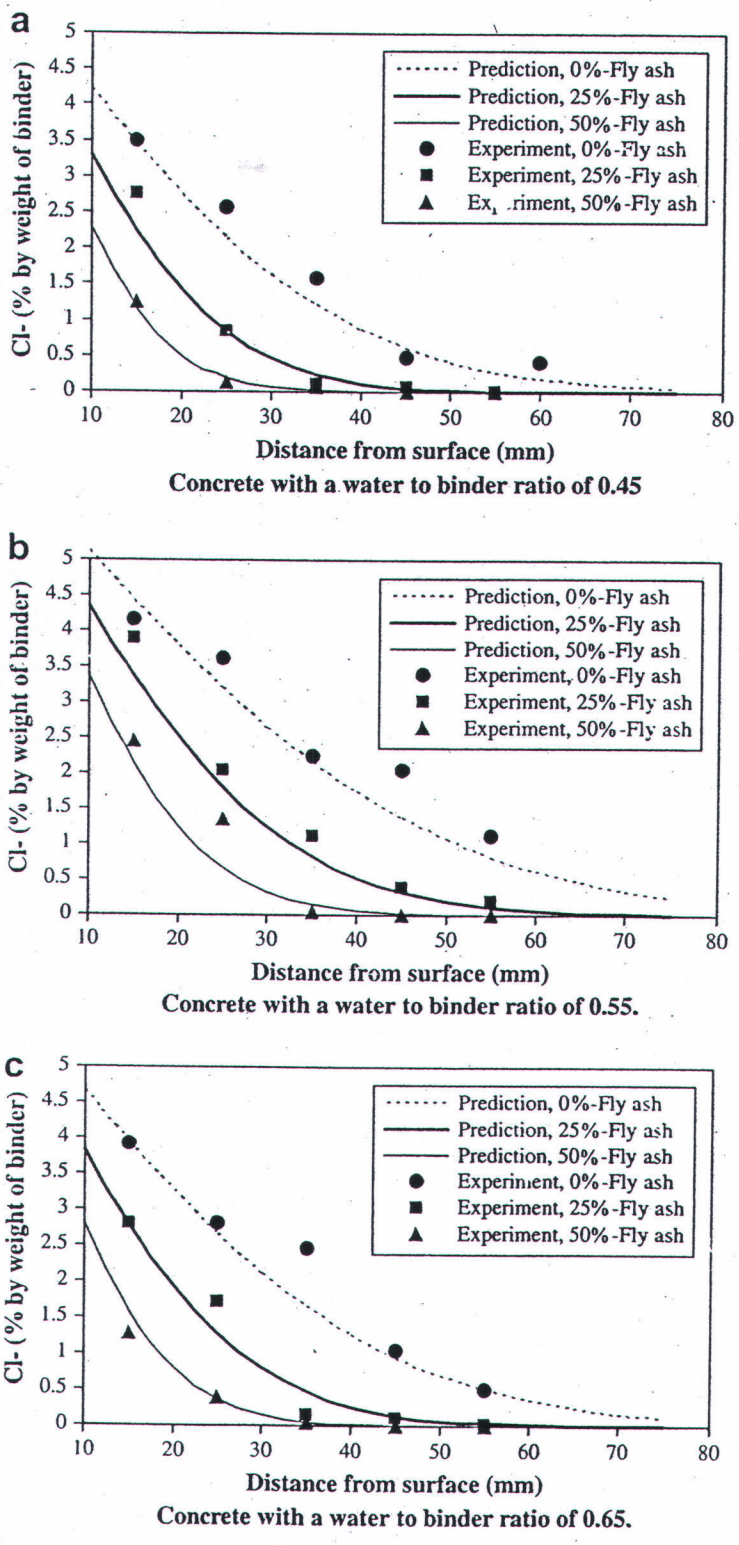

Fig. 4. Comparison of the predicted and experimental chloride penetration profiles of concrete exposed to a marine environment in Thailand for 5 years.

the empirical model that were plotted with actual experimental data at a 5-year exposure. Most experimental data fit well with the predicted curve. Fig. 5 shows the relationship between the predicted and experimental chloride concentrations at 15, 25, 35, and 45 mm concrete depths with *W/B* ratios of 0.45, 0.55, and 0.65 at 4- and 5-year exposures. Most of the data are below the line of equality, so the estimated chloride concentration at all depths was lower than the experimental results. However, most estimates were within a ±25% margin of error based on the test data ($R^2 = 0.91 - 0.99$), especially for chloride concentrations of more than 0.5% by weight of binder. Although most of the data with the chloride concentration lower than 0.5% by weight of binder lie out of this interval, this does not significantly affect the predicted values. Even though very low chloride concentrations yielded high percentages of error, the predicted chloride concentrations differed minimally from the actual data. For example, the model predicted a chloride concentration of 0.2% by weight of binder, while the actual experimental data revealed a concentration of 0.1% on the same basis at the same depth of concrete. In this case, the prediction error was as high as 50%, but the predicted chloride concentration only differed by 0.1% by weight of binder. A chloride content of 0.1% or 0.2% by weight of binder in concrete will not result in a significantly different corrosion in reinforcing steel. Therefore, predictions using the empirical model are reasonably accurate compared to experimental data.

4.2. Comparison to other experimental results

We compared the model's predictions to experimental results obtained from Thomas and Matthews [4], Castro et al. [10], Mcpolin et al. [11], and Mohammed et al. [12]. Thomas carried out an experiment using concrete exposed for 10 years under an English tidal zone BRE marine site with chloride and sulfate compositions of 18,200 ppm and 2600 ppm, respectively. The major chemical compositions of seawater at that site did not differ greatly from those in the Gulf of Thailand, but other physical factors (such as temperature, humidity, and abrasion–erosion) did. In 2005, Castro et al. [10] published a chloride profile of normal concrete with a *W/B* ratio of 0.50 under 24- and 45-month exposures in a Mexican marine site that varied greatly in humidity and temperature from 60% to 95% and 20 °C to 30 °C, respectively. Mcpolin et al. [11] conducted a laboratory investigation of chloride content in concrete specimens at 2-, 3-, and 4-year exposures in 0.55 M NaCl (3.2% by weight). These specimens were exposed to the solution for 24 h and then removed to dry for 6 days before being reimmersed. Throughout, Mohammed et al. [12] reported chloride content in cement concrete under 30-year exposure in marine environment. In this investigation, the specimens were exposed to 5 h of wetting and seven hours of drying cycle. The average temperature of seawater is about 8 °C to 24 °C with

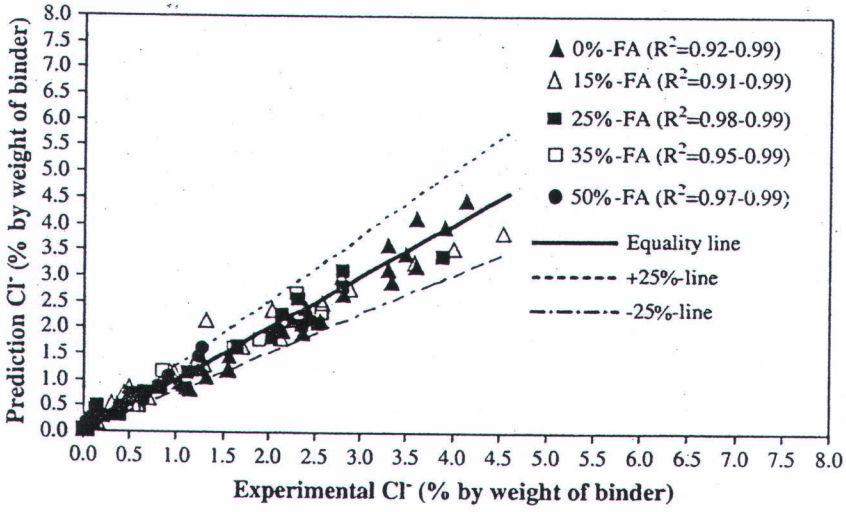

Fig. 5. Comparison of the predicted and experimental results of chloride concentrations at 15, 25, 35, and 45 mm depth in concrete with *W/B* ratios of 0.45, 0.55, and 0.65 under 4- and 5-year exposures to a marine environment.

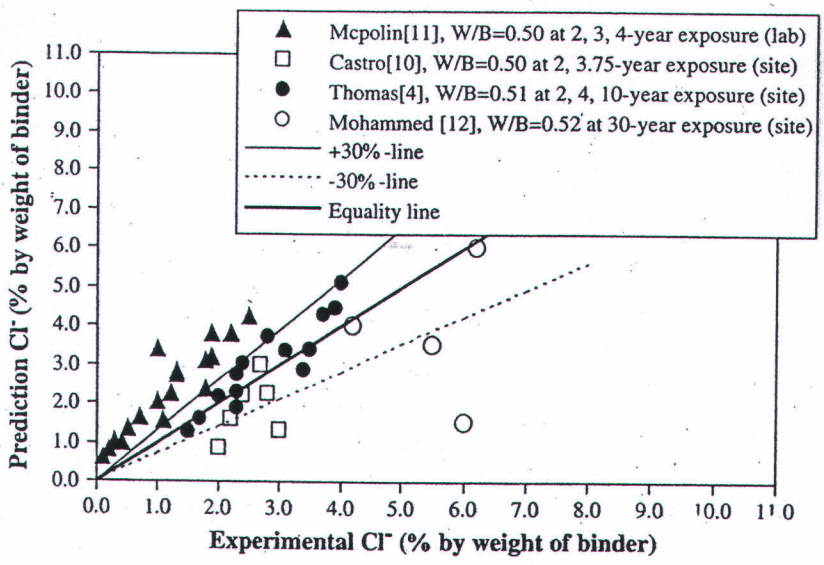

Fig. 6. Comparison of the predicted and experimental results of chloride concentrations based on data from Thomas and Matthews [4], Castro et al. [10], Mcpolin et al. [11] and Mohammed et al. [12].

chloride and sulfate compositions of 17,136 ppm and 2412 ppm, respectively. We compared these experimental data with the results obtained from our proposed model (see Fig. 6).

Fig. 6 indicates that Mcpolin's [11] data are above the line of equality; thus, compared to those results, our proposed model overestimated the chloride concentration. However, most of Thomas's [4], Castro's [10] and Mohammed's [12] data are within a ±30% margin of error, and Thomas's [4] data are between Mcpolin's [11] and Castro's [10]. All Mohammed's data are below the line of equality, it presents the lower estimate of chloride content in cement concrete as compared with the tested results. Note that data obtained from marine sites differ from laboratory data. The data from both marine sites were similar to the results obtained from the proposed model, while laboratory tests produced lower chloride ingress than the predicted results. This is likely caused by the physical impact of an actual marine environment, which damages concrete. Therefore, the results indicate that durability testing in a laboratory setting (which can easily control many factors) may not sufficiently mimic an actual marine environment. Fig. 7 compares the chloride penetration profiles for 30% fly ash concrete from the proposed model and experimental results obtained from Thomas and Matthews [4].

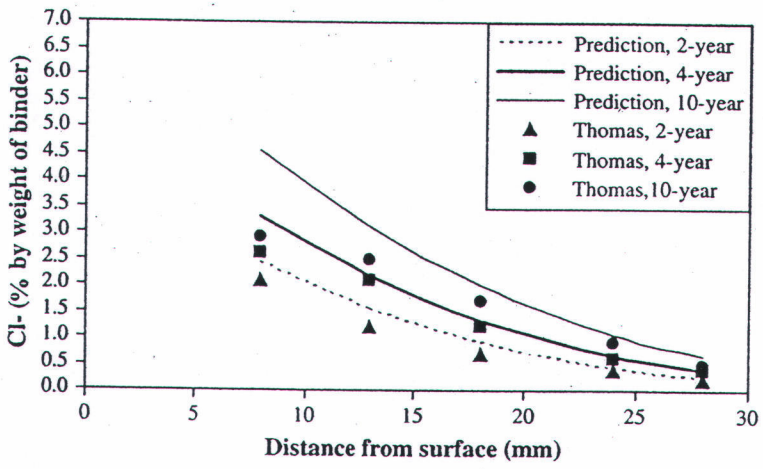

Fig. 7. Comparison of the predicted and experimental results of chloride penetration profiles of 30% fly ash concrete with *W/B* ratio of 0.45 based on data from Thomas and Matthews [4] under 2-, 4-, and 10-year exposures in a marine environment.

The experimental results fit well with the predicted curves, especially at deeper concrete covering depths. These comparisons demonstrate that the proposed model is reasonable for predicting chloride penetration profiles in fly ash concrete at tidal zones of a marine environment. This validation was based on experimental data over a 10-year exposure period. However, the model will require further validation using experimental data over longer exposure periods and various exposure zones. Because of limited information in the literature, the existing experimental data are insufficient to confirm this model. As a starting point, this empirical model can be used to efficiently predict long-term chloride diffusion in cement concrete as well as in fly ash concrete.

5. Practical uses of the proposed model

Generally, a chloride penetration profile presents the chloride concentration at any depth of concrete. If a chloride penetration profile can be estimated at any exposure time, it will enable estimation of initial corrosion and the deterioration of reinforcing steel after this initial period. Fig. 8 shows predicted chloride concentrations for 20- and 50-year exposures at any depth of concrete with a *W/B* ratio of 0.50. The predicted chloride concentration in 30% fly ash concrete over a 30-year period (from 20- to 50-year exposures) changed less than in cement concrete; these changes correspond reasonably to the actual behavior of chloride ingress because concrete containing fly ash is more resistant to chloride and has a smaller pore size than concrete without fly ash [13–16]. Fig. 9 shows estimated chloride concentrations at a 40 mm concrete covering depth at any time of exposure up to 60 years in concrete with a *W/B* ratio of 0.50. According to this prediction, the highest chloride content will appear in concrete without fly ash, and the chloride content decreases with increased fly ash replacement in concrete. Throughout the experiment, cement concrete had the highest rate of chloride buildup at this covering depth, about 0.04% by weight of binder per year, while the use of fly ash in concrete (up to 40% on the same basis) clearly reduced the rate of chloride buildup from 0.04 to 0.003% by weight of binder per year.

Fig. 10 shows the time to initial corrosion of fly ash concrete for a covering depth of 40 mm. This estimate was based on the proposed model and threshold chloride levels reported in several studies (Threshold chloride values of 0.9%, 0.6%, 0.4% and 0.3% for 0%, 15%, 25% and 35% fly ash concretes, respectively) [17,18]. The use of fly ash to replace Portland cement in concrete can extend the time to initial corrosion. In addition, a lower *W/B* ratio clearly resulted in superior corrosion resistance due to the low permeability of concrete. Thus, the most effective way to reduce chloride penetration is to decrease the *W/B* ratio and increase the fly ash replacement in concrete. While a high volume of fly ash can greatly improve chloride resistance of concrete, it can also negatively affect some mechanical properties, for example, cause low compressive strength at an early age [19,20]. These mechanical

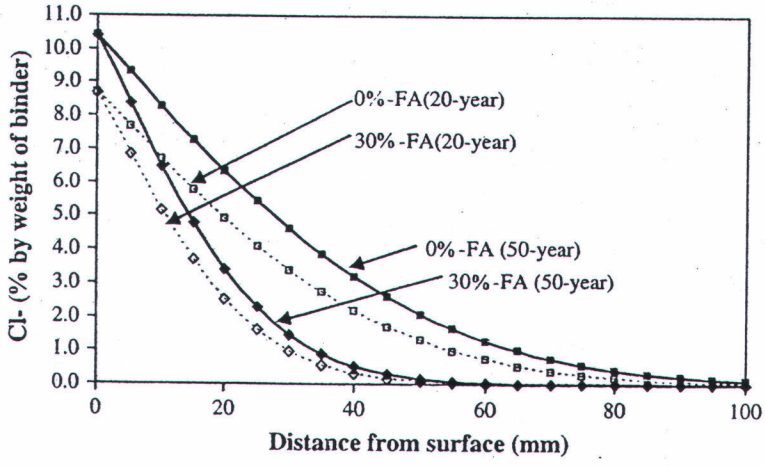

Fig. 8. Predicted chloride penetration profiles in fly ash concrete with *W/B* ratio of 0.50 and exposed to a marine environment for 20 and 50 years based on the proposed model.

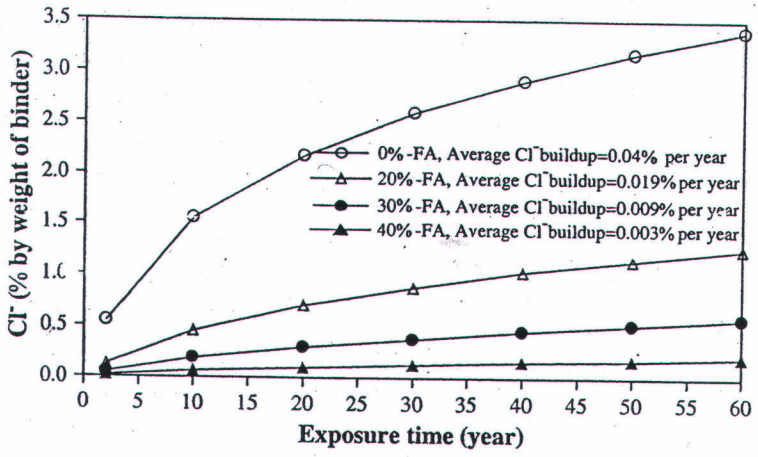

Fig. 9. Estimated chloride concentration in fly ash concrete at a covering depth of 40 mm with *W/B* ratio of 0.50 based on the proposed model.

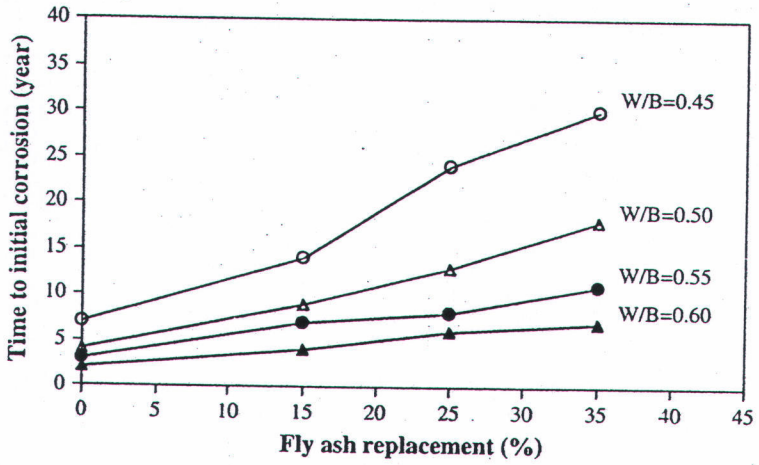

Fig. 10. Estimated time to initial corrosion of fly ash concrete at a covering depth of 40 mm based on the proposed model.

properties also influence the rate of corrosion and the service life of reinforced concrete structures under loading conditions. Therefore, increasing the durability of reinforced concrete structures in a marine environment requires not only incorporating resistance to chloride ingress, but also maintaining other properties of concrete such as the compressive strength, permeability, and abrasion–erosion resistance.

6. Conclusion

In this study a model for predicting chloride diffusion in cement and fly ash concretes under long-term marine exposure in the Gulf of Thailand is proposed. The model can predict chloride concentration at any depth of cement and fly ash concretes in a marine environment at any exposure period longer than 2 years. Accurate results could be obtained for concrete with *W/B* ratios from 0.45 to 0.65 and fly ash replacement from 0 to 50%. The model's application, however, is limited because it only produces a one-dimensional ingress of chloride into a reinforced concrete structure. The results indicated that both fly ash and *W/B* ratio strongly affected chloride diffusion in concrete; higher fly ash replacement and lower *W/B* ratios clearly produced better chloride resistance in concrete under a marine environment.

Acknowledgments

The authors gratefully acknowledge financial supports from the Research and Development Funds, Faculty of Engineering, Burapha University, Thailand contact No. 74/2551 and the Thailand Research Fund (TRF) under TRF Senior Research Scholar, contract No. RTA5080020 and from the Commission on Higher Education, Ministry of Education, Thailand.

References

[1] Rabiah AR, Rasheeduzzafar, Baggott R. Durability requirements for reinforced concrete construction in aggressive marine environments. Mar Struct 1990;3:285–300.
[2] Arora P, Popov BN, Haran B, Ramasubramanian M, Popova S, White RE. Corrosion initiation time of steel reinforcement in a chloride environment-a one dimensional solution. Corrosion Sci 1997;39:739–59.
[3] Jung Woo-Yong, Yoon Young-Soo, Sohn Young-Moo. Predicting the remaining service life of land concrete by steel corrosion. Cement Concr Res 2003;33:663–77.
[4] Thomas MDA, Matthews JD. Performance of pfa concrete in a marine environment-10-year results. Cement Concr Res 2004;26:5–20.
[5] Mangat PS, Limbachiya MC. Effect of initial curing on chloride diffusion in concrete repair materials. Cement Concr Res 1999;29:1475–85.
[6] ASTM. Standard test method for acid-soluble chloride in mortar and concrete, C1152. In: Annual book of ASTM standards. vol. 04.01; 1997; p. 627–9.
[7] Crank J. The mathematic of diffusion. 2nd ed. London: Oxford Press; 1975.
[8] Tanaka Y, Kawano H, Watanabe H, Nakajo T. Study on required cover depth of concrete highway bridges in coastal environment. Seventeenth U.S.–Japan bridge engineering workshop. Tsukuba; 2001; p. 1–16.
[9] Diaz B, Novoa XR, Perez MC. Study of the chloride diffusion in mortar: a new method of determining diffusion coefficients based on impedance measurements. Cement Concr Comp 2006;28:237–45.
[10] Castro P, De Rincon CT, Pazini EJ. Interpretation of chloride profiles from concrete exposed to tropical marine environments. Cement Concr Res 2001;31:529–37.
[11] McPolin D, Basheer PAM, Long AE, Grattan KTV, Sun T. Obtaining progressive chloride profiles in cementitious materials. Constr Build Mater 2005;19:666–73.
[12] Mohammed TU, Hamada H, Yamaji T. Marine durability of 30-year old concrete made with different. J Adv Concr Technol 2003;01:63–75.
[13] Chindaprasirt P, Jaturapitakkul C, Sinsiri T. Effect of fly ash fineness on compressive strength and pore size of blended cement paste. Cement Concr Comp 2005;27:425–8.
[14] Bai J, Wild S, Sabir BB. Chloride ingress and strength loss in concrete with different PC-PFA-MK binder compositions exposed to synthetic seawater. Cement Concr Res 2003;33:353–62.
[15] Sujjavanich S, Sida V, Suwanvitaya P. Chloride permeability and corrosion risk of high volume fly ash concrete with mid-range water reducer. ACI Mater J 2005;102:177–82.
[16] Sengul O, Tasdemir C, Tasdemir AT. Mechanical properties and rapid chloride permeability of concrete with ground fly ash. ACI Mater J 2005;102:414–21.
[17] Thomas MDA. Chloride threshold in marine concrete. Cement Concr Res 1996;26:513–9.
[18] Chalee W, Teekavanit M, Kiattikomol K, Siripanichgorn A, Jaturapitakkul C. Effect of W/C ratio on covering depth of fly ash concrete in marine environment. Constr Build Mater 2007;21:965–71.
[19] Jaturapitakkul C, Kiattikomol K, Sata V, Leekeeratikul T. Use of ground coarse fly ash as a replacement of condensed silica fume in producing high-strength concrete. Cement Concr Res 2004;34:549–55.
[20] Kiattikomol K, Jaturapitakkul C, Songpiriyakij S, Chutubtim S. A study of ground coarse fly ashes with different finenesses from various sources as pozzolanic materials. Cement Concr Comp 2001;23:335–43.

4. W. Chalee, C. Jaturapitakkul. Effects of W/B ratios and fly ash finenesses on chloride diffusion coefficient of concrete in marine environment, Materials and Structures, 42 (2009), 505-514. (IF 0.892)

Materials and Structures (2009) 42:505–514
DOI 10.1617/s11527-008-9398-2

ORIGINAL ARTICLE

Effects of W/B ratios and fly ash finenesses on chloride diffusion coefficient of concrete in marine environment

W. Chalee · C. Jaturapitakkul

Received: 30 October 2007 / Accepted: 16 June 2008 / Published online: 1 July 2008

Abstract The objectives of this investigation were to study the effect of W/B ratios and fly ash finenesses on chloride diffusion coefficient (D_c) of concrete under marine environment. Original and classified fly ashes were used as a partial replacement of Portland cement type I at 0%, 15%, 25%, 35%, and 50% by weight of binder. Water to binder ratios (W/B) were varied as 0.45, 0.55, and 0.65. Concrete cube specimens of 200 mm were cast and removed from the molds after casting 1 day and then cured in fresh water for 27 days. After that, the specimens were placed to the tidal zone of marine environment in the Gulf of Thailand. Subsequently, the specimens were tested for chloride penetration profile after being exposed to the tidal zone for 2, 3, 4, and 5 years. The regression analysis of investigated data was carried out and Fick's second law of diffusion was applied to calculate the chloride diffusion coefficient (D_c) and chloride concentration at concrete surface (C_o) based on one-dimensional analysis. The results showed that D_c of all concrete mixtures decreased with an exposure time and the decrease of W/B ratio resulted in the decrease of D_c. When the W/B ratio of concrete was reduced, the decrease of D_c in cement concrete was higher than that of the fly ash concrete. The use of fly ash with high fineness clearly reduced the rate of chloride ingress into concrete. In addition, fly ash with high fineness has more effective on reducing of D_c in concrete with higher W/B ratio than that with lower W/B ratio.

Keywords Chloride diffusion · W/B ratio · Finenesses · Fly ash · Marine environment

W. Chalee
Department of Civil Engineering, Faculty of Engineering, Burapha University, Chonburi, Thailand

C. Jaturapitakkul (✉)
Department of Civil Engineering, Faculty of Engineering, King Mongkut's University of Technology Thonburi (KMUTT), Bangkok 10140, Thailand
e-mail: chai.jat@kmutt.ac.th

1 Introduction

Chloride penetration into concrete is a main cause of the corrosion of steel in reinforced concrete under marine environment. The level of corrosion in reinforcing steel is primarily based on the penetration of chloride ions to the steel surface. Generally, a study of chloride attack in reinforced concrete structure is emphasized on the corrosion at the initial state which causes by a threshold chloride level. In particular, a threshold chloride presented in term of the level of chloride concentration required to initiate the corrosion of reinforcing steel. This chloride concentration has led to the finding of sufficient concrete covering and time to start the initial corrosion of steel under marine environment. In

addition, a high rate of chloride ingress into concrete significantly leads to a short period of initial corrosion. The penetration rate of chloride ingress into concrete depends on the diffusion coefficient since a higher rate causes a higher diffusion coefficient.

In general, Fick's law of diffusion is popular to be used to simulate the transportation of chloride into concrete. The applying of Fick's law to fit curve with the chloride penetration profile yields the diffusion coefficient and chloride concentration at concrete surface. Most of researchers investigated the chloride diffusion coefficient based on electrical techniques because the testing time can be reduced by the accelerative diffusion of chloride into concrete under the action of an electric filed [1–4]. This method has some disadvantage because it cannot present the actual diffusion of chloride into concrete. In addition, some researchers also investigated the chloride diffusion coefficient based on the diffusion from laboratory [5–7]. However, the results from laboratory cannot present the actual behavior of chloride ingress from marine site because all physical influences such as abrasion, temperature, moisture etc. cannot be simulated in the laboratory. In 2004, Thomas and Matthews [8] had published the chloride diffusion coefficient of concrete in the practice site of England. In fact, D_c is changing with time and the simulation of chloride ingress into concrete for long term exposure should consider together with the changing of D_c. However, most researchers suggested a constant value of D_c with a specific exposure time for supporting the design of marine concrete structures [9, 10]. Throughout, the acceptable chloride diffusion coefficient should be determined based on the actual exposure from marine environment because it will present the real case of concrete structure. The objectives of this investigation are to study the effect of W/B ratios and fly ash finenesses on chloride diffusion coefficient of concrete under practice site of marine environment.

2 Experimental program

2.1 Materials

Portland cement type I and fly ash obtained from Mae Moh power plant in Thailand, graded sand, and crushed limestone with maximum size of 19 mm were used in this study for casting concrete.

The original fly ash (fly ash as received from the power plant) had the median particle size of 30.6 μm, and then was classified by an air classifier to have median particle size of 9.7 μm. For chemical compositions, the sums of SiO_2, Al_2O_3, and Fe_2O_3 in original and classified fly ashes were 79.45% and 78.47%, respectively, indicating the class F fly ash in accordance with ASTM C 618. It was also concluded that the chemical compositions of classified fly ash were not different from those of the original fly ash.

2.2 Specimens

Concrete cube specimens of 200 mm were prepared. Fly ash concretes were cast by using original and classified fly ashes to replace Portland cement type I at percentages of 0, 15, 25, 35, and 50 by weight of binder. Water to binder ratios (W/B) of concretes were varied as 0.45, 0.55, and 0.65. The mix proportions of all concretes are shown in Table 1. The specimens were demoulded after 1 day of casting and then cured in water for 27 days. After that, they were transferred to the tidal zone of the marine site in Chonburi, Thailand. Normally, the temperature at this site is between 25 and 35°C. Chloride and sulfate compositions in the sea water are ranging from 16,000 to 18,000 mg/l and 2,200 to 2,600 mg/l, respectively. The concretes were tested to determine the chloride penetration profile after being exposed to sea water in wet-dry condition for 2, 3, 4, and 5 years.

2.3 Tested program

After exposure period of 2, 3, 4, and 5 years in the marine site, the concrete sample was dry-cored to obtain a cored concrete with 50-mm in diameter at the center of the cube specimen. The cored sample was cut from surface having each slide of 10-mm thickness then each slide of the concrete was ground into fine particles. The powder sample was used to test for chloride content by auto titration equipment in order to determine the total chloride content in concrete, in accordance with ASTM C1152 [11]. The chloride content was plotted against the distance from the top surface, presenting the total chloride diffusion profile in concrete. The details and results of this investigation can be found from [12].

Table 1 Mixture proportions of concretes

Mix	Mixture proportions of concretes (kg/m^3)						W/B
	Cement	Original fly ash	Classified fly ash	Fine aggregate	Coarse aggregate	Water	
I45	478	–	–	639	1,024	215	0.45
I55	478	–	–	639	971	262	0.55
I65	478	–	–	639	922	311	0.65
I45O15	406	72	–	639	1,004	215	0.45
I45O25	359	119	–	639	990	215	0.45
I45O35	311	167	–	639	977	215	0.45
I45O50	239	239	–	639	957	215	0.45
I55O15	406	72	–	639	948	262	0.55
I55O25	359	119	–	639	933	262	0.55
I55O35	311	167	–	639	918	262	0.55
I55O50	239	239	–	639	897	262	0.55
I65O15	406	72	–	639	898	311	0.65
I65O25	359	119	–	639	881	311	0.65
I65O35	311	167	–	639	864	311	0.65
I65O50	239	239	–	639	840	311	0.65
I45F15	406	–	72	639	1,004	215	0.45
I45F25	359	–	119	639	990	215	0.45
I45F35	311	–	167	639	977	215	0.45
I45F50	239	–	239	639	957	215	0.45
I55F15	406	–	72	639	948	262	0.55
I55F25	359	–	119	639	933	262	0.55
I55F35	311	–	167	639	918	262	0.55
I55F50	239	–	239	639	897	262	0.55
I65F15	406	–	72	639	898	311	0.65
I65F25	359	–	119	639	881	311	0.65
I65F35	311	–	167	639	864	311	0.65
I65F50	239	–	239	639	840	311	0.65

3 Calculation of chloride diffusion coefficient (D_c)

In this paper, D_c was evaluated based on Fick's second law of diffusion as given by Eq. 1 [13]

$$\frac{\partial C}{\partial t} = D_c \frac{\partial^2 c}{\partial x^2}. \quad (1)$$

If D_c in this equation is a constant value at a specific exposure time, a general solution of Eq. 1 is given in Eq. 2

$$C_{x,t} = C_o\left[1 - erf\left(\frac{x}{2\sqrt{D_c t}}\right)\right] \quad (2)$$

where $C_{x,t}$ is the total chloride concentration (% by weight of binder) at the position x and exposure time t; x the distance from concrete surface (mm); t the exposure time (s); C_o the chloride concentration at concrete surface (% by weight of binder) at exposure time t; D_c the diffusion coefficient (mm^2/s) at exposure time t; and erf the error function.

The general solution in Eq. 2 provides the chloride concentration at any depth and at any exposure time under the constant values of D_c and C_o. Thus, the value of D_c by this equation can only be obtained when the value of D_c is a constant at a specific exposure time. In order to obtain the value of C_o, the chloride profile has to be extrapolated at x = 0.

The determination of D_c can be evaluated by fitting the Fick's second law on the chloride penetration profile from experiment. Figure 1 shows the

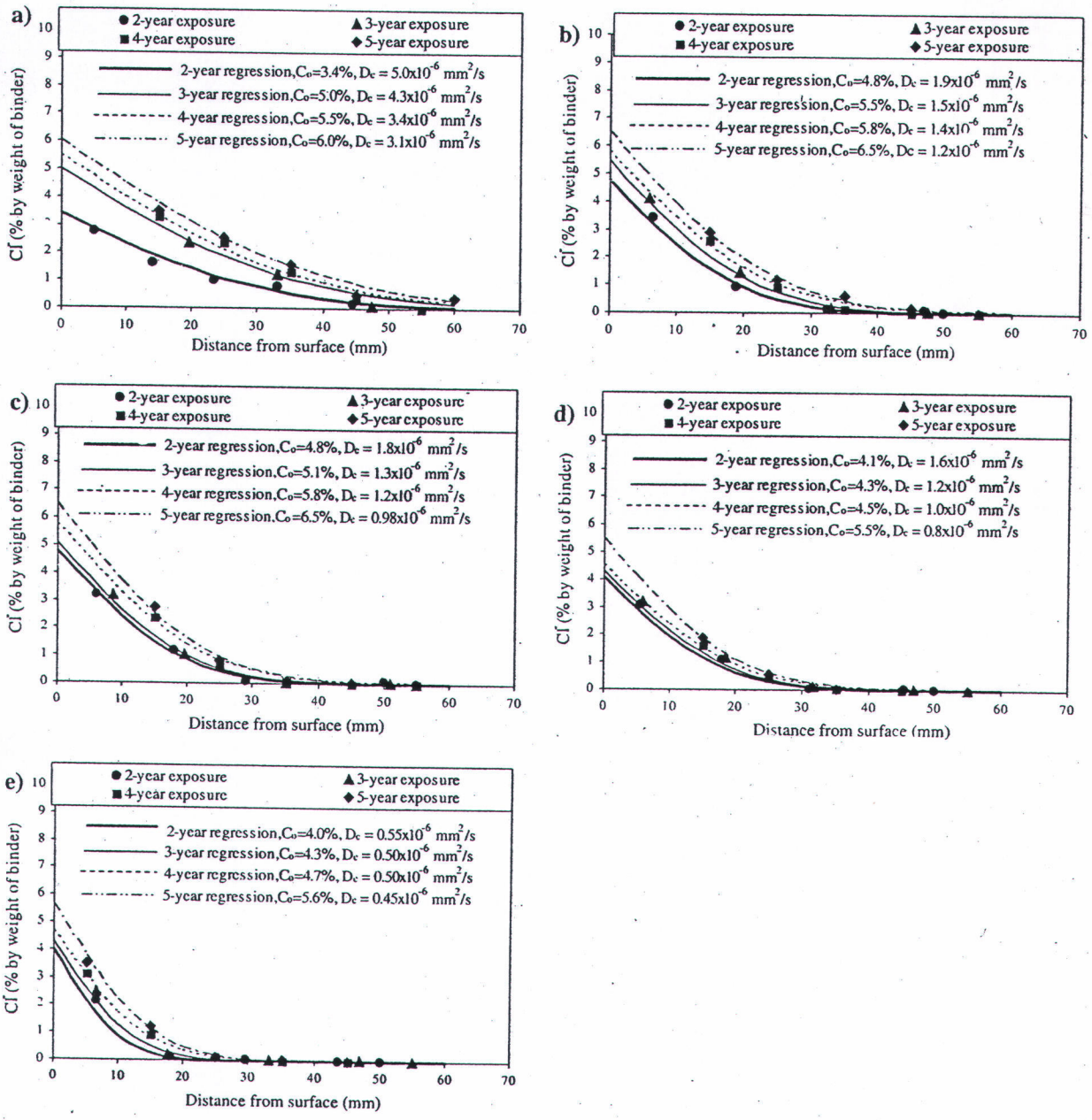

Fig. 1 Chloride penetration profiles of original fly ash concretes with W/B ratio of 0.45 at 2, 3, 4, and 5-year exposure in tidal zone of the marine environment. **(a)** Normal concrete; **(b)** 15%-fly ash concrete; **(c)** 25%-fly ash concrete; **(d)** 35%-fly ash concrete; and **(e)** 50%-fly ash concrete

fitting curve of Fick's second law on chloride penetration profile of original fly ash concretes with W/B ratio of 0.45 at 2, 3, 4, and 5-year exposure. The regression analysis yielded D_c and C_o at 2, 3, 4, and 5-year exposure in the marine environment. For the same procedure, the values of D_c and C_o could be evaluated in the other concrete mixtures as shown in Table 2.

Table 2 Chloride diffusion coefficient (D_c) and chloride concentration at concrete surface (C_o) of concretes under 2, 3, 4, and 5-year exposure in marine environment

Mix no.	Chloride diffusion coefficient, $D_c \times 10^{-6}$ (mm^2/s)				Chloride concentration at concrete surface, C_o (% by weight of binder)			
	2-year exposure	3-year exposure	4-year exposure	5-year exposure	2-year exposure	3-year exposure	4-year exposure	5-year exposure
I45	5.00	4.30	3.40	3.10	3.40	5.00	5.50	6.00
I55	5.70	5.50	5.10	4.00	4.00	4.70	5.00	6.00
I65	8.70	8.00	7.00	5.60	4.20	5.20	5.70	6.20
I45O15	1.90	1.50	1.40	1.20	4.80	5.50	5.80	6.50
I45O25	1.80	1.30	1.20	0.98	4.80	5.10	5.80	6.50
I45O35	1.60	1.20	1.00	0.80	4.10	4.30	4.50	5.50
I45O50	0.55	0.50	0.50	0.45	4.00	4.30	4.70	5.60
I55O15	2.50	2.10	1.80	1.50	4.60	5.60	6.00	7.00
I55O25	1.80	1.60	1.40	1.30	5.20	5.40	5.50	6.30
I55O35	1.80	1.50	1.20	1.10	4.80	5.50	6.00	6.40
I55O50	0.85	0.65	0.55	0.55	4.60	5.50	6.40	6.60
I65O15	3.10	2.80	2.20	2.10	5.30	6.50	6.90	7.30
I65O25	2.50	2.00	1.90	1.90	5.50	6.00	6.30	7.00
I65O35	2.00	1.50	1.30	1.20	4.80	5.40	5.70	6.30
I65O50	1.60	1.30	1.00	0.95	4.80	5.40	5.80	6.20
I45F15	1.40	1.30	1.20	1.10	4.10	5.40	5.60	6.00
I45F25	1.60	1.30	1.10	0.95	4.40	5.30	5.50	5.80
I45F35	1.00	0.75	0.70	0.60	3.70	4.30	4.50	5.20
I45F50	0.55	0.40	0.35	0.30	4.00	4.30	4.50	4.70
I55F15	2.30	1.60	1.30	1.10	4.40	5.00	5.30	5.70
I55F25	1.80	1.40	1.30	1.20	5.10	5.40	5.60	6.20
I55F35	1.30	1.10	1.00	0.90	4.00	4.40	5.00	5.20
I55F50	0.75	0.60	0.45	0.45	4.60	5.00	5.50	5.90
I65F15	2.40	1.80	1.50	1.35	5.00	5.50	6.50	7.30
I65F25	1.70	1.50	1.40	1.20	4.80	5.00	5.30	5.90
I65F35	1.40	1.20	1.00	1.00	4.40	5.40	6.00	6.40
I65F50	1.10	0.90	0.85	0.80	4.80	5.20	5.70	6.20

4 Results and discussion

4.1 Effects of W/B ratio and fly ash on chloride diffusion coefficient (D_c)

Generally, the effect of W/B ratio on durability of concrete is well reported in literatures that the low W/B ratio has improved the durability of concrete. Interestingly, this study found that the decrease of W/B ratio is more effective on reducing D_c in cement concrete than in fly ash concrete as shown in Fig. 2. The results show the similar trend for all concrete mixtures that the concrete with lower W/B ratio has lower value of D_c, particularly in the concrete without fly ash. For example, the decreasing of W/B ratio from 0.65 to 0.45, the values of D_c of the cement concretes (I65 and I45 concretes) at 5-year exposure decreased from 5.6×10^{-6} to 3.1×10^{-6} mm^2/s while the D_c of the 35%-original fly ash concretes (I65O35 and I45O35 concretes) decreased from 1.2×10^{-6} to 0.8×10^{-6} mm^2/s, respectively. Generally, the W/B ratio is very important parameter in Portland cement concrete since it directly affects the rate of hydration and strength development. Throughout, the water permeability of concrete without fly ash is mainly depended on W/B ratio. In

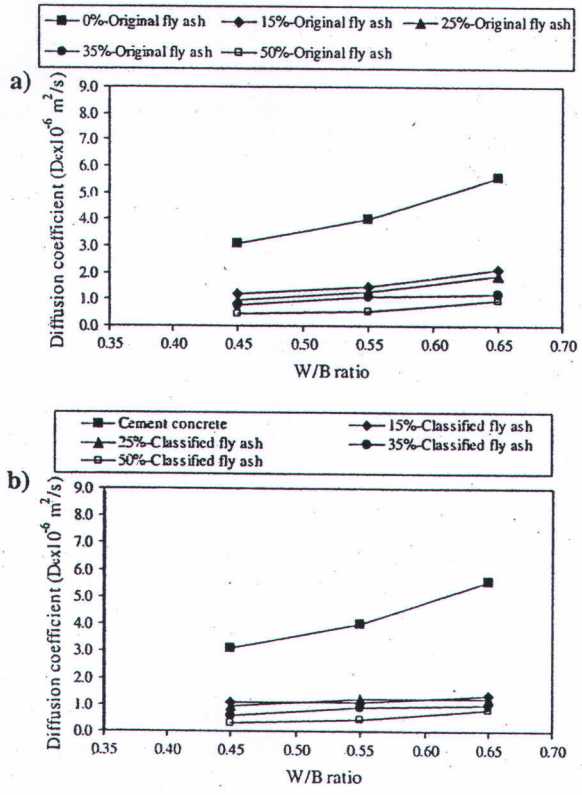

Fig. 2 Effect of W/B ratio on chloride diffusion coefficient of fly ash concrete at 5-year exposure in the marine environment. (a) Original fly ash and (b) classified fly ash

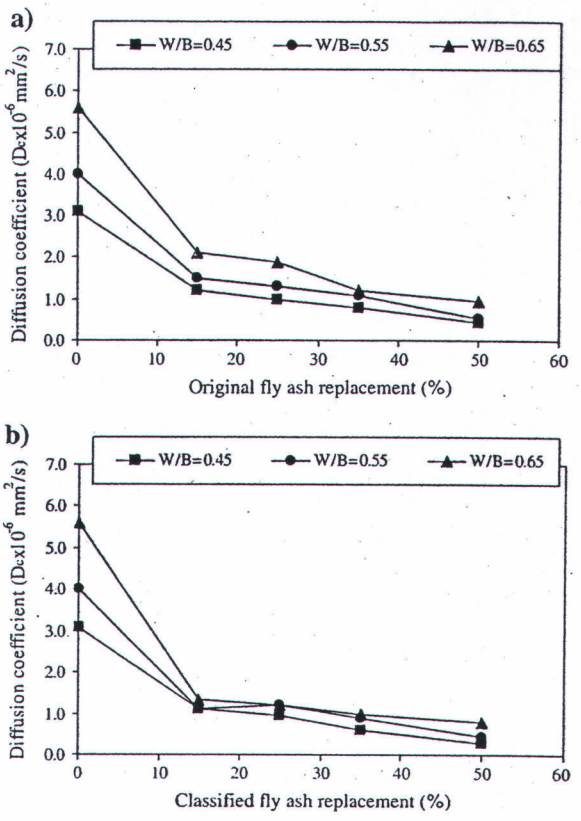

Fig. 3 Effect of fly ash on chloride diffusion coefficient of concrete at 5-year exposure in the marine environment. (a) Original fly ash and (b) classified fly ash

2005, Chindaprasirt et al. [14] also found that the increase of fly ash content in blended cement paste could reduce the pore size distribution and average pore diameter, but it also decreased the compressive strength. In addition, packing effect and pozzolanic reaction of fly ash in concrete are depended on the spherical particle and chemical composition of fly ash [15]. Thus, it should be noted that the chloride resistance in fly ash concrete does not solely depend on the compressive strength of concrete. Owing to the results, W/B ratio was more effective on reducing the chloride penetration rate of cement concrete than original or classified fly ash concretes.

Figure 3 shows the effect of fly ash on D_c of concretes at 5-year exposure in marine environment. The results showed that the use of both original and classified fly ashes clearly reduced the rate of chloride ingress in concrete and it was strongly confirmed by several studies [16–18]. This is due to the packing effect and pozzolanic reaction of fly ash in concrete help the concrete to resist the chloride penetration [19]. Interestingly, all fly ash concretes with W/B ratio of 0.65 had D_c at 5-year exposure lower than that of I45 concrete (cement concrete with W/B ratio of 0.45). This clearly explains that the replacement of cement by fly ash at least 15% by weight of binder in concrete with W/B ratio of 0.65 provides lower rate of chloride ingress than the cement concrete with W/B ratio of 0.45.

4.2 Effect of fly ash finenesses on chloride diffusion coefficient (D_c)

Figure 4 shows the effect of fly ash finenesses on D_c of concrete with W/B ratios of 0.45 and 0.65 at 5-year exposure in the marine environment. The result shows that concrete with classified fly ash gave a good result in lower D_c than the concrete with original fly ash. It can be seen that the use of fly ash with high fineness and high W/B ratio in concrete has more effect on reducing D_c than the one with low W/B ratio. For instance, the concretes with W/B ratio of

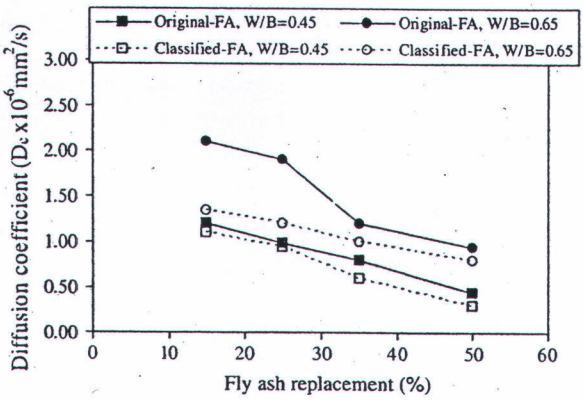

Fig. 4 Effect of fly ash finenesses on chloride diffusion coefficient of concrete with W/B ratios of 0.45 and 0.65 at 5-year exposure in marine environment

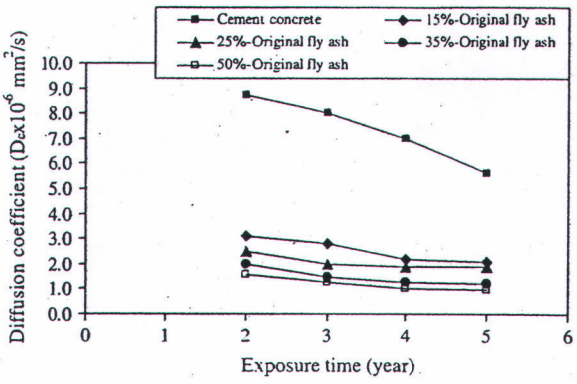

Fig. 5 Relationship between chloride diffusion coefficient of original fly ash concrete with W/B ratio of 0.65 and exposure time in marine environment

0.65 and 25%-fly ash replacement (I65F25 and I65O25 concretes), the use of classified fly ash instead of original fly ash in concrete could decrease D_c at 5-year exposure of 0.7×10^{-6} mm^2/s (from 1.9×10^{-6} to 1.2×10^{-6} mm^2/s) while D_c of the concrete with W/B ratio of 0.45 (I45F25 and I45O25 concretes) decreased only 0.03×10^{-6} mm^2/s (from 0.98×10^{-6} to 0.95×10^{-6} mm^2/s). Chindaprasirt et al. [19] reported the similar trend of this result that the incorporation of high fineness fly ash in low strength concrete (high W/B ratio) was more effect on reducing chloride penetration into concrete than in high strength concrete (low W/B ratio). This result is confirmed to the study in the laboratory and in the site. However, the effective improvement of concrete under marine environment, based on the strength and durability of concrete, is to use high fineness fly ash as a cement replacement and to use low W/B ratio of concrete.

4.3 Effect of exposure time on chloride diffusion coefficient (D_c)

Figure 5 shows the effect of exposure time on D_c of original fly ash concretes with W/B ratio of 0.65. The result showed the general trend in all concrete mixtures that the values of D_c decreased with exposure time. *The D_c of cement concretes decrease at higher rate than that of fly ash concrete* (see Fig. 5). Typically, the value of D_c in cement concrete with W/B ratio of 0.65 (I65 concrete) decreased from 8.7×10^{-6} to 5.6×10^{-6} mm^2/s during the exposure period of 2–5 years while that of 25% and 50%-original fly ash concretes (I65O25 and I65O50 concretes, respectively) decreased from 2.5×10^{-6} to 1.9×10^{-6} mm^2/s and 1.6×10^{-6} to 0.95×10^{-6} mm^2/s, respectively. The decrease of D_c with exposure time was confirmed by Thomas and Matthews [8]. The decrease of D_c with exposure time is conceivable normality because the pore size distribution and average pore diameter in concrete decreases with time [14, 20]. Throughout, the use of fly ash in concrete could efficiently improve the pore system, especially in long term performance, leading to the good resistance of chloride ingress into concrete. This can be explained that at the early age, the concrete containing fly ash has a higher permeability than that of cement concrete, but in longer period, fly ash concrete can provide a very low permeability due to pozzolanic reaction [21]. In this study, the value of D_c truly decreased with exposure time but it showed a slow decreasing and almost be constant as a longer period. Mangat and Limbachiya [5] had published the relationship between D_c and exposure time in form of the inverse exponential function. This function demonstrates that the value of D_c decreases slowly when the exposure time increases.

At present, numerous authors have reported different chloride diffusion coefficient (D_c) with various methods for several concrete mixtures as shown in Table 3 [1, 2, 5, 6, 8, 22]. Those of them identically concluded that D_c had several values depending on several parameters, for instance, type of cement and cementitious materials, W/B ratio, exposure condition, migration, diffusion, detection method, etc.

Table 3 Chloride diffusion coefficient of concrete from several literatures

Specimens	Environment	Detection method	Diffusion coefficient, D_c (mm^2/s)			References
			Detail of specimen	Time	D_c	
Cement concrete	Concrete was exposed below ground in a coastal area of the Arabian Gulf	Fitting chloride diffusion curve by Fick's law	w/c = 0.40	4.5 years	1.18×10^{-8}	Bader [22]
			w/c = 0.50	4.5 years	5.95×10^{-8}	
			w/c = 0.65	4.5 years	6.92×10^{-8}	
Fly ash concrete	Concrete was exposed to tidal zone of BRE marine site, England	Fitting chloride diffusion curve by Fick's law	0%-FA, w/c = 0.68	2 years	15.3×10^{-6}	Thomas and Matthews [8]
				4 years	16.2×10^{-6}	
			15%-FA, w/c = 0.61	2 years	3.36×10^{-6}	
				4 years	2.39×10^{-6}	
				10 years	0.99×10^{-6}	
			30%-FA, w/c = 0.54	2 years	3.34×10^{-6}	
				4 years	1.67×10^{-6}	
				10 years	0.55×10^{-6}	
			50%-FA, w/c = 0.44	2 years	2.46×10^{-6}	
				4 years	2.48×10^{-6}	
				10 years	0.42×10^{-6}	
Cement concrete	Concrete was immersed in sodium chloride solution in laboratory (17.5% by weight)	Fitting chloride diffusion curve by Fick's law	Cement concrete (compressive strength of 41 MPa at 28 day)	28 days	22.7×10^{-5}	Mangat and Limbachiya [5]
				90 days	4.5×10^{-5}	
				180 days	3.6×10^{-5}	
Cement concrete	Concrete was immersed in sodium chloride solution in laboratory (3% by weight)	Fitting chloride diffusion curve by Fick's law	23 MPa at 28 days	1 year	29×10^{-6}	Khatri and Sirivivatnanon [6]
			50 MPa at 28 days	1 year	8×10^{-6}	
			56 MPa at 28 days	1 year	2.5×10^{-6}	
Cement concrete	Concrete was cured at temperature of 18–20°C	Based on concrete via a gas diffusion technique	w/c = 0.40	14 days	10.3×10^{-6}	Sharif et al. [1]
			w/c = 0.50	14 days	33.7×10^{-6}	
Fly ash concrete	Concrete was cured at 12% relative humidity and temperature of 20°C	Based on rapid chloride penetration test	0%-FA, w/c = 0.55	16 weeks	8×10^{-7}	Shafiq [2]
			40%-FA, w/c = 0.49	16 weeks	1.1×10^{-7}	
			50%-FA, w/c = 0.48	16 weeks	1.0×10^{-7}	

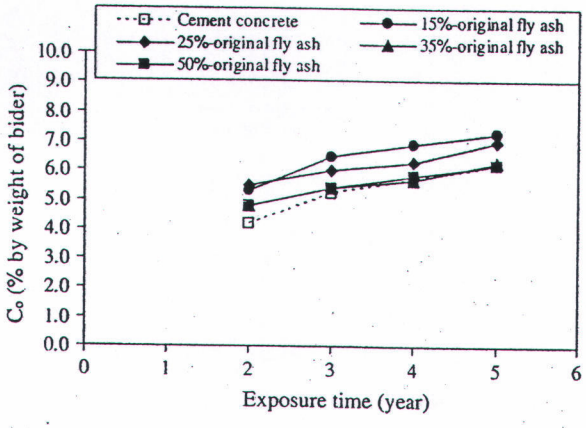

Fig. 6 Relationship between chloride concentration at concrete surface of original fly ash concrete with W/B ratio of 0.65 and exposure time in marine environment

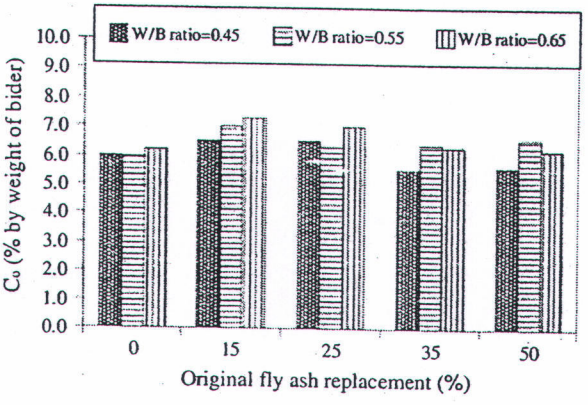

Fig. 7 Effects of original fly ash and W/B ratio on chloride concentration at concrete surface at 5-year exposure in marine environment

4.4 Chloride concentration at concrete surface (C_o)

The determination of C_o is evaluated by the extrapolation of chloride profile at $x = 0$ (at surface of concrete) and the values of C_o for all concrete mixtures at any exposure time are shown in Table 2.

Figure 6 shows the effect of exposure time on C_o of original fly ash concrete with W/B ratio of 0.65. This figure indicated that C_o increased with the increase of exposure time. It is noted that the value of C_o in this study does not relate to fly ash replacement or W/B ratio (see Fig. 7).

Generally, C_o must be determined prior to obtain the chloride penetration in concrete under marine environment. At present, little research has study in this point because it is so complicated and so difficult to present the actual value of C_o. Generally, C_o depends on many factors such as airborne chlorides, exposure time, surface roughness of concrete, types of structural member, rain, wind speed, and so on [23]. Some literature had published C_o based on some parameters as mentioned above [24], but it did not clearly present the actual behavior. However, the study of C_o based on airborne chloride is useful in the case of concrete is far away from the sea water (at atmospheric zone). The damaging of reinforced concrete structure in this zone is mainly caused by the chloride ions diffusion into the concrete and induces the steel to be corroded. Besides, in the case of concrete directly subjected to sea water or chloride solution, the value of C_o is needed to support the boundary condition of diffusion equation for simulation chloride penetration profile in concrete. Many researches had evaluated C_o for initial concentration in Fick's second law of diffusion to obtain the chloride penetration profile in concrete [5, 8].

5 Conclusion

Based on the results and discussions, the following conclusions are made.

1. Decrease of W/B ratio resulted in the decrease of chloride diffusion coefficient (D_c). It is also found that the decrease of W/B ratio is more effective on reducing D_c in cement concrete than in fly ash concrete.
2. The increase of fly ash fineness, fly ash replacement of cement, and exposure time of concrete resulted in the decrease of chloride diffusion coefficient (D_c).
3. The use of fly ash with higher W/B ratio has more effective on reducing of chloride diffusion coefficient (D_c) than that of concrete with lower W/B ratio.
4. Concrete with W/B ratio of 0.65 and use fly ash to replace cement at least 15% by weight of binder can provide the chloride diffusion coefficient (D_c) lower than that of the cement concrete with W/B ratio of 0.45.

Acknowledgments The authors gratefully acknowledge the financial supports from Thailand Research Fund (TRF) under TRF Senior Research Scholar Contact No. RTA5080020 and

the Commission on Higher Education, Ministry of Education, Thailand. Thanks also extend to the departments of civil engineering, King Mongkut's University of Technology Thonburi, and Burapha University, Thailand for providing facilities and equipments.

References

1. Sharif A, Loughlin KF, Azad AK, Navaz CM (1997) Determination of effective chloride diffusion coefficient in concrete via a gas diffusion technique. ACI Mater J 94(3):227–233
2. Shafiq N (2004) Effects of fly ash on chloride migration in concrete and calculation of cover depth required against the corrosion of embedded steel reinforcement. Struct Concrete 5(1):5–9
3. Maltais Y, Samson E, Marchand J (2004) Predicting the durability of Portland cement systems in aggressive environments-laboratory validation. Cement Concrete Res 34(9):1579–1589
4. Biaz B, Novoa XR, Perez MC (2006) Study of the chloride diffusion in mortar: a new method of determining diffusion coefficients based on impedance measurements. Cement Concrete Comp 28(3):237–245
5. Mangat PS, Limbachiya MC (1999) Effect of initial curing on chloride diffusion in concrete repair materials. Cement Concrete Res 29(9):1475–1485
6. Khatri RP, Sirivivatnanon V (2004) Characteristic service life for concrete exposed to marine environments. Cement Concrete Res 34(5):745–752
7. Persson B (2004) Chloride migration coefficient of self-compacting concrete. Mater Struct 37:82–91
8. Thomas MDA, Matthews JD (2004) Performance of pfa concrete in a marine environment-10-year results. Cement Concrete Res 26(1):5–20
9. Arora P, Popov BN, Haran B, Ramasubramanian M, Popova S, White RE (1997) Corrosion initiation time of steel reinforcement in a chloride environment-a one dimensional solution. Corros Sci 39(4):739–759
10. Jung W-Y, Yoon Y-S, Sohn Y-M (2003) Predicting the remaining service life of land concrete by steel corrosion. Cement Concrete Res 33(5):663–677
11. ASTM C1152 (1997) Standard test method for acid-soluble chloride in mortar and concrete. Annual Books of ASTM Standards V. 04.01 Philadelphia, pp 627–629
12. Chalee W, Teekavanit M, Kiattikomol K, Siripanichgorn A, Jaturapitakkul C (2007) Effect of W/C ratio on covering depth of fly ash concrete in marine environment. Constr Build Mater 21(5):965–971
13. Crank J (1975) The mathematic of diffusion, 2nd edn. Oxford Press, London
14. Chindaprasirt P, Jaturapitakkul C, Sinsiri T (2005) Effect of fly ash fineness on compressive strength and pore size of blended cement paste. Cement Concrete Comp 27(4):425–4[illegible]
15. Tangpagasit J, Cheerarot R, Jaturapitakkul C, Kiattikomol K (2005) Packing effect and pozzolanic reaction of fly ash in mortar. Cement Concrete Res 35(6):1145–1151
16. Sengul O, Tasdemir C, Tasdemir AT (2005) Mechanical properties and rapid chloride permeability of concrete with ground fly ash. ACI Mater J 102(6):414–421
17. Sujjavanich S, Sida V, Suwanvitaya P (2005) Chloride permeability and corrosion risk of high-volume fly ash concrete with mid-range water reducer. ACI Mater J 102(3):177–182
18. Sumranwanich T, Tangtermsirikul S (2004) A model for predicting time-depending chloride binding capacity of cement-fly ash cementitious system. Mater Struct 37:387–396
19. Chindaprasirt P, Chotithanorm C, Cao HT, Sirivivatnanon V 2007) Influence of fly ash fineness on the chloride penetration of concrete. Constr Build Mater 21(2):356–361
20. Van Der Wegen G, Bijen J, Van Selst R (1993) Behavior of concrete affected by sea water under high pressure. Mater Struct 26:549–556
21. Naik TR, Singh SS, Hossain MM (2004) Permeability of concrete containing large amounts of fly ash. Cement Concrete Res 24(5):913–922
22. Bader MA (2003) Performance of concrete in coastal environment. Cement Concrete Comp 25(4):539–548
23. Swatekititham S (2004) Computational model for chloride concentration at surface of concrete under actual environmental condition. A dissertation for the degree of Doctor of Engineering submitted to Kochi University of Technology, Japan, pp 1–178
24. Tanaka Y, Kawano H, Watanabe H, Nakajo T (2001) Study on required cover depth of concrete highway bridges in coastal environment. In: 17th U.S.-Japan bridge engineering workshop, Tsukuba, pp 1–16

5. W. Tangchirapat, C. Jaturapitakkul, P. Chindaprasirt. Use of palm oil fuel ash as a supplementary cementitious material for producing high-strength concrete, Construction and Building Materials, 23 (2009), 2641-2646. (IF 0.947).

Construction and Building Materials 23 (2009) 2641–2646

Contents lists available at ScienceDirect

Construction and Building Materials

journal homepage: www.elsevier.com/locate/conbuildmat

Use of palm oil fuel ash as a supplementary cementitious material for producing high-strength concrete

Weerachart Tangchirapat [a], Chai Jaturapitakkul [a,*], Prinya Chindaprasirt [b]

[a] Department of Civil Engineering, Faculty of Engineering, King Mongkut's University of Technology Thonburi, Bangkok 10140, Thailand
[b] Department of Civil Engineering, Faculty of Engineering, Khon Kaen University, Khon Kaen 40002, Thailand

ARTICLE INFO

Article history:
Received 7 November 2008
Received in revised form 9 January 2009
Accepted 28 January 2009
Available online 3 March 2009

Keywords:
Palm oil fuel ash
Compressive strength
Drying shrinkage
Water permeability
Sulfate resistance

ABSTRACT

The objective of this study is to investigate the use of ground palm oil fuel ash with high fineness (GPA) as a pozzolanic material to produce high-strength concrete. Samples were made by replacing Type I Portland cement with various proportions of GPA. Properties such as the compressive strength, drying shrinkage, water permeability, and sulfate resistance, were then investigated. After aging for 28 days, the compressive strengths of these concrete samples were found to be in the range of 59.5–64.3 MPa. At 90-day the compressive strength of concrete containing GPA 20% was as high as 70 MPa. The drying shrinkage and water permeability were lower than those of high-strength concrete made from Type I Portland cement. When the concrete samples were immersed in a 10% $MgSO_4$ solution for 180 days, the sulfate resistance in terms of the expansion and loss of compressive strength was improved. The results indicated that GPA is a reactive pozzolanic material and can be used as a supplementary cementitious material for producing high-strength concrete.

1. Introduction

High-strength concrete is widely used in civil engineering projects throughout the world because most of its mechanical and durability properties are better than those of normal-strength concrete. In addition to the advantageous properties, using high-strength concrete enables reduction of the size of structural members that are essential in high-rise buildings, such as beams and columns. The use of lighter and slender structures reduces the volume of concrete needed in building structures, resulting in cost savings for construction projects.

According to ACI 363 [1], concrete with a 28-day compressive strength higher than 41 MPa is considered high-strength concrete. Typically, high-strength concrete has a low water to binder ratio of 0.20–0.45 with high binder content [2] and superplasticizer is used to increase its workability. In addition, supplementary cementing materials, such as fly ash and silica fume, are widely used as pozzolanic materials in high-strength concrete. They are normally used to create extra strength by pozzolanic reactions, to reduce the permeability, and to improve the durability of the concrete.

Palm oil fuel ash (POFA) is one of agro-waste ash from which palm oil residue, such as palm fiber and shells, are burnt at temperatures of about 800–1000 °C to produce steam for electricity generation in biomass thermal power plants. In Thailand, more than 100,000 tons of POFA are produced annually, and this amount increases every year because palm oil is one of the major raw materials used in the production of bio-diesel. POFA contains large amounts of silica and has recently been accepted as a pozzolanic material in concrete [3,4]. However, the utilization of POFA as a pozzolanic material to partially replace Portland cement has not been investigated extensively, especially in high-strength concrete.

In this study, an effort was made to evaluate the usefulness of POFA as a cement replacement for producing high-strength concrete. The effects of POFA on the compressive strength and durability of high-strength concrete in terms of drying shrinkage, water permeability, and sulfate resistance were investigated. If POFA can be used as a pozzolanic material in producing high-strength concrete and can improve its durability, it will lead to reductions in cement usage and the cost of high-strength concrete and will also be beneficial for the environment by reducing the volume of waste disposed of in landfills. Furthermore, using POFA as a replacement for cement will also encourage researchers to investigate the use of other by-products from biomass power plants, which will ultimately lead to their development as a more environmentally friendly way of generating energy.

2. Experiment

2.1. Materials

2.1.1. Cement

The physical properties and chemical compositions of the Type I and Type V Portland cement used in this study are shown in Tables 1 and 2, respectively.

* Corresponding author. Tel.: +66 2470 9131; fax: +66 2427 9063.
E-mail address: chai.jat@kmutt.ac.th (C. Jaturapitakkul).

0950-0618/$ - see front matter © 2009 Elsevier Ltd. All rights reserved.
doi:10.1016/j.conbuildmat.2009.01.008

Table 1
Physical properties of materials.

Materials	Specific gravity	Retained on a 45-μm (No. 325) sieve (%)	Median particle size, d_{50} (μm)
Cement Type I	3.14	N/A	14.6
Cement Type V	3.17	N/A	7.5
Original POFA (OP)	1.97	41.2	65.6
High-fineness POFA (GPA)	2.33	1.5	10.1

Table 2
Chemical composition of materials.

Chemical composition (%)	Cement Type I	Cement Type V	GPA
Silicon dioxide (SiO_2)	20.9	22.1	65.3
Aluminum oxide (Al_2O_3)	4.7	3.5	2.5
Iron oxide (Fe_2O_3)	3.4	5.5	1.9
Calcium oxide (CaO)	65.4	62.4	6.4
Magnesium oxide (MgO)	1.2	0.9	3.0
Sodium oxide (Na_2O)	0.2	0.0	0.3
Potassium oxide (K_2O)	0.3	0.1	5.7
Sulfur trioxide (SO_3)	2.7	1.0	0.4
Loss on ignition (LOI)	0.9	1.6	10.0
$SiO_2 + Al_2O_3 + Fe_2O_3$	–	–	69.7
Bogue chemical compositions (%)			
Tricalcium silicate (C_3S)	62.8	51.2	–
Dicalcium silicate (C_2S)	12.5	24.8	–
Tricalcium aluminate (C_3A)	6.8	0.0	–
Tetracalcium aluminoferrite (C_4AF)	10.3	16.9	–

2.1.2. Aggregate

Local river sand with a fineness modulus of 2.68, specific gravity of 2.60, and water absorption of 0.63% was used as a fine aggregate. Crushed limestone with a maximum size of 12.5 mm, specific gravity of 2.72, and water absorption of 0.80% was used as coarse aggregate.

2.1.3. Palm oil fuel ash

Palm oil fuel ash (POFA) used in this study was collected from a biomass power plant located in Southern Thailand. To improve its reactivity, it was ground with a ball mill to reduce the particle sizes. The particle morphologies are shown in Fig. 1 and the physical properties of the materials are shown in Table 1. The original POFA (OP) that came directly from the power plant had large particles with a median particle size of 65.6 μm, and most of the particles had a porous texture (see Fig. 1a). After the POFA was ground to reduce the particle size (GPA), irregular particles with a crushed shape were found (see Fig. 1b) and the median particle size was reduced to 10.1 μm. The fineness in terms of the weight of particles retained on a 45-μm (No. 325) sieve and the specific gravity of the materials are shown in Table 1. It was found that 41.2% of the OP particles were retained on the sieve, while only 1.5% by weight of the particles of ground POFA with high fineness (GPA) was retained. The specific gravity of OP was 1.97 and increased to 2.33 for GPA. The grinding process increased both the fineness of POFA and the specific gravity. This was due to the crushing of porous particles, which usually have low specific gravity, into smaller particles with lower porosity [5]. This result agreed with those of other researchers who ground fly ash and bottom ash [6,7].

The chemical composition of ground POFA with high fineness (GPA) is listed in Table 2. The main component of GPA is SiO_2 which is 65.3%. The total amount of SiO_2, Al_2O_3, and Fe_2O_3 was 69.7%. The amounts of LOI and SO_3 were within the respective limits of 10.0% and 4.0% as specified by ASTM C618 [8]. Although GPA is not a natural pozzolan, it can be classified as a Class N (natural) pozzolan based on the chemical composition according to ASTM C618 [8].

2.2. Mix proportions and test specimens

GPA was used to partially replace Type I Portland cement at proportions of 10%, 20%, and 30% by weight of binder. The targeted compressive strength of concrete incorporating GPA at 28 days was at least 55 MPa. All mix proportions of high-strength concretes as shown in Table 3 had the same binder content of 550 kg/m^3, and the water to binder (W/B) ratio was kept at 0.32. Superplasticizer was used in the high-strength concrete mixtures in order to obtain high workability with slump of fresh concrete between 200 and 250 mm. Concrete cylinders of 100 mm in diameter and 200 mm in height were cast and used to determine the compressive strength at 7, 28, 90, and 180 days. Three concrete cylinders were tested and used for each data point.

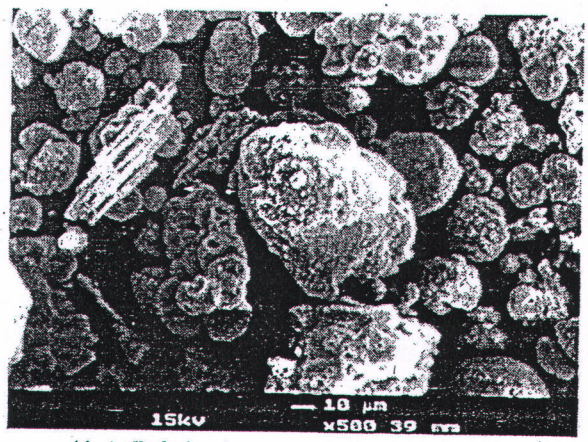

(1a) Original palm oil fuel ash (OP)

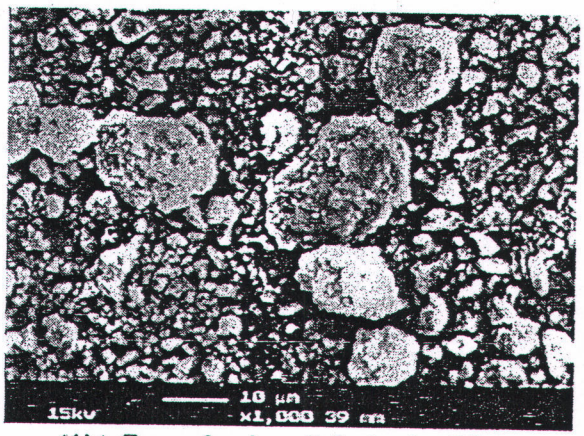

(1b) Ground palm oil fuel ash (GPA)

Fig. 1. Scanning electron microscopy (SEM) images of palm oil fuel ash.

To determine the drying shrinkage of concrete, prismatic concrete specimens 75 × 75 mm^2 in cross-section and 285 mm in length were used. Each specimen was fitted with stainless steel studs at both ends. After casting for 24 h, the specimens were removed from the molds and cured in tap water for 1 day. After the age of 3 days, the specimens were removed from the water, wiped with damp cloth, and measured immediately to determine the initial length of the concrete specimens. The concrete specimens were subsequently placed in an air storage cabinet with a controlled temperature of 23 ± 2 °C and a relative humidity of 50 ± 5% as prescribed by ASTM C596 [9]. The drying shrinkage of all concrete samples was monitored up to 6 months.

To conduct the water permeability test, a slice 40 mm thick was sawn from the middle of the 100 × 200 mm concrete cylinder. A layer of epoxy resin 25 mm thick was then cast around the slice of concrete and allowed to harden for 24 h. The resulting specimen was then installed in a permeability housing cell (Fig. 2). Water pressure of 0.5 MPa or 5.0 bar was applied to the cell. The amount of water flowing through the concrete specimen was measured by reading the drop in water level within a manometer tube. The results were plotted with a curve of the cumulative amount of water flowing *vs.* the cumulative time to determine the steady-state flow. At this stage, the steady flow rate was obtained and the coefficient of water permeability was calculated using Darcy's law and continuity equation. This experimental setup for testing the water permeability of concrete was recommended by Khatri and Sirivivatnanon [10] and Chindaprasirt et al. [11]. The values of water permeability of concretes were investigated at the age of 90 days.

Two types of test for sulfate resistance of concretes, expansion and loss in compressive strength, were performed by exposing the samples to a 10% $MgSO_4$ solution. The expansion of a prismatic concrete specimen 75 × 75 mm^2 in cross-section and 285 mm in length was measured. The concrete bars were immediately immersed in a 10% $MgSO_4$ solution after being removed from the molds (24 h after casting). The expansion of all concrete bars was measured during a period of 180 days (about 6 months).

To examine the loss of compressive strength, concrete cylinders of 100 mm in diameter and 200 mm in height were used. Fifteen specimens were cured in water and another 15 specimens were immersed in a 10% $MgSO_4$ solution. After 180 days,

Table 3
Mix proportions of high-strength concretes.

Mixes	Mix proportion (kg/m³)						W/B	Slump (mm)
	Cement	GPA	Sand	Limestone	Water	Superplasticizer		
CTI	550	–	760	968	176	6.4	0.32	245
CTV	550	–	760	968	176	6.4	0.32	250
GPA10	495	55	753	959	176	6.8	0.32	250
GPA20	440	110	745	950	176	8.6	0.32	240
GPA30	385	165	738	940	176	11.6	0.32	250

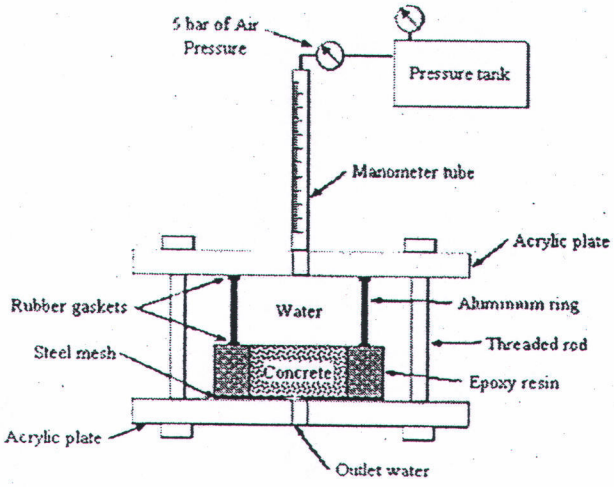

Fig. 2. Experimental setup to test the water permeability of concrete.

the compressive strengths of the two types of specimen were examined. The loss of compressive strength of concrete was evaluated by measuring the difference in compressive strength compared to the same type of concrete cured in water at the same age.

To compare the sulfate resistance of concretes containing GPA with that of concrete made from high sulfate resistance cement, high-strength concrete made from Type V Portland cement (CTV) was also prepared and tested. The mix proportion of the concrete is also shown in Table 3.

3. Results and discussion

3.1. Compressive strength

The results of compressive strength and normalized compressive strength of concretes containing GPA with high fineness are shown in Table 4. Normalized compressive strength is defined as the ratio (in percentage) between the compressive strength of concrete containing GPA and the compressive strength of CTI concrete. For concrete mixtures containing various proportions of GPA, the compressive strength at 28 days was more than 55.0 MPa, with GPA30 and GPA20 concrete samples showing values of 58.8 and 60.9 MPa, respectively. These results were comparable to those of CTI and CTV concretes, which had compressive strengths of 58.5 and 57.9 MPa, respectively, at the same age. Therefore, all of these concrete mixtures could be categorized as high-strength concrete.

The effects of GPA on the high compressive strength of concretes are shown in Fig. 3. At an early age of 7 days, replacing Type I Portland cement with 10–30% GPA was found to yield a compressive strength that was comparable to CTI concrete. The compressive strengths of GPA10, GPA20, and GPA30 concretes were 55.6, 54.6, and 53.2 MPa, respectively. These values represent 101%, 99%, and 97% of the compressive strength of CTI concrete, respectively. After 28 days, the compressive strengths of all concretes containing GPA were higher than that of CTI concrete. The compressive strengths of GPA10, GPA20, and GPA30 concretes were 59.5, 60.9, and 58.8 MPa, respectively. Among all the samples examined in this study, the highest compressive strengths were found in the sample containing 20% GPA with values at 28, 90, and 180 days of 60.9, 69.4, and 73.7 MPa, respectively, representing 104%, 107%, and 108% of the compressive strength of CTI concrete. The increase in the compressive strength of GPA concretes at an early age was due to the high fineness of GPA particles, which filled the voids between the cement and the aggregates. At later ages, the SiO_2 contained in GPA reacts with the $Ca(OH)_2$ generated by the hydration process of cement to form additional calcium silicate hydrate (C–S–H) and improves interfacial bonding between the aggregates and pastes. These characteristics have been shown to improve the compressive strength and increase the density of concrete [12,13].

The use of 20% GPA gave a compressive strength as high as 70.0 MPa at age of 90 days. Furthermore, GPA can be used as a cement replacement up to 30% in producing high-strength concrete, and the compressive strength obtained is higher than that of high-strength concrete made from Type I Portland cement. The results suggested that ground POFA with high fineness (GPA) is a reactive pozzolanic material and can be used as a mineral admixture in producing high-strength concrete. The material is similar to other pozzolanic materials, such as silica fume and fly ash.

3.2. Drying shrinkage

Fig. 4 shows the results of drying shrinkage of high-strength concretes. The drying shrinkage developed rapidly at an early stage, with approximately 70% of the maximum shrinkage occur-

Table 4
Compressive strength and water permeability of high-strength concretes.

Mixes	Compressive strength (MPa) – normalized compressive strength (%)				Water permeability at 90 days ($K \times 10^{-14}$), m/s–K/K_{CTI}
	7-D	28-D	90-D	180-D	
CTI	54.9–100	58.5–100	64.7–100	68.5–100	6.67–1.00
GPA10	55.6–101	59.5–102	67.5–104	72.0–105	4.17–0.63
GPA20	54.6–99	60.9–104	69.4–107	73.7–108	3.11–0.47
GPA30	53.2–97	58.8–101	66.1–102	69.0–101	3.83–0.57

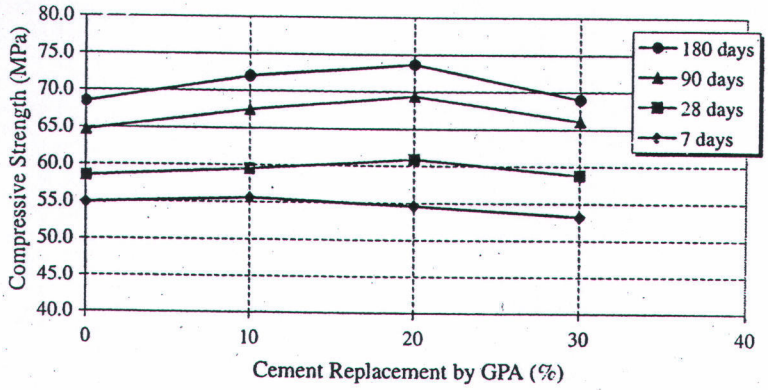

Fig. 3. Relationship between compressive strength and cement replacement by GPA.

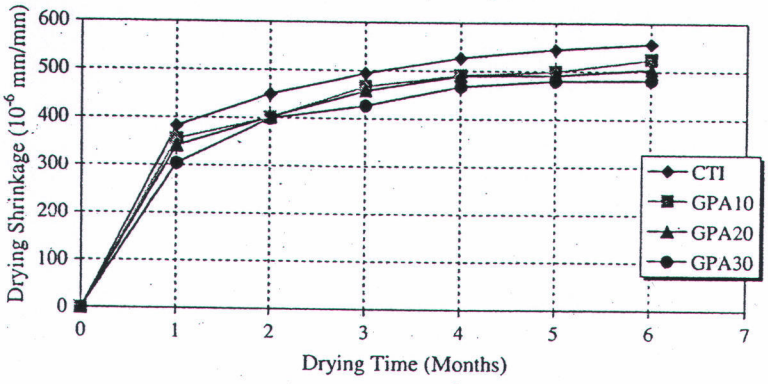

Fig. 4. Drying shrinkage of high-strength concrete.

ring during the first 3 months. The drying shrinkage curve patterns agreed with the observations reported by Barr et al. [14] and Huo et al. [15]. At 6 months, the drying shrinkage values were found to vary between 494×10^{-6} and 557×10^{-6} mm/mm. For high-strength concretes with high binder contents, the drying shrinkage values were moderate and agreed with those reported by Haque [16] for concretes of similar binder contents.

At 6 months, the drying shrinkage of CTI was 557×10^{-6} mm/mm while those of GPA concretes were slightly lower than that of CTI concrete. At 6 months, the drying shrinkage values of GPA10, GPA20, and GPA30 concretes were 525×10^{-6}, 505×10^{-6}, and 494×10^{-6} mm/mm, respectively. The lower values of the drying shrinkage were attributed to densification of the concrete due to pozzolanic reaction and the high fineness of the ash. In addition, the high fineness of the ash caused pore refinement, *i.e.*, the transformation of large pores into fine pores. This process reduced the evaporation of water and thus decreased the drying shrinkage of concrete. Haque and Kayali [17] reported that most specifications allow drying shrinkage performance in the range of 600–800 microstrain at 56 days. Therefore, the drying shrinkage characteristics of these high-strength concretes were in compliance with these specifications. The above results suggested that the use of GPA up to 30% slightly reduces the drying shrinkage of high-strength concrete. From this viewpoint, concretes incorporating GPA with high fineness are also considered to be within the high performance category.

3.3. Water permeability

The water permeability of high-strength concretes at the age of 90-day was investigated and the results are shown in Table 4. The water permeability of all the high-strength concretes varied between 3.11×10^{-14} and 8.47×10^{-14} m/s, which were consistent with the results of El-Dieb and Hooton [18], who reported water permeability values of high-strength concrete ranging from 1×10^{-12} to 1×10^{-16} m/s. At 90 days, the water permeability value of CTI concrete was 6.67×10^{-14} m/s while those of GPA10, GPA20, and GPA30 concretes were 4.17×10^{-14}, 3.11×10^{-14}, and 3.83×10^{-14} m/s, respectively. These results indicated that the use of GPA at all proportions examined in this study reduced the water permeability of high-strength concrete. Using up to 30% GPA in high-strength concrete resulted in greater impermeability to water than CTI concrete. The above results suggested that the pozzolanic reaction and the filler effect of the GPA with high fineness filled voids and thus increased the density of the resultant concrete [11].

The water permeability was compared between concrete samples with different proportions of GPA. The results indicated that concrete containing 20% GPA had the lowest water permeability as compared to the other replacement rates, and the water permeability of concrete increased slightly when the replacement of cement by GPA was up to 30% by weight of binder. In addition, all high-strength concretes containing GPA had water permeability about half that of the CTI concrete, suggesting that GPA can help

refine the porosity and pore size in concrete to produce a highly impermeable and dense concrete.

3.4. Sulfate resistance

3.4.1. Expansion of concrete

The results of the expansion test of the high-strength concrete bars immersed in a 10% $MgSO_4$ solution for up to 180 days are shown in Fig. 5. At 180 days, the amount of expansion of the CTV concrete bar (0.016%) was not much different from that of the CTI concrete bar (0.021%). This was despite the lack of C_3A in Portland cement Type V, while Type I Portland cement had a C_3A content of 6.8%. These results confirmed earlier findings that the presence of C_3A is not the only cause of expansion due to sulfate attack [19]. Gonzalez and Irassar [20] investigated the sulfate attack mechanism on four types of cement with low C_3A contents (varying between 0% and 1%) and with C_3S content varying between 40% and 74%. They found increased expansion of the cement mortar with increasing C_3S content. Moreover, this lack of a significant difference in expansion between CTV and CTI concrete bars may be due to the Type I Portland cement used in this study has a C_3A content of 6.8%, which is lower than the allowable C_3A content for ASTM C150 [21] Type II moderate sulfate resistance cement (8.0%) and is slightly higher than that allowable for Type V high sulfate resistance cement (5.0%).

It was clearly seen that the use of GPA in high-strength concrete reduced the expansion of the concrete bars. At 180 days of immersion, the GPA10, GPA20, and GPA30 concrete bars expanded by 0.016%, 0.015%, and 0.017%, respectively, values which were lower than that of CTI concrete (0.021%). In addition, the amount of expansion of GPA20 concrete bars was slightly lower than that of CTV concrete bars. The lower expansion of concrete bars containing GPA was due to the replacement of cement by high fineness POFA, which was responsible for the pozzolanic reaction and the reduction of $Ca(OH)_2$ in concrete. Our results were similar to those of other studies in which pozzolanic materials were used as cement replacements to improve sulfate resistance [22,23]. The pozzolanic reaction led to a refinement of the pore structure, resulting in a highly impermeable matrix. A reduction in $Ca(OH)_2$ led to reductions in the formation of gypsum and ettringite [24].

3.4.2. Concrete strength reduction

Fig. 6 shows the compressive strengths of high-strength concrete samples immersed in 10% $MgSO_4$ solution and cured in water for 180 days. The compressive strength of high-strength concretes made from Type I Portland cement and Type V Portland cement placed in sulfate solution showed the same behavior as those cured in water. After 180 days of immersion in sulfate solution, the compressive strength of CTV concrete was 63.8 MPa, while that of CTI concrete was 59.7 MPa, representing reductions of the compressive strength of 10.4% and 12.8%, respectively.

The changes in compressive strength of GPA concrete samples stored in a 10% $MgSO_4$ sulfate solution and water are also shown in Fig. 6. Under the same curing conditions, GPA10, GPA20, and GPA30 concretes showed higher compressive strength than CTI concrete, and also showed a lower percentage reduction in compressive strength as compared to CTI concrete. Again, this can be explained by the pore refinement process that occurs as a result of pozzolanic reactions, the filler effects from the fine particles of GPA, and the reduction of $Ca(OH)_2$ from the hydration reaction,

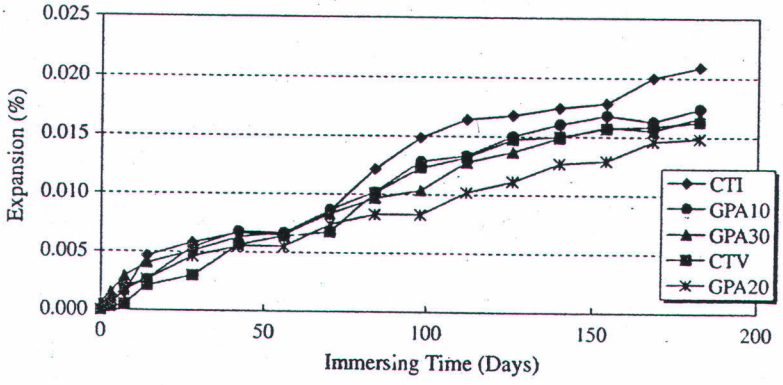

Fig. 5. Expansion of high-strength concrete due to 10% $MgSO_4$ solution.

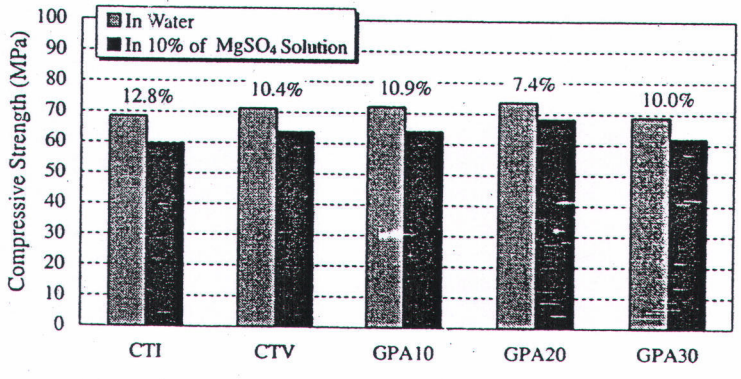

Fig. 6. Compressive strength of high-strength concretes cured in water and immersed in a 10% $MgSO_4$ solution for 180 days (values indicate the percentage loss in compressive strength of concrete).

all of which act together to enhance the resistance of concrete to sulfate attack [23,25]. In addition, the concrete samples incorporating 10% and 20% GPA had higher compressive strengths than that of CTV concrete even after storage in sulfate solution for up to 180 days. At 180 days, the compressive strengths of GPA10, GPA20, and GPA30 concretes placed in sulfate solution were 64.1, 68.3, and 62.1 MPa, respectively. Compared to the samples cured in water, these values represent reductions in compressive strength of 10.9%, 7.4%, and 10.0%, respectively. GPA20 concrete showed the highest compressive strength and the lowest loss of compressive strength among the GPA concretes. The obtained results suggested that the use of 20% GPA produces concrete with sulfate resistance comparable to that of Type V Portland cement concrete.

4. Conclusions

Based on the results of this study, the following conclusions can be made.

1. Ground POFA with high fineness (GPA) can be used as a cement replacement to produce high-strength concrete with a compressive strength as high as 70 MPa at 90 days when used to replace Type I Portland cement at 20% by weight of binder. At the age of 28 days, concretes containing 10–30% GPA exhibited higher compressive strength than concrete made from Type I Portland cement.
2. Use of GPA in high-strength concrete resulted in a slight reduction of concrete drying shrinkage as compared to the high-strength concrete made from Type I Portland cement, depending on the amount of GPA added.
3. Increasing the proportion of GPA in high-strength concrete reduces the water permeability of concrete. All high-strength concretes containing GPA had water permeability between 3.11×10^{-14} and 4.62×10^{-14} m/s, which were about half that of high-strength concrete made from Type I Portland cement.
4. High-strength concrete containing GPA showed better resistance in a 10% $MgSO_4$ solution. Concretes containing GPA showed a smaller degree of expansion and loss in compressive strength than high-strength concrete made from Type I Portland cement. In addition, the use of 20% GPA in high-strength concrete showed the highest resistance to a 10% $MgSO_4$ solution attack, comparable to that of high-strength concrete made from Type V Portland cement.

Acknowledgments

The authors are grateful for financial supports from the Thailand Research Fund (TRF) under the TRF Senior Research Scholar, Contract No. RTA5080020, the Royal Golden Jubilee Ph.D. Program, and the Commission on Higher Education, Ministry of Education, Thailand.

References

[1] American Concrete Institute (ACI) Committee 363. State-of-the-art report on high-strength concrete. ACI 363R-92. In: ACI manual of concrete practice part I; 2005.
[2] Kosmatka SH, Kerkhoff B, Panarese WC. Design and control of concrete mixtures. 14th ed. Portland Cement Association; 2002.
[3] Hussin MW, Awal ASMA. Palm oil fuel ash—a potential pozzolanic material in concrete construction. In: International conference on urban engineering in Asian cities in the 21st century, Bangkok, Thailand; 1996. p. D361–6.
[4] Jaturapitakkul C, Kiattikomol K, Tangchirapat W, Saeting T. Evaluation of the sulfate resistance of concrete containing palm oil fuel ash. Constr Build Mater 2007;21(7):1399–405.
[5] Paya J, Monzo J, Borrachero MV, Mora EP, Lopez EG. Mechanical treatment of fly ashes part II: particles morphologies in ground fly ashes (GFA) and workability of GFA mortar–cement mortars. Cem Concr Res 1995;26(2):225–35.
[6] Cheerarot R, Jaturapitakkul C. A study of disposed fly ash from landfill to replace Portland cement. Waste Manage 2004;24(7):701–9.
[7] Kiattikomol K, Jaturapitakkul C, Songpiriyakij S, Chutubtim S. A study of ground coarse fly ashes with different finenesses from various sources as pozzolanic materials. Cem Concr Compos 2001;23(4–5):335–43.
[8] ASTM C618. Standard specification for coal fly ash and raw or calcined natural pozzolan for use as a mineral admixture in concrete. Annual book of ASTM standards, vol. 04.02; 2001. p. 310–3.
[9] ASTM C596. Standard test method for drying shrinkage of mortar containing hydraulic cement. Annual book of ASTM standards, vol. 04.01; 2001. p. 331–3.
[10] Khatri RP, Sirivivatnanon V. Methods for the determination of water permeability. ACI Mater J 1997;94(3):257–61.
[11] Chindaprasirt P, Homwuttiwong S, Jaturapitakkul C. Strength and water permeability of concrete containing palm oil fuel ash and rice husk–bark ash. Constr Build Mater 2007;21(7):1492–9.
[12] Zhang MH, Malhotra VM. High-performance concrete incorporating rice husk ash as a supplementary cementing material. ACI Mater J 1996;93(6):629–36.
[13] Isaia GC, Gastaldini ALG, Moraes R. Physical and pozzolanic action of mineral additions on the mechanical strength of high-performance concrete. Cem Concr Compos 2003;25(1):69–76.
[14] Barr B, Hoseinian SB, Beygi MA. Shrinkage of concrete stored in natural environments. Cem Concr Compos 2003;25(1):19–29.
[15] Huo XS, Al-Omaishi N, Tadros MK. Creep, shrinkage, and modulus of elasticity of high-performance concrete. ACI Mater J 1998;98(6):440–9.
[16] Haque MN. Strength and drying shrinkage of high-strength concretes. Cem Concr Compos 1996;18(5):333–42.
[17] Haque MN, Kayali O. Properties of high-strength concrete using a fine fly ash. Cem Concr Res 1998;28(10):1445–52.
[18] El-Dieb AS, Hooton RD. Water-permeability measurement of high performance concrete using a high-pressure triaxial cell. Cem Concr Res 1995;25(6):1199–208.
[19] Tian B, Cohen MD. Does gypsum formation during sulfate attack on concrete lead to expansion? Cem Concr Res 2000;30(1):117–23.
[20] Gonzalez MA, Irassar EF. Ettringite formation in low C_3A Portland cement exposed to sodium sulfate solution. Cem Concr Res 1997;27(7):1061–72.
[21] ASTM C150. Standard specification for Portland cement. Annual book of ASTM standards, vol. 04.01; 2001. p. 149–55.
[22] Irassar EF, Gonzalez M, Rahhal V. Sulphate resistance of type V cements with limestone filler and natural pozzolan. Cem Concr Compos 2000;22(5):361–8.
[23] Thomas KK, Savva AE. Resistance of fly ash and natural pozzolans blended cement mortars and concrete to carbonation, sulfate attack, and chloride ion penetration. In: Proceedings of the seventh CANMET/ACI international conference on fly ash, silica fume, slag, and natural pozzolan in concrete, Chennai, India; 2001. p. 276–93.
[24] Cao HT, Bucea L, Ray A, Yozghatlian S. The effect of cement composition and pH of environment on sulfate resistance of Portland cements and blended cements. Cem Concr Compos 1997;19(2):161–71.
[25] Shannag MJ, Shaia HA. Sulfate resistance of high-performance concrete. Cem Concr Compos 2003;25(3):363–9.

6. W. Tangchirapat, C. Jaturapitakkul, K. Kiattikomol. Compressive strength and expansion of blended cement mortar containing palm oil fuel ash, Journal of Materials in Civil Engineering, Technical Note, 21 (2009), 426-431. (IF 0.526)

Compressive Strength and Expansion of Blended Cement Mortar Containing Palm Oil Fuel Ash

Weerachart Tangchirapat[1]; Chai Jaturapitakkul[2]; and Kraiwood Kiattikomol[3]

Abstract: This research aims to utilize palm oil fuel ash (POFA) as a pozzolanic material for replacing portland cement. POFA was ground by ball milling until the median particle sizes were 19.91 (G1P) and 10.18 μm (G2P). portland cement Type I was replaced by all POFA of 10–40% by weight of the binder. The effects of POFA fineness on the setting times, compressive strength, and expansion of mortars exposed to a 5% $MgSO_4$ solution were investigated. It was found that the use of POFA to replace portland cement Type I caused an increase in water demand for normal consistency and setting times, depending on the fineness and level replacement of POFA. With 10% replacement of portland cement Type I by G1P or G2P, the compressive strengths of the POFA mortars were 102–104% of that of portland cement Type I mortar at 90 days. For sulfate resistance, the expansions at 1 year for all mortar bars containing G1P or G2P were less than those of mortar bars made from portland cement Types I and V. The results suggest that ground POFA is a good pozzolanic material and can be used to increase both the compressive strength and the sulfate resistance of mortar.

DOI: 10.1061/(ASCE)0899-1561(2009)21:8(426)

CE Database subject headings: Ashes; Cements; Mortars; Recycling; Compressive strength.

Introduction

Thailand is an agricultural country; so, besides the agricultural products, the agroindustries also produce agrowastes. Palm oil residue, obtained from palm oil mills, is one of those products. In 2004, the production of palm oil fruits in Thailand was about 5.18 million tons (Office of the Agricultural Economics 2006) and its residue was estimated to be 2.59 million tons. Nowadays, palm oil residue is used as a fuel in biomass power plants and a by-product, in the form of ash, is produced that is about 5% by weight of the residue or about 0.13 million tons per year. The utilization of palm oil fuel ash (POFA) is minimal while its quantity increases annually. Most POFA is disposed of as waste in landfills, thus causing environmental problems.

POFA is one of the agrowaste ashes that has a large amount of silica in its chemical composition, which may be used as a cement replacement like rice-husk ash (Ikpong and Okpala 1992) and sawdust ash (Elinwa and Mahmood 2002). However, the use of POFA as a pozzolanic material to partially replace portland cement is not well known and only a small amount of research has been undertaken on this topic. Tay (1990) had used ash from palm oil waste to replace portland cement and had shown that it had low pozzolanic properties; he recommended that POFA should not be used as a cement substitute for more than 10% by weight of a binder. The low pozzolanic property of POFA from Tay's work is due to the large size of the ash particles, thus resulting in a very low rate of pozzolanic reaction.

Sulfate in soils, groundwater, and seawater reacts with various phases of hydrated cement paste leading to expansion, cracking, and spalling. Many researchers reported that the low water to binder ratio, the low C_3A content in cement, and using pozzolans can improve the sulfate resistance of concrete (Irassar et al. 2000; Shasiprakash and Thomas 2001; Ramyar and Inan 2006). Sideris and Savva (2001) studied the sulfate resistance of cement mortar and concrete that contain fly ash and natural pozzolans in their blend. They concluded that the use of natural pozzolans and fly ashes increased the sulfate resistance of concrete. The improved sulfate resistance of mortar or concrete mixed with pozzolans is attributed to the pozzolanic reaction, which leads to a refinement of the pore structure and also a reduction in $Ca(OH)_2$.

Therefore, the objective of this research was to study the potential of using POFA as a pozzolanic material in cement mortar. Grinding was used to improve the reactivity of POFA. The effects of ground POFA with two different degrees of fineness on compressive strength and expansion of cement mortar exposed to a 5% $MgSO_4$ solution were investigated.

Materials

The main materials used in this investigation were: portland cement Types I (CT1) and V (CT5), river sand, POFA, and $MgSO_4$ (commercial grade). POFA was collected from a biomass power

[1]Lecturer, Faculty of Engineering, Dept. of Civil Engineering, Khon Kaen Univ. (KKU), Khon Kaen 40002, Thailand. E-mail: taishici@hotmail.com

[2]Professor, Faculty of Engineering, Dept. of Civil Engineering, King Mongkut's Univ. of Technology Thonburi (KMUTT), Bangkok 10140, Thailand (corresponding author). E-mail: chai.jat@kmutt.ac.th

[3]Associate Professor, Faculty of Engineering, Dept. of Civil Engineering, King Mongkut's Univ. of Technology Thonburi (KMUTT), Bangkok 10140, Thailand. E-mail: kraiwood.kia@kmutt.ac.th

Note. This manuscript was submitted on April 2, 2008; approved on February 5, 2009; published online on July 15, 2009. Discussion period open until January 1, 2010; separate discussions must be submitted for individual papers. This technical note is part of the *Journal of Materials in Civil Engineering*, Vol. 21, No. 8, August 1, 2009. ©ASCE, ISSN 0899-1561/2009/8-426–431/$25.00.

plant in the south of Thailand. It is a by-product of burning palm oil residue at a controlled temperature of 800–900°C. The original POFA—received directly from the power plant—was sieved through a 1.18 mm (No. 16) sieve to remove large particles, foreign materials, and unburnt palm fibers, which comprised about 5% by weight of the ash. The sieved POFA was called G0P. To study the effect of fineness on the pozzolanic reaction, the quality of the G0P was improved by grinding it into two different finenesses with a ball mill. The abbreviations G1P and G2P were used to identify the ground POFA as small and very small particle sizes with median particle sizes (d_{50}) of 19.91 and 10.18 μm, respectively.

Experimental Program

The physical properties of CT1, CT5, and all POFA (G0P, G1P, and G2P), were investigated for the specific gravity and weight retained on a 45 μm (No. 325) sieve. In addition, the morphology of the materials was recorded by a scanning electron microscope (SEM). The chemical compositions of CT1, CT5, and POFA (G2P) were analyzed by an X-ray fluorescence spectrometer.

CT1 was partially replaced by G0P, G1P, or G2P at rates of 0, 10, 20, 30, and 40% by weight of the binder. The Vicat needle was used to study the normal consistency and setting times of the cement pastes and pastes containing POFA.

The effects of POFA with different particle sizes and levels of cement replacement on the compressive strength and sulfate resistance of mortar were investigated. A standard mortar cube of 50 mm was used to determine the compressive strength. A ratio of binder materials (portland cement plus POFA) to river sand was set at a constant of 1:2.75 with a maintained flow of mortar in the range of 105–115%. All samples were removed from the molds after casting for 24 h and were cured in water at room temperature. The mortars were tested for compressive strength at the ages of 7, 28, 60, and 90 days. The average of compressive strength for each age was obtained from three mortars. The maximum permissible range between specimens at the same tested, age and the same mix proportion is 8.7% of the average as specified by ASTM C109 (2001d).

To test for the ability of sulfate resistance, the change in length of mortars was measured with a prism (cross section 25 × 25 mm, length 285 mm). After casting for 24 h, all specimens were removed from the molds. They were then immersed in a 5% $MgSO_4$ solution. The expansions of the mortar bars were measured during 364 days (about a year). The expansions of the POFA mortar bars were compared to those of the mortar bars made from CT1 and CT5.

Results and Discussion

Particle Shape

Fig. 1 shows the particle morphologies of all POFA. Most particles of G0P had a rather spherical and porous structure with an agglomeration of several particles [see Fig. 1(a)], whereas G1P and G2P had irregular and crushed shapes as shown in Figs. 1(b and c), respectively.

Specific Gravity and Fineness

The specific gravity and fineness of the materials used in this study are shown in Table 1. Fig. 2 shows the particle-size distributions of CT1, CT5 and all POFA. It was found that the percentage of G0P retained on a 45 μm (No. 325) sieve was 41.2%, which was higher than 34.0%. The percentages of G1P and G2P retained were 17.1 and 1.5%, respectively. The median particle size of G0P was 62.5 μm. After grinding, the median particle sizes of G1P and G2P were 19.9 and 10.1 μm or reduced by about 3 and 6 times, respectively. The specific gravity of G0P was 1.97 and increased to 2.17 and 2.33 for G1P and G2P, respec-

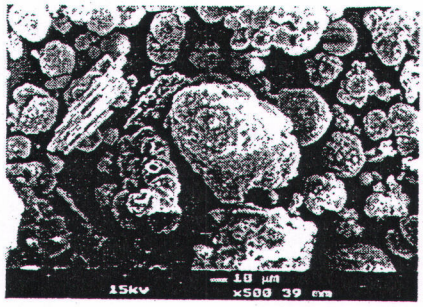

(a) Unground palm oil fuel ash (G0P)

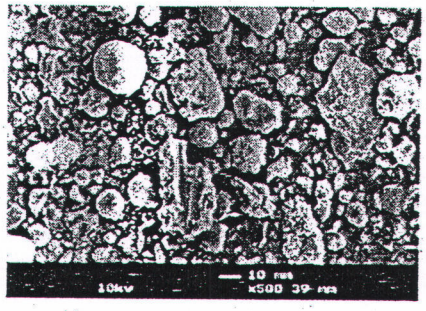

(b) Small size of palm oil fuel ash (G1P)

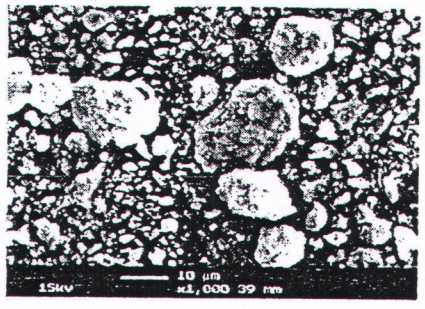

(c) Very small size of palm oil fuel ash (G2P)

Fig. 1. SEM images of POFA: (a) underground palm oil fuel ash (G0P); (b) small size of palm oil fuel ash (G1P); and (c) very small size of palm oil fuel ash (G2P)

Table 1. Physical Properties of Materials

Sample	Specific gravity	Retained on sieve No. 325 (%)	Median particle size, d_{50} (μm)
CT1	3.14	N/A	14.6
CT5	3.17	N/A	7.5
G0P	1.97	41.2	62.5
G1P	2.17	17.1	19.9
G2P	2.33	1.5	10.1

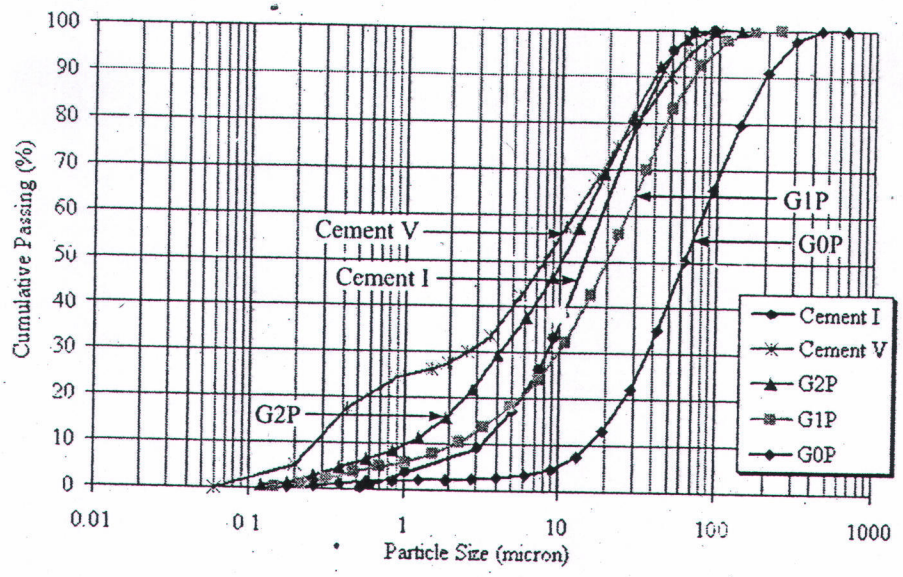

Fig. 2. Particle-size distribution of the materials

tively. It should be noted that the grinding process not only increased the fineness of the POFA, but also increased the specific gravity because the porous particles, which usually had low specific gravities, were crushed into smaller particles with lower porosity (Paya et al. 1995; Bouzoubaa et al. 1997; Jaturapitakkul and Cheerarot 2003).

Chemical Composition

The chemical compositions of the powders are tabulated in Table 2. Bogue compositions of cement, calculated in accordance with ASTM C 150 (2001c), showed that portland cement Type I had 6.8% of C_3A while portland cement Type V had 0% of C_3A.

The major chemical component of ground POFA (G2P) was 65.3% of SiO_2 which was more than one-half of the total chemical content. POFA had a total of 69.7% of SiO_2, Al_2O_3, and Fe_2O_3, which was close to the minimum requirement (70%) specified by ASTM C 618 (2001b). The loss on ignition (LOI) and SO_3 were 10.0 and 0.4%, respectively. According to the chemical compositions, POFA may be classified as a Class N pozzolan as prescribed by ASTM C 618 (2001b).

Table 2. Chemical Compositions of Materials

Chemical compositions (%)	CT1	CT5	POFA (G2P)
Silicon dioxide (SiO_2)	20.9	22.1	65.3
Aluminium oxide (Al_2O_3)	4.7	3.5	2.5
Iron oxide (Fe_2O_3)	3.4	5.5	1.9
Calcium oxide (CaO)	65.4	62.4	6.4
Magnesium oxide (MgO)	1.2	0.9	3.0
Sodium oxide (Na_2O)	0.2	0.0	0.3
Potassium oxide (K_2O)	0.3	0.1	5.7
Sulfur trioxide (SO_3)	2.7	1.0	0.4
Loss on ignition (LOI)	0.9	1.6	10.0
Tricalcium silicates (C_3S)	62.8	51.1	—
Dicalcium silicates (C_2S)	12.5	24.9	—
Tricalcium aluminate (C_3A)	6.8	0.0	—
Tetracalcium aluminoferrite (C_4AF)	10.3	16.8	—

Normal Consistency and Setting Time

Table 3 shows the normal consistency and setting times of cement paste and pastes incorporating POFA. All pastes mixed with G0P had higher normal consistencies (29.9–39.8%) than those of CT1 and CT5 pastes (25.9% and 27.1%, respectively). Pastes containing POFA also had longer initial setting times than the CT1 paste by about 14–33 min. After grinding to increase the fineness of the POFA (G1P and G2P), the normal consistencies of POFA pastes were in the range 26.6–31.9% with initial setting times between

Table 3. Normal Consistency and Setting Times of Cement Pastes and Pastes Mixed with POFA

Type of paste	Water requirement of paste (%)	Initial setting time (min)	Final setting time (min)
CT1	25.9	114	180
CT5	27.1	120	210
G0P10	29.9	128	210
G0P20	32.1	132	225
G0P30	34.5	139	225
G0P40	39.8	147	240
G1P10	27.3	124	195
G1P20	28.7	127	195
G1P30	30.1	131	210
G1P40	31.9	137	225
G2P10	26.6	120	180
G2P20	28.1	124	195
G2P30	29.2	130	210
G2P40	30.9	133	210

Note: G0P, G1P, and G2P=unground, small, and very small palm oil fuel ash, respectively. 10, 20, 30, and 40=percent replacement of palm oil fuel ash in portland cement Type 1 by weight of the binder.

Table 4. Compressive Strength of Mortars

Mortar	$\frac{W}{(C+P)}$	Flow	Water requirement (%)	Compressive strength (MPa–%) 7 days	28 days	60 days	90 days
CT1	0.67	111	100	32.7–***100***	42.8–***100***	48.9–***100***	51.5–***100***
CT5	0.67	108	100	28.1–***86***	42.1–***98***	49.5–***101***	53.2–***103***
G0P10	0.68	105	101	27.0–***83***	37.4–***87***	45.3–***93***	48.4–***94***
G0P20	0.70	109	104	24.8–***74***	31.3–***73***	36.8–***75***	39.9–***77***
G0P30	0.72	107	107	17.6–***54***	28.3–***66***	32.5–***66***	35.0–***68***
G0P40	0.73	108	109	13.1–***40***	18.9–***44***	24.5–***50***	25.9–***50***
G1P10	0.66	107	99	31.2–***96***	40.3–***94***	48.8–***100***	52.5–***102***
G1P20	0.67	111	100	29.3–***90***	38.1–***89***	46.4–***95***	50.0–***97***
G1P30	0.68	112	101	25.3–***78***	35.4–***83***	43.4–***89***	46.4–***90***
G1P40	0.69	107	103	21.3–***65***	30.3–***71***	35.9–***73***	38.4–***75***
G2P10	0.66	107	99	31.9–***98***	42.0–***98***	50.0–***102***	53.6–***104***
G2P20	0.67	111	100	29.5–***90***	40.6–***95***	48.9–***100***	52.1–***101***
G2P30	0.67	106	100	27.7–***85***	38.7–***90***	46.0–***94***	49.2–***95***
G2P40	0.68	109	101	25.5–***78***	33.8–***79***	40.1–***82***	42.9–***83***

Note: Bold-italic number indicate percentage of compressive strength as compared to that of CT1 mortar.

120 and 137 min. The normal consistencies and setting times of all pastes containing POFA were higher than those of the CT1 paste, depending on the levels of replacement and fineness of the POFA. The use of a finer POFA decreased the normal consistency and reduced the setting times of the pastes as compared to the coarser one. These results support the finding that G0P has high porosity, thus absorbing water during mixing. The higher POFA content resulted in reducing the C_3S, increasing the LOI in the pastes, and thus increasing the setting times (Berg and Kukko 1991).

The final setting times of all pastes containing POFA were in the range of 180–240 min while those of the CT1 and CT5 pastes were 180 and 210 min, respectively. According to ASTM C 595 (2001a), for blended cement the initial and final setting times of the blended cement paste should not be less than 45 min and not more than 420 min, respectively. In this study, the setting times of all POFA pastes were within the specified limits.

Effect of POFA on Compressive Strength of Mortar

The compressive strength of mortars and their strength relative to that of the CT1 mortar are given in Table 4. The water to binder ratio of all mortars containing POFA, when keeping a constant flow of 110 ± 5%, varied in the range of 0.66–0.73, while the CT1 and CT5 mortars had the same water to binder ratio of 0.67.

The compressive strengths of all mortars mixed with G0P were always lower than that of the CT1 mortar at the same age up to 90 days. The result also revealed that the higher the percentage of replacement by G0P in portland cement, the lower the compressive strength of the G0P mortar. For example, the compressive strengths of G0P10, G0P20, G0P30, and G0P40 mortars at the age of 7 days were 27.0, 24.8, 17.6, and 13.1 MPa, respectively, while those of CT1 and CT5 mortars were 32.7 and 28.2 MPa, respectively. It was also observed that the compressive strength of G0P mortars was reduced by one-half with an increase in the replacement of G0P from 10 to 40%. The G0P20 mortar had compressive strengths of 24.8 and 31.3 MPa or 74 and 73% of CT1 mortar at 7 and 28 days, respectively. These compressive strengths are lower than 75% of CT1 mortar and indicate that unground POFA is not suitable for use as a pozzolanic material as specified by ASTM C 618 (2001b).

After increasing the fineness of the POFA by grinding, the compressive strength of G1P10, G1P20, G1P30, and G1P40 mortars increased to be 31.2, 29.3, 25.3, and 21.3 MPa or 96, 90, 78, and 65% of CT1 mortar, respectively, at 7 days. At 28 days, the G1P20 mortar had a compressive strength of 38.1 MPa or 89% of CT1 mortar, which was 14% higher than the minimum value specified by ASTM C 618 (2001b), and tended to increase above this value at later ages.

The compressive strengths of the G2P mortars were slightly greater than those of the G1P mortars. For example, at 90 days, the compressive strengths of G1P20 and G2P20 mortars were 50.0 and 52.1 MPa, respectively. Additionally, when G2P is used at 10 and 20% replacement levels, the compressive strength of the G2P mortars were as high as that of the CT1 mortar (101–104%) at the age of 90 days. This indicated that POFA is not an inert material. Thus, the additional compressive strength of G2P mortars is due to the pozzolanic reaction between $Ca(OH)_2$ and SiO_2 as well as the filler effect of the small particle sizes of G2P, which enhance the compressive strength of mortars. This behavior was also found as the result of using ground bottom ash and ground coarse fly ash as pozzolanic materials (Kiattikomol et al. 2001; Jaturapitakkul and Cheerarot 2003).

The effects of replacement and fineness of POFA on the compressive strength of mortars are shown in Fig. 3. It can be observed in Fig. 3(a) that the higher is the replacement level of G0P, the lower is the compressive strength of the mortar. However, the use of improved quality POFA (G1P and G2P) to replace portland cement gives better results. Figs. 3(b and c) show that the replacements of G1P and G2P at the rates of 10 and 20% by weight of the binder give the highest compressive strengths of G1P and G2P mortars, respectively, after 90 days. The results of compressive strength of the mortars suggest that G1P and G2P are good pozzolanic materials. Their fineness is one of the major factors that increases the compressive strength and confirms the results for other pozzolanic materials such as fly ash (Kiattikomol et al. 2001) and rice-husk ash (Ikpong and Okpala 1992).

Effect of POFA on Expansion of Mortar Bar

The CT1 mortar bar was cracked along its edges and the specimen was bent due to uneven and fast expansion. The relationship

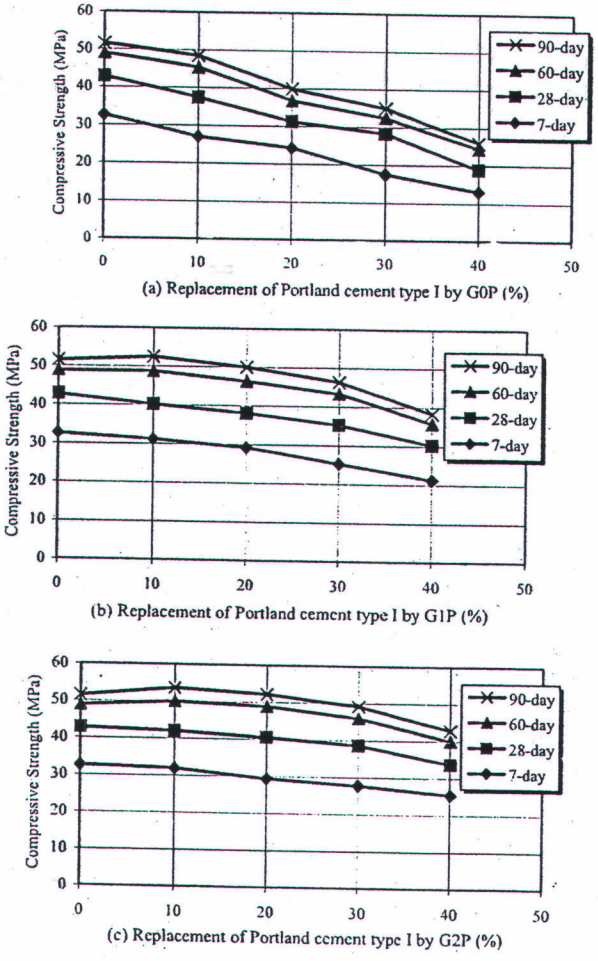

Fig. 3. Relationship between compressive strength of mortar and percent replacement of CT1 by POFA: replacement of CT1 by (a) G0P (%); (b) G1P (%); and (c) G2P (%)

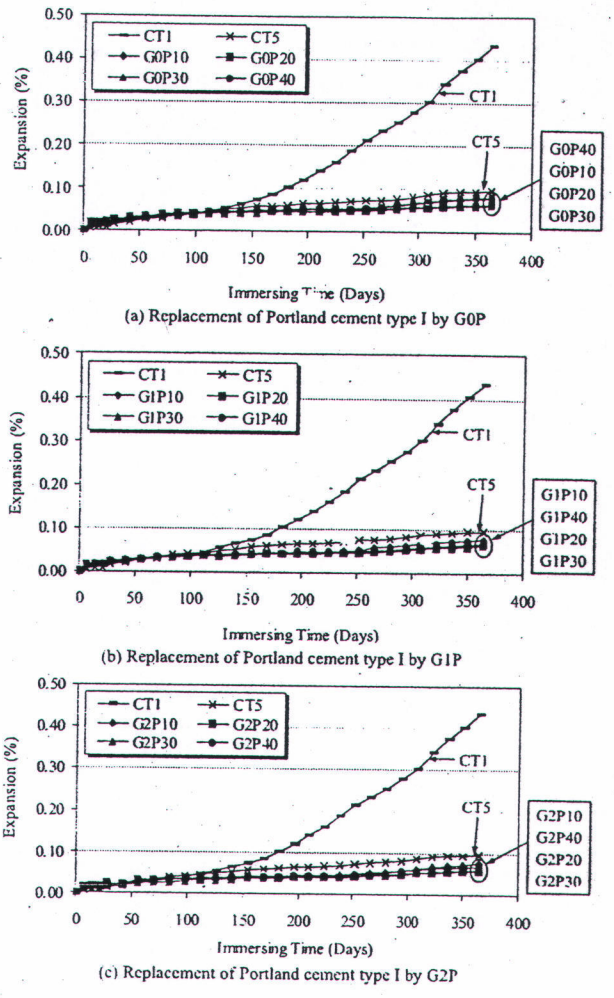

Fig. 4. Relationship between expansion and immersing time of mortar bars in a 5% $MgSO_4$ solution: replacement of CT1 by (a) G0P; (b) G1P; and (c) G2P

between the expansion of the mortar bars and the time for which they were immersed in a 5% $MgSO_4$ solution is shown in Fig. 4.

It was found that the CT1 mortar bar had the highest expansion and was 0.434% at 364 days while the CT5 mortar bar had 0.097% expansion at the same age. It was observed that the expansion values of the CT5 mortar bar was still about 0.1%, even though CT5 does not contain C_3A. These results indicated that C_3A was not the sole parameter causing the mortar to expand in a sulfate environment (Al-Amoudi 1998).

The values for the expansion of the G0P, CT1, and CT5 mortar bars are shown in Fig. 4(a). The use of G0P at all replacement rates can reduce the expansion of the mortar bar. The expansions of the G0P mortar bars were in the range of 0.065–0.083% at 364 days. It should be noted that the replacement of CT1 by 10–40% of G0P significantly reduced the expansion of mortar bars as compared to the CT1 mortar bar, although the compressive strengths of G0P mortars at all test ages were lower than those of the CT1 mortar. In addition, the amount of mixing water in the G0P mortar bars was higher than that in the CT1 mortar bar, especially in G0P40 mortar. This resulted in increased porosity of the G0P mortar bars. Additionally, the G0P mortar bars had many voids due to their large and porous particles [see Fig. 1(c)]. These voids and pore structures may allow space for ettringite and for gypsum formation during a sulfate attack. Similar results were obtained by Moukwa (1990) and Irassar and Batic (1989), who found that the ettringite crystals develop slowly by filling pore structures.

Although the expansions of the mortar bars were reduced by using G0P to replace portland cement, the compressive strengths of the G0P mortars were too low. Thus, G0P is not suitable for use as a pozzolanic material in concrete.

Figs. 4(b and c) show the expansion of mortar bars using G1P and G2P, respectively, to replace CT1. The expansions of the G1P and G2P mortar bars were lower than those of CT1 and CT5 mortar bars and were also lower than those of G0P mortar bars. This occurs because the replacement of CT1 by G1P or G2P reduces not only the C_3A but also the $Ca(OH)_2$, which affects the expansion of the mortar bar. After 364 days of immersion in a sulfate solution, G1P10, G1P20, G1P30, and G1P40 mortar bars had expansions of 0.079, 0.065, 0.062, and 0.069%—or about 6 to 7 times lower than that of the CT1 mortar bar. The mortar bars mixed with G2P had expansions at 364 days of 0.076, 0.061, 0.059, and 0.067% for replacement rates of 10, 20, 30, and 40%, respectively. It was observed that 30% replacement of G1P and G2P resulted in the lowest expansion for each group, and the

expansion was slightly increased when the replacement of G1P or G2P was increased to be 40%. However, the expansion of mortar bars mixed with 40% of G1P and G2P was lower than that of the control mortar bars (CT1 and CT5).

Environmental and Economic Consideration

The results suggested that ground POFA (G1P and G2P) is a good pozzolanic material to be used as a partial cement replacement to increase sulfate resistance. The fineness of POFA does not have much influence on expansion but has a major effect on the compressive strength of mortar. However, the utilization of POFA is minimal while its quantity increases annually with an increase in energy demands since palm oil is one of the major raw materials used to produce biodiesel. Thus, most POFA is disposed of as waste in landfills, which is expensive and is a major threat to the environment. The use of POFA as a partial cement replacement in concrete not only reduces the disposal waste in landfill, but also leads to the reduction of cement usage, results in a reduction of CO_2 emissions, and is good for the environment. For economic considerations, the cost of a pozzolanic material is usually low and certainly well below that of portland cement. Since POFA is a by-product the cost of POFA is, therefore, zero. The major cost of POFA depends on the process of reducing its particle size to an effective size. In this study, the cost of ground POFA is cheaper than portland cement. Additionally, the writers think that the grinding energy of POFA is still lower than that of portland cement clinker.

Conclusions

Based on the experimental results of this study, the following conclusions can be drawn:

1. The use of POFA to replace CT1 gives a higher normal consistency and longer setting times than those of CT1 paste.
2. Although unground POFA can reduce the expansion of mortar bars exposed to a 5% $MgSO_4$ solution, it is not suitable for use as a pozzolanic material because it produces mortar with a low compressive strength.
3. The mortars containing 10 and 20% of G1P and G2P exhibit a compressive strength as high as that of mortar made from CT1 at 90 days. At a replacement rate of 30%, the compressive strengths of mortars G1P or G2P at 90 days are more than 90% of those of CT1 mortar and produce a very low expansion in a sulfate environment.
4. The use of 10–20% of ground POFA to replace CT1, result in a sulfate resistance as good as is achieved with the use of CT5. The results also encourage the researchers to undertake further study on the use of POFA in concrete, which we hope will lead to a reduction in the cost of concrete as well as a method for the disposal of POFA.

Acknowledgments

The writers gratefully acknowledge financial support from the Thailand Research Fund (TRF) under TRF Senior Research Scholar (Contract No. RTA5080020) and the Royal Golden Jubilee Ph.D. Program, and the Commission on Higher Education, Ministry of Education, Thailand.

References

Al-Amoudi, O. S. B. (1998). "Sulfate attack and reinforcement corrosion in plain and blended cements exposed to sulfate environments." *Build. Environ.*, 33(1), 53–61.

ASTM. (2001a). "Standard specification for blended hydraulic cements." *ASTM C595*, West Conshohocken, Pa.

ASTM. (2001b). "Standard specification for coal fly ash and raw or calcined natural pozzolan for use as a mineral admixture in portland cement concrete." *ASTM C618*, West Conshohocken, Pa.

ASTM. (2001c). "Standard specification for portland cement." *ASTM C150*, West Conshohocken, Pa.

ASTM. (2001d). "Standard test method for compressive strength of hydraulic cement mortars using 2-in. or [50-mm] cube specimens." *ASTM C109*, West Conshohocken, Pa.

Berg, V. W., and Kukko, H. (1991). "Fly ash in concrete properties and performance." *RILEM Rep. No. 7*, E & FN Spon, London.

Bouzoubaa, N., Zhang, M. H., Bilodeau, A., and Malhotra, V. M. (1997). "The effect of grinding on the physical properties of fly ashes and a portland cement clinker." *Cem. Concr. Res.*, 22(12), 1861–1874.

Elinwa, A. U., and Mahmood, Y. A. (2002). "Ash from timber waste as cement replacement material." *Cem. Concr. Compos.*, 24(2), 219–222.

Ikpong, A. A., and Okpala, D. C. (1992). "Strength characteristics of medium workability ordinary portland cement-rice husk ash concrete." *Build. Environ.*, 27(1), 105–111.

Irassar, E. F., and Batic, O. (1989). "Effects of low calcium fly ash on sulfate resistance of OPC cement." *Cem. Concr. Res.*, 19(2), 1945–202.

Irassar, E. F., Gonzalez, M., and Rahhal, V. (2000). "Sulphate resistance of type V cements with limestone filler and natural pozzolana." *Cem. Concr. Compos.*, 22(5), 361–368.

Jaturapitakkul, C., and Cheerarot, R. (2003). "Development of bottom ash as pozzolanic material." *J. Mater. Civ. Eng.*, 15(1), 48–53.

Kiattikomol, K., Jaturapitakkul, C., Songpiriyakij, S., and Chutubtim, S. (2001). "A study of ground coarse fly ashes with different finenesses from various sources as pozzolanic materials." *Cem. Concr. Compos.*, 23(4), 335–343.

Moukwa, M. (1990). "Charateristics of the attack of cement paste by $MgSO_4$ and $MgCl_2$ from the pore structure measurements." *Cem. Concr. Res.*, 20(1), 148–158.

Office of the Agricultural Economics. (2007). *Agricultural statistics of Thailand crop year 2006*, Center of Agricultural Information, Ministry of Agriculture and Cooperatives, Bangkok, Thailand.

Paya, J., Monzo, J., Borrachero, M. V., and Mora, E. P. (1995). "Mechanical treatment of fly ash. Part I: Physical-chemical characterization of ground fly ashes." *Cem. Concr. Res.*, 25(7), 1469–1479.

Ramyar, K., and Inan, G. (2007). "Sodium sulfate attack on plain and blended cements." *Build. Environ.*, 42(3), 1368–1372.

Shasiprakash, S. G., and Thomas, M. D. A. (2001). "Sulfate resistance of mortars containing high-calcium fly ashes and combinations of highly reactive pozzolans and fly ash." *Proc., Int. Conf. on Fly Ash, Silica Fume, Slag, and Natural Pozzolan in Concrete*, SP-199, American Concrete Institute, Mich., 221–237.

Sideris, K. K., and Savva, A. E. (2001). "Resistance of fly ash and natural pozzolans blended cement mortars and concrete to carbonation, sulfate attack and chloride ion penetration." *Proc., Int. Conf. on Fly Ash, Silica Fume, Slag, and Natural Pozzolan in Concrete*, SP-199, American Concrete Institute, Mich., 276–293.

Tay, J. H. (1990). "Ash from oil-palm waste as concrete material." *J. Mater. Civ. Eng.*, 2(2), 94–105.

7. N. Chusilp, C. Jaturapitakkul, K. Kiattikomol. Utilization of bagasse ash as a pozzolanic material in concrete, Construction and Building Materials, 23 (2009), 3352-3358. (IF 0.947)

Construction and Building Materials 23 (2009) 3352–3358

Contents lists available at ScienceDirect

Construction and Building Materials

journal homepage: www.elsevier.com/locate/conbuildmat

Utilization of bagasse ash as a pozzolanic material in concrete

Nuntachai Chusilp, Chai Jaturapitakkul *, Kraiwood Kiattikomol

Department of Civil Engineering, Faculty of Engineering, King Mongkut's University of Technology Thonburi, Bangkok 10140, Thailand

ARTICLE INFO

Article history:
Received 7 August 2008
Received in revised form 3 June 2009
Accepted 18 June 2009
Available online 24 July 2009

Keywords:
Bagasse ash
Pozzolanic material
Compressive strength
Heat evolution of concrete
Water permeability

ABSTRACT

The physical properties of concrete containing ground bagasse ash (BA) including compressive strength, water permeability, and heat evolution, were investigated. Bagasse ash from a sugar factory was ground using a ball mill until the particles retained on a No. 325 sieve were less than 5wt%. They were then used as a replacement for Type I Portland cement at 10, 20, and 30wt% of binder. The water to binder (W/B) ratio and binder content of the concrete were held constant at 0.50 and 350 kg/m^3, respectively.

The results showed that, at the age of 28 days, the concrete samples containing 10–30% ground bagasse ash by weight of binder had greater compressive strengths than the control concrete (concrete without ground bagasse ash), while the water permeability was lower than the control concrete. Concrete containing 20% ground bagasse ash had the highest compressive strength at 113% of the control concrete. The water permeability of concrete decreased as the fractional replacement of ground bagasse ash was increased. For the heat evolution, the maximum temperature rise of concrete containing ground bagasse ash was lower than the control concrete. It was also found that the maximum temperature rise of the concrete was reduced 13, 23, and 33% as compared with the control concrete when the cement was replaced by ground bagasse ash at 10, 20, and 30wt% of binder, respectively. The results indicate that ground bagasse ash can be used as a pozzolanic material in concrete with an acceptable strength, lower heat evolution, and reduced water permeability with respect to the control concrete.

1. Introduction

Type I Portland cement is currently widely used to build various constructions because of its high compressive strength. However, as the quantity of cement needed for construction projects increases, increasing amounts of raw materials from natural resources are consumed. If some of these raw materials can be replaced by cheaper materials of similar composition, the concrete production cost could be reduced without affecting its quality. For this reason, bagasse ash, the by-product from burning sugar cane (or bagasse) as a fuel to heat steam for electricity generation as well as the sugar extraction process, has been chosen for further investigation.

In general, bagasse ash is disposed of in landfills and is now becoming an environmental burden. It is estimated that more than 200,000 tons of bagasse ash are produced every year in Thailand [1], and this increases annually. Our study of bagasse ash for potential application in concrete production was introduced by Martirena et al. [2], who used different waste ashes from the sugar industry as pozzolanic materials in lime-pozzolan binders. They found that the sugar cane bagasse ash produced in the boilers of the sugar industry could be classified as a pozzolanic material. Subsequently, Singh et al. [3] found that the presence of 10% bagasse ash in concrete gave a higher compressive strength than that of their control concrete at all ages, and the chemical deterioration of the blended cement was less than that of the control concrete due to the pozzolanic reaction induced permeability reduction of bagasse ash. Ganesan et al. [4] studied the effects of bagasse ash content as a partial replacement for cement on the physical and mechanical properties of hardened concrete. They found that the bagasse ash is an effective mineral admixture, with 20% constituting an optimal cement replacement ratio.

Raw bagasse ash has a large particle size and a high porosity, so it needs more water content in the concrete mixture and thus results in a lower compressive strength of concrete. However, when bagasse ash is ground up into small particles, the compressive strength of concrete containing this ground bagasse ash improves significantly [5]. The optimum proportion of bagasse ash was found to be in the range of 10–20wt% of binder. Most studies of bagasse ash focus on the pozzolanic activity and hydration reaction of mortar. Very few studies have been carried out studying the water permeability and heat evolution of concrete containing bagasse ash. These are the properties of interest for concrete in isolated environments. Before application of bagasse ash in concrete, these properties must be investigated to make sure that it is a suitable material to use.

The aim of this paper is to study the compressive strength, water permeability, and heat evolution of concrete containing ground bagasse ash. The results are compared with the control concrete, i.e., concrete made using Portland cement as the sole

* Corresponding author. Tel.: +66 2 470 9131; fax: +66 2 427 9063.
E-mail address: chai.jat@kmutt.ac.th (C. Jaturapitakkul).

0950-0618/$ - see front matter © 2009 Elsevier Ltd. All rights reserved.
doi:10.1016/j.conbuildmat.2009.06.030

cementitious material. This knowledge could be beneficial for using this type of waste product in concrete, especially regarding the durability and heat reduction in mass concrete.

2. Experimental program

2.1. Materials

2.1.1. Cement and bagasse ash

ASTM Type I ordinary Portland cement was used in all concrete mixtures. Bagasse ash from a sugar factory in central Thailand was ground using a ball mill until the particles retained on a No. 325 sieve (with openings of 45 μm) were less than 5wt% and was assigned as BA. The physical properties and chemical composition of the cement and ground bagasse ash are listed in Tables 1 and 2, respectively.

2.1.2. Aggregates

Crushed limestone with a maximum size of 20 mm and a specific gravity of 2.67 was used as a coarse aggregate. River sand with a fineness modulus of 2.44 and a specific gravity of 2.65 was used as a fine aggregate.

2.2. Concrete mixtures

Ground bagasse ash (BA) was used to replace Type I Portland cement at 10, 20, and 30wt% of binder. The binder content and water to binder (W/B) ratio of all types of concrete were adjusted to be constant at 350 kg/m^3 and 0.50, respectively. The mix proportions are presented in Table 3. The slump of fresh concrete was controlled to remain in the range of 150–200 mm using superplasticizer.

2.3. Compressive strength

Concrete cylinders 100 mm in diameter and 200 mm in height were used to determine the compressive strength. The concrete samples were removed from their molds after casting for 24 h and cured in water until their testing age. The compressive strength of all concrete samples was determined at ages of 28 and 90 days.

Table 1
Physical properties of Type I Portland cement and ground bagasse ash (BA).

Sample	Retained on a 45-μm sieve (%)	Specific gravity
Cement	–	3.14
BA	2.8	2.20

Table 2
Chemical compositions of Type I Portland cement and ground bagasse ash (BA).

Chemical composition (%)	Type of sample	
	Cement	BA
Silicon dioxide, SiO_2	20.90	64.88
Aluminum oxide, Al_2O_3	4.76	6.40
Iron oxide, Fe_2O_3	3.41	2.63
Calcium oxide, CaO	65.41	10.69
Magnesium oxide, MgO	1.25	1.55
Sulfur trioxide, SO_3	2.71	1.56
Loss on ignition, LOI	0.96	8.16
$SiO_2 + Al_2O_3 + Fe_2O_3$	–	73.91

2.4. Water permeability

A steady flow method was applied to test the permeability of the concrete. The coefficient of the water permeability was determined by measuring the amount of water passing through the specimen and calculated using Darcy's Law and the equation of continuity [6].

$$K_f = \frac{\rho L g Q}{PA} \quad (1)$$

where K_f is the coefficient of water permeability of the specimen (m/s), ρ the density of water (kg/m^3), L the length of the specimen (m), g the acceleration due to gravity (m/s^2), Q the net flow rate (m^3/s), A the cross-sectional area of the specimen (m^2), and P is the water pressure [(kg m s^{-2})/(m^2)].

The samples were prepared by sawing 40 mm thick slice from the middle of the cylinder before testing the water permeability two days. After drying in the laboratory for 24 h, the concrete slices were cast in a 25 mm thick layer of non-shrinkage epoxy resin to prevent water leakage. The epoxy resin was allowed to harden and dry for another 24 h. The specimens were then installed in the housing cells, as shown in Fig. 1a, upon which a water pressure of 0.5 MPa was applied. This pressure was also used by both Chan and Wu [7] and Chindaprasirt et al. [8]. The time and the amount of water that passed through each of the specimens were monitored until a constant flow rate was obtained. The water permeability test apparatus is shown in Fig. 1b.

2.5. Heat evolution of concrete

The heat evolution of concrete containing ground bagasse ash under semi-adiabatic conditions was investigated. Ground bagasse ash (BA) was used to replace the Type I Portland cement at 10, 20, and 30wt% of binder. The mix proportion of the concrete used in this investigation was the same as that for the study of the compressive strength and water permeability. Concrete samples were cast in 450 mm cube molds lined with an insulator made of 50 mm expanded polystyrene on each side. The heat evolution, in terms of temperature rise, was measured by inserting a thermocouple into the center of the concrete specimen for a period of 168 h (7 days). The temperature rise of the concrete containing ground bagasse ash was compared with that of the control concrete. Fig. 2 shows a schematic representation of the concrete heat evolution test.

Note that the heat evolution of the concrete containing original bagasse ash was not examined since its compressive strength was much lower than that of the control concrete. This was because the particles of the original bagasse ash were large compared with those of Portland cement [9]. Thus, original bagasse ash is not suitable for use as a replacement for Portland cement.

3. Results and discussion

3.1. Physical properties of Portland cement and ground bagasse ash

The particle shapes of the cement and ground bagasse ash are shown in Fig. 3. The cement particles were angular and irregular while the original bagasse ash, particles had rough surfaces with high porosity ("spongy") and large surface areas. After the bagasse ash particles were ground, their shapes were small but they still had rough, porous surfaces.

It should be noted that the particle shape of bagasse ash is completely different from that of fly ash. Fly ash, melts at a temperature of about 1500 °C, forming spherically shaped particles. If the burn temperature is below 1500 °C, fly ash fails to melt and irregular particles are formed [10]. It has been reported that spongy particles are associated with partially burnt fragments of coal (carbon) resulting from incomplete combustion [11]. Bagasse ash, burns at a temperature of 600–800 °C; the sponge-like particle shape is obtained because this temperature is lower than the

Table 3
Mix proportions of concrete.

Sample	Mix proportion (kg/m^3)						W/B	Slump (mm)
	Cement	Bagasse ash	Fine aggregate	Coarse aggregate	Water	Super P		
35CT	350	–	824	1055	175	–	0.50	150
35BA10	315	35	816	1047	175	3.15	0.50	160
35BA20	280	70	808	1039	175	5.25	0.50	180
35BA30	245	105	800	1028	175	7.35	0.50	190

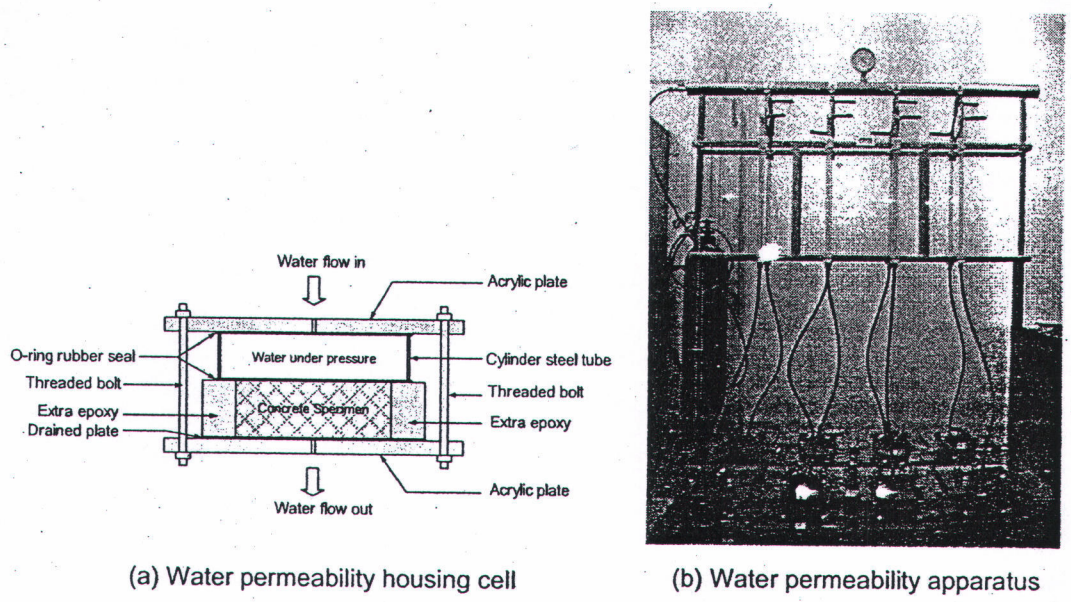

Fig. 1. Water permeability test.

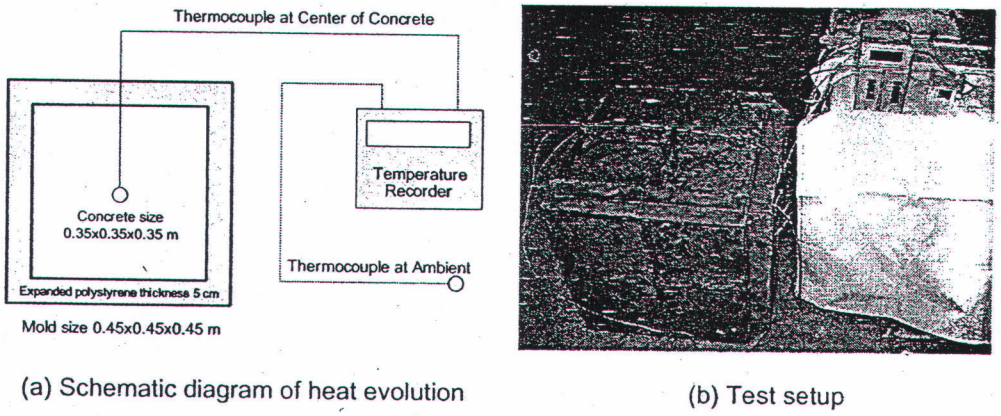

Fig. 2. Heat evolution test.

melting point of the bagasse ash. Spongy particles absorb the water used to mix the concrete, which decreases the functionality of concrete compared with that of concrete mixed with spherical fly ash particles.

The particle size distribution curves of the original and ground bagasse ash are shown in Fig. 4. The mean particle size of the original bagasse ash was 23 μm. After grinding, the bagasse ash had a mean particle size of 10 μm; the fraction of particles retained on a 45-μm sieve (No. 325) was 2.8%. The ground bagasse ash had a specific gravity of 2.2, which is lower than 3.14, the specific gravity of Type I Portland cement.

3.2. Chemical compositions of materials

Based on an assessment of the chemical compositions listed in Table 2, it follows that the $SiO_2 + Al_2O_3 + Fe_2O_3$ content of ground bagasse ash comprises more than 70% of the overall material composition. Note that the proportion of SiO_2 in bagasse ash is 64.88%, suggesting that bagasse ash contains a high content of important oxides suitable for a pozzolanic material.

The loss on ignition (LOI) content of ground bagasse ash is rather high at 8.16%, which close to the limit of 10% specified by the ASTM C 618 standard for class N pozzolan [12]. Other pozzolanic materials, such as rice husk ash have LOIs that can be as high as 66% [13]. However, the LOI of the ash decreases when the calcination temperature increases. Ganesan et al. [4] used bagasse ash with a LOI of 4.9% and found that this did not significantly affect the compressive strength of the concrete. For classified fly ash, LOI content increased the water demand of fresh concrete [14]. However, effects of LOI of bagasse ash on the properties of concrete have not been published.

3.3. Properties of fresh concrete

The control concrete (35CT) did not need superplasticizer to maintain the slump of fresh concrete at values between 150 and 200 mm. However, concretes containing ground bagasse ash required superplasticizer to maintain the specified slump (see Table 3). When the replacement of cement by ground bagasse ash was increased in proportion, the concrete needed more

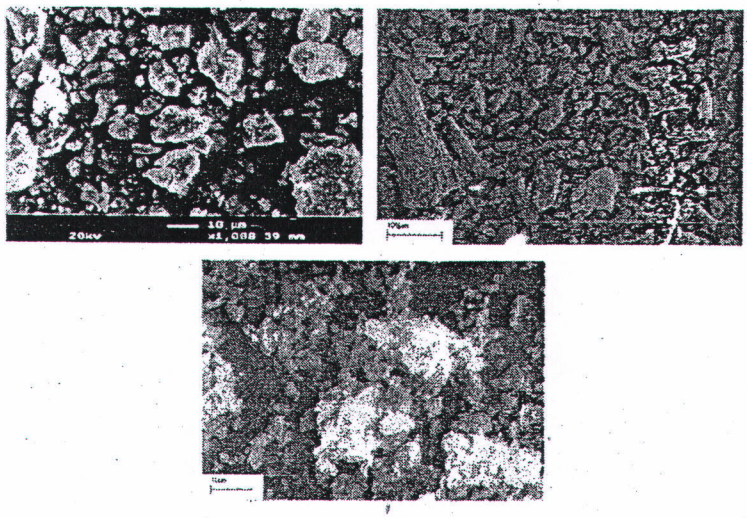

(a) Type I Portland cement (b) Origina bagasse ash (c) Ground bagasse ash

Fig. 3. Particle images of Portland cement and bagasse ashes.

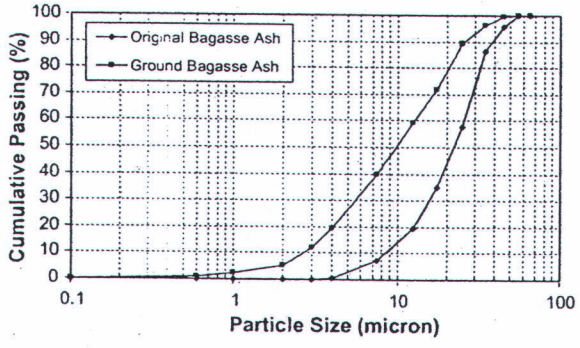

Fig. 4. Particle size distribution of bagasse ashes.

superplasticizer. For example, the control concrete did not require superplasticizer while concretes containing 10%, 20%, and 30% ground bagasse ash by weight of binder required 3.15, 5.25, and 7.35 kg/m^3, respectively, of superplasticizer. Because the particles of ground bagasse ash are angular, irregularly shaped, and characterized by a high porosity, like palm oil fuel ash and rice husk-bark ash [8], bagasse ash required more superplasticizer for lubrication to maintain the same workability as the control concrete.

3.4. Compressive strength of concrete

The compressive and normalized strength of concretes containing ground bagasse ash are included in Table 4. The control concrete (35CT) had a compressive strength of 36.9 MPa at the age of 28 days, which increased to 41.8 MPa after 90 days. Concretes containing 10%, 20%, and 30% ground bagasse ash by weight of binder (35BA10, 35BA20, and 35BA30, respectively) had compressive strengths of 38.2, 40.5, and 39.3 MPa or 104%, 110%, and 107% of the control concrete, and 44.4, 47.4, and 45.0 MPa, or 106%, 113%, and 108% of the control concrete at the ages of 28 and 90 days, respectively. These results show that ground bagasse ash is a good

Table 4
Compressive strength of concrete.

Sample	Compressive strength (MPa) – normalized compressive strength (%)	
	28 days	90 days
35CT	36.9–100	41.8–100
35BA10	38.2–104	44.4–106
35BA20	40.5–110	47.4–113
35BA30	39.3–107	45.0–108

pozzolanic material. "There are two factors responsible for the early strength (at 28 days) of the ground bagasse ash concrete compared to that of the control concrete (35CT). First, the pozzolanic reaction can be highly activated when the particle size is small [15]. In this experiment, the bagasse ash was ground by ball mill until the particles retained on a 45-μm sieve were less than 5wt% and had a mean particle size, d_{50}, of 10 μm. Thus, the pozzolanic reaction of the ground bagasse ash is very fast and can improve the compressive strength of concrete at an early age (at 28 days). Secondly, small particles of ground bagasse ash can fill the voids or air spaces in the concrete structure and thus produces denser concrete. This referred to as the filler or packing effect [16]".

The optimum fraction of ground bagasse ash replacing cement in concrete is 20wt% of binder, as this proportion exhibits the highest normalized compressive strength. Concretes containing 10% and 30% of ground bagasse ash by weight of binder also had a higher compressive strength than the control concrete. Note that the variation in the strength of the various concrete mixes was not large. The compressive strengths of concretes containing 10% and 30% of ground bagasse ash was 3–6% lower than that of the other bagasse ash concrete.

3.5. Water permeability of concrete

The water permeability and the water permeability ratio of concrete mixes are also given in Table 5. The water permeability ratio was defined as the water permeability of concrete containing

Table 5
Water permeability of concrete.

Sample	Permeability × 10^{-12}, k (m/s) – k/k_{CT}	
	28 days	90 days
35CT	1.32–1.00	1.26–1.00
35BA10	1.22–0.92	0.73–0.58
35BA20	1.08–0.82	0.48–0.38
35BA30	0.66–0.50	0.39–0.31

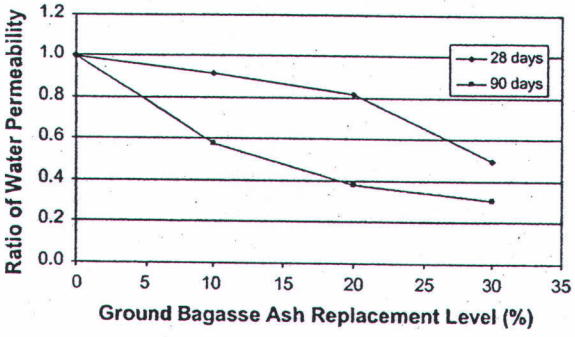

Fig. 5. Relationship between the ratio of water permeability of concrete and fraction replacement by ground bagasse ash.

ground bagasse ash with respect to that of the control concrete at the same age. The water permeability of the control concrete was 1.32×10^{-12} and 1.26×10^{-12} m/s at 28 and 90 days, respectively. These results agree with previous studies [8,17]. It is also found that the water permeability values of all concretes decreased with their curing age. For example, the water permeability values of the 35BA10 concrete were 1.22×10^{-12} and 0.73×10^{-12} m/s, with water permeability ratios of 0.92 and 0.58, at 28 and 90 days, respectively. These results suggest that the low water permeability of concrete was affected by the pozzolanic reaction of the ground bagasse ash. Note that the compressive strengths of 35CT and 35BA10 at the age of 90 days were not very different, at 41.8 and 44.4 MPa, respectively.

The relationship between the ratio of the water permeability of concrete and the fractional replacement by ground bagasse ash is shown in Fig. 5. The water permeability ratio of concrete decreased with increasing ground bagasse ash proportion in concrete. At the age of 28 days, water permeability ratios of 0.92 and 0.82 were obtained for concretes containing 10% and 20% ground bagasse ash. This result suggests that small particles of ground bagasse ash can help to fill the voids in the concrete structure, so that the water permeability of 35BA10 and 35BA20 was 80–90% of that of the control concrete. Concrete containing 30% ground bagasse ash had a water permeability ratio of 0.50 at the age of 28 days due to the high number of small particles from the ground bagasse ash filling the voids in the concrete. At 90 days, the water permeability ratios of 35BA10, 35BA20, and 35BA30 were 0.58, 0.38, and 0.31, respectively. The low water permeability values of concretes containing ground bagasse ash at 90 days were mostly caused by the pozzolanic reaction, which filled up the voids and increased the concrete density [8].

3.6. Relationship between compressive strength and water permeability of concrete

The relationship between the water permeability and the compressive strength of the concrete at 28 and 90 days are illustrated

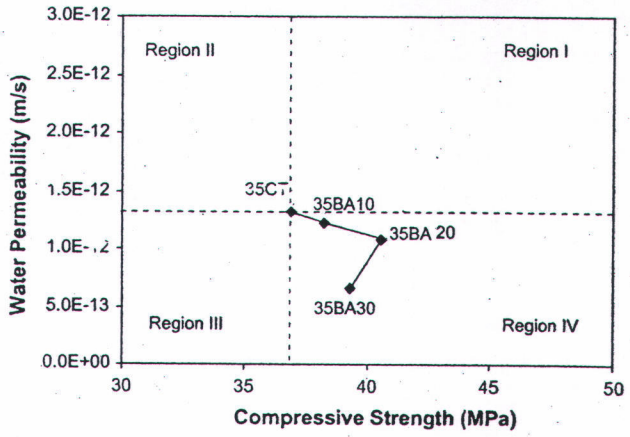

Fig. 6. Relationship between water permeability and compressive strength of concrete at age of 28 days.

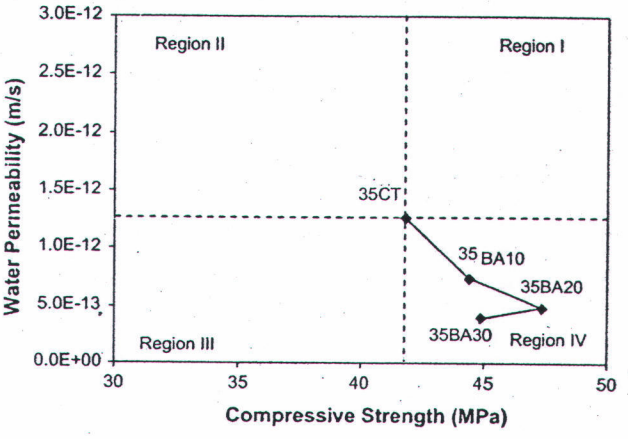

Fig. 7. Relationship between water permeability and compressive strength of concrete at age of 90 days.

in Figs. 6 and 7, respectively. The figures are divided into four regions. Region I represents concrete that has both a higher compressive strength and higher water permeability than the control concrete. Region II includes concrete of lower compressive strength but higher water permeability. Region III represents concrete that has both lower compressive strength and lower water permeability than the control concrete. Finally, concrete containing 10–30% ground bagasse ash by weight of binder are located in region IV; these are more impervious, or have lower water permeability, and also have a higher compressive strength than the control concrete. The water permeability of concrete decreased with an increasing proportion of ground bagasse ash. However, to obtain the highest compressive strength, it is recommended to use ground bagasse ash at 20% by weight of binder. At a replacement fraction of 10–20%, the combination of the pozzolanic reaction and the filling effect of the ground bagasse ash can improve the concrete property and make it more impervious. For a 30% replacement fraction, the pozzolanic reaction and filling effect still continues to cause low water permeability. However, the pozzolanic reaction filling effect does not compensate the loss of compressive strength due to high replacement of Portland cement, thus leading to a lower compressive strength of bagasse concrete as compared with the control concrete.

Table 6
Heat evolution of concrete.

Sample	Initial temp. (°C)	Max. temp. (°C)	Highest temp. rise (°C)	Reduce temp. (°C)	Reduce temp. (%)	Highest temp. rise (°C/100 kg of binder)	Time of highest temp. rise after casting (h)
35CT	27	57	30	–	0	8.57	13
35BA10	28	54	26	4	13	7.43	14
35BA20	30	53	23	7	23	6.57	15
35BA30	30	50	20	10	33	5.71	15

3.7. Heat evolution of concrete

Table 6 lists the highest temperature rise, the reduction in the temperature rise compared to the control concrete, and the time of the highest temperature rise after casting of concrete. The control concrete with a cement content of 350 kg/m^3 had a highest temperature rise of 30 °C after mixing for 13 h. For 35BA10, 35BA20, and 35BA30 concretes, the highest temperature rises were 26, 23, and 20 °C, respectively. The relationship between the temperature rise of the concretes containing ground bagasse ash and the time after casting is shown in Fig. 8.

The results of this study showed that the highest temperature rises of concrete with 10%, 20%, and 30% ground bagasse ash were lower than that of the control concrete by 4, 7, and 10 °C, or by 13%, 23%, and 33%, respectively. Higher replacement fractions of ground bagasse ash lower the cement content in the concrete, and thus reduce the concrete heat evolution [18].

The highest temperature rises in concrete per 100 kg of binder using different pozzolanic materials to replace Portland cement are shown in Fig. 9. The control concrete had the highest temperature rise of 8.57 °C/100 kg of binder. It should be noted that this result does not directly represent the temperature rise in thick sections or in mass concrete. Bamforth [19] reported that the temperature rise when casting a 300 mm cube of concrete in a block "hot box" was only 7 °C per 100 kg of ordinary Portland cement (OPC), compared with the measured in situ values of 12–13 °C per 100 kg of OPC. In addition, for a slab with a thickness greater than 2.5 m, the temperature rise was approximately constant at 12 °C per 100 kg of binder [20]. According to the recommendation of the ACI 207 [21] for the heat generated by cement hydration in the presence of little heat loss, 0.3–0.5 m thick concrete can be expected to reach a maximum temperature of 9 °C per 100 kg of OPC above its initial temperature at the age of 18–72 h.

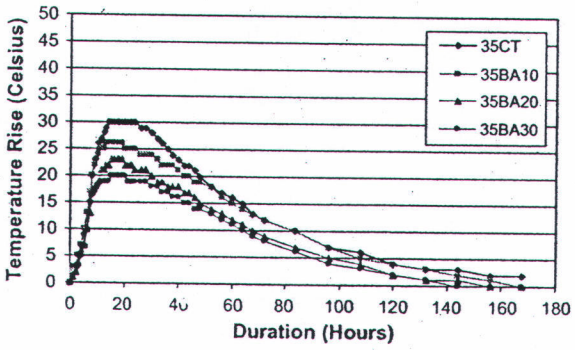

Fig. 8. Temperature rise of concrete versus duration time.

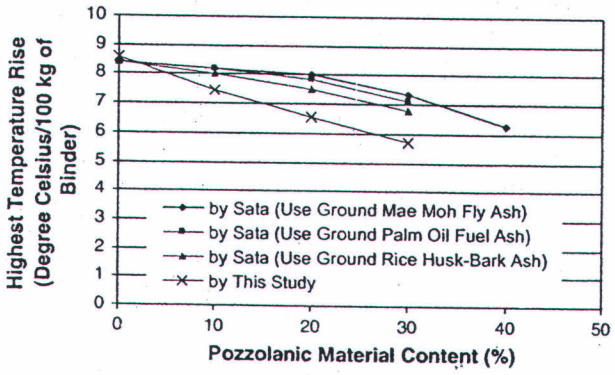

Fig. 9. Highest temperature rise in concrete per 100 kg of binder using different pozzolanic materials to replace Portland cement.

This study showed that concrete with ground bagasse ash replacements of 10, 20, and 30wt% of binder had the highest temperature rises of 7.43, 6.57, and 5.71 °C/100 kg of binder, respectively. This result is similar to that reported by Sata et al. [22], who used ground Mae Moh fly ash (MFA), ground palm oil fuel ash (POFA), and ground rice husk-bark ash (RHBA) as pozzolanic materials to replace Portland cement at 10%, 20%, and 30wt% of binder in concrete. They reported the highest temperature rises of 8.2, 8.0, and 7.3 °C/100 kg of binder for MFA, 8.2, 7.9, and 7.1 °C/100 kg of binder for POFA, and 8.0, 7.5, and 6.8 °C/100 kg of binder for RHBA, respectively. It should be noted that the concrete mix proportion in Sata's study had a W/B ratio of 0.28, while in this experiment used a W/B ratio of 0.50.

The time required to reach the highest temperature rise in ground bagasse ash concrete was delayed by 1–2 h compared with the control concrete (see Table 6). The higher the replacement fraction of Portland cement by ground bagasse ash, the longer the delay time to obtain the highest temperature rise. This may be due to the superplasticizer, which can delay the hydration reaction of concrete [23,24]. Alternatively, this could be caused by the smaller cement content in the ground bagasse ash concrete compared with the control concrete.

4. Conclusions

The following conclusions can be drawn based on the study of using ground bagasse ash to replace Type I Portland cement in concrete.

1. Concrete containing up to 30% ground bagasse ash had a higher compressive strength and a lower water permeability than the control concrete, both at ages of 28 and 90 days.
2. The optimum cement replacement fraction by ground bagasse ash was 20wt% of binder. A higher replacement proportion (30%) resulted in concrete with a lower water permeability and a lower compressive strength.
3. The maximum temperature rise of concrete containing 10–30% ground bagasse ash was lower than the control concrete. As the cement replacement fraction by ground bagasse ash was increased, the corresponding temperature rise in concrete became smaller.

4. Ground bagasse ash is a suitable pozzolanic material for use in concrete. The above results show a beneficial application of this by-product material.

Acknowledgement

We would like to thank the Office of the Higher Education Commission, Thailand for supporting by grant fund under the program Strategic Scholarships for Frontier Research Network for the Ph. D. Program Thai Doctoral degree for this research. Thank also extend to the Thailand Research Fund (TRF) for the financial support under the TRF Senior Research Scholar, Contract No. RTA5080020.

References

[1] Office of Cane and Sugar Board. Report on total cane crushing and sugar production 2006/2007. Thailand: Ministry of Industry; 2007.
[2] Martirena JF, Middendorf B, Gehrke M, Budelmann H. Use of wastes of sugar industry as pozzolana in lime-pozzolana binders: study of the reaction. Cem Concr Res 1998;28:1525–36.
[3] Singh NB, Singh VD, Rai S. Hydration of bagasse ash-blended Portland cement. Cem Concr Res 2000;30:1485–8.
[4] Ganesan K, Rajagopal K, Thangavel K. Evaluation of bagasse ash as supplementary cementitious material. Cem Concr Comp 2007;29:515–24.
[5] Cordeiro GC, Toledo Filho RD, Tavares LM, Fairbairn EMR. Pozzolanic activity and filler effect of sugar cane bagasse ash in Portland cement and lime mortars. Cem Concr Comp 2008;30:410–8.
[6] Khatri RP, Sirivivatnanon V. Methods for the determination of water permeability of concrete. ACI Mater J 1997;94(5):257–61.
[7] Chan WWJ, Wu CML. Durability of concrete with high cement replacement. Cem Concr Res 2000;30(6):865–79.
[8] Chindaprasirt P, Homwuttiwong S, Jaturapitakkul C. Strength and water permeability of concrete containing palm oil fuel ash and rice husk-bark ash. Constr Build Mater 2007;21:1492–9.
[9] Chindaprasirt P, Jaturapitakkul C, Sinsiri T. Effect of fly ash fineness on compressive strength and pore size of blended cement paste. Cem Concr Comp 2005;27:425–8.
[10] Alonso JL, Wesche K. Characterization of fly ash. In: Wesche K, editor. Fly ash in concrete properties and performance. RILEM report; 1991. vol. 7. p. 3–23.
[11] Helmult R. Fly ash in cement and concrete. Illinois: Portland Cement Association; 1987. p. 42–61.
[12] ASTM C 618: Standard specification for coal fly ash and raw or calcined natural pozzolan for use as a mineral admixture in concrete; 1997; 04.02:294–6.
[13] Chandrasekhar S, Pramada PN. Rice husk ash as an adsorbent for methylene blue-effect of ashing temperature. Adsorption 2006;12:27–43.
[14] Atis CD. Strength properties of high-volume fly ash roller compacted and workable concrete and influence of curing condition. Cem Concr Res 2005;35:1112–21.
[15] Kiattikomol K, Jaturapitakkul C, Songpiriyakit S, Chutubtim S. A study of ground coarse fly ashes with different finenesses from various sources as pozzolanic materials. Cem Concr Comp 2001;23:335–43.
[16] Isaia GC, Gastaldini ALG, Moraes R. Physical and pozzolanic action of mineral additions on the mechanical strength of high performance concrete. Cem Concr Comp 2003;25:69–76.
[17] Li Z, Chau CK. New water permeability test scheme for concrete. ACI Mater J 2000;97(1):84–90.
[18] Sanchez MI, Frias M. The pozzolanic activity of different materials, its influence on the hydration heat in mortars. Cem Concr Res 1996;26:203–13.
[19] Bamforth PB. Heat of hydration of PFA concrete and its effect on strength development. In: Conference proceedings, Ashtech'84, the second international conference on ash technology, London; 1984. p. 287–94.
[20] Davies DR, Kitchener JN. Massive use of pulverized fuel ash in concrete for the construction of a U.K. power station. Waste Manage 1996;16:169–80.
[21] ACI Committee 207. Mass concrete. ACI manual of concrete practice part I. Detroit (USA): American Concrete Institute; 2000. 20 p.
[22] Sata V, Jaturapitakkul C, Kiattikomol K. Utilization of palm oil fuel ash in high-strength concrete. J Mater Civil Eng 2004;16:1–6.
[23] Atis CD. Heat evolution of high-volume fly ash concrete. Cem Concr Res 2002;32:751–6.
[24] Zhang Y, Sun W, Lui S. Study on the hydration heat of binder paste in high-performance concrete. Cem Concr Res 2002;32:1483–8.

8. N. Chusilp, C. Jaturapitakkul, K. Kiattikomol. Effects of LOI of ground bagasse ash on the compressive strength and sulfate resistance of mortars, Construction and Building Materials, 23 (2009), 3523-3531. (IF 0.947)

Construction and Building Materials 23 (2009) 3523–3531

Contents lists available at ScienceDirect

Construction and Building Materials

journal homepage: www.elsevier.com/locate/conbuildmat

Effects of LOI of ground bagasse ash on the compressive strength and sulfate resistance of mortars

Nuntachai Chusilp, Chai Jaturapitakkul *, Kraiwood Kiattikomol

Department of Civil Engineering, Faculty of Engineering, King Mongkut's University of Technology Thonburi (KMUTT), Bangkok 10140, Thailand

ARTICLE INFO

Article history:
Received 16 March 2009
Received in revised form 26 June 2009
Accepted 26 June 2009
Available online 22 July 2009

Keywords:
Compressive strength
Sulfate resistance
Mortar
LOI
Bagasse ash

ABSTRACT

Raw bagasse ash collected from the Thai sugar industry has a high loss on ignition (LOI) of ~20%. When ground and ignited at 550 °C for 45 min, the LOI was reduced to ~5%. These high and low LOI of ground bagasse ashes were blended in the ratios of 1:2 and 2:1 by weight to give ground bagasse ashes with LOIs of 10% and 15%, respectively. Each of these ground bagasse ashes was used to replace Portland cement type I at 10%, 20%, 30%, and 40% by weight of binder to cast mortar.

The results showed that the development of compressive strengths of mortars containing ground bagasse ash with high LOI was slower than that of mortar containing ground bagasse ash with low LOI. However, at the later age, both types of ground ash mortars displayed similar compressive strengths. Mortars containing high LOI (~20%) of ground bagasse ash at 20% and 30% by weight of binder could produce higher compressive strengths than a control mortar after 28 and 90 days, respectively. Mortar bars containing ground bagasse ash at 10% showed a greater potential sulfate resistance and displayed a reduce expansion compared to a control mortar. However, mortar bars containing high LOI (*larger than* 10%) of ground bagasse ashes showed greater deterioration from sulfate attack than the mortar bars containing low LOI (*less than* 10%) of ground bagasse ashes, especially at high replacement levels (30–40%).

1. Introduction

Loss on ignition (LOI) is defined by ACI 116 [1] as a percent loss in mass of a constant weight sample ignited at temperatures of 900–1000 °C. ASTM C 618 [2] limits the LOI of pozzolanic materials to less than 6%, largely because higher LOI levels commonly result in discoloration, poor air entrainment, segregation, and low compressive strength of the mixed components. However, this standard is specified principally for fly ashes. Atis [3] found that the LOI increased the water demand of fresh concrete. A high carbon content provides one source of elevated LOI and is believed to interfere the hydration reactions in cement, as well as reducing the workability and increasing the water demand in concrete. LOI of fly ash consists of unburned carbon generally presented in the form of cellular particles. Berry et al. [4] found that an increase in LOI was not necessarily related to an increase in the carbon content of fly ash. Numerous studies of LOI of fly ashes show that LOI has a detrimental effect on concrete. For other pozzolanic materials, such as calcined natural pozzolans, the ASTM C618 limits the upper limit for LOI at 10%, since these materials are produced at lower burning temperatures (500–800 °C) and contain higher LOI levels.

Bagasse ash is recently accepted as a pozzolanic material which is obtained as a by-product of the sugar industry. However, the study of using bagasse ash as a pozzolan is not well-known especially the effects of LOI *of bagasse ash* on the compressive strength and sulfate resistance. A survey from many sources in Thailand found that LOI of bagasse ash is very high (*larger than* 10%) and well over the limit for pozzolan in concrete [2]. Bagasse ash contains amorphous silica and displays good pozzolanic properties [5–9], but its uses are limited and most of it is disposed in landfills. Moreover, sugar factories use different process of burning and collecting which affects the physical and chemical properties of the ash. Batra et al. [10] examined the unburned carbon in bagasse ash and suggested that it might be separated from oxide fractions by water floataion. This process increased LOI of the ash from 20% to 80%, and the unburned carbon found to be amorphous with a cellular morphology. Umamaheswaran et al. [11] compared bagasse ash, ground nut shell ash, cashew shell ash, and rice husk ash, all used in fabricating inorganic membrane filters and found that the bagasse ash was the most suitable in terms of handling strength, porosity, and pore size distribution, even though its LOI was as high as 24.84%. Subsequently, Frías et al. [12] found that LOI of bagasse ashes could vary from 1.81% to 0.52% depending on whether the ignited temperature at 800 or 1000 °C, respectively. At both temperatures, the ignited ash displayed very high pozzolanic activity. However, to date, few studies have been

* Corresponding author. Tel.: +66 2 470 9131; fax: +66 2 427 9063.
E-mail address: chai.jat@kmutt.ac.th (C. Jaturapitakkul).

0950-0618/$ - see front matter © 2009 Elsevier Ltd. All rights reserved.
doi:10.1016/j.conbuildmat.2009.06.046

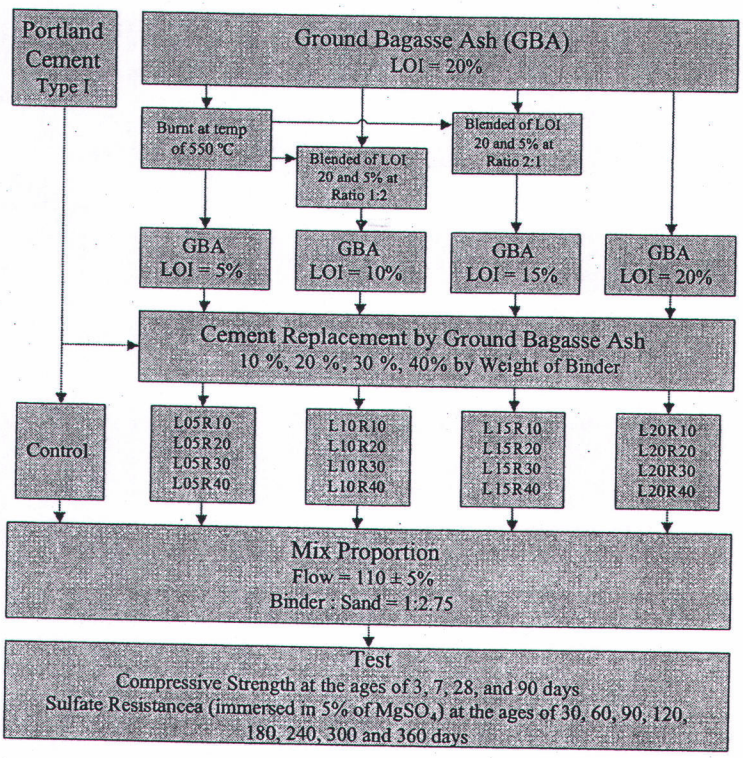

Fig. 1. Flow chart to study the effects of LOI of ground bagasse ash on the compressive strength and the sulfate resistance of mortar.

undertaken to examine the impact the LOIs of bagasse ashes on the mechanical properties of mortars and concretes.

Many researchers have found pozzolanic materials such as fly ash, rice husk ash, or palm oil fuel ash are effective in reducing sulfate attacks [13–15], but scant attention has been paid to the similar effects of bagasse ashes when used as a pozzolanic material in concrete.

In this study, ground bagasse ashes of different LOIs were used as a partial replacement for Portland cement in mortar, and the effects on compressive strength and sulfate resistance of mortars were compared. This experiment studied mortar not concrete because it was easier to control the quality of mix proportion and material. In addition, the use of mortar instead of concrete can avoid the effects of many factors such as bond strength between aggregate and paste or the uniformity of the mixture. The results demonstrate that the ground bagasse ash with high fineness can be used in concrete by engineers, designers, contractors, and other users with a high degree of confidence.

2. Experimental program

2.1. Materials and test methods

The primary materials used in this investigation were Portland cement type I, natural river sand, bagasse ash, and water.

Bagasse ash with high LOI of about 20% was obtained from one of the sugar industries in central Thailand. The bagasse ash was improved by grinding in a ball mill until the particles retained on a 45-μm sieve were less than 5% and was then put in an oven at 550 °C for about 45 min. This process reduced LOI of the ground bagasse ash to about 5%. The two ground bagasse ashes were then prepared with LOI contents of 10% and 15% by blending the ground bagasse ash of 20% LOI with 5% LOI in the weight ratios of 1:2 and 2:1, respectively.

Details of the four ground bagasse ashes, symbolized as L05, L10, L15, and L20, are shown in Fig. 1. The analytical LOI values of the four were determined by comparing the weights of the samples before and after ignition for 45 min at 550 °C, as specified in ASTM C 311 [16]. The chemical compositions of the four ash samples were determined using X-ray fluorescence spectrometry (XRF).

X-ray diffraction (XRD) examination of the four ground bagasse ashes was carried out by using a Bruker-AXS D8 Discover diffractometer operating with Co K_α radiation and a scanning angle (2θ) from 20° to 80°.

The particle size distributions of ground bagasse ashes were measured by laser particle size analysis.

The morphology of ground bagasse ash particles was investigated by scanning electron microscopy (SEM) using an accelerating voltage of 15 kV, and followed by gold coating of the samples.

2.2. Compressive strength

Standard-sized 50 mm mortar cubes were prepared using each of the four different LOI ashes to partially replace Portland cement type I at rates of 10%, 20%, 30%, and 40% by weight of binder. The binder to sand ratio was constant at 1:2.75 by weight [17], and a standard flow of 110 ± 5, as specified by ASTM C 230 [18], was maintained by adjusting the quantity of mixing water. This is to control the mortars to have the same workability and to reduce the effect of compaction during casting the mortars into the moulds. However, by following this standard, a disadvantage was found since the W/B ratios of the mortar mixtures were rather high and varied with the percent replacement of ground bagasse ash. The compressive strength of mortar was measured after curing for 3, 7, 28, and 90 days.

2.3. Sulfate resistance of the mortar

The sulfate resistance, was determined on 25 × 25 × 285 mm prismatic test specimens with two stainless steel probes inserted at both ends in order to monitor any changes in length of the mortar, in accordance with ASTM C1012 [19]. After 24 h of casting, one-half of the specimens were taken from the moulds and cured

Table 1
Physical properties of Portland cement type I, original bagasse ash, and ground bagasse ash with different LOI.

Physical properties		Ground bagasse ash				
	Cement	L05	L10	L15	L20	OBA
Retained on a 45-μm sieve	–	–	–	–	2.8	47.1
Specific gravity	3.14	2.50	2.37	2.35	2.29	2.08
Mean particle size, d_{50} (μm)	14.6	–	–	–	10.0	23.0

Remark: OBA = original bagasse ash received from the power plant.

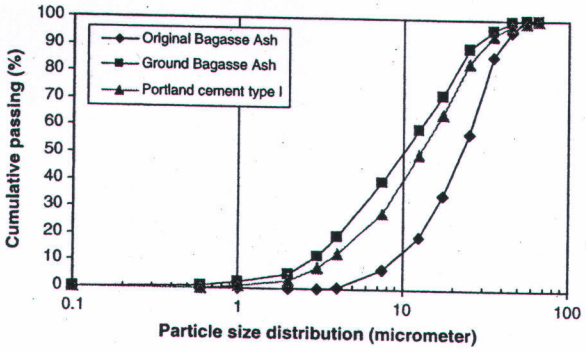

Fig. 2. Particle size distribution of materials.

in water. The second half the specimens were exposed to a 5% magnesium sulfate solution ($MgSO_4$). The changes in length of the water-cured samples and those immersed in the magnesium sulfate solution were compared for up to 360 days.

3. Results and discussion

3.1. Physical properties of the materials

Table 1 shows the physical properties of Portland cement type I, the original bagasse ash (OBA), and the blended ground bagasse ashes. The OBA had a specific gravity of 2.08, and the ground bagasse ashes had the specific gravities of 2.50, 2.37, 2.35, and 2.29 for L05, L10, L15, and L20, respectively. That is, the specific gravity of the ground bagasse ash decreased as the LOI increased, reflecting a reduction in low-density substances upon decomposition during burnt at 550 °C.

The particle size distributions of ground bagasse ashes are shown in Fig. 2, with some 2.8% of the particles of ground bagasse ash L20 retained on a 45-μm sieve compared with 47.1% of the OBA. The OBA had large particles with a mean particle size (d_{50}) of 23 μm. Following grinding, the mean particle size was reduced to near 10 μm. For Portland cement, the mean particle size was 14.6 μm.

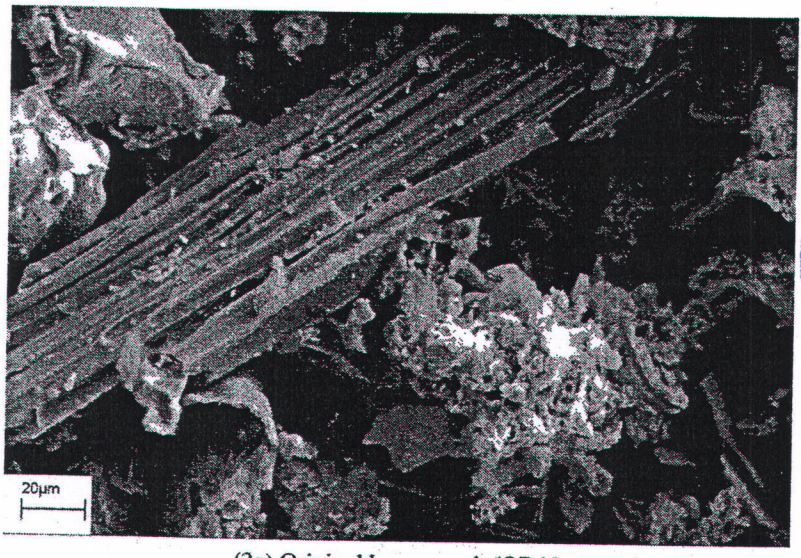

(3a) Original bagasse ash (OBA)

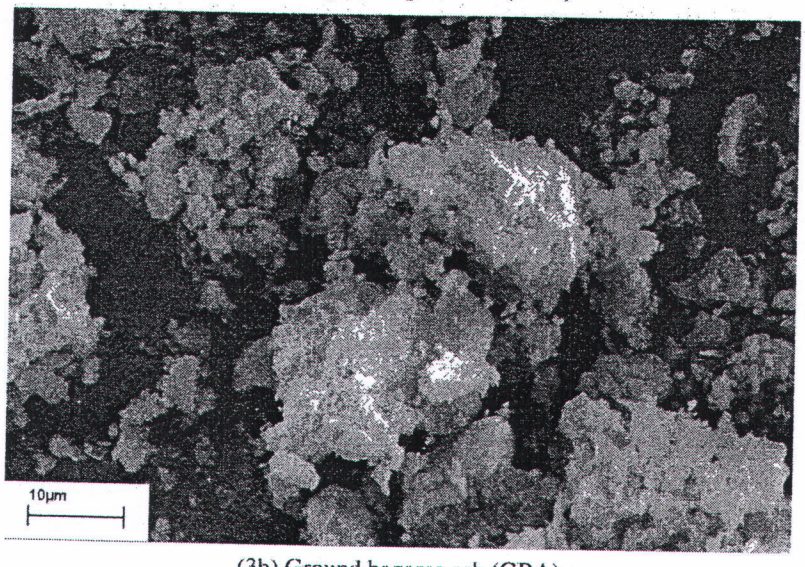

(3b) Ground bagasse ash (GBA)

Fig. 3. Scanning electron microscopies of original and ground bagasse ashes.

Table 2
Chemical compositions of Portland cement type I, original bagasse ash, and ground bagasse ash with different LOI.

Chemical composition (%)	Cement	Ground bagasse ash				OBA	Requirement of ASTM C 618
		L05	L10	L15	L20		
Silicon dioxide, SiO_2	20.90	77.37	70.64	60.67	54.45	54.10	–
Aluminum oxide, Al_2O_3	4.76	3.59	3.68	4.30	6.06	5.69	–
Iron oxide, Fe_2O_3	3.41	4.66	4.06	4.02	3.23	3.54	–
Calcium oxide, CaO	65.41	7.81	10.68	15.85	15.41	15.37	–
Magnesium oxide, MgO	1.25	1.32	1.41	1.46	1.37	1.41	–
Sulfur trioxide, SO_3	2.71	0.15	0.15	0.09	0.04	0.03	<4.0
Loss on ignition, LOI	0.96	5.08	9.29	13.59	19.39	19.36	<10.0
$SiO_2 + Al_2O_3 + Fe_2O_3$	–	85.62	78.38	68.99	63.74	63.33	>70.0

Remark: OBA = original bagasse ash received from the power plant.

The morphologies of the original and ground bagasse ashes are shown in Fig. 3. The OBA had large tubular-shaped particles with highly irregular shapes and high porosity (Fig. 3a). After grinding, the particle size become smaller, the particle shape was still highly irregular and the ground bagasse ash become more dense (Fig. 3b).

3.2. Chemical compositions of the materials

The XRF chemical analyses of the original bagasse ash (OBA), ground bagasse ashes, and Portland cement type I, are tabulated in Table 2. The Portland cement type I had high CaO and SiO_2 contents of 65.41% and 20.90%, respectively. The analytical LOI of the ground bagasse ashes were 5.08%, 9.29%, 13.59%, and 19.39% for L05, L10, L15, and L20, respectively, and their SiO_2 contents were 77.37%, 70.64%, 60.67%, and 54.45%, respectively, with SiO_2 decreasing as LOI increased. CaO, however, increased with increasing LOI. As the ignition temperature increased to 550 °C, the LOI declined to become almost constant thereafter, as shown in Fig. 4.

3.3. Mineralogical composition of ground bagasse ash

The results of the XRD mineralogical analysis of bagasse and ground bagasse ashes are shown in Fig. 5. Before ignition, bagasse displayed a wide scattering band centered at about 27° 2θ, consistent with the presence of amorphous silica, but with small quantities of crystalline quartz, calcite, and cristobalite also present (Fig. 5a).

After bagasse being burnt and ground, the ground bagasse ash L20 exhibited a high content of quartz, graphite, and calcite (Fig. 5b), but after ignition at 550 °C for 45 min, and with now reduced LOI (L05), the calcite peak was reduced, consistent with a decrease in the CaO content of this ash, and the quartz (SiO_2) peak of ground bagasse ash increased (Fig. 5c).

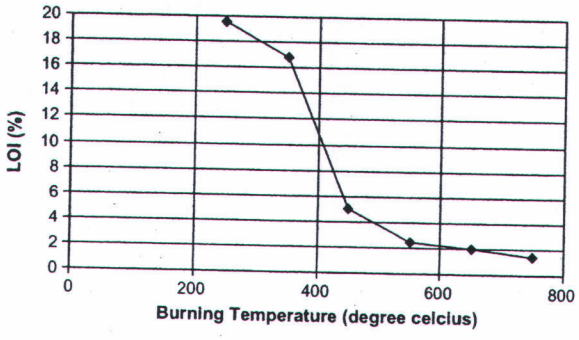

Fig. 4. Relationship between the LOI of ground bagasse ash and the burning temperature.

3.4. Effect of the LOI on the water requirement of mortar

The water to binder (W/B) ratios of all mortars to produce a standard flow of 110 ± 5 are shown in Table 3. All mix proportion of mortars containing ground bagasse ash had higher water

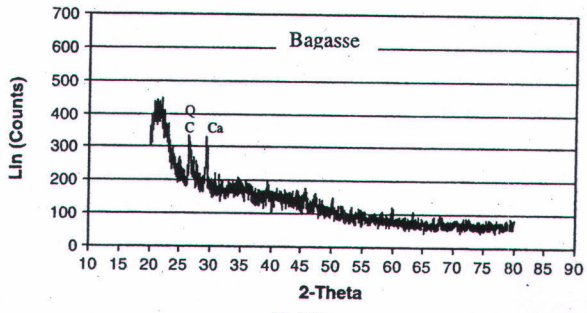

(5a) Bagasse

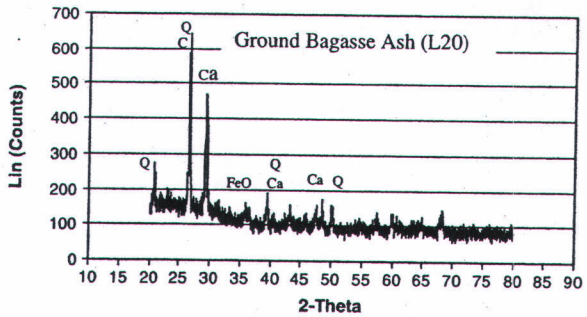

(5b) Ground bagasse ash (L20)

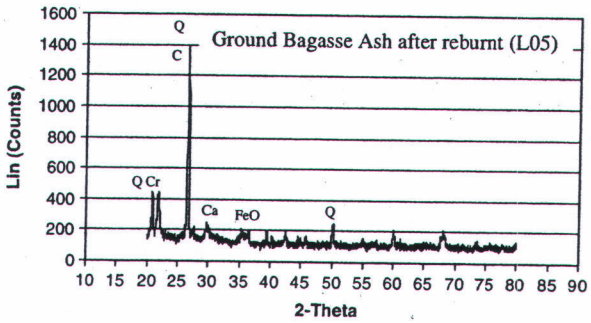

(5c) Ground bagasse ash after reburnt(L05)

Q: Quartz, Ca: Calcite, FeO: Iron oxide, Cr: Cristobalite, C: Graphite

Fig. 5. Mineralogical composition of (a) bagasse, (b) ground bagasse ash, and (c) ground bagasse ash after reburnt at 550 °C.

requirements than the control mortar. The water requirement of the mortars increased with the increase in ground bagasse ash replacement. For example, mortar containing OBA at rates of 10%, 20%, 30%, and 40% by weight of binder had the water requirements of 0.75, 0.82, 0.92, and 1.03, respectively. For mortars containing ground bagasse ash L20 to replace Portland cement of 10%, 20%, 30%, and 40% by weight of binder, the water requirements were 0.73, 0.74, 0.75, and 0.77, respectively. The water requirements of mortars containing original bagasse ash (OBA) were extremely high (W/B ratios between 0.75 and 1.03) and more than the mortars containing ground bagasse ash and also increased with the increased of the percent replacement of ground bagasse ash. At the same replacement, mortars containing ground bagasse ash with different LOI have slightly different in W/B ratio. The high water requirement of original bagasse mortar was due to the porous nature of the particles and their higher surface area, both enhancing the absorption of water by the mixture. At the same replacement, the ground bagasse ash mortars had much lower water requirements (W/B ratios between 0.73 and 0.79) compared to the original bagasse ash mortar due to their lower particle porosity [20].

The above results point to both high and low LOI of ground bagasse ashes having little effect on the water requirement of mortar.

Table 3
Mix proportions of mortar.

Mix no.	Symbol	Mix proportion (by weight)							W/B ratio	Flow (%)
		Cement (g)	Ground bagasse ash (g)				OBA (g)	Sand (g)		
			L05	L10	L15	L20				
1	Control	100	–	–	–	–	–	275	0.71	110
2	L05R10	90	10	–	–	–	–	275	0.73	109
3	L05R20	80	20	–	–	–	–	275	0.74	109
4	L05R30	70	30	–	–	–	–	275	0.75	111
5	L05R40	60	40	–	–	–	–	275	0.77	110
6	L10R10	90	–	10	–	–	–	275	0.75	111
7	L10R20	80	–	20	–	–	–	275	0.76	109
8	L10R30	70	–	30	–	–	–	275	0.78	112
9	L10R40	60	–	40	–	–	–	275	0.79	111
10	L15R10	90	–	–	10	–	–	275	0.75	109
11	L15R20	80	–	–	20	–	–	275	0.76	112
12	L15R30	70	–	–	30	–	–	275	0.77	108
13	L15R40	60	–	–	40	–	–	275	0.78	110
14	L20R10	90	–	–	–	10	–	275	0.73	109
15	L20R20	80	–	–	–	20	–	275	0.74	108
16	L20R30	70	–	–	–	30	–	275	0.75	111
17	L20R40	60	–	–	–	40	–	275	0.77	112
18	OBAR10	90	–	–	–	–	10	275	0.75	108
19	OBAR20	80	–	–	–	–	20	275	0.82	105
20	OBAR30	70	–	–	–	–	30	275	0.92	108
21	OBAR40	60	–	–	–	–	40	275	1.03	113

Remark: OBA = original bagasse ash as received from the power plant.

Table 4
Compressive strength of mortars.

Mix No.	Symbol	Compressive strength (MPa) – normalized compressive strength (%)			
		3 days	7 days	28 days	90 days
1	Control	22.3–100	27.4–100	33.3–100	34.2–100
2	L05R10	25.6–115	34.3–125	42.1–126	44.1–129
3	L05R20	23.3–104	31.1–114	38.8–117	39.9–117
4	L05R30	17.1–77	28.5–104	35.9–108	38.0–111
5	L05R40	15.9–71	24.5–89	30.7–92	36.3–106
6	L10R10	25.0–112	33.9–124	41.7–125	43.5–127
7	L10R20	20.6–92	30.0–109	37.5–113	38.7–113
8	L10R30	18.0–81	27.2–99	36.1–108	37.2–109
9	L10R40	14.3–64	23.8–87	30.0–90	35.0–102
10	L15R10	24.4–109	30.9–113	39.1–117	41.2–120
11	L15R20	17.5–78	28.5–104	34.8–105	35.9–105
12	L15R30	14.1–63	24.0–88	33.5–101	34.6–101
13	L15R40	10.0–45	17.8–65	28.1–84	31.5–92
14	L20R10	19.5–87	25.0–91	38.6–116	41.4–121
15	L20R20	17.2–77	22.8–83	33.8–102	34.9–102
16	L20R30	12.8–57	19.1–70	29.3–88	34.4–101
17	L20R40	9.4–42	13.5–49	23.1–69	31.2–91
18	OBAR10	13.6–61	18.3–67	28.2–85	31.4–92
19	OBAR20	9.8–44	16.9–62	23.6–71	28.2–82
20	OBAR30	7.6–34	11.6–42	15.5–47	18.8–55
21	OBAR40	4.0–18	5.1–19	10.4–31	15.0– 44

For example, mortars L05R40, L10R40, L15R40, and L20R40 that used ground bagasse ashes L05, L10, L15, and L20 had water requirements of 0.77, 0.79, 0.78, and 0.77, respectively. The results also demonstrate that the replacement rate of ground bagasse ash exercised a greater effect on water requirement of mortar than that of the LOI of the ground bagasse ash.

3.5. Effect of the LOI on the compressive strengths of mortar

The compressive strengths of the control mortar and mortars containing ground bagasse ashes with different LOI are shown in Table 4.

The compressive strengths of mortars containing original bagasse ash (OBA) at 28 days were very low at 10.4 MPa and 15.5 MPa for mortars OBAR40 and OBAR30, respectively. This is due to the extremely high W/B ratios (W/B ratios of 1.03 and 0.92, respectively), high replacement, and low pozzolanic reaction of OBA [21]. However, the mortars containing ground bagasse ash with different LOI have compressive strength between 23.1 MPa and 42.1 MPa, depending on the values of LOI and percent replacement. Moreover, the compressive strengths at 90 days of ground bagasse ash are rather high and varied between 31.2 MPa and 44.1 MPa, depending on the percent replacement of ground bagasse ash.

Mortars containing ground bagasse ash L05 had higher compressive strengths than the control mortar at 3 days or more when the ground bagasse ash L05 was used to replace Portland cement at 20% by weight of binder. Moreover, those mortars containing ground bagasse ash L10 and L15 also had higher compressive strengths than the control mortar at all tested ages when Portland cement was replaced by the ground bagasse ash at 10% by weight of binder. These results consistent with those of Ganesan et al. [22]

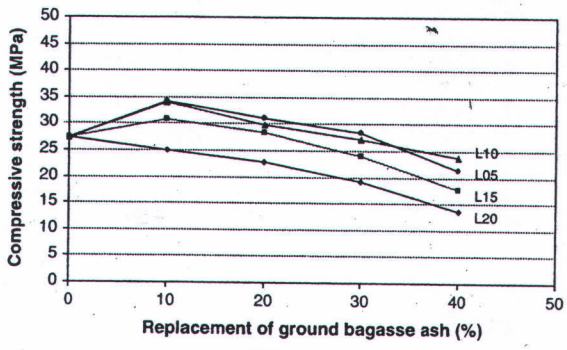

(7a) At 7 days

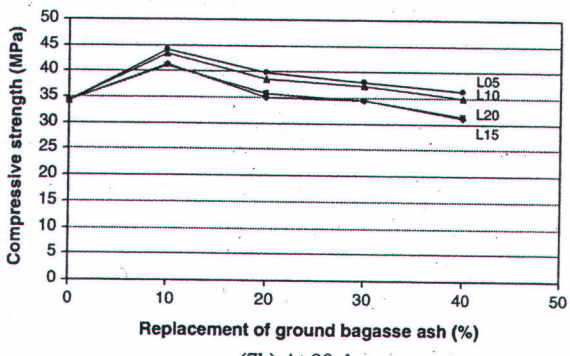

(7b) At 90 days

Fig. 7. Relationship between compressive strength of mortar at 7 and 90 days and replacement of ground bagasse ash.

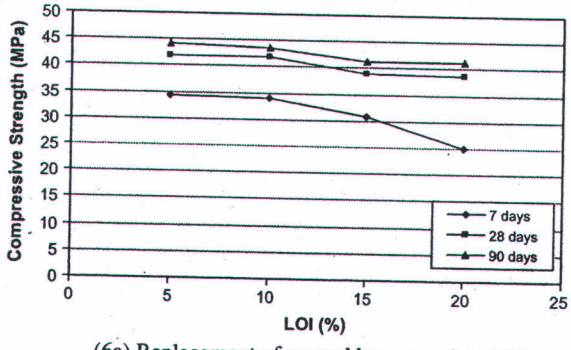

(6a) Replacement of ground bagasse ash at 10%

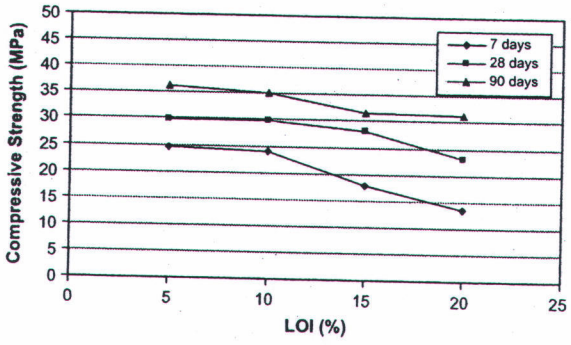

(6b) Replacement of ground bagasse ash at 40%

Fig. 6. Relationship between compressive strength of mortar and LOI of ground bagasse ash at replacement of ground bagasse ash at 10% and 40% by weight of binder.

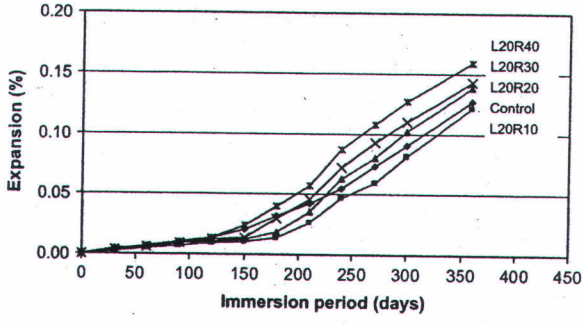

(8a) Replacement of ground bagasse ash L20

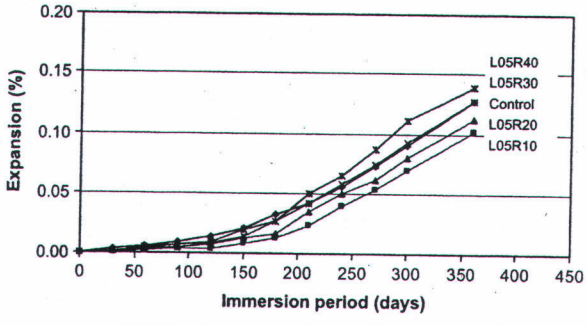

(8b) Replacement of ground bagasse ash L05

Fig. 8. Relationship between expansions and immersion time in a 5% magnesium sulfate solution of mortar bars containing ground bagasse ash L20 and L05.

and Cordeiro et al. [23] who found bagasse ash to provide an effective mineral admixture; replacing 10–20% of the Portland cement proved optimal.

For 30% replacement, mortars containing ground bagasse ash L05 and L10 (*less than or equal* 10%) had higher compressive strength than the control mortar at 7 days, while mortars containing ground bagasse ash L15 and L20 (*larger than* 10%) had higher compressive strength than the control mortar at 28 and 90 days, respectively. At 40% replacement, mortars containing ground bagasse ash L05 and L10 (*less than or equal* 10%) had higher compressive strength than the control mortar at 90 days, while the mortars containing bagasse ash L15 and L20 (*larger than* 10%) had lower compressive strength than the control mortar at all ages up to 90 days.

Clearly, the compressive strength of a mortar tends to decrease with an increase of ground bagasse ash in the mortar. The development of compressive strength in mortars containing ground bagasse ash having high LOI (*larger than* 10%) were slightly slower than mortars containing ground bagasse ash having low LOI (*less than* 10%). However, at the later age (90 days), mortars containing either low or high LOI of ground bagasse ash had similar compressive strengths. Further, all mortars containing ground bagasse ash with LOIs of 5–10% had the compressive strengths over 30 MPa. Only mortar OBAR10 had a compressive strength higher that 30 MPa while the rests of OBAR mortar had lower compressive strength than 30 MPa.

The relationship between the compressive strength and the LOI of ground bagasse ash was shown in Fig. 6. At the early age of 7 days and with 10% replacement of ground bagasse ash (Fig. 6a), the compressive strength of a mortar tended to decrease when the LOI of the ground bagasse ash was higher than 10%. However, the compressive strengths of mortars containing ground bagasse ashes with LOIs between 5% and 20% were almost the same from 28 to 90 days. This is arises from the replacement rate being low (10%) thus the effect of LOI is minimal. For the replacement rate of 40% (Fig. 6b), the effect of the LOI on reducing the compressive strength of mortar at 7 days was enhanced regardless of whether L15 and L20 were used. At the ages of 28 and 90 days, the effect of the LOI of ground bagasse ash (L15 and L20) was reduced. These results indicate that a high LOI (*larger than* 10%) effectively reduced the compressive strengths of mortars at the early age but exercised less influence at the later ages.

Fig. 7 shows the relationship between the compressive strength of a mortar and the percent replacement of Portland cement by ground bagasse ash at 7 and 90 days. The mortars containing ground bagasse ash having high LOI (*larger than* 10%) tended to have lower compressive strengths than the mortar containing ground bagasse ash having low LOI (*less than* 10%). This was due to the low LOI of ground bagasse ashes containing more active particles than the high LOI of ground bagasse ashes. In addition, the replacement rate of ground bagasse ash had a more pronounced effect on reducing compressive strengths at the early age (7 days)

Fig. 9. Deterioration of mortar bars immersed in a 5% magnesium sulfate solution at 360 days.

than the later age (90 days). At 90 days, the compressive strengths of mortars containing ground bagasse ashes with different LOIs (5–20%) and replacement rates of 10% or 40% were little different. With 10–30% replacement of Portland cement, the compressive strengths of ground bagasse ash mortars were higher or equal to the control mortar. These results confirmed that the ground bagasse ash was a good pozzolan and its reactivity was mainly dependent on particle size and fineness [24].

3.6. *Effect of the LOI on the sulfate resistances of mortars*

The relationship between expansion and immersion time in a 5% magnesium sulfate solution of mortar bars containing ground bagasse ash L20 and L05 are shown in Fig. 8a and b, respectively. In Fig. 8a, mortar bar L20R10 had lower expansion compared to the control mortar bar. At the higher replacements (20% or more) of ground bagasse ash L20 in mortar, the greater expansion of mortar bar was a result. When using ground bagasse ash L05 to replace Portland cement, mortar bars L05R10 and L05R20 produced less expansion compared to the control mortar bar. The lower expansions found in ground bagasse ash mortars came from the small particles of the ash filling voids and increasing the density of the mortar bar. However, where high levels of replacement of ground bagasse ash were used, the opposite result occurred due to the great surface area of the ground bagasse ash, which had a high water requirement in the mortar bar, giving the resulting mortar bar reduced compressive strength and resulted in a higher expansion [25]. Mortar bars containing ground bagasse ashes with high LOI (*larger than* 10%) tended to show a higher expansion than the mortar bars containing ground bagasse ashes with low LOI (*less than or equal* 10%).

Fig. 9 shows the deterioration of a control mortar bar and mortar bars containing ground bagasse ash immersed in a 5% magnesium sulfate solution for 360 days. Mortar bars containing ground bagasse ash L20 had a greater degree of deterioration than the mortar bars containing ground bagasse ash L05 for the same level of replacement of ground bagasse ash.

Mortar bars L05R10, L05R20, L05R30, and L05R40 did not show any cracking while mortar bars L20R10, L20R20, L20R30, and L20R40 showed major cracks due to their enhanced expansion. The CaO and Al_2O_3 contents in ground bagasse ash increased with an increase in the LOI, and combined to form C_3A that was susceptible to sulfate attacks. In low LOI of ground bagasse ashes, the high Fe_2O_3 and low Al_2O_3 contents increased their resistance to sulfate attacks, consistent with other researches that showed a low LOI could increase sulfate resistance [26–29].

4. Conclusions

The principal conclusions of this investigation are summarized as follows:

1. The replacement rate of Portland cement type I by ground bagasse ash had a greater effect on the compressive strength of the mortar than did the LOI values (5–20%) of ground bagasse ash.
2. Mortar bars made using ground bagasse ashes at 10–20% (LOI between 5% and 20%) to replace Portland cement type I showed little deterioration after being submersed in a 5% magnesium sulfate solution for 360 days. However, the use of 30–40% of ground bagasse ashes with high LOI (*larger than* 10%) caused severe deterioration in the mortar bar.
3. The high LOI (*larger than* 10%) of ground bagasse ash had a marked effect on lowering the compressive strength of the mortar at the early age (7 days). However, the LOI content of up to 20% had only a slight effect on lower the compressive strength of mortar at the later age (more than 28 days).
4. A high degree of sulfate resistance could be obtained by using a mortar containing ground bagasse ash of either a high or low LOI to replace Portland cement type I not more than 20% by weight of binder.
5. A high LOI of a ground bagasse ash, whether it was due to the carbon content or the unignited bagasse, had no adverse affect on the properties of a mortar. Nonetheless, ground bagasse ash with an LOI *less than* 10% provided an excellent pozzolanic material and could be used to partially replace Portland cement in concrete. This use of ground bagasse ashes will reduce the amount disposed as waste and be good for the environment.

Acknowledgements

We would like to thank the Office of the Higher Education Commission, Thailand for supporting by grant fund under the program Strategic Scholarships for Frontier Research Network for the Ph.D. Program Thai Doctoral degree for this research. Thank also extend to the Thailand Research Fund (TRF) for the financial support under the TRF Senior Research Scholar, Contract No. RTA5080020.

References

[1] ACI Committee 116, ACI 116R-00. Cement and concrete terminology. American Concrete Institute; 2000. 73p.
[2] ASTM C 618. Standard specification for coal fly ash and raw or calcined natural pozzolan for use as a mineral admixture in concrete. ASTM C 618-2001. In: Annual book of ASTM standards, vol. 04.02; 2001.
[3] Atis CD. Strength properties of high-volume fly ash roller compacted and workable concrete, and influence of curing condition. Cem Concr Res 2005;35:1112–21.
[4] Berry EE, Hemmings RT, Langley WS, Carrette GG. Beneficated fly ash: hydration, microstructure, and strength development in Portland cement. In: Proceedings of the first international conference on fly ash, silica fume, slag, and natural pozzolans in concretes, SP-114, Detroit, USA; 1989. p. 241–73.
[5] Martirena JF, Middendorf B, Gehrke M, Budelmann H. Use of waste of sugar industry as pozzolana in lime-pozzolana binders: study of reaction. Cem Concr Res 1998;28:1525–36.
[6] Singh NB, Singh VD, Rai S. Hydration of bagasse ash-blended Portland cement. Cem Concr Res 2000;30:1485–8.
[7] Villar-Cociña E, Valencia-Morales E, González-Rodríguez R, Hernández-Ruíz J. Kinetics of the pozzolanic reaction between lime and sugar cane straw ash by electrical conductivity measurement: a kinetic-diffusive model. Cem Concr Res 2003;33:517–24.
[8] Villar-Cocina E, Frias Rojas M, Valencia Morales E. Sugar cane wastes as pozzolanic materials: application of mathematical model. ACI Mater J 2008;105:258–64.
[9] Kantiranis N. Re-cycling of sugar-ash: a raw feed material for rotary kilns. Waste Manage 2004;24:999–1004.
[10] Batra VS, Urbonaite S, Svensson G. Characterization of unburned carbon in bagasse fly ash. Fuel 2008;87:2972–6.
[11] Umamaheswaran K, Batra VS, Bhagavanulu DVS. Development of biomass ash filters for high temperature applications. In: International symposium of research students on materials science and engineering, Chennai, India; 20–22 Decemberm 2004.
[12] Frías M, Villar-Cociña E, Valencia-Morales E. Characterisation of sugar cane straw waste as pozzolanic material for construction: calcining temperature and kinetic parameters. Waste Manage 2007;27:533–8.
[13] Chindaprasirt P, Kanchanda P, Sathonsaowaphak A, Cao HT. Sulfate resistance of blended cements containing fly ash and rice husk ash. Construct Build Mater 2007;21:1356–61.
[14] Ghrici M, Kenai S, Said-Mansour M. Mechanical properties and durability of mortar and concrete containing natural pozzolana and limestone blended cements. Cem Concr Compos 2007;29:542–9.
[15] Tangchirapat W, Saeting T, Jaturapitakkul C, Kiattikomol K, Siripanichgorn A. Use of waste ash from palm oil industry in concrete. Waste Manage 2007;27:81–8.
[16] ASTM C 311-00. Standard test method for sampling and testing fly ash or natural pozzolans for use as a mineral admixture in Portland-cement concrete. In: Annual book of ASTM standards, vol. 04.02; 2001. p. 191–9.
[17] ASTM C 109-99. Standard test method for compressive strength of hydraulic cement mortars (using 2-in. or [50 mm] cube specimens). In: Annual book of ASTM standards, vol. 04.01; 2001. p. 83–8.
[18] ASTM C 230-98. Specification for flow table for use in tests of hydraulic cement. In: Annual book of ASTM standards, vol. 04.01; 2001. p. 203–9.

[19] ASTM C 1012-95a. Standard test method for length change of hydraulic-cement mortars exposed to a sulfate solution. In: Annual book of ASTM standards, vol. 04.01; 2001. p. 503–7.
[20] Chindaprasirt P, Homwuttiwong S, Jaturapitakkul C. Strength and water permeability of concrete containing palm oil fuel ash and rice husk-bark ash. Construct Build Mater 2007;21:1492–9.
[21] Chindaprasirt P, Jaturapitakkul C, Sinsiri T. Effect of fly ash fineness on microstructure of blended cement paste. Construct Build Mater 2007;21:1534–41.
[22] Ganesan K, Rajagopal K, Thangavel K. Evaluation of bagasse ash as supplementary cementitious material. Cem Concr Compos 2007;29:515–24.
[23] Cordeiro GC, Toledo Filho RD, Fairbairn EMR. Use of ultra-fine sugar cane bagasse ash as mineral admixture for concrete. ACI Mater J 2008;105:487–93.
[24] Cordeiro GC, Toledo Filho RD, Tavares LM, Fairbairn EMR. Pozzolanic activity and filler effect of sugar cane bagasse ash in Portland cement and lime mortars. Cem Concr Compos 2008;30:410–8.
[25] Moon HY, Lee ST, Kim SS. Sulphate resistance of silica fume blended mortars exposed to various sulphate solutions. Canadian J Civ Eng 2003;30:625–36.
[26] Odler I, Jawed J. Expansion reaction in concrete. In: Skalny J, Mindess S, editors. Materials science of concrete. Westerville (OH): American Ceramic Society; 1989.
[27] Kalousek GL, Porter LC, Benton EJ. Cement for long-term service in sulfate environment. Cem Concr Res 1972;2:79–89.
[28] Tikalaky PJ, Roy D, Scheetz B, Krize T. Redefining cement characteristics for sulfate-resistant Portland cement. Cem Concr Res 2002;32:1239–46.
[29] Jaturapitakkul C, Kiattikomol K, Tangchirapat W, Saeting T. Evaluation of the sulfate resistance of concrete containing palm oil fuel ash. Contruct Build Mater 2007;21:1399–405.

9. W. Chalee, P. Ausapanit , C. Jaturapitakkul. Utilization of fly ash concrete in marine environment for long term design life analysis, Materials & Design, 31 (2010), 1242-1249. (IF 1.107).

Materials and Design 31 (2010) 1242–1249

Contents lists available at ScienceDirect

Materials and Design

journal homepage: www.elsevier.com/locate/matdes

Utilization of fly ash concrete in marine environment for long term design life analysis

W. Chalee [a], P. Ausapanit [b], C. Jaturapitakkul [c,*]

[a] Department of Civil Engineering, Faculty of Engineering, Burapha University 20131, Thailand
[b] Toyo-Thai Co., Ltd., Asok, Dindaeng, Bangkok 10400, Thailand
[c] Department of Civil Engineering, Faculty of Engineering, King Mongkut's University of Technology Thonburi, Bangkok 10140, Thailand

ARTICLE INFO

Article history:
Received 15 December 2008
Accepted 12 September 2009
Available online 16 September 2009

Keywords:
Fly ash concrete
Marine environment
Prediction

ABSTRACT

This paper presents the performance of 7-year fly ash concrete exposed to hot and high humidity climate in marine conditions. Control concrete and fly-ash concrete cube specimens of 200 mm were cast and steel bars of 12 mm in diameter and 50 mm in length were embedded at various cover depths. The concrete specimens were exposed to tidal zone of marine environment in the Gulf of Thailand. The concrete specimens were tested for chloride penetration profile, chloride content at the position of embedded steel bar, and corrosion of embedded steel bar after being exposed to tidal zone of sea water up to 7 years. Consequently, these experimental data were used to generate the empirical equation for predicting long term required cover depth of cement and fly ash concretes to protect against the initial corrosion of reinforcing steel in a marine environment.

The results showed that the increase of fly ash replacement in concrete clearly reduced the chloride penetration, chloride *penetration* coefficient, and steel corrosion in concrete. Interestingly, concretes with the fly ash replacement of 25–50% by weight of binder with a W/B ratio of 0.65 did not have corrosion of embedded steel bar at 50 mm concrete cover depth at 7-year exposure in a marine environment and presented the corrosion resistance as good as the cement concrete with a W/B ratio of 0.45. In addition, the empirical model indicated that all predicted data were within ±15% error of the tested data (up to 7 years). Also, the model was verified by using the investigated data of concrete exposed to a marine environment up to 10 years from other researchers; most predicted results were within ±25% error of the investigated data.

1. Introduction

Presently, there has been a renewed emphasis on improving durability and increasing service life of concrete structures. Since, the financial impact of rehabilitating structures that have failed prematurely due to improper design and construction methods is enormous. Therefore, the study on material design method for supporting concrete structures under the severe condition is very important. Under the severe condition, marine concrete structure is widely concerned for long term serviceability. It is well known that the destroying of concrete structure in marine environment is mainly due to sulfate attack and the corrosion of steel under chloride attack. However, all of these mechanisms are combination of many influences, such as moisture, temperature, impacted force, abrasion by sand in sea water and [1,2]. One way to increase service life is to design, specify, and build structures using concrete with particular properties. These properties can easily be improved by using concrete with a low water–binder (W/B) ratio or by using fly ash to replace some of Portland cement in concrete [3,4]. Throughout, the compromise between material and durable design method are necessary. The field indicator of concrete in marine site is preferred to achieve the suitable design and development for high durability concrete.

Many researchers have obtained the durability data of marine concrete structure in long-term exposure [5–7]. However, a few researches studied on the corrosion of fly ash concrete relating to fly ash replacement level, various concrete cover depths, corrosion of steel, and chloride penetration profile [7,8]. Moreover, it has not been found the long term durable data of concrete in a marine environment of Southeast Asia which is in a hot and high humidity climate. Besides, the prediction of long term performance of marine concrete is needed for durability design. Furthermore, the development of empirical model to predict the corrosion of steel reinforcement in fly ash concrete over long-term exposure to a marine environment requires investigated data gathered from experimental sites. Thus, the performances of 7-year fly ash concretes exposed to a hot climate in marine condition were presented

* Corresponding author.
E-mail address: chai.jat@kmutt.ac.th (C. Jaturapitakkul).

0261-3069/$ - see front matter © 2009 Elsevier Ltd. All rights reserved.
doi:10.1016/j.matdes.2009.09.024

Table 1
Chemical composition of Portland cement type I and fly ash.

Chemical composition (%)	Sample	
	Cement type I	Fly ash
Silicon dioxide, SiO_2	20.80	44.95
Aluminum oxide, Al_2O_3	5.50	23.70
Iron oxide, Fe_2O_3	3.16	10.80
Calcium oxide, CaO	64.97	13.80
Magnesium oxide, MgO	1.06	3.47
Sodium oxide, Na_2O	0.08	0.07
Potassium oxide, K_2O	0.55	2.38
Sulfur trioxide, SO_3	2.96	1.31
Loss on ignition, LOI	2.89	0.52
Tricalcium silicate, C_3S	56.50	–
Dicalcium silicate, C_2S	17.01	–
Tricalcium aluminate, C_3A	9.23	–
Tetracalcium aluminoferrite, C_4AF	9.62	–

in this study. Consequently, the prediction of cover depth of fly ash concrete required to protect reinforcing steel against initial corrosion in a marine environment for a specified period was developed based on experimental data. The model's validity was verified using data obtained from specimens in a marine environment in Thailand and from previous researches.

2. Specimen preparation and testing

The specimens used were 200 mm concrete cubes containing 0%, 15%, 25%, 35%, and 50% fly ash as a replacement of Portland cement type I. Concrete samples had W/B ratios of 0.45, 0.55, and 0.65. Round bars (grade SR 24 yield strength of 240 MPa) with a diameter of 12 mm and a length of 50 mm were embedded in the concrete samples at cover depths of 10, 20, 50, and 75 mm. Tables 1 and 2 list the chemical properties of cementitious materials and mix proportions of concretes, respectively. After casting for 28 days, the concrete specimens were transferred to a seashore at Chonburi Province, Thailand (Fig. 1). Concrete samples at this marine site were exposed to two wet-dry conditions daily. Annual temperatures at this site range from 25°C to 35°C. Table 3 lists the chemical analysis of the sea water. After exposure to this environment for 2, 3, 4, 5 and 7 years, the samples were dry-cored and tested to determine the chloride penetration profile and chloride content at the position of the embedded steel bar. Chloride concentrations were determined using the acid-soluble chloride method set out by ASTM C1152 [9], resulting in the total chloride content (by weight of binder) in concrete. Besides, the concrete cubes were cored to obtain cylindrical concretes of 50 mm in diameter and 100 mm in height. The compressive strength of the cored concretes were determined and the result was the average of 3 samples. Finally, the 200 mm concrete samples were then crushed, and the corrosions of the embedded steel bars were measured in term of the percentage of rusted area.

3. Experimental results

3.1. Chloride penetration

Fig. 2 shows the chloride penetration profiles of cement concrete and fly ash concretes with a W/B ratio of 0.45 at 7-year exposure in a marine environment. It is seen that fly ash concretes provide lower chloride content than concrete without fly ash. This result is confirmed by several researches that the pozzolanic reaction of fly ash in concrete performs lower permeability, thus leads to lower chloride ingress than normal concrete [10–16]. Interestingly, all fly ash concretes with a W/B ratio of 0.65 had chloride penetration at 7-year exposure lower than that of cement concrete

Table 2
Mixture proportions of concrete samples.

Water to binder ratio	Fly ash replacement (%)	Mixture proportion of concrete (kg/m³)					28 days strength (MPa)
		Cement	Fly ash	Fine aggregate	Coarse aggregate	Water	
0.45							
	0	478	–	639	1024	215	50.4
	15	406	72	639	1004	215	47.4
	25	359	119	639	990	215	43.2
	35	311	167	639	977	215	45.0
	50	239	239	639	957	215	33.8
0.55							
	0	478	–	639	971	262	37.0
	15	406	72	639	948	262	32.0
	25	359	119	639	933	262	30.3
	35	311	167	639	918	262	32.7
	50	239	239	639	897	262	20.9
0.65							
	0	478	–	639	922	311	29.0
	15	406	72	639	898	311	19.9
	25	359	119	639	881	311	21.0
	35	311	167	639	864	311	22.9
	50	239	239	639	840	311	16.6

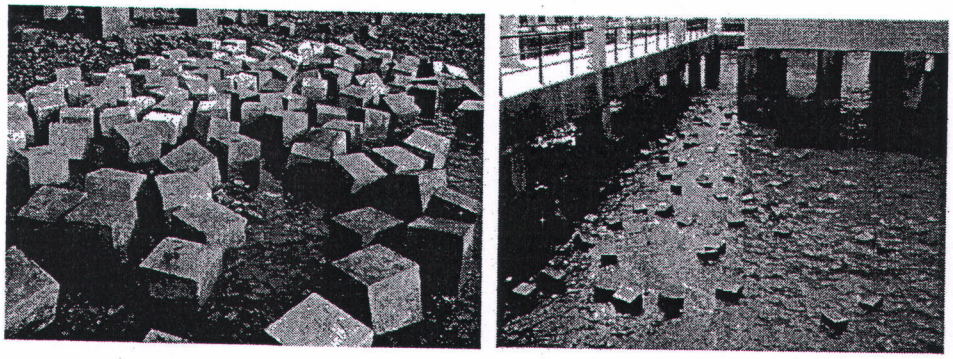

Fig. 1. Concrete specimens at a tidal zone in the Gulf of Thailand (Chonburi Province).

Table 3
Chemical analysis of sea water.

Parameter	January 2002	May 2002	August 2003	December 2003	April 2004	February 2006
pH	8.2	8.2	7.9	8.2	8.1	8.0
Chloride (mg/l)	18.035	16.210	17.125	18.820	17.620	18.380
Sulphate (mg/l)	2.240	2.500	2.230	2.680	2.480	2.510

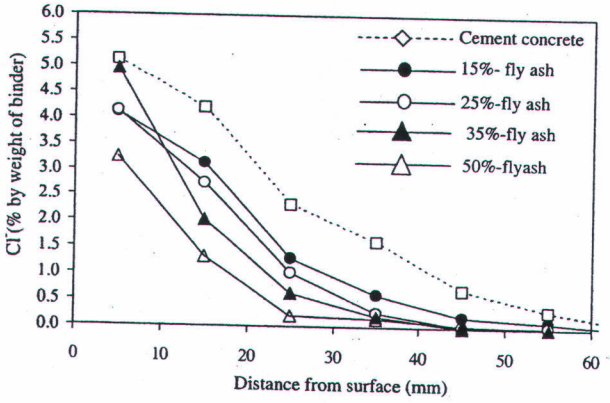

Fig. 2. Chloride penetration profiles of fly ash concretes with a W/B of 0.45 at 7-year exposure in a marine environment.

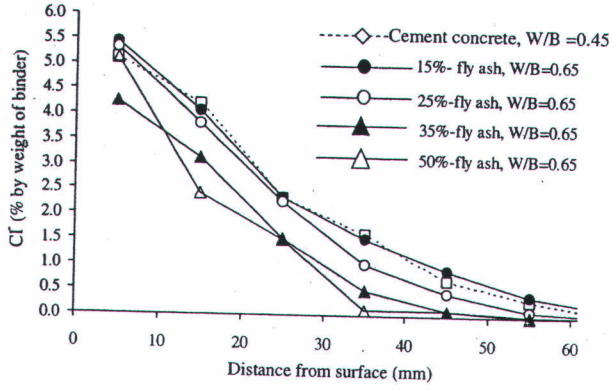

Fig. 3. Chloride penetration profiles of cement concrete with a W/B ratio of 0.45 and fly ash concretes with a W/B of 0.65 at 7-year exposure in a marine environment.

with a W/B ratio of 0.45 as shown in Fig. 3. This result indicated that the use of fly ash in concrete with lower strength grade (W/B of 0.65) has higher resistance to chloride ingress than the one with higher strength grade (W/B of 0.45). For instance, concretes containing fly ash of 15%, 25%, 35%, and 50% by weight of binder with a W/B ratio of 0.65 had chloride concentration at 35 mm cover depth of 1.5%, 1.0%, 0.5%, and 0.1% by weight of binder, respectively while cement concrete with W/B ratio of 0.45 had the chloride concentration at the same cover depth of 1.6% by weight of binder.

3.2. Relationship between compressive strength at 28 days and chloride penetration coefficient

In this study, chloride *penetration* coefficient (D_c) was evaluated based on the general solution of Fick's second law of diffusion as given in Eq. (1) [17].

$$C_{x,t} = C_o\left[1 - erf\left(\frac{x}{2\sqrt{D_c t}}\right)\right] \quad (1)$$

where $C_{x,t}$ is the total chloride concentration (% by weight of binder) at the position x and exposure time t; x, the distance from concrete surface (mm); t, the exposure time (seconds); C_o, the chloride concentration at concrete surface (% by weight of binder) at exposure time t; D_c, the *chloride penetration* coefficient (mm^2/s) at exposure time t and *erf* is the error function.

The determination of D_c can be evaluated by fitting the Fick's second law on chloride penetration profile of the specimens from experimental site. Fig. 4 shows the fitting curve of Fick's second law on chloride penetration profile of concrete with a W/B ratio

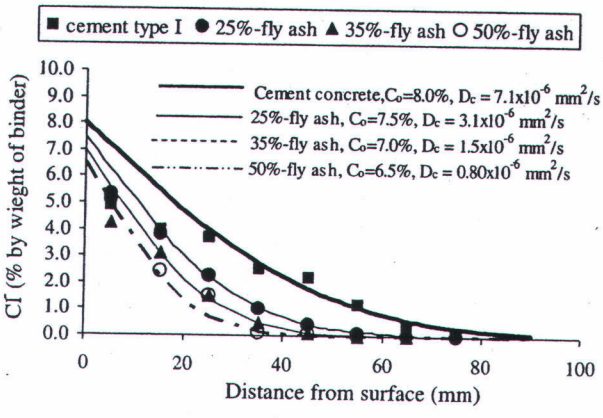

Fig. 4. The fitting curve of general solution of Fick's second law on chloride penetration profile in concrete with a W/B ratio of 0.65 at 7-year exposure.

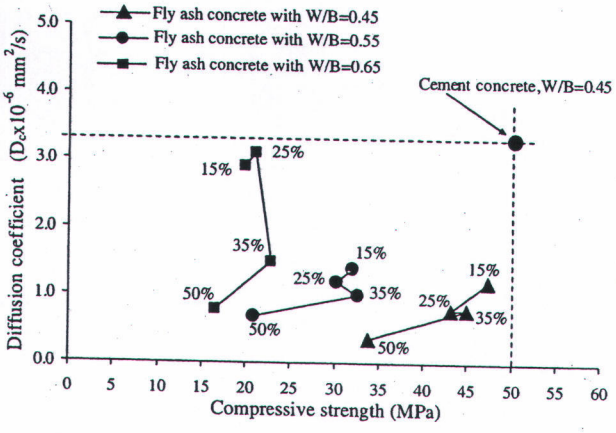

Fig. 5. Relationship between compressive strength at 28 days and chloride penetration coefficient (D_c) of fly ash concretes at 7-year exposure.

of 0.65 at 7-year exposure. After the chloride concentration at concrete surface (C_o) was obtained, the regression analysis yielded the chloride *penetration* coefficient (D_c) at 7-year exposure in a marine environment. For the same procedure, the values of D_c and C_o could be evaluated in the other concrete mixtures.

Fig. 5 shows relationship between compressive strength at 28 days and chloride *penetration* coefficient (D_c) of fly ash concretes at 7-year exposure. These results were also compared with cement concrete with a W/B ratio of 0.45. The results indicated that all fly ash concretes had lower D_c than cement concrete even though they provided lower compressive strength at 28 days than that of cement concrete. All concretes containing fly ash with W/B ratios of 0.45, 0.55, and 0.65 had lower compressive strength than those of cement concretes with the same W/B ratios. It should be noted that the use of fly ash in concrete with low strength grade (high W/B ratio) had more effect on decreasing chloride *penetration* coefficient than the one with high strength grade (low W/B ratio). For instance, in low strength grade concrete (W/B ratio of 0.65), the D_c of concrete at 7-year exposure decreases from 2.9×10^{-6} mm^2/s (15% fly ash replacement) to 0.8×10^{-6} mm^2/s (50% fly ash replacement) while the D_c of concrete with high strength grade (W/B ratio of 0.45) decreases from 1.2×10^{-6} to 0.4×10^{-6} mm^2/s with the same replacement of fly ash. This result was confirmed by other researcher [18]. However, the effective improvement of concrete under marine environment, based on strength and durability of concrete, is to use fly ash as a cement replacement and to use low W/B ratio of concrete. *Since the use of fly ash in concrete with a low W/B ratio produces the high strength and low permeability, achieving a high durable concrete.*

In this study, 25% and 35%-fly ash concretes with a W/B ratio of 0.45 provided the best performance of concrete to be used in a marine environment as it processed the high strength and relatively low chloride penetration. Nevertheless, 50%-fly ash concretes had the lowest compressive strength as compared with the other concrete mixtures (having the same W/B ratio) but it presented the lowest chloride penetration.

3.3. Steel corrosion

After coring, the cube concrete was broken and the embedded steel bars were removed from the cube concrete. The corrosions of embedded steel bars were measured in terms of the percentage of rusted area and image recording. Fig. 6 shows the effects

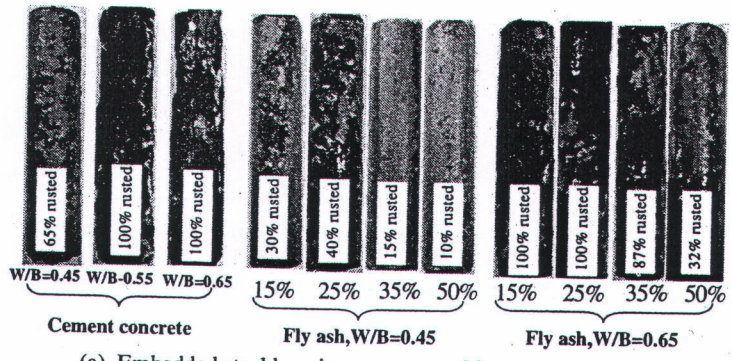

(a) Embedded steel bars in concretes at 20-mm cover depth

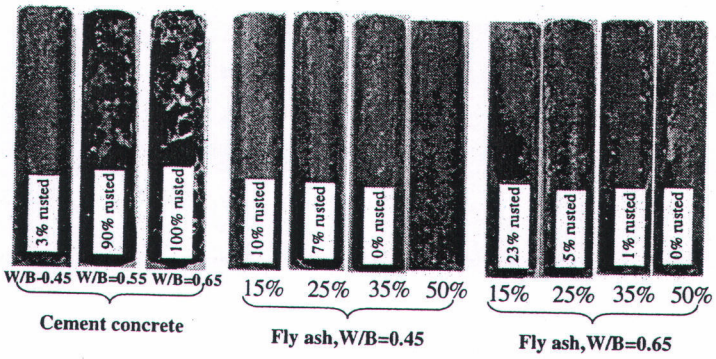

(b) Embedded steel bars in concretes at 50-mm cover depth

Fig. 6. Corrosion of embedded steel bars in concretes at 7-year exposure in tidal zone of marine environment.

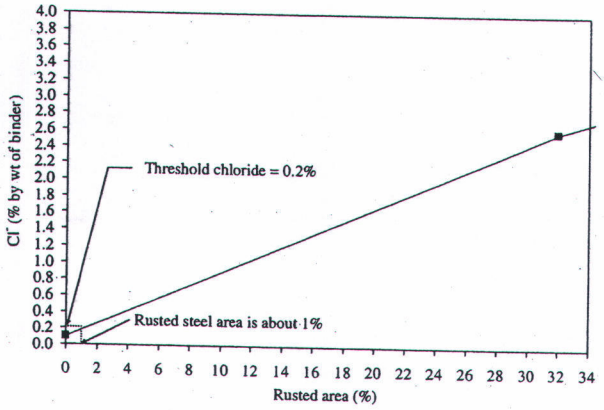

Fig. 7. Relationship between chloride content and rusted area of 50%-fly ash concrete with a W/B ratio of 0.65 at 7-year exposure.

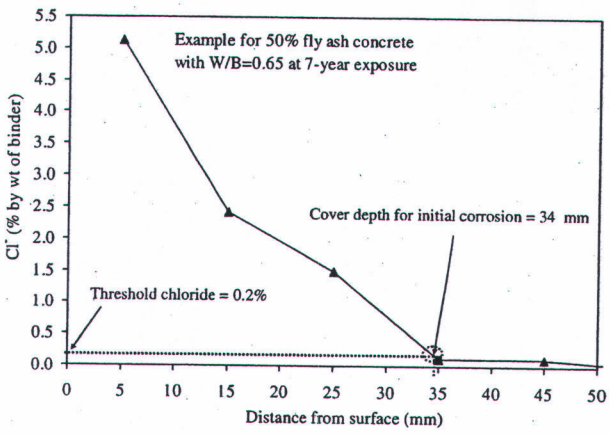

Fig. 8. Chloride penetration profile of 50%-fly ash concrete with a W/B ratio of 0.65 at 7-year exposure.

of W/B ratio and fly ash replacement on the corrosion of embedded steel bars at 20 and 50 mm cover depths at 7-year exposure. The use of fly ash is found to reduce the corrosion of the embedded steel bars as shown in Fig. 6a. For instance, concretes containing fly ash 15%, 25%, 35%, and 50% by weight of binder with a W/B ratio of 0.45 had percentages of rusted area at 20 mm cover depth of 30%, 40%, 15% and 10%, respectively. In Fig. 6b, the embedded steel bars with 50 mm cover depth are rustless in all fly ash concretes, however, slightly rusted of embedded steel bar can be seen in the concrete with high W/B ratio and low fly ash replacement (W/B ratio of 0.65% and 15%-fly ash concrete). Interestingly, the use of fly ash between 25% and 50% in concretes with a W/B ratio of 0.65 did not show the corrosion of embedded steel bar at 50 mm cover depth and presented the corrosion resistance as good as cement concrete with W/B a ratio of 0.45. In cement concrete, it was found that the corrosion was reduced with the decrease of W/B ratio. At 7-year exposure, the embedded steel bars in cement concrete with W/B ratios of 0.55 and 0.65 were severely corroded at the cover depth of 50 mm. This can be suggested that cement concrete with a W/B ratio of more than 0.55 is not appropriate for practical use in a marine environment because it is rapidly destroyed by sea water within 7-year exposure, however, small corrosion (3% rusted area) is found in cement concrete with a W/B ratio of 0.45. In this study, it can be concluded that a direct relationship between the steel corrosion and chloride penetration in concrete under marine environment are found.

Table 4
Required cover depths of concretes against the initial corrosion of embedded steel bar after 2, 3, 4, 5 and 7 years of exposure in a marine environment in Thailand.

Water to binder ratio	Fly ash replacement (%)	Required cover depth (mm)				
		2-year exposure	3-year exposure	4-year exposure	5-year exposure	7-year exposure
0.45						
	0	25	32	38	43	50
	15	22	28	30	37	38
	25	23	27	29	35	40
	35	19	24	27	29	32
	50	17	22	25	26	29
0.55						
	0	26	37	47	48	60
	15	25	32	35	39	47
	25	23	31	33	38	44
	35	22	30	32	33	38
	50	21	25	28	30	32
0.65						
	0	45	53	60	70	75
	15	35	46	48	54	63
	25	30	36	38	47	52
	35	28	33	35	40	43
	50	22	30	31	32	34

4. Utilization of experimental data for long term design life analysis

4.1. Cover depth for initial corrosion

The cover depth of concrete required to protect against the initial corrosion of embedded steel bar was defined by the penetration depth of threshold chloride in concrete. The threshold chloride values were determined from the amount of chloride required to cause the initial corrosion of the steel bars embedded in the concrete samples. In this study, initial corrosion was defined as the initial occurrence of rusted steel, approximately 1% of the total area. The rusted areas were used to determine the threshold chloride values using the relationship between the rusted area and the chloride concentration near the embedded steel bar. Throughout, penetration depths of the threshold chloride could be extrapolated from chloride penetration profiles or from the relationship between chloride content and the distance from the concrete surface.

Fig. 7 shows the relationship between chloride content and rusted area of 50% fly ash concrete with a W/B ratio of 0.65 after 7 years of exposure. At the initial occurrence of rust (~1% of the steel area), the chloride content was 0.20% by weight of binder; this was defined as the threshold chloride content for 50% fly ash concrete with a W/B ratio of 0.65 after 7 years of exposure. This threshold chloride content was used to determine the cover depth of concrete required to protect against the initial corrosion of embedded steel bar in fly ash concrete (Fig. 8).

4.2. Generating empirical equation for prediction of concrete cover depth

Table 4 lists the required concrete cover depths to protect against the initial corrosion of embedded steel bar. The data were plotted to obtain the relationship between the required concrete cover depth to protect against the initial corrosion of embedded steel bar and the exposure period of fly ash concretes with W/B ratios of 0.45, 0.55, and 0.65 (shown in Fig. 9). The relationship between the required cover depth to protect against the initial corrosion of embedded steel bar and the exposure period of fly-ash concrete can be established using a logarithm function, producing the following equation to predict the required cover depth of fly ash concrete to protect reinforcing steel from initial corrosion at a specified exposure period:

$$CD = [\alpha(F) + \beta]\ln(T) + \gamma(F) + \delta \quad (2)$$

where CD is the required cover depth to protect against the initial corrosion of embedded steel bar in concrete (mm); T, the exposure period in a marine environment (years); F, the fly ash replacement (%) and α, β, γ and δ are the coefficients for a specified W/B ratio, obtained from the following regressions:

$$\alpha = 6.03(W/B)^2 - 7.31(W/B) + 1.87 \quad (3)$$

$$\beta = -233.1(W/B)^2 + 292.09(W/B) - 65.67 \quad (4)$$

$$\gamma = -15.99(W/B)^2 + 16.76(W/B) - 4.29 \quad (5)$$

$$\delta = 677.65(W/B)^2 - 682.81(W/B) + 181.69 \quad (6)$$

where W/B = water to binder ratio, ranging from 0.45 to 0.65.

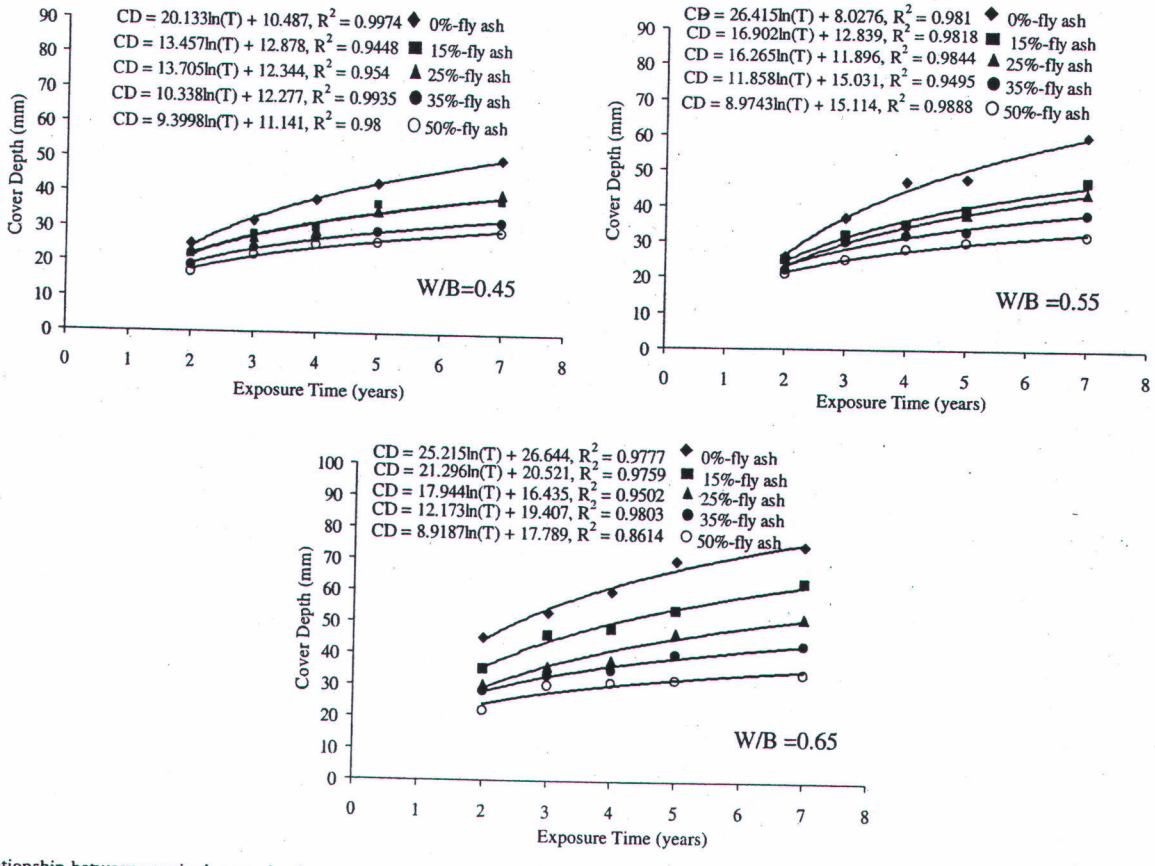

Fig. 9. Relationship between required cover depth to protect against the initial corrosion of embedded steel bar and exposure time in a marine environment for fly ash concrete.

Eq. (2) can be re-written in the other form for predicting the time for initial corrosion of embedded steel bar in fly ash concrete, as follows:

$$T = Exp[CD - (\gamma(F) + \delta)]/[\alpha(F) + \beta] \quad (7)$$

Furthermore, Eq. (7) can predict deactivation time of reinforcing steel or the maintenance period if the details of the reinforced concrete structure are known (cover depth, W/B ratio, fly ash replacement, and exposure time).

The empirical model was developed based on durable data obtained from an actual experimental site in a marine environment. It should be noted that it is difficult to control various parameters in a field site, especially a site with physical effects such as temperature, humidity, and abrasion–erosion damage. However, the empirical equation (which was based on data obtained from the actual experimental site) also included physical and chemical parameters that damaged concrete structures.

The empirical model can predict the required cover depth of concrete to protect against the initial corrosion of reinforcing steel bar in fly ash concrete at any duration of exposure in a marine environment. It yields good results when W/B ratios range from 0.45 to 0.65, fly ash replacement values range from 0% to 50% by weight of binder, and the duration of exposure in a marine environment is longer than 2 years. However, the model's ability to predict cover depth is limited; because the model was developed based on the chloride penetration profile (obtained from dry-cored 200 mm concrete cube specimens), it used only the one-dimensional dispersion of chloride. Therefore, it is limited to a one-dimensional perspective of chloride ingress from the concrete surface to its centre. The model is applicable to practical reinforced concrete structures such as slabs, footings, and other structures when they are assumed to have one-dimensional chloride ingress.

4.3. Model validation

The empirical model was validated using data obtained from an experimental marine environment in Thailand and from previous researches. Fig. 10 compares predicted and actual cover depth results at 2, 3, 4, 5 and 7 years of exposure. Solid and dotted lines represent the range within +15% and −15% error of the tested data, respectively. All predictions were within 15% error of the empirical results. The predictions were also compared with the results obtained from Thomas and Matthew [7] in a marine environment in which the cover depths for threshold chloride levels in fly ash concretes at 2, 4, and 10 years of exposure in a UK marine environment were investigated. Fig. 11 compares Thomas and Matthews's results [7] to the predicted values; most predictions were within 25% error of the tested data.

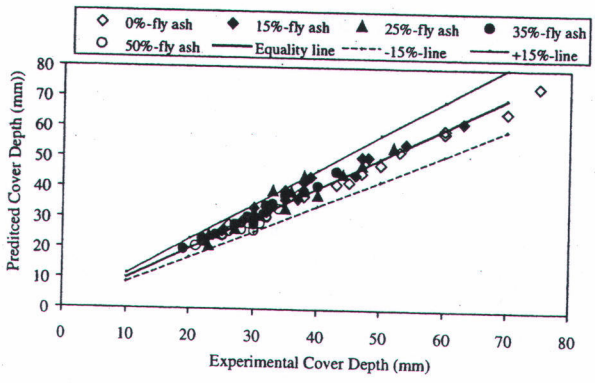

Fig. 10. Comparison of predicted and experimental required cover depth to protect against the initial corrosion of embedded steel bar in fly ash concrete after 7 years of exposure in a marine environment.

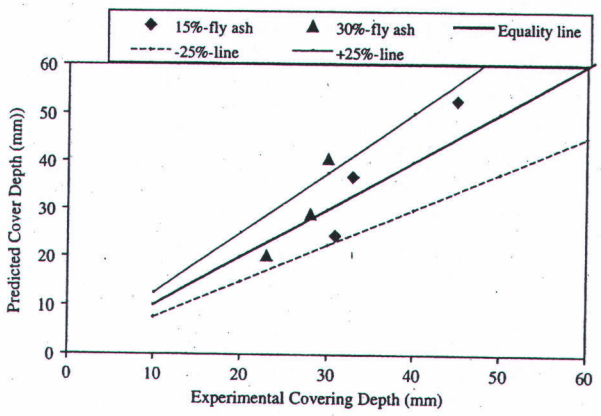

Fig. 11. Relationship between predicted and experimental cover depths of concretes to protect against the initial corrosion of reinforcing steel bar based on Thomas's data [7].

Fig. 12 shows the required cover depths of cement concrete and 30% fly-ash concrete to protect against the initial corrosion of reinforcing steel, according to the predictions by Thomas [19] and our empirical model. The predictions differed slightly for fly ash concretes within a 40-year exposure period, after which the models yielded quite different predictions; the empirical model predicted that less concrete cover depth would be required. The two models predicted the same cover depth for cement concrete within a 10-year exposure period. Thomas's model [19] is based on the *penetration* coefficient of chloride, calculated from the fitting of data over four years and threshold chloride values of 0.7% for cement concrete and 0.5% for fly ash concrete. These data were gathered from specimens exposed to the tidal zone of a marine site in Essex, UK, where the climate varies greatly from warm summers to cool winters. In contrast, the empirical model was based on experimental data from a marine site in Southeast Asia, which is always hot and humid. However, the predictions of both models indicated that use of fly ash in concrete considerably reduces the required cover depth to protect against the initial corrosion of steel. Predictions by Thomas's model [19] and by the empirical model indicated that for a 50 mm cover depth, the time to initiate corrosion in reinforcing steel was approximately 7 and 8 years for cement concrete and 30 and 24 years for concrete containing 30% fly ash, respectively.

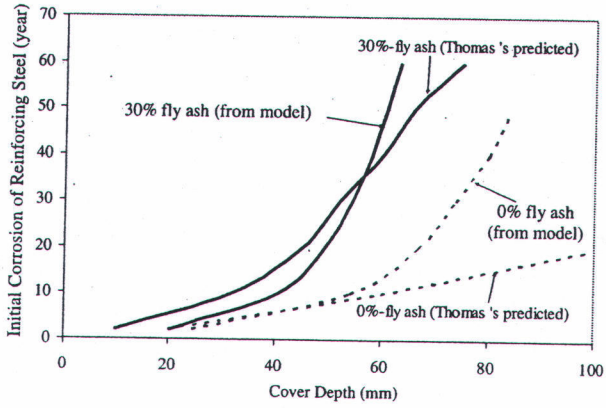

Fig. 12. Comparison of the cover depths of concretes to protect against the initial corrosion of reinforcing steel bar in cement concrete and 30%-fly ash concrete in a marine environment from the empirical model and from Thomas's model [14].

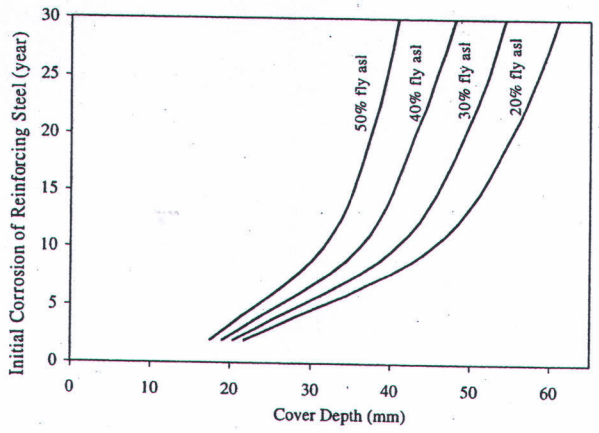

Fig. 13. Relationship between the initial corrosion of reinforcing steel and the cover depth of fly ash concrete with a W/B ratio of 0.45 after exposure to a marine environment for 30 years, based on the empirical model.

Another study, Shafiq [20] predicted the required cover depths for specified service lifetimes of 50 and 120 years based on the corrosion by 1% chloride content in fly ash concrete. Shafiq [20] predicted that 40% fly ash concrete with a W/B ratio of 0.50 would require a cover depth of 50 mm for 50 years and 75 mm for 120 years to protect against the initial corrosion of reinforcing steel; the empirical model predicted a required cover depth of 55 and 65 mm for the same conditions. The different predictions may be that Shafiq's prediction [20] is based on corrosion damage by 1% chloride content, whereas the empirical model is based on the defined initial corrosion of 1% rusted area of embedded steel in a practice site which has a chloride content of 0.4% by weight of binder. However, the two models still yielded fairly similar results.

4.4. Use of the empirical model

The empirical model could be very useful to help engineers to determine a suitable concrete cover depth for a reinforced concrete structure in sea water. In addition, the time for initial corrosion of the reinforcing steel in concrete can be predicted and then, the maintenance of the reinforced concrete structure will be followed. The empirical model can predict the time to the initial corrosion of reinforcing steel in concrete when the cover depth and the characteristics of concrete are known. Fig. 13 shows the relationship between the time to initial corrosion in reinforcing steel and the required cover depths of 20%, 30%, 40% and 50% fly ash concretes with a W/B ratio of 0.45. For example, if a 50 mm cover depth is required to last 20 years (time to initial corrosion), up to 30% of fly ash will be needed to replace Portland cement in concrete with a W/B ratio of 0.45. Furthermore, the model can predict the deactivation time or maintenance schedule for concrete structures that are already in service in a marine environment when the details of the concrete are known (i.e., cover depth, W/B ratio, fly ash replacement, and exposure time).

5. Conclusions

1. The increase of fly ash replacement in concrete clearly reduces the chloride penetration, chloride *penetration* coefficient, and steel corrosion in concrete.
2. Decrease of W/B ratio results in the decrease of chloride *penetration* coefficient (D_c). It is also found that the decrease of W/B ratio is more effective on reducing D_c in low volume fly ash concrete (15–25% replacement) than in high volume fly ash concrete (35–50% replacement).
3. At 7-year exposure in sea water, concretes containing 25–50% of fly ash as a cement replacement and having a W/B ratio of 0.65 have equivalent or better resistance of steel corrosion than that of cement concrete with a W/B ratio of 0.45.
4. The empirical model can predict the required concrete cover depth to protect against the initial corrosion of reinforcing steel in cement and fly ash concretes for exposure period longer than two years in a marine environment. It yields good results for concretes with W/B ratios ranging from 0.45 to 0.65 and fly ash replacement from 0% to 50% by weight of binder. However, the application of the model is limited to a one-dimensional ingress of chloride into concrete structures.

Acknowledgements

The authors gratefully acknowledge financial supports from the Research and Development Funds, Faculty of Engineering, Burapha University, Thailand, the Thailand Research Fund (TRF) under TRF New Researcher Scholar Contact no. MRG5280003, and TRF Senior Research Scholar Contact no. RTA5080020, and the Commission on Higher Education, Ministry of Education, Thailand.

References

[1] Wong Song H, Saraswathy V. Studies on the corrosion resistance of reinforced steel in concrete with ground granulated blast-furnace slag–an overview. J Hazard Mater 2006;138:226–33.
[2] Dimitri Val V, Mark Stewart G. Life cycle cost analysis of reinforced concrete structure in marine environments. Struct Saf 2003;25:343–62.
[3] Kiattikomol K, Jaturapitakkul C, Songpiriyakij S, Chutubtim S. A study of ground course fly ashes with different finenesses from various sources as a pozzolanic materials. Cem Concr Compos 2001;23:335–43.
[4] Jaturapitakkul C, Kiattikomol K, Sata V, Leekeeratikul T. Use of ground coarse fly ash as a replacement of condensed silica fume in producing high-strength concrete. Cem Concr Res 2004;34:549–55.
[5] Troconis de Rincon O, Castro P, Moreno EI, Torres-Acosta AA, Moron de Bravo O, Arrieta I, et al. Chloride penetration profile in two marine structures-meaning and some predictions. Build Environ 2004;39:1065–70.
[6] Dehwah HAF, Maslehuddin M, Austin SA. Long-term effect of sulfate ions and associated cat ion type on chloride-induced reinforcement corrosion in Portland cement concretes. Cem Concr Compos 2002;24:17–25.
[7] Thomas MDA, Matthews JD. Performance of PFA concrete in a marine environment-10-year results. Cem Concr Res 2004;26:5–20.
[8] Chalee W, Jaturapitakkul C, Chindaprasirt P. Predicting the chloride penetration of fly ash concrete in seawater. Mar Struct 2009;22:341–53.
[9] ASTM C1152. Standard test method for acid-soluble chloride in mortar and concrete. Annual books of ASTM standards V. 04.01, Philadelphia; 1997. p. 627–69.
[10] Chindaprasirt P, Jaturapitakkul C, Sinsiri T. Effect of fly ash fineness on compressive strength and pore size of blended cement paste. Cem Concr Compos 2005;27(4):425–8.
[11] Arya C, Xu Y. Effect of cement type on chloride binding and corrosion of steel in concrete. Cem Concr Res 1995;25:893–902.
[12] Ilker Bekir Topcu, Karakurt Cenk, Sardemir Mustafa. Predicting the strength development of cements produced with different pozzolans by neural net work and fuzzy logic. Mater Des 2008;29:1986–91.
[13] Sezer Gozdelnan, Ramyar Kambiz, Karasu Bekir, Burak Goktepe A, Sezer Alper. Image analysis of sulfate attack on hardened cement paste. Mater Des 2008;29:224–31.
[14] Sujjavanich S, Sida V, Suwanvitaya P. Chloride permeability and corrosion risk of high-volume fly ash concrete with mid-range water reducer. ACI Mater J 2005;102:177–82.
[15] Sengul O, Tasdemir C, Tasdemir AT. Mechanical properties and rapid chloride permeability of concrete with ground fly ash. ACI Mater J 2005;102:414–21.
[16] Ramezanianpour AA, Malhotra VM. Effect of curing on the compressive strength, resistance to chloride-ion penetration and porosity of concretes incorporating slag, fly ash or silica fume. Cem Concr Compos 1995;17:125–33.
[17] Crank J. The mathematics of diffusion. 2nd ed. London: Oxford Press; 1975.
[18] Chindaprasirt P, Chotithanorm C, Cao HT, Sirivivatnanon V. Influence of fly ash fineness on the chloride penetration of concrete. Construct Build Mater 2007;21:356–61.
[19] Thomas MDA. Author's reply to discussion of paper chloride thresholds in marine concrete. Cem Concr Res 1996;26:1603–4.
[20] Shafiq N. Effects of fly ash on chloride migration in concrete and calculation of cover depth required against the corrosion of embedded steel reinforcement. Struct Concr 2004;5:5–9.

10. S. Songpiriyakij, T. Kubprasit, C. Jaturapitakkul, P. Chindaprasirt. Compressive strength and degree of reaction of biomass-fly ash –based geopolymer, Construction and Building Materials, 24 (2010), 236-240. (IF 0.947)

Construction and Building Materials 24 (2010) 236–240

Contents lists available at ScienceDirect

Construction and Building Materials

journal homepage: www.elsevier.com/locate/conbuildmat

Compressive strength and degree of reaction of biomass- and fly ash-based geopolymer

Smith Songpiriyakij [a,*], Teinsak Kubprasit [b], Chai Jaturapitakkul [b], Prinya Chindaprasirt [c]

[a] College of Industrial Technology, King Mongkut's University of Technology, North Bangkok, Bangkok, Thailand
[b] Department of Civil Engineering, Faculty of Engineering, King Mongkut's University of Technology, Thonburi, Bangkok, Thailand
[c] Department of Civil Engineering, Faculty of Engineering, Khon Kaen University, Khon Kaen, Thailand

ARTICLE INFO

Article history:
Received 10 April 2009
Received in revised form 31 July 2009
Accepted 7 September 2009
Available online 7 October 2009

Keywords:
Geopolymer
Fly ash
Rice husk and bark ash
Degree of reaction

ABSTRACT

Rice husk and bark ash (RHBA) was used as a rich SiO_2 source to partially replace fly ash in making geopolymer. Consequently, the SiO_2/Al_2O_3 ratio was extended to the wide range of 4.03–1035. Compressive strength, degree of reaction, and microstructure of the geopolymers were investigated to observe the effect of SiO_2/Al_2O_3 ratio. Results revealed that the optimum SiO_2/Al_2O_3 ratio to obtain the highest compressive strength was 15.9. Fly ash was more reactive than RHBA. It was also shown that not only the reactivity of the source materials but also the quality of the matrix contributed to the enhancement of compressive strength of the geopolymer paste.

1. Introduction

Unlike high-volume fly ash (HVFA) concrete, geopolymer is synthesized by the polycondensation of silico-aluminate structures. Highly alkaline solutes such as NaOH and KOH are incorporated with source materials rich in SiO_2 and Al_2O_3. There is no Portland cement involved in this cementing material. Normal hydration or pozzolanic reaction processes cannot be used to describe the geopolymeric reaction. Davidovits [1] described three basic forms of silico-aluminate structures corresponding to Si/Al ratios of 1, 2, and 3 as polysialate, polysialate-siloxo, and polysialate-disiloxo. The matrix is bonded together by any form of 3D cross-linked chain. Many researchers [2–4] have considered the role of the SiO_2/Al_2O_3 ratio in the properties of geopolymer. However, with constrained material sources such as fly ash and kaolin, SiO_2/Al_2O_3 varies in a narrow range of 1–4. Fletcher et al. [5] extended the limit of studies by observing the effect of SiO_2/Al_2O_3 ratios from 0.5 to 300 on the setting and hardening properties of geopolymer. It is interesting to observe that increasing the SiO_2/Al_2O_3 ratio to 16 results in higher compressive strength. Beyond this ratio, compressive strength rapidly reduces and the geopolymer becomes elastic rather than brittle.

Other work [5] used dehydroxylated kaolinite and fine amorphous silica as starting materials. In practice, it is costly to use materials rich in Si and Al other than byproduct materials. We focus primarily on using rice husk and bark ash (RHBA) as a Si-rich material, incorporating it with lignite fly ash as starting materials, and testing the product's compressive strength over a wide range of SiO_2/Al_2O_3 ratios. Moreover, degrees of reaction corresponding to the SiO_2/Al_2O_3 ratio are presented.

2. Experimental program

2.1. Materials

Fly ash and RHBA were used as starting materials. RHBA was obtained from a biomass electricity power plant from burning of rice husks and bark at a ratio of 70:30. The burning temperature was around 400 °C. The chemical compositions are shown in Table 1. RHBA was ground in a ball mill until 98% of the particles were smaller than 45 μm. Fly ash was not processed as 66% of the particles were smaller than 45 μm. Sodium hydroxide solutions of 14 and 18 M concentration were prepared by dissolving NaOH pellets in distilled water. Sodium silicate solution with composition of 8.9 wt.% Na_2O, 28.7 wt.% SiO_2, 62.5 wt.% H_2O was also used.

2.2. Mix proportions

Ashes were dry blended in a jar at proportions of FA:RHBA of 100:0, 80:20, 60:40, 20:80, and 0:100 by weight. NaOH and sodium silicate solutions were also premixed in plastic containers and left overnight to cool to room temperature. A total of 11 mix proportions were used, as shown in Table 2.

Two series of mixes were used in this experiment. For the first series, seven mixes were prepared with varying SiO_2/Al_2O_3 ratios by varying RHBA:FA ratios. For the second series, four mixes were prepared to vary the liquid fractions (activator) by changing sodium silicate/NaOH ratios. The list of key chemical ratios is shown in Table 3. It should be noted here that SiO_2/Al_2O_3 ratios could be varied in a wide range by varying FA:RHBA ratios.

* Corresponding author. Tel.: +66 2 2131524; fax: +66 2 587 6930.
E-mail address: ssy@kmutnb.ac.th (S. Songpiriyakij).

0950-0618/$ - see front matter © 2009 Elsevier Ltd. All rights reserved.
doi:10.1016/j.conbuildmat.2009.09.002

Table 1
Chemical composition of starting materials.

	SiO_2	Al_2O_3	Fe_2O_3	CaO	SO_3	LOI
RHBA	84.75	0.16	–	2.78	0.60	3.72
FA	36.02	20.58	15.91	18.75	2.24	0.07

2.3. Test details

Samples were cast in 30 mm diameter by 60 mm height cylindrical molds and vibrated for 5 min to reduce entrained air. The pastes with high RHBA content were quite sticky and required extra effort in casting in a mold. All samples were demolded 24 h after casting. They were wrapped with polyurethane sheet to prevent moisture loss. A mixture was chosen to observe the effect of curing temperatures. Two curing conditions, room curing at 27 °C and oven curing at 60 °C for 24 h were used. Samples were then left at room temperature until the tested ages. Samples were tested for compressive strength at 3, 7, 14, 28, and 90 days. Portions of broken sample at the age of 28 days were used for the scanning electron microscopy and energy dispersive spectroscopy (SEM/EDAX) studies.

Degrees of reaction of some samples were tracked by chemical processes. Geopolymer product was ground and attacked by picric acid (5 g dissolved in methyl alcohol 10 g and 20 g distilled water added). The sample was stirred for 45 min and poured through filter paper with a pore size of 2.5 μm. The remains were oven dried at 100 °C for 24 h and then heated in an oven at 1000 °C for 3 h. The residue was considered to be the unreacted portion of the fly ash. This method was used to determine the degree of pozzolanic reaction [6–8]. A similar method with other media was also used to determine the degree of geopolymerization by Fernandez-Jimenez et al. [9].

3. Results and discussion

3.1. Effect of SiO_2/Al_2O_3 ratios on compressive strength

The SiO_2/Al_2O_3 ratios were varied from 4.03 for the 100% FA mixture to 1035 for the 100% RHBA mixture, as shown in Table 4. The compressive strength results of series 1 are shown in Fig. 1. It should be noted here that the other chemicals were kept optimum and varied within a narrow range. Compressive strength increased as the SiO_2/Al_2O_3 ratio increased. The compressive strength at 3 days was 10.9 MPa at an SiO_2/Al_2O_3 ratio of 4.03 (100% FA). The strength increased rapidly when some RHBA was added. The addition of RHBA enriched the Si in the matrix, which allowed stronger Si–O–Si bonds to form. When the ratio of about 10 (65FA60 18M25 mix) was reached, the rate of compressive strength development became slower. The strength actually dropped when the ratio exceeded 15.9. When the SiO_2/Al_2O_3 ratio was greater than eight, the mixtures were very sticky and difficult to pour into the mold. The compressive strength at 3 days of 65FA60 18M25 (SiO_2/Al_2O_3 = 15.9) paste with room temperature

Table 4
Compressive strength of pastes.

Symbol	Compressive strength (MPa)				
	3 days	7 days	14 days	28 days	90 days
65FA100 18M25	10.9	17.0	25.7	34.0	35.3
65FA80 18M25	13.4	20.3	30.6	40.4	42.6
65FA60 18M25	23.1	30.3	36.1	44.5	54.0
65FA40 18M25	24.3	33.5	40.9	51.0	62.4
65FA40 18M25H[a]	49.2	49.2	54.9	56.0	72.8
65FA30 18M25	23.2	29.9	37.9	42.2	NA
65FA20 18M25	19.6	25.7	33.1	39.3	NA
65FA00 18M25	NA	NA	NA	NA	NA
65FA40 14M05	0.8	6.9	16.0	21.8	22.5
65FA40 14M15	13.9	27.6	32.8	42.0	49.7
65FA40 14M25	25.4	34.6	39.4	46.4	53.4
65FA40 14M35	26.3	37.3	43.2	49.4	51.6

[a] H = cured at 60 °C for 24 h after demolding.

Table 2
Mixture proportions.

Series	Symbol	Mix proportion by weight (g per 1000 g)				
		RHBA	FA	Na_2OSiO_2	NaOH 14 M	NaOH 18 M
1	65FA100 18M25	–	650	250		100
	65FA80 18M25	130	520	250		100
	65FA60 18M25	260	390	250		100
	65FA40 18M25	390	260	250		100
	65FA30 18M25	455	195	250		100
	65FA20 18M25	520	130	250		100
	65FA00 18M25	650	–	250		100
2	65FA40 14M05	390	260	117	233	
	65FA40 14M15	390	260	210	140	
	65FA40 14M25	390	260	250	100	
	65FA40 14M35	390	260	272	78	

*xx*FA*yy zz*Mn: *xx* = % of solid fraction, *yy* = % of fly ash in solid fraction, *zz* = molarities of NaOH, and *n* = Na_2OSiO_2/NaOH ratio.

Table 3
Key chemical ratios of mixtures.

Symbol	SiO_2/Al_2O_3	Na_2O/SiO_2	Na_2O/Al_2O_3	Si/Al input	Si/Al of end product[a]
65FA100 18M25	4.03	0.27	1.07	2.09	3.75
65FA80 18M25	6.02	0.22	1.33	3.14	6.02
65FA60 18M25	9.34	0.19	1.77	4.86	6.39
65FA40 18M25	15.91	0.17	2.64	8.28	6.57
65FA30 18M25	22.39	0.16	3.51	11.65	7.19
65FA20 18M25	35.11	0.15	5.19	18.27	8.75
65FA00 18M25	1035.0	0.13	138.0	538.0	–
65FA40 14M05	14.51	0.23	3.37	7.55	NA
65FA40 14M15	15.49	0.17	2.67	8.06	NA
65FA40 14M25	15.91	0.15	2.38	8.28	NA
65FA40 14M35	16.14	0.14	2.21	8.40	NA

[a] Randomly taken from dense matrix.

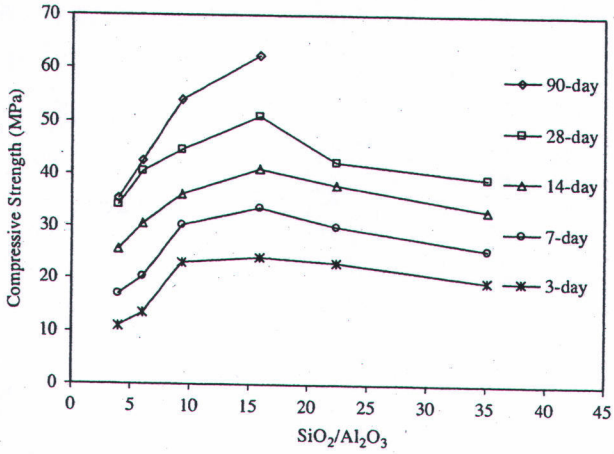

Fig. 1. Compressive strength vs. SiO_2/Al_2O_3 ratio.

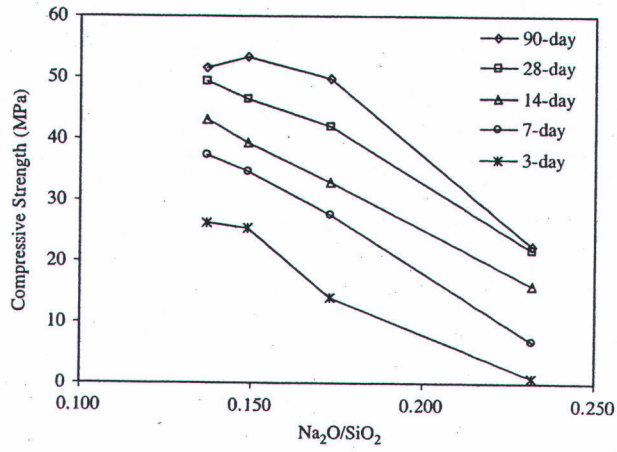

Fig. 2. Compressive strength vs. Na_2O/SiO_2 ratio.

curing was 24.3 MPa. After demolding at age of 2 days, the same mixture was cured at 60 °C for 24 h. The compressive strength of this paste reached 49.2 MPa within 3 days, comparable with the 28-day strength of paste cured at room temperature. The compressive strength of all mixtures increased with time similar to the normally observed Portland cement materials.

For the mixtures with SiO_2/Al_2O_3 ratios higher than 15.9, expansion of the specimens with time was observed and cracking started to occur after a month. This leads to the need for more research on expansion and the mechanism of this behavior. A 65FA00 18M25 paste specimen (SiO_2/Al_2O_3 = 1035) expanded and cracked within the first day after demolding. The 65FA20 18M25 and 65FA30 18M25 paste specimens cracked after 1–2 months. There was no compressive strength gain for adding more RHBA when the SiO_2/Al_2O_3 ratio was higher than 15.9, as shown in Fig. 1. Previous work [2–4] on fly ash geopolymer reported optimum Si/Al ratios of 1.70–1.90 for maximizing compressive strength.

Fletcher et al. [5] synthesized geopolymer from dehydroxylated kaolinite and amorphous silica with SiO_2/Al_2O_3 from 0.5 to 300 (Si/Al = 0.26–156) and showed that the compressive strength of the geopolymer paste increased as the SiO_2/Al_2O_3 ratios increased. When the SiO_2/Al_2O_3 ratio was higher than 16, the compressive strength tended to drop and the failure mode changed from crushing to deformation. We also found this transformation from brittle to elastic materials at SiO_2/Al_2O_3 at 15.9.

3.2. Influence of Na_2O on compressive strength

Although the main point of this research was to identify the influence of the SiO_2/Al_2O_3 ratio on the compressive strength of geopolymer paste, the effect of Na_2O was not completely ignored. Na_2O/SiO_2 and Na_2O/Al_2O_3 ratios represented the amount of OH^- in the mixtures. The observation of the influence of Na_2O on the compressive strength of geopolymer paste was carried out in series 2. In this series, the proportion of powder was kept constant and the proportion of activator was varied to obtain a wide range of NaOH in the mixtures. Table 3 shows that SiO_2/Al_2O_3 ratios changed in a narrow range between 14.51 and 16.14. The results shown in Fig. 1 indicated that this small range had negligible effect on compressive strength. Na_2O/SiO_2 and Na_2O/Al_2O_3 ratios were the main variables affecting compressive strength in this series. Na_2O/SiO_2 ratios were between 0.14 and 0.23 and Na_2O/Al_2O_3 ratios were between 2.21 and 3.37.

The results as shown in Figs. 2 and 3 indicated that the decrease in Na_2O/SiO_2 and Na_2O/Al_2O_3 (or less Na_2O) resulted in increases in

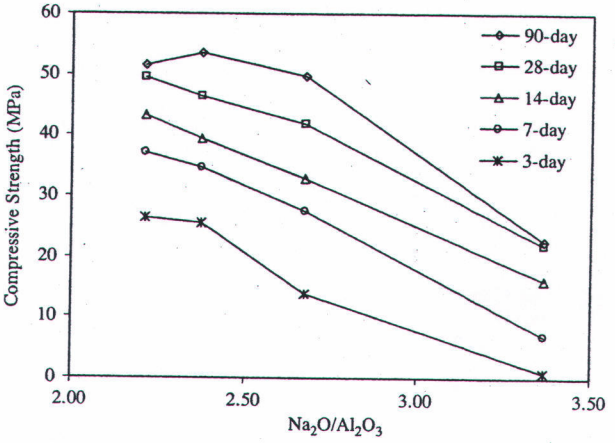

Fig. 3. Compressive strength vs. Na_2O/Al_2O_3 ratio.

compressive strength of the geopolymer. High Na_2O content was found to promote an amorphous–crystalline transformation in the system. The dense amorphous matrix exhibited the higher compressive strength [10]. The results conformed to previous research [10,11]; however, our work provided the results at very high SiO_2/Al_2O_3 ratios (between 14.51 and 16.14). Thus, we have validated the effect for a wide range of SiO_2/Al_2O_3 (3–16.14). Chindaprasirt et al. [11] reported that the optimum sodium silicate/NaOH ratios of fly ash geopolymer were between 0.67 and 1.0, and NaOH concentrations between 10 and 20 M had a small effect on compressive strength.

3.3. Rate of reaction

Three proportions of paste, 100% FA, 40% FA–60% RHBA, and 100% RHBA mixtures were selected for the investigation of degree of reaction. The 65FA40 18M25 (SiO_2/Al_2O_3 = 15.91) paste was cured both at room temperature and oven cured. The results are shown in Table 5. Some particles reacted immediately in the dissolution stage, because silicon and aluminum ions were released into solution to form Si–O–Si, Si–O–Al, and Al–O–Al structures. These matrixes were easily washed by mild acid, and unreacted particles remained. The degree of reaction of the 100% FA mixture was 23.47% immediately after mixing and increased rapidly to 55.44% at 24 h during the hardening process. Afterward, the reaction

Table 5
Degree of reaction.

Symbol	Degree of reaction (%)						
	0 h	1 h	6 h	1 days	2 days	7 days	28 days
65FA100 18M25	23.47	36.44	41.51	55.44	61.46	63.83	65.21
65FA40 18M25	15.57	22.93	28.86	32.14	33.31	35.36	46.25
65FA40 18M25H[a]	15.57	22.93	28.86	32.14	41.25	48.73	55.25
65FA00 18M25	13.29	30.70	31.52	31.58	37.96	39.10	40.20

[a] H = cured at 60 °C for 24 h after demolding.

was relatively slow. However, the compressive strength of the paste continued to develop after that time. It is noted that the reaction in the solid phase of geopolymeric paste does not require moist curing to the same extent as the hydration.

The 100% RHBA mixture showed less reaction than the 100% FA mixture. A degree of reaction of 13.29% was obtained immediately after mixing and only 40.20% was obtained after 28 days. However, the compressive strength did not match the degree of reaction results. This mixture expanded and cracked after demolding. Previous work [12] has reported that the Al ion is always required, to form the stronger aluminosilicate compound. However, silicate gel or glass gel did not provide compressive strength. The sample 65FA40 18M25 with a SiO_2/Al_2O_3 ratio of 15.91 gave the expected result. The degree of reaction was lower than that of 100% FA but higher than that of 100% RHBA. However, it was observed that the lesser reaction resulted in the relatively high strength of 51.0 MPa at 28 days with degree of reaction of 46.25%. In contrast, sample 65FA100 18M25 reacted faster to 65.21%, but had a lower compressive strength of 34.0 MPa. It was evident that not only the degree of reaction but also the quality of the matrix was responsible for the compressive strength. With higher SiO_2/Al_2O_3 ratios, complex frameworks were formed and consequently exhibited higher compressive strength.

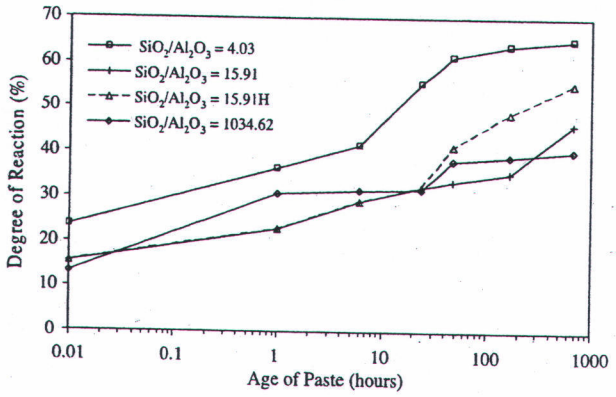

Fig. 4. Degree of reaction, H = cured at 60 °C for 24 h after demolding.

To observe the effect of curing temperature, samples of 65FA40 18M25 were cured at room temperature of 27 °C and oven cured at 60 °C for 24 h. The results shown in Fig. 4 indicate that the rate of reaction was enhanced with high-temperature curing. The rate of reaction jumped from 32.14% to 41.25% within 24 h while it gradually increased to 33.31% for normal room temperature curing. This resulted in significant gain in compressive strength.

3.4. SEM and EDAX description

SEM and EDAX were taken from broken portions of 28-day compressive strength test samples. Fig. 5 shows that the matrix

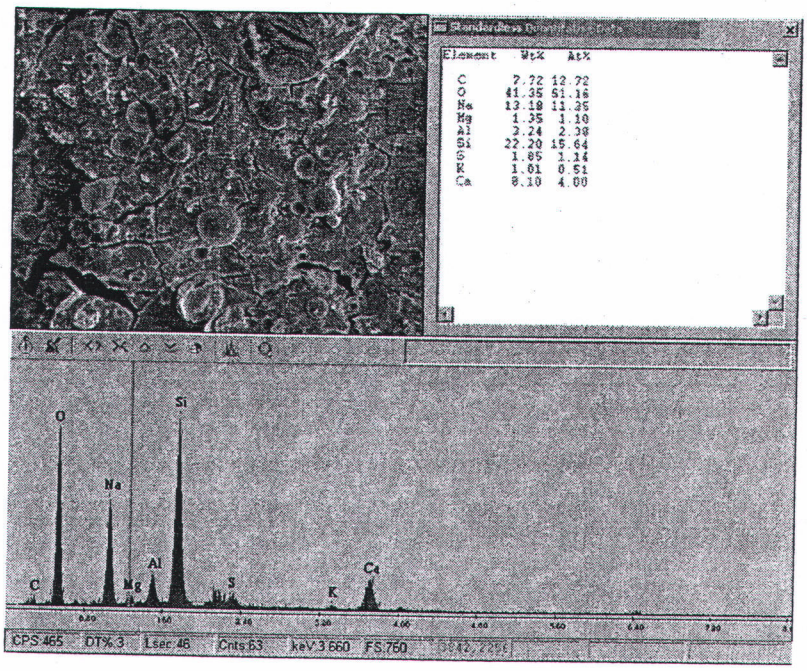

Fig. 5. SEM and EDAX taken from a broken portion of a 28-day sample of mix.

was not homogenous: some fly ash particles remained unreacted, but were bonded in the matrix. Xu and Van Deventer [13] suggested that these unreacted mineral particles are not acting as filler. The bonding is the result of complex reactions between the mineral surfaces, adding to the late strength of the matrix.

It was found that the Si/Al ratios of geopolymer products were slightly different from the input Si/Al ratios (see Table 3). However, there was a tendency that as the Si/Al input increased, the Si/Al of the end product increased as well. The same result was found in previous work [14].

4. Conclusions

Our systematic study of the effect of Si/Al ratio of geopolymer paste allows us to conclude as follows.

1. RHBA is a good silicon-rich source and can be used to partially replace fly ash to produce high Si/Al ratio geopolymers. Its incorporation can change the geopolymer's mechanical properties.
2. The optimum Si/Al ratio for maximum compressive strength of this FA–RHBA geopolymer was eight (SiO_2/Al_2O_3 = 15.9). A geopolymer with the relatively high compressive strength of 73 MPa could be obtained.
3. The behavior of the geopolymer changed from brittle to relatively elastic materials as SiO_2/Al_2O_3 ratios increased above 15.9. Care should be taken when the SiO_2/Al_2O_3 ratio is increased to a very high value, as the geopolymer expanded and cracked with aging.
4. In this study, the Na_2O/SiO_2 ratios were between 0.14 and 0.23 and Na_2O/Al_2O_3 ratios were between 2.21 and 3.37. The compressive strength of the geopolymer increased with decreases in the Na_2O/SiO_2 and Na_2O/Al_2O_3 ratios.

Acknowledgments

We gratefully acknowledge financial support from the Thailand Research Fund (TRF) under the TRF New Researcher Scholar Grant No. MRG4980104 and the TRF Senior Research Scholar Grant No. RTA5080020, and the Commission on Higher Education, Ministry of Education, Thailand.

References

[1] Davidovits J. Chemistry of geopolymeric systems, terminology. In: Davidovits J, Davidovits R, James C, editors. Proceedings of geopolymer '99 international conference. France; 1999. p. 9–40.
[2] Duxson P, Provis JL, Lukey GC, Mallicoat SW, Kriven WM, Van Deventer JSJ. Understanding the relationship between geopolymer composition, microstructure and mechanical properties. Colloid Surface 2005;269(1–3):47–58.
[3] Duxson P, Mallicoat SW, Lukey GC, Kriven WM, Van Deventer JSJ. The effect of alkali and Si/Al ratio on the development of mechanical properties of metakaolin-based geopolymers. Colloid Surface 2007;292(1):8–20.
[4] De Silva P, Sagoe-Crenstil K, Sirivivatnanon V. Kinetics of geopolymerization: role of Al_2O_3 and SiO_2. Cem Concr Res 2007;37(4):512–8.
[5] Fletcher RA, MacKenzie KJD, Nicholson CL, Shimada S. The composition range of aluminosilicate geopolymers. J Eur Ceram Soc 2005;25(9):1471–7.
[6] Ohsawa S, Asaga K, Goto S, Daimon M. Quantitative determination of fly ash in the hydrated fly ash – $CaSO_4{\cdot}2H_2O$–Ca $(OH)_2$ system. Cem Concr Res 1985;15(2):357–66.
[7] Lam L, Wong YL, Poon CS. Degree of hydration and gel/space ratio of high-volume fly ash/cement systems. Cem Concr Res 2000;30(5):747–56.
[8] Rattanasak U. Microstructural study of pozzolan–cement composites in combination with superplasticising admixtures. Ph.D. Thesis, Department of Chemical Engineering. England: University of Birmingham; 2004.
[9] Fernandez-Jimenez A, De La Torre AG, Palomo A, Lopez-Olmo G, Alonso MM, Aranda MAG. Quantitative determination of phases in the alkaline activation of fly ash. Part II: degree of reaction. Fuel 2006;85:1960–9.
[10] De Silva P, Sagoe-Crenstil K. Medium-term phase stability of Na_2O–Al_2O_3–SiO_2–H_2O geopolymer system. Cem Concr Res 2008;38(6):870–6.
[11] Chindaprasirt P, Chareerat T, Sirivivatnanon V. Workability and strength of coarse high calcium fly ash geopolymer. Cem Concr Compos 2006;29(3):224–9.
[12] Fernandez-Jimenez A, Palomo A, Sobrados I, Sanz J. The role played by the reactive alumina content in the alkaline activation of fly ashes. Micropor Mesopor Mater 2006;91:111–9.
[13] Xu H, Van Deventer JSJ. The geopolymerisation of alumino-silicate minerals. Int J Miner Process 2000;59(3):247–66.
[14] Chindaprasirt P, Chalee W, Jaturapitakkul C, Rattanasak U. Comparative study on characteristics of fly ash and bottom ash geopolymers. Waste Manage 2009;29:539–43.

11. T. Cheewaket, C. Jaturapitakkul, W. Chalee. Long term performance of chloride binding capacity in fly ash concrete in a marine environment, Construction and Building Materials, 24 (2010), 1352-1357. (IF 0.947)

Construction and Building Materials 24 (2010) 1352–1357

Contents lists available at ScienceDirect

Construction and Building Materials

journal homepage: www.elsevier.com/locate/conbuildmat

Long term performance of chloride binding capacity in fly ash concrete in a marine environment

T. Cheewaket [a], C. Jaturapitakkul [a], W. Chalee [b,*]

[a] Department of Civil Engineering, Faculty of Engineering, King Mongkut's University of Technology Thonburi, Bangkok 10140, Thailand
[b] Department of Civil Engineering, Faculty of Engineering, Burapha University, Chonburi 20131, Thailand

ARTICLE INFO

Article history:
Received 16 September 2009
Received in revised form 6 November 2009
Accepted 25 December 2009
Available online 21 January 2010

Keywords:
Chloride binding capacity
Total chloride
Free chloride
Fly ash
Concrete
Marine environment
Thailand

ABSTRACT

The capacity of binding chloride ions in fly ash concrete under marine exposure was studied. The free and total chloride contents in concrete were determined by water and acid-soluble methods, respectively. In order to study the effects of *W/B* ratios, exposure time, and fly ash contents on chloride binding capacity of concrete in a marine site, a class F fly ash was used as a partial replacement of Portland cement type I at 0%, 15%, 25%, 35%, and 50% by weight of binder. Water to binder ratios (*W/B*) were varied at 0.45, 0.55, and 0.65. Concrete cube specimens of 200 mm were cast and placed into the tidal zone of a marine environment in the Gulf of Thailand. Consequently, acid-soluble and water-soluble chlorides in the concrete were measured after the concrete was exposed to the tidal zone for 3, 4, 5, and 7 years. It was found that the percentage of chloride binding capacity compared to total chloride content increased with the increase of fly ash in the concrete. The percentage of chloride binding capacity significantly decreased within 3–4 years after the concrete was exposed to the marine environment, and then its value was almost constant. The research also showed that the *W/B* ratio does not noticeably affect the chloride binding capacity of concrete.

1. Introduction

At present, the development of concrete mixtures that are highly resistant to the ingress of chloride ions is very important for concrete in marine environments. In order to achieve durable concrete, the concrete should have low permeability and high resistance to chloride ingress. For concrete in marine environments, several factors must be considered, such as the chloride diffusion coefficient, threshold chloride, chloride binding capacity, and so on [1–4]. The binding of chlorides in hydrated cement paste affects the transport rate of chlorides into concrete as well as the steel corrosion rate and the amount of chlorides necessary to initiate active corrosion [5–7]. Generally, the chloride binding ability depends on calcium aluminate, which reacts with chloride ions to form chloroaluminates. The remaining chloride ions in the pore solution (free chloride) lead to reinforcement corrosion. The effect of the cement type on the bound chloride was also investigated by Mohammed and Hamada [8]. Their research confirmed that a high chloride binding capacity was found in a higher calcium aluminate cement than in a lower calcium aluminate cement. In addition, the use of pozzolanic materials can increase the binding ability of chloride, which has been confirmed by several studies [9–11]. Chloride binding in concrete is very important for the development of models for service life predictions of reinforced concrete with respect to reinforcement corrosion. Efficient models to predict long term corrosion of reinforced concrete should be generated based on field exposure investigation with long term monitoring [12–15]. The combined destruction of reinforced concrete due to chemicals and the physical properties of an actual environment is complicated and requires a long term study. Thus, the goal for constructing concrete in a marine environment is to employ methods and materials that will develop and provide a longer service life for concrete.

2. Materials and method

2.1. Concrete materials and properties

Portland cement types I and V and class F fly ash ($SiO_2 + Al_2O_3 + Fe_2O_3 = 79.45\%$) from Thailand with a 30-μm mean particle size (d_{50}) were used as cementitious materials. The chemical properties of fly ash and Portland cement types I and V are shown in Table 1. Graded river sand and crushed limestone with a maximum size of 19 mm were used as a fine and course aggregates, respectively.

2.2. Mix proportions and specimen preparation

Control concretes were designed by using Portland cement types I and V to have compressive strengths of about 30, 40, and 50 MPa at 28 days, which *corresponded* to the *W/B* ratios of 0.65, 0.55, and 0.45, respectively. Fly ash concretes were cast using fly ash to replace Portland cement type I at 15%, 25%, 35%, and 50% by weight of binder with the same *W/B* ratio of the control concretes. The detailed mixture proportions of concretes are given in Table 2. Concrete cube specimens of $200 \times 200 \times 200$ mm^3 were prepared and transferred to the tidal zone of a marine site in the Gulf of Thailand after being cured in water for 28 days as shown in Fig. 1.

* Corresponding author. Tel.: +66 38 102 2222; fax: +66 38 102 2222x3355.
E-mail address: wichian@buu.ac.th (W. Chalee).

0950-0618/$ - see front matter © 2009 Elsevier Ltd. All rights reserved.
doi:10.1016/j.conbuildmat.2009.12.039

Table 1
Chemical compositions of the Portland cements and fly ash.

Chemical compositions (%)	Sample		
	Cement type I	Cement type V	Fly ash (FA)
Silicon dioxide, SiO_2	20.80	21.52	44.95
Aluminium oxide, Al_2O_3	5.50	3.56	23.70
Iron oxide, Fe_2O_3	3.16	4.51	10.80
Calcium oxide, CaO	64.97	66.70	13.80
Magnesium oxide, MgO	1.06	1.20	3.47
Sodium oxide, Na_2O	0.08	0.10	0.07
Potassium oxide, K_2O	0.55	0.24	2.38
Sulfur trioxide, SO_3	2.96	2.11	1.31
Loss on ignition, LOI	2.89	1.74	0.52
Tricalcium silicate, C_3S	56.50	71.60	–
Dicalcium silicate, C_2S	17.01	7.68	–
Tricalcium aluminate, C_3A	9.23	1.80	–
Tetracalcium aluminoferrite, C_4AF	9.62	13.72	–

2.3. Exposed site condition

The ambient temperature at the exposed site ranges from 25 °C to 35 °C, and the pH of the seawater ranges from 7.9 to 8.2 *while* chloride and sulfate compositions in the seawater range from 16,000 to 18,000 ppm and from 2200 to 2600 ppm, respectively [16]. The concrete specimens were exposed to two wet–dry cycles of seawater daily.

2.4. Tested program

After the concrete samples were exposed to the seawater for 3, 4, 5, and 7 years, the chloride contents of the concretes were investigated to measure the chloride ingress *into* the concrete specimens. The concrete specimens were cored to obtain 100-mm diameter cylinders. The core *specimen was* dry-cut from the surface which was 10 mm thick, and then ground into small powdery particles (see Fig. 2). Ten grams of *the* concrete powder was needed for chloride tests by acid-soluble and water-soluble chloride methods, to determine the total and free chloride contents, respectively. For the acid-soluble chloride test, the analysis conforms to ASTM C 1152 [17], and the analysis conforms to ASTM C1218 [18] for the water-soluble chloride *test.*

3. Results and discussion

3.1. Chloride binding capacity

Generally, the chloride binding capacity in concrete can be calculated by subtracting the free chloride content from total chloride content. In this study, the chloride binding capacity was analysed in term of percentage chloride binding capacity compared to the total chloride content. Fig. 3 illustrates the relationship between free chloride and total chloride content in concretes with *W/B* ratios of 0.45, 0.55, and 0.65, which were exposed to a marine environment for 7 years. Regression analyses were then performed to obtain their relations. For example, $C_f = (0.8556)C_t$, where C_f is the free chloride content and C_t is the total chloride content of I45 concrete after 7 years exposure. According to the relation, the percentage chloride binding capacity (P_{cb}) as compared to the total chloride content can be easily determined from Eq. (1):

$$P_{cb} = \frac{[(C_t - C_f) \times 100]}{C_t} \quad (1)$$

By substituting C_f in terms of C_t [$C_f = (0.8556)C_t$] in Eq. (1), the percentage chloride binding capacity (P_{cb}) of I45 concrete after

Table 2
Mixture proportions of the concretes.

Mix	Mixture proportion of concrete (kg/m^3)						*W/B*
	Cement type I	Cement type V	Fly ash	Fine aggregate	Coarse aggregate	Water	
I45	478	–	–	639	1024	215	0.45
I55	478	–	–	639	971	262	0.55
I65	478	–	–	639	922	311	0.65
V45	–	478	–	639	1024	215	0.45
V55	–	478	–	639	971	262	0.55
V45	–	478	–	639	922	311	0.65
I45FA15	406	72	72	639	1004	215	0.45
I45FA25	359	119	119	639	990	215	0.45
I45FA35	311	167	167	639	977	215	0.45
I45FA50	239	239	239	639	957	215	0.45
I55FA15	406	72	72	639	948	262	0.55
I55FA25	359	119	119	639	933	262	0.55
I55FA35	311	167	167	639	918	262	0.55
I55FA50	239	239	239	639	897	262	0.55
I65FA15	406	72	72	639	898	311	0.65
I65FA25	359	119	119	639	881	311	0.65
I65FA35	311	167	167	639	864	311	0.65
I65FA50	239	239	239	639	840	311	0.65

Fig. 1. Concrete specimens under wet–dry cycles in the marine environment.

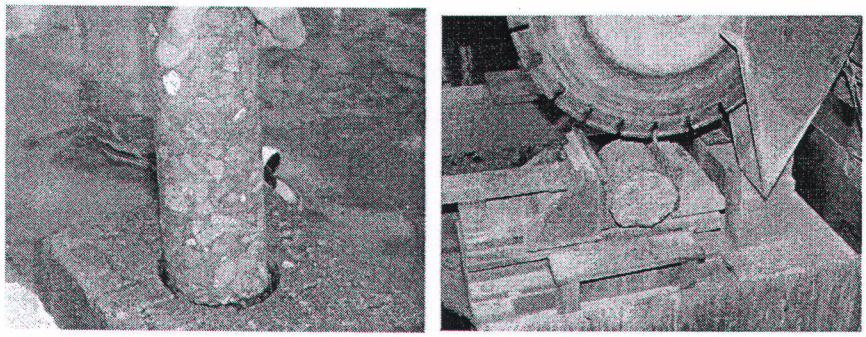

Fig. 2. Concrete coring and cutting for chloride test.

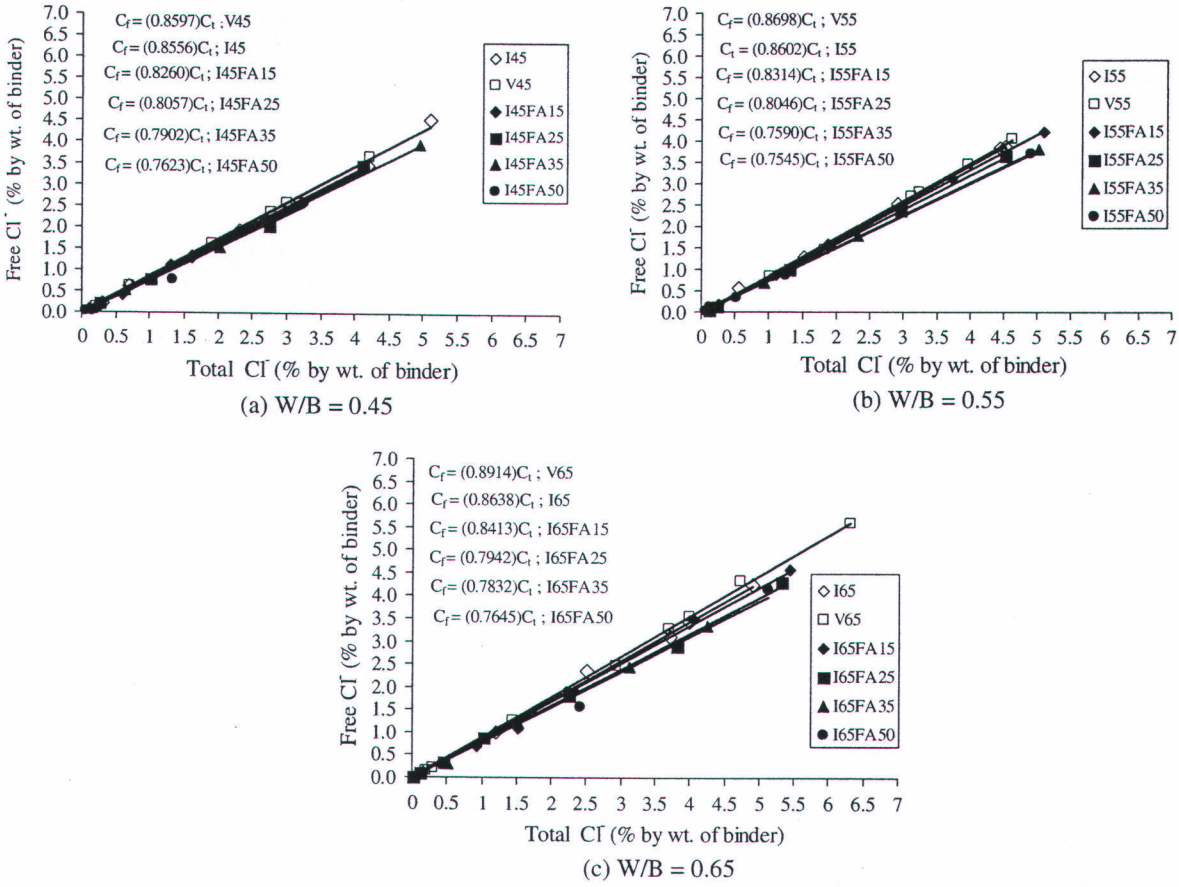

Fig. 3. Relationship between the free and total chloride contents of concrete after 7 years exposure in the marine environment: (a) *W/B* = 0.45, (b) *W/B* = 0.55, (c) *W/B* = 0.65.

7 years exposure is 14.4%. The percentage chloride binding capacity of the other concrete mixtures at 3, 4, 5, and 7 years exposure can also be calculated similarly, as shown in Table 3.

Fig. 4 presents the effect of fly ash content on the chloride binding capacity of concrete at 4, 5, and 7 years after *being exposed* in the marine environment. The results showed that the use of fly ash clearly increased the chloride binding capacity in concrete, and this was also confirmed by several studies [19,20]. *Generally, chloride binding capacity of concrete depends on the two main mechanisms of physical adsorption and chemical reactions* [21,22]. *For chemical binding,* there is a chemical reaction between bound chloride and C_3A that produces calcium chloroaluminate hydrate ($3CaO{\cdot}Al_2O_3{\cdot}CaCl_2{\cdot}10H_2O$), sometimes called Friedel's salt. Therefore, chloride is bound more when the C_3A content in the binder is higher. Based on this study, fly ash contains aluminium oxide (Al_2O_3) at 23.7%, whereas Portland cement type I contains Al_2O_3 at only 5.5%. For this reason, increasing the amount of fly ash in concrete *also* increases the amount of Al_2O_3, which results in

Table 3
Chloride binding capacity of concrete exposed to a marine environment.

Mix	Chloride binding capacity (% of total chloride content)			
	3 years of exposure	4 years of exposure	5 years of exposure	7 years of exposure
I45	22.4	13.7	16.6	14.4
I55	16.0	14.3	14.3	14.0
I65	15.0	13.7	15.2	13.6
V45	14.9	12.6	15.1	14.0
V55	13.2	13.3	13.1	13.0
V45	13.5	12.4	11.0	10.9
I45FA15	24.8	17.8	17.5	17.4
I45FA25	25.7	22.0	21.6	19.4
I45FA35	28.2	21.9	24.7	21.0
I45FA50	36.5	26.0	24.1	23.8
I55FA15	19.2	16.2	16.5	16.9
I55FA25	21.4	20.0	20.6	19.5
I55FA35	26.4	24.1	23.1	24.1
I55FA50	26.6	24.3	24.0	24.6
I65FA15	20.7	16.4	16.0	15.9
I65FA25	22.5	21.8	18.5	20.6
I65FA35	21.2	24.5	21.7	21.7
I65FA50	30.3	23.8	23.2	23.6

enhancing chloride binding capacity as well [23,24]. For instance, the concretes containing fly ash 0%, 15%, 25%, 35%, and 50% by weight of binder with a *W/B* ratio of 0.45 had P_{cb} values at 7 years exposure of 14.4%, 17.4%, 19.4%, 21.0%, and 23.8%, respectively. In addition, Portland cement type I used in this study had a higher C_3A content than type V by about a factor of 5. Consequently, type I concrete had more P_{cb} than type V concrete at all *W/B* ratios for a given exposure time. For instance, P_{cb} values at 3 years exposure for the I45, I55, and I65 concretes were 22.4%, 16.0%, and 15.0%, while those of the V45, V55, and V65 concretes were 14.9%, 13.2%, and 13.5%, respectively (see Table 3). *For the physical binding, chloride can be physically adsorbed on the surface of hydration or pozzolanic reaction products, such as C–S–H, C–A–H, ettringite, and monosulfate. Previous research had reported that the physical bound of chloride content in cement paste increases with the increasing of total chloride and W/B ratio* [21,25].

Fig. 5 shows the relation between percentage chloride binding capacity and *W/B* ratio of concretes at 7 *years exposure*. It was found that P_{cb} is not correlated with the *W/B* ratio. As a result, the *W/B* ratio does not affect the ratio of bound chloride compared to total chloride ingress in concrete. This result was also confirmed by previous research [26]. Although the P_{cb} of each concrete mix did not change with the *W/B* ratio, the chloride binding capacity increased as the *W/B* ratio increased. *This result is due to the physical binding of chloride in concrete* [25]. *Besides*, the total chloride content in concrete increases when the *W/B* ratio increases. *This is due to* a higher *W/B* ratio results in higher porosity in concrete and thus greater chloride ingresses into the concrete.

Fig. 6 illustrates the effect of the exposure time on the chloride binding capacity of concrete with a *W/B* ratio of 0.45 in *the* marine environment. The results showed that P_{cb} decreased with *the* exposure time. For example, I45FA50 concrete at 3, 4, 5, and 7 years had P_{cb} values of 36.5%, 26.0%, 24.1%, and 23.8%, respectively. Interestingly, P_{cb} obviously decreased at 4 years and then remained almost constant for longer periods (from 4 to 7 years). Previous research proposed a model for predicting the time-dependent chloride binding based on experimental data in the laboratory [25]. Their model states that a larger chloride binding capacity is expected for longer exposure periods for paste. However, it did not present the bound chloride content as compared to the total chloride content in cement paste. With increasing exposure time, more total chloride ingress was found, and the bound chloride content was greater, even though the percentage chloride binding capacity (P_{cb}) as compared to the total chloride content was smaller.

3.2. Utilization of chloride binding capacity in marine concrete

The ability to bind chloride ions in concrete can indicate the free chloride content, which deteriorates reinforced steel of concrete in a marine environment. As the total ingressing chloride in concrete is increasingly bound, the free chloride cannot corrode reinforcing steel as much, and hence the life of the concrete structure can be prolonged [27]. Therefore, the selection of binding material in order to protect against the corrosion of reinforcing steel by chloride attack should be taken into account. The selection of concrete should consider not only low water permeability and high strength but also the chloride binding capacity of binding material in order to prevent chloride ingress. This study proposes the percentage chloride binding capacity (P_{cb}) compared to the total chloride content, which leads to the amount of bound chloride as well as free chloride content in the pores of cement paste. The results are based on exposed concrete specimens in *the* marine conditions for 7 years. Furthermore, the mathematical models were generated using field data over a long period to achieve the precise prediction of the steel corrosion and service life of concrete in *the* marine environment [28]. Thus, the results in this research can be used to develop a high efficiency model for predicting the corrosion of reinforced concrete in a marine site. In addition, the data can assist in the selection of concrete mixtures suitable for marine environments.

3.3. Relationship between free and total chloride in concrete in marine environment

In general, the free chloride content causes corrosion in reinforcing steel, but determining its value (by the water-soluble method) is more difficult than conducting the total chloride content test (by the acid-soluble method). Therefore, this research proposes an equation for determining the free chloride content from the total chloride content ingress in concrete by using the data gathered from *the* marine site over 7 years. Fig. 7 shows the relationship between free and total chloride contents of concretes with *W/B* ratios of 0.45, 0.55, and 0.65 at 3, 4, 5, and 7 years exposures. Using the experimental data, the following linear relationships are proposed for cement and fly ash concrete as shown in Eqs. (2)–(7):

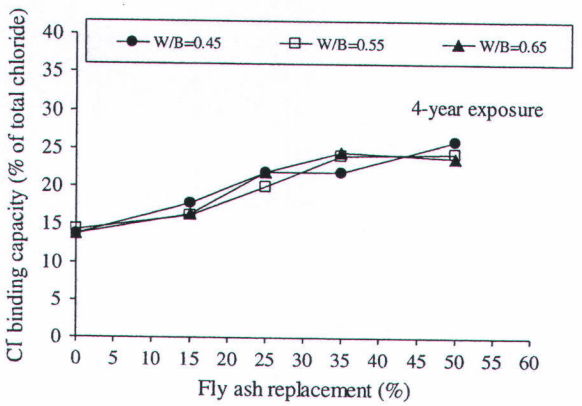

a) 4 years of exposure

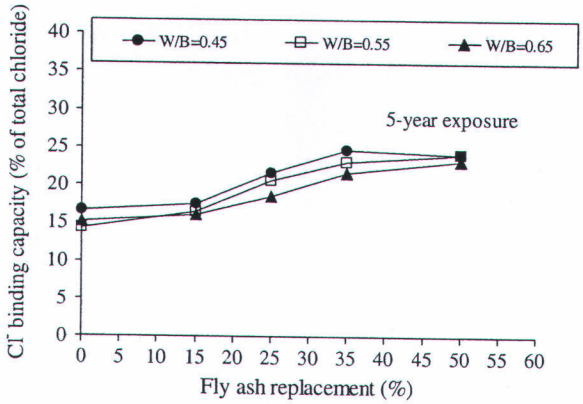

b) 5 years of exposure

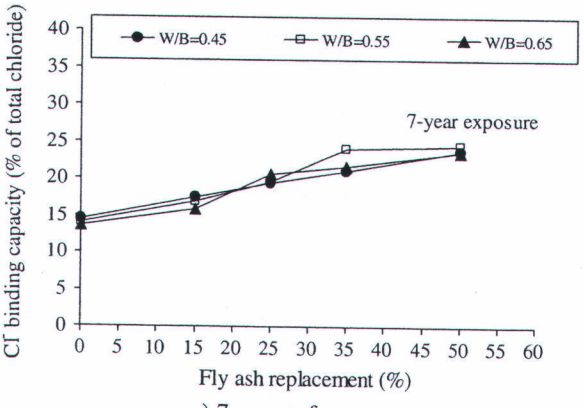

c) 7 years of exposure

Fig. 4. Effect of fly ash on the chloride binding capacity of concretes at 4, 5, and 7 years exposures in the marine environment.

$$C_f = 0.8541(C_t);\ (R^2 = 0.9963),\ \text{for Portland cement type I concrete} \quad (2)$$

$$C_f = 0.8773(C_t);(R^2 = 0.9977),\ \text{for Portland cement type V concrete} \quad (3)$$

$$C_f = 0.8350(C_t);(R^2 = 0.9985),\ \text{for 15\%-fly ash concrete} \quad (4)$$

$$C_f = 0.8011(C_t);(R^2 = 0.9979),\ \text{for 25\%-fly ash concrete} \quad (5)$$

$$C_f = 0.7734(C_t);(R^2 = 0.9986),\ \text{for 35\%-fly ash concrete} \quad (6)$$

$$C_f = 0.7661(C_t);(R^2 = 0.9949),\ \text{for 50\%-fly ash concrete} \quad (7)$$

Here, C_f and C_t are the free and total chloride contents in concrete, respectively. According to the equations, the free chloride contents

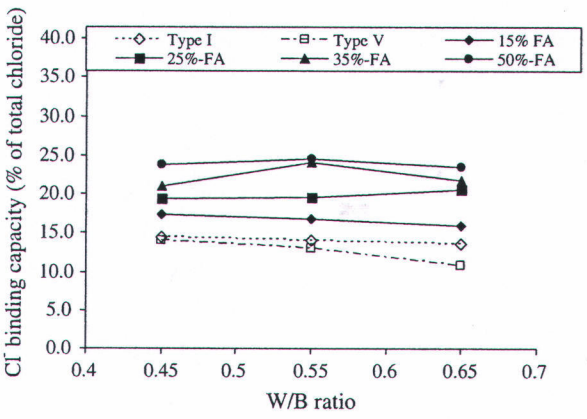

Fig. 5. Effect of *W/B* ratio on the chloride binding capacity of concrete after 7 years exposure in the marine environment.

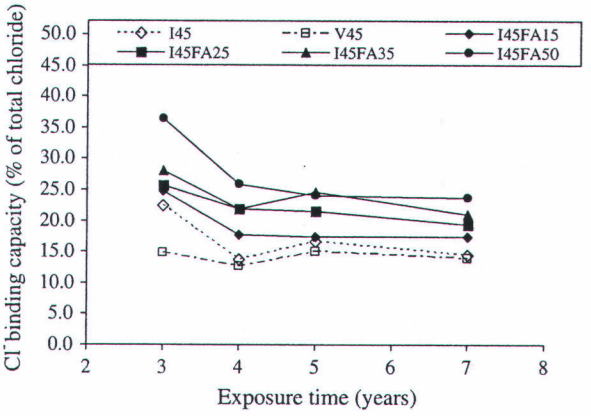

Fig. 6. Effect of exposure time on the chloride binding capacity of concrete with a *W/B* ratio of 0.45 in the marine environment.

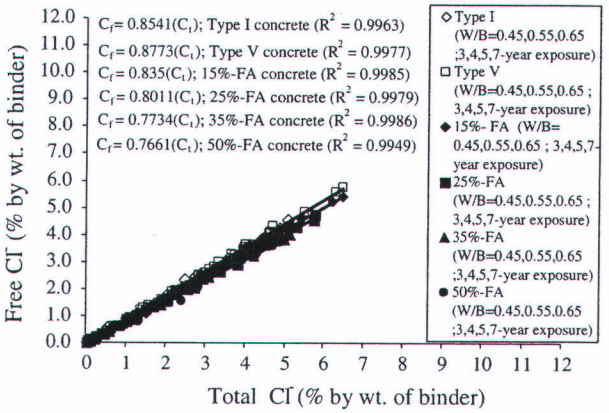

Fig. 7. Relationship between free and total chloride contents of concrete with *W/B* ratios of 0.45, 0.55, and 0.65 at 3, 4, 5, and 7 years exposures.

of Portland cement types I and V, 15%-fly ash, 25%-fly ash, 35%-fly ash, and 50%-fly ash concretes are 85.41%, 87.73%, 83.5%, 80.11%, 77.34%, and 76.61% of the total chloride content, respectively. The relations show that as the percentage replacement of fly ash increases, the free chloride content in terms of the total chloride content decreases, which corresponds to the increase in the chloride

binding as previously presented. These equations are very useful in determining the free chloride content, which affects steel corrosion. In addition, they could also be used to determine the threshold chloride with regard to the design of concrete durability.

4. Conclusions

Based on the results and discussions, the following conclusions are made.

1. The increase of fly ash replacement of cement in concrete resulted in an increasing *the percentage chloride binding capacity* (P_{cb}) as compared to the total chloride content.
2. Increasing the exposure time of concrete resulted in a decreasing *the* percentage of chloride binding capacity (P_{cb}) as compared to the total chloride content.
3. The *W/B* ratio of concrete has small effect on the chloride binding capacity of concrete exposed to a marine environment.
4. The proposed linear relationships between the free and total chloride contents in concretes show reasonably good correlation with field data obtained from the marine exposure site.

Acknowledgments

The authors gratefully acknowledge the financial supports from the Research and Development Funds, Faculty of Engineering, Burapha University, Thailand, Contract No. 74/2551; from the Thailand Research Fund (TRF) under TRF Senior Research Scholar, Contract No. RTA5080020; from the Commission on Higher Education, Ministry of Education, Thailand; from the Thailand Research Fund (TRF) under TRF New Researcher Scholar Contract No. MRG5280003 and from the financial supports from the Thailand Research Fund (TRF) who sponsored the research under the Royal Golden Jubilee Ph.D. program, Contract No. PHD/0320/2550.

References

[1] Han Sang-Hun. Influence of diffusion coefficient on chloride ion penetration of concrete structure. Constr Build Mater 2007;21:370–8.
[2] Chalee W, Jaturapitakkul C. Effect of *W/B* ratios and fly ash finenesses on chloride diffusion coefficient of concrete in marine environment. Mater Struct 2009;42:505–14.
[3] Fajardo G, Valdez P, Pacheco J. Corrosion of steel rebar embedded in natural pozzolan based mortars exposed to chlorides. Constr Build Mater 2009;23:768–74.
[4] Ann Ki Yong, Song Ha-Won. Chloride threshold level for corrosion of steel in concrete. Corros Sci 2007;49:4113–33.
[5] Yuan Q, Shi C, Schutter GD, Audenaert K, Deng D. Chloride binding of cement-based materials subjected to external chloride environment – a review. Constr Build Mater 2009;23:1–13.
[6] Baweja D, Roper H, Sirivivatnanon V. Chloride-induced steel corrosion in concrete; part 1 corrosion rates, corrosion activity, and attack areas. ACI Mater J 1998;23:207–17.
[7] Huang R, Chang Jiang-Jhy, Wu Jiann-Kuo. Correlation between corrosion potential and polarisation resistance of rebar in concrete. Mater Lett 1996;28:445–50.
[8] Mohammed TU, Hamada H. Relationship between free chloride and total chloride contents in concrete. Cem Concr Res 2003;33:1487–90.
[9] Dhir RK, El-Mohr MAK, Dyer TD. Chloride binding in GGBS concrete. Cem Concr Res 1996;26:1767–73.
[10] Jensen OM, Korzen MSH, Jakobsen HJ, Skibsted J. Influence of cement constitution and temperature on chloride binding in cement paste. Adv Cem Res 2000;12:57–64.
[11] Arya C, Xu Y. Effect of cement type on chloride binding and corrosion of steel in concrete. Cem Concr Res 1995;25:893–902.
[12] Sandberg P. Studies of chloride binding in concrete exposed in a marine environment. Cem Concr Res 1999;29:473–7.
[13] Tamimi AK, Abdalla JA, Sakka ZI. Prediction of long term chloride diffusion of concrete in harsh environment. Constr Build Mater 2008;22:829–36.
[14] Chalee W, Jaturapitakkul C, Chindaprasirt P. Predicting the chloride penetration of fly ash concrete in seawater. Mar Struct 2009;22:341–53.
[15] Yüzer Nabi, Aköz Fevziye, Kabay Nihat. Prediction of time to crack initiation in reinforced concrete exposed to chloride. Constr Build Mater 2008;22:1100–7.
[16] Chalee W, Teekavanit M, Kiattikomol K, Siripanichgorn A, Jaturapitakkul C. Effect of *W/C* ratio on covering depth of fly ash concrete in marine environment. Constr Build Mater 2007;21:965–71.
[17] ASTM. Standard test method for acid-soluble chloride in mortar and concrete, C1152/C1152M. Annual book of ASTM Standards, vol. 04.02; 2001. p. 621–9.
[18] ASTM. Standard test method for water-soluble chloride in mortar and concrete, C1218/C1218M. Annual book of ASTM Standards, vol. 04.02; 2001. p. 645–7.
[19] Dhir RK, El-Mohr MAK, Dyer TD. Developing chloride resisting concrete using PFA. Cem Concr Res 1997;27:1633–9.
[20] Dhir RK, Jones MR. Development of chloride-resisting concrete using fly ash. Fuel 1999;78:137–42.
[21] Luo Rui, Cai Yuebo, Wang Changyi, Huang Xiaoming. Study of chloride binding and diffusion in GGBS concrete. Cem Concr Res 2003;33:1–7.
[22] Hirao Hiroshi, Yamada Kazuo, Takahashi Haruka, Zibara Hassan. Chloride binding of cement estimated by binding isotherms of hydrates. J Adv Concr Tech 2005;3:77–84.
[23] Castellote M, Andrade C, Alonso C. Chloride-binding isotherms in concrete submitted to non-steady-state migration experiments. Cem Concr Res 1999;29:1799–806.
[24] Jensen HU, Pratt PL. The binding of chloride ions by pozzolanic product in fly ash cement blends. Adv Cem Res 1989;7:121–9.
[25] Sumranwanich T, Tangtermsirikul S. A model for predicting time-dependent chloride binding capacity of cement-fly ash cementitious system. Mater Struct 2004;37:387–96.
[26] Delagrave A, Marchand J, Jean-Pierre O, Julien S, Hazrati K. Chloride binding capacity of various hydrated cement paste systems. Adv Cem Based Mater 1997;6:28–35.
[27] Broomfield JP. Corrosion of steel in concrete. England, Taylor: Francis Ltd.; 1996. p. 1–10.
[28] Val VD, Stewart MG. Life cycle cost analysis of reinforced concrete structure in marine environments. Struct Saf 2003;25:343–62.

12. W. Tangchirapat, R. Buranasing, C. Jaturapitakkul. Use of high fineness of fly ash to improve properties of recycled aggregate concrete, Journal of Materials in Civil Engineering ASCE, 22, No. 6 (2010), 565-571.(IF 0.526).

Use of High Fineness of Fly Ash to Improve Properties of Recycled Aggregate Concrete

Weerachart Tangchirapat[1]; Rak Buranasing[2]; and Chai Jaturapitakkul[3]

Abstract: This study used high fineness of fly ash as a cement replacement to improve recycled aggregate concrete properties. The mixture proportions of recycled aggregate concretes were first prepared using 100% recycled coarse aggregate, and then river sand was replaced with recycled fine aggregate at 0, 50, and 100% by weight of the fine aggregate (river sand plus recycled fine aggregate). Results indicated that use of 35–50% fly ash (with respect to total cementitious content) of high fineness could improve slump loss behavior in recycled aggregate concretes. Greater proportions of recycled fine aggregates decreased the compressive strength of concrete. However, use of high fineness of fly ash (1.2% retained on a No. 325 sieve) in recycled aggregate concrete could produce greater compressive strength than that of the recycled aggregate concrete alone. The splitting tensile strength of the recycled aggregate concretes containing high fineness of fly ash was 8.2% of its compressive strength, slightly lower than that of the normal aggregate concrete. The modulus of elasticity of recycled aggregate concrete, with or without high fineness of fly ash, was lower than that of the normal aggregate concrete and about 5.9% lower than the value predicted by ACI 318. The results suggest that high fineness of fly ash can be used to improve various properties of recycled aggregate concrete.

DOI: 10.1061/(ASCE)MT.1943-5533.0000054

CE Database subject headings: Fly ash; Concrete; Elasticity; Aggregates; Tensile strength.

Author keywords: Fly ash; High fineness; Modulus of elasticity; Recycled aggregate; Splitting tensile strength.

Introduction

Globally, the concrete industry consumes large quantities of natural resources, which are becoming insufficient to meet increasing demands. At the same time, many old buildings have reached the end of their service life and are being demolished, resulting in wasted concrete; some concrete waste is used as backfill material, and much being sent to landfills. Recycling concrete by using it as new aggregate in concrete could reduce concrete waste and conserve natural sources of aggregate.

Many studies have attempted to use recycled aggregate in concrete and have concluded that it reduces the compressive strength of concrete (De Oliveira and Vazquez 1996; Katz 2003; Tangchirapat et al. 2008). Chen et al. (2003) conducted a literature review and reported that the compressive strength of concrete containing 100% recycled coarse aggregate (RCA) could be as low as 60% of the compressive strength of concrete made from normal aggregate. Poon et al. (2004) found that concrete should contain no more than 50% RCA in the air-dried state to yield normal strength recycled aggregate concrete. In addition to producing low compressive strength, recycled aggregate allows high water absorption and results in low concrete workability. Topçu and Sengel (2004) reported that concrete containing more than 50% recycled aggregate is especially problematic for workability. More details on considerations for evaluating and processing waste concrete for production of aggregates suitable for reuses in concrete construction are presented in ACI 555R-01 [American Concrete Institute (ACI) Committee 2005b].

Due to the low compressive strength and low workability of concrete containing recycled aggregates, most previous studies of recycled aggregate in concrete have focused on replacing either coarse or fine aggregate and have been limited to low replacement levels of recycled aggregate. Several methods were used to improve concrete containing recycled aggregates. Otsuki et al. (2003) used a double mixing method in the case of high water-binder ratio to increase strength, chloride penetration, and carbonation resistance of concrete using recycled aggregates. Montgomery (1998) used ball mill to treat the aggregate in order to remove the old cement paste from the aggregate and found that this method could be used to increase the strength of recycled aggregate concrete. Katz (2004) treated the recycled aggregate by impregnation of silica fume solution and by ultrasonic cleaning. He found that an increase of 30 and 15% in the compressive strength at the ages of 7 and 28 days was found after the silica fume treatment and the improvement of 7% was observed in the ultrasonic treatment. Another method to overcome these shortcomings is to incorporate a pozzolanic material in the concrete mixture.

Fly ash is known to be a good pozzolanic material and has been used to increase the ultimate compressive strength and workability of fresh concrete (Mehta 1985). Naik and Ramme

[1]Dept. of Civil Engineering, Faculty of Engineering, King Mongkut's Univ. of Technology Thonburi (KMUTT), Bangkok 10140, Thailand. E-mail: weerachart.tan@kmutt.ac.th

[2]Dept. of Civil Engineering, Faculty of Engineering, King Mongkut's Univ. of Technology Thonburi (KMUTT), Bangkok 10140, Thailand. E-mail: rak_structure@hotmail.com

[3]Dept. of Civil Engineering, Faculty of Engineering, King Mongkut's Univ. of Technology Thonburi (KMUTT), Bangkok 10140, Thailand (corresponding author). E-mail: chai.jat@kmutt.ac.th

Note. This manuscript was submitted on December 2, 2008; approved on October 22, 2009; published online on October 24, 2009. Discussion period open until November 1, 2010; separate discussions must be submitted for individual papers. This paper is part of the ***Journal of Materials in Civil Engineering***, Vol. 22, No. 6, June 1, 2010. ©ASCE, ISSN 0899-1561/2010/6-565–571/$25.00.

Table 1. Physical Properties of Portland Cement Type I and Fly Ash before and after Grinding

Sample	Specific gravity	Retained on a 45-μm sieve (Number 325) (%)	Median particle size, d_{50} (μm)
Portland cement	3.15	NA	14.6
Fly ash before grinding	2.19	42.5	27.1
Fly ash after grinding	2.72	1.2	7.7

Note: NA is not applicable.

(1989) produced concrete mixes containing large quantities of fly ash which achieved compressive strengths of 21 and 28 MPa within 28 days. Influence of fly ash as a cement replacement on the compressive strengths, tensile strengths, and static modulus of elasticity values of recycled aggregate concrete was also shown in studies by Kou et al. (2007). They found that the mentioned properties decreased as the recycled aggregate and the fly ash content increased. It should be noted that fly ash used in this study did not have high fineness. High fineness of fly ash is accepted to be an excellent pozzolanic material. It was found that high fineness of fly ash (mean diameter, d_{50}, about 3.8 μm) can be used to produce high-strength concrete of 70 MPa at the age of 7 days (Jaturapitakkul et al. 2004). In Thailand, the Mae Moh power plant is the largest producer of fly ash, approximately 9,000 tons per day or 3 million tons per year. Because of this massive quantity, considerable funds are expended on transporting and disposing of the fly ash and minimizing environmental impacts. Therefore, using high fineness of fly ash as a cement replacement in recycled aggregate concrete cannot only increase the compressive strength and workability of recycled aggregate concrete, but also increase use of fly ash and reduce the amount of fly ash sent to landfills.

This study investigated high fineness of fly ash as a cement replacement in concrete containing high levels of recycled aggregate. Only recycled aggregate concrete containing a high percentage of recycled aggregates (i.e., 100% RCA) was used, and then recycled fine aggregate (RFA) was used to replace river sand at 0, 50, and 100% by weight of the fine aggregate. Slump loss of fresh concretes and mechanical properties of recycled aggregate concretes such as compressive strength, splitting tensile strength, and modulus of elasticity were investigated and compared with those of normal aggregate concrete (NAC). Using of the two often wasted materials, recycled aggregate and fly ash, will reduce the volume of waste, thereby improving the environment, and use of recycled aggregate will also help conserve supplies of natural aggregates.

Table 2. Chemical Compositions of Portland Cement Type I and High Fineness of Fly Ash

Chemical composition (%)	Portland cement type I	High fineness of fly ash
Silicon dioxide (SiO_2)	20.9	41.9
Aluminum oxide (Al_2O_3)	4.7	21.5
Iron oxide (Fe_2O_3)	3.4	12.7
Calcium oxide (CaO)	65.4	13.9
Magnesium oxide (MgO)	1.2	2.6
Sodium oxide (Na_2O)	0.2	2.7
Potassium oxide (K_2O)	0.3	2.5
Sulfur trioxide (SO_3)	2.7	0.6
Loss on ignition (LOI)	0.9	0.7

Experimental Program

Materials

Cement

Portland cement type I was used in NAC and recycled aggregate concretes. Tables 1 and 2 list its physical and chemical properties, respectively.

Fly Ash

Fly ash class F was obtained from the Mae Moh power plant located in Northern Thailand. Table 1 lists the physical properties of Portland cement type I and fly ash before and after grinding while Table 2 shows the chemical composition of Portland cement and high fineness of fly ash. To improve its reactivity, the fly ash was ground until the particles retained on a No. 325 sieve (45-μm opening) were 1.2% by weight. It is noted that the high fineness of fly ash is from grinding and not from separating process, thus the particles of the ground fly ash are in irregular shape. After that, the ground fly ash was then used as a pozzolanic material to partially replace Portland cement type I (20 to 50% by weight of binder) in recycled aggregate concrete.

Fine and Coarse Aggregates

Local river sand with a fineness modulus of 3.04 was used as a fine aggregate. Crushed limestone with a maximum size of 20 mm was used as a coarse aggregate. The fine and coarse aggregates had specific gravities of 2.60 and 2.67 and water absorptions of 0.94 and 0.46%, respectively.

Recycled Aggregates

Recycled aggregates used in this investigation were obtained from concrete test cylinders and not from demolition. The concrete cylinders were made from river sand and crushed limestone which were the same types of aggregate used in NAC. Cylinder concrete samples (150 × 300 mm) that had compressive strengths between 25 and 40 MPa; these were crushed using swing hammer mills. The crushed concrete was screened by sieving to produce RCA and RFA. Table 3 lists the physical properties of recycled

Table 3. Physical Properties of Normal and Recycled Aggregates

	Normal aggregates		Recycled aggregates	
Properties	River sand	Limestone	Fine	Coarse
Fineness modulus	3.04	6.79	3.55	6.40
Specific gravity [saturated surface dry (SSD)]	2.60	2.67	2.31	2.45
Absorption (%)	0.94	0.46	11.91	5.61
Los Angeles abrasion loss (%)	N/A	21.70	N/A	33.08

Note: NA is not applicable.

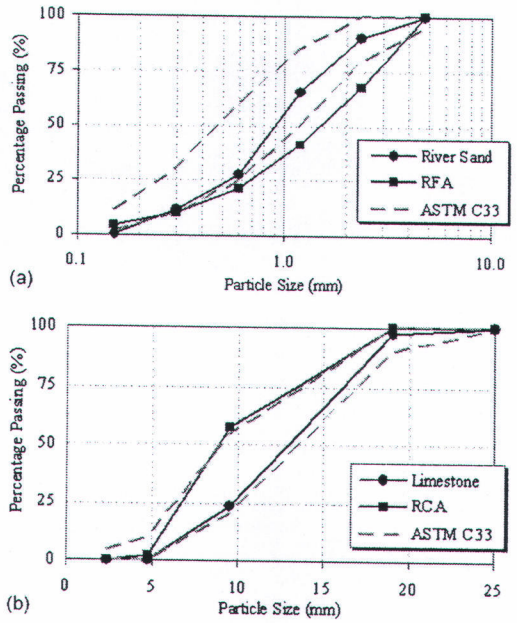

Fig. 1. Grading sizes of river sand, limestone, and recycled aggregates (RFA and RCA): (a) river sand and RFA; (b) limestone and RCA

aggregates. Figs. 1(a and b) compare the grading size of the recycled aggregates with ASTM C-33 (ASTM 2001a) requirements for fine and coarse aggregates, respectively. The RFA had a fineness modulus of 3.55, slightly coarser than the limit specified by ASTM C-33 (ASTM 2001a), while the RCA had a fineness modulus of 6.40, which met ASTM C-33 (ASTM 2001a) grading requirements.

The RCA and RFA had specific gravities of 2.45 and 2.31 and water absorptions of 5.61 and 11.91%, respectively. The low specific gravities and high water absorption of these recycled aggregates were caused by residue from old mortar (Katz 2003). Based on the Fig. 1(b), and assuming that the limestone was used in the concrete cylinders, the difference of about 30% between crushed limestone and RCA passing 10 mm indicated that many of the RCA would be from original coarse aggregates below 10 mm with attached mortar. This is a major factor lowering the specific gravity and increasing the water absorption of RCA. In the case of RFA, there would also be crushed partially hydrated cement paste and hence even produced a higher difference in specific gravity and absorption. The RCA had a Los Angeles abrasion of 33.08%, higher than that of crushed limestone (21.70%). This was caused by the adhering cement paste, which is usually weaker than the normal aggregate (Shayan and Xu 2003).

Mixture Proportions and Test Specimens

Table 4 summarizes the mixture proportions in NAC and recycled aggregate concretes. Both the normal and recycled aggregates used in this study were in an air-dried state. A constant effective water/binder ratio (w/b) was calculated and maintained at 0.48 (or effective water of 182.4 kg/m^3) for all concrete mixtures. Since the recycled aggregates had greater water absorption than normal aggregates, they required more water to maintain the slump of fresh concrete from 50 to 100 mm. Since the fine and coarse recycled aggregates are in air-dried condition, the amount of mixing water was adjusted to compensate for water absorption by the recycled aggregates.

The mixture proportions of recycled aggregate concretes were first prepared using 100% RCA, and local river sand was replaced with RFA at the levels of 0, 50, and 100% by weight of the fine aggregate (denoted as concrete groups AF, BF, and CF, respectively). The ratio of fine to coarse aggregate was 45:55 by volume. In addition, high fineness of fly ash was used to replace Portland cement type I at rates of 20, 35, and 50% by weight of the binder.

After mixing, the slump loss of fresh concrete was measured using the standard slump test apparatus. Initial slump value was recorded, and slump values were then measured every 15 min. Cylinder concretes (100 mm in diameter, 200 mm in height) were prepared and cast for 24 h, after which they were removed from the molds and cured in water. They were then tested for the mechanical properties of concrete, including compressive strength,

Table 4. Mixture Proportions of Normal Aggregate and Recycled Aggregate Concretes

	Mix proportion (kg/m^3)									
Mix	Cement	High fineness of fly ash	Limestone	Sand	RFA[a]	RCA[b]	Mixing water	Effective water	W/B[c]	Slump (mm)
NAC	380	—	1006	800	—	—	191.0	182.4	0.48	60
AF	380	—	—	800	—	1006	214.5	182.4	0.48	70
AF20	304	76	—	785	—	1006	214.5	182.4	0.48	70
AF35	247	133	—	780	—	1006	214.5	182.4	0.48	80
AF50	190	190	—	770	—	1006	214.5	182.4	0.48	85
BF	380	—	—	400	400	1006	235.5	182.4	0.48	60
BF20	304	76	—	395	395	1006	235.5	182.4	0.48	70
BF35	247	133	—	390	390	1006	235.5	182.4	0.48	80
BF50	190	190	—	385	385	1006	235.5	182.4	0.48	80
CF	380	—	—	—	800	1006	256.5	182.4	0.48	50
CF20	304	76	—	—	785	1006	256.5	182.4	0.48	60
CF35	247	133	—	—	780	1006	256.5	182.4	0.48	70
CF50	190	190	—	—	770	1006	256.5	182.4	0.48	80

[a]RFA in air-dried condition.

[b]RCA in air-dried condition.

[c]W/B ratio was based on the SSD condition of recycled coarse and fine aggregates.

splitting tensile strength, and modulus of elasticity. At each testing age for compressive strength and splitting tensile strength, the average of three concrete specimens were used to represent the mechanical properties of the concretes. The acceptable ranges of the tested results (three specimens) were within 7.8% as specified by ASTM C-39/C-39M-01 (ASTM 2001b).

Results and Discussion

Fresh Concrete and Slump Loss of Concrete

Table 4 lists the amounts of water mixed into the concrete to maintain an initial slump of 50–100 mm in fresh concrete. Recycled aggregate concretes required more mixing water than NAC, and the quantity of mixing water increased with increased RFA. For example, the AF, BF, and CF concretes required 214.5, 235.5, and 256.5 kg/m^3 amount of mixing water, respectively, while NAC required 191.0 kg/m^3. This was due to the water absorption by the recycled aggregates, which is about 12–13 times greater than NAC. Similar results were also reported elsewhere (Tangchirapat et al. 2008; Katz 2004).

When the slump of fresh concrete was maintained between 50 and 100 mm, recycled aggregate concrete containing high fineness of fly ash required the same amount of mixing water as recycled aggregate concrete without fly ash. Fly ash is spherical, and when used in concrete typically increases slump or reduces the required mixing water. Because of its high fineness (and thus increased surface area) and irregular shape, ground fly ash tends not to yield significantly better workability when used in recycled aggregate concrete. However, results indicated that the initial slump of fresh concretes containing recycled aggregates and fly ash increased slightly with increased fly ash replacement. For example, CF, CF20, CF35, and CF50 concretes had initial slumps of 50, 60, 70, and 80 mm, respectively. The slightly greater initial slump of fresh concrete containing greater fly ash replacement could have been caused by greater quantities of fly ash replacement containing a greater volume of paste (ground fly ash had a much lower specific gravity than Portland cement type I), leading to reduced aggregate particle interference and enhanced concrete workability. In addition, perhaps not all of the fly ash particles were ground and sufficient spherical particles exist to help lubricate the mixture.

Fig. 2 presents slump loss for NAC and the recycled aggregate concretes. The initial slump value for NAC was 60 mm, which decreased to zero at 105 min after mixing. Loss of slump was faster in recycled aggregate concretes than in the control concrete, particularly in the sample in which river sand was replaced with RFA. For example, the slumps of AF, BF, and CF concretes decreased to zero at 90, 75, and 60 min after mixing, respectively. This might have been caused by water absorption by the fine recycled aggregate, which quickly reduced the amount of water in the mixture.

Incorporating 20% high fineness of fly ash into recycled aggregate concrete resulted in a time for the initial slump to loss to zero about 15 min quicker than that of the recycled aggregate concrete without fly ash. This faster slump loss might have been due to the fineness of the fly ash, which provided more surface area to react with water. However, the slump loss of recycled aggregate concretes decreased when the high fineness of fly ash was replaced Portland cement at 35 and 50% by weight of the binder. For example, AF, AF20, AF35, and AF50 concretes had slump loss to zero value at 90, 75, 105, and 120 min, respectively.

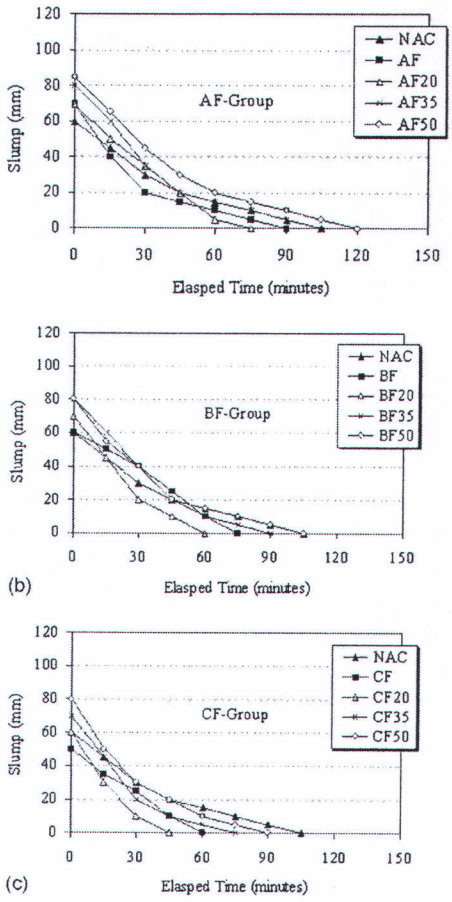

Fig. 2. Slump loss of concretes containing recycled aggregates: (a) concrete containing 100% RCA and 0% RFA (100% river sand); (b) concrete containing 100% RCA and 50% RFA; and (c) concrete containing 100% RCA and 100% RFA

The least slump loss occurred in the mix of concrete made from 100% RCA and river sand, and 50% high fineness of fly ash. This might have been attributable to two factors: first, the use of fly ash in concrete typically increases the concrete setting time, and second, the cement content in the concrete mixture decreases due to the replacement of fly ash (Kiattikomol et al. 2001). In addition, the slump loss for AF35 concrete was the same as for NAC, while slump loss was slower for AF50 concrete. This result suggests that incorporating high fineness of fly ash could reduce the slump loss of recycled aggregate concrete. This result was similar to Ravina (1984) who found that fly ash can reduce slump loss when it is partially used to replace cement.

Compressive Strength

Fig. 3 presents the compressive strengths of recycled aggregate concretes. At 28 days, NAC had a compressive strength of 47.0 MPa; after the same period, AF, BF, and CF concretes containing recycled aggregate had respective compressive strengths of 44.1, 41.3, and 35.9 MPa (94, 88, and 76% of NAC). Therefore, use of 100% RCA reduced the compressive strength of concrete by about 6% compared to NAC. In addition, increased replacement with RFA corresponded with a reduced compressive strength of

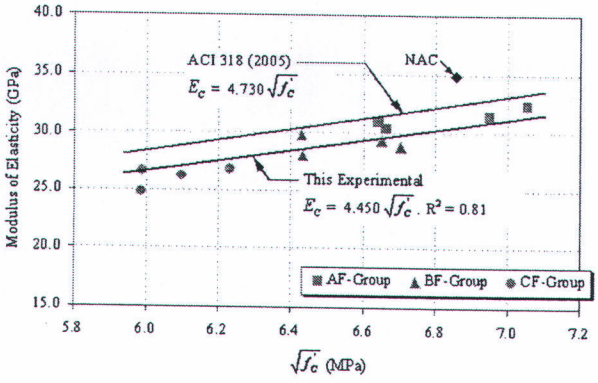

Fig. 5. Relationship between the modulus of elasticity and square root of the compressive strength of recycled aggregate concretes

gregate concrete ranged from 8.9 to 12.1%. Sri Ravindrarajah and Tam (1985) reported that the splitting tensile strength of recycled aggregate concrete made with RCA and natural sand did differ significantly from that of NAC. In this study, however, incorporating high fineness of fly ash did not alter the splitting tensile strength of recycled aggregate concrete samples.

Modulus of Elasticity

Fig. 5 presents the modulus of elasticity values for recycled aggregate concretes based on 100×200-mm cylindrical concrete samples. At 28 days, modulus of elasticity values ranged from 24.9 to 32.4 GPa, with compressive strengths from 35.8 to 49.7 MPa; the corresponding values for NAC were 34.9 GPa and 47.0 MPa. These results indicate that incorporating recycled aggregate into concrete decreases the modulus of elasticity values, particularly when both RCA and RFA are used. For example, at 28 days, AF, BF, and CF samples had modulus of elasticity values of 31.0, 29.8, and 26.7 GPa, respectively. Concretes made from 100% RCA and river sand had a modulus of elasticity 11% lower than that of NAC, and those made from 100% RCA and 100% RFA had a modulus of elasticity 24% lower than that of NAC. Gerardu and Hendriks (1985) obtained similar results, and reported that recycled aggregate concrete made with RCA and natural sand yielded a maximum modulus of elasticity 15% lower than that of NAC.

Recycled aggregate concretes that contained high fineness of fly ash had lower modulus of elasticity values than NAC, even though some mixtures of recycled aggregate concretes had equivalent or greater compressive strengths than NAC. For example, AF35 concrete had a 32.4 GPa modulus of elasticity with a corresponding compressive strength of 49.7 MPa, while NAC had a 34.9 GPa modulus of elasticity and a 47.0 MPa compressive strength. In concrete, the modulus of elasticity is usually related to the strength of aggregates rather than the strength of cement paste (Neville 1997). In addition, use of a pozzolanic material as a cement replacement slightly decreases the aggregate content of the concrete mixture compared to levels in NAC, resulting in a decreased modulus of elasticity (Cetin and Carrasquillo 1998). However, modulus of elasticity values of recycled aggregate concretes (with and without high fineness of fly ash) was still related to compressive strength, increasing with increased compressive strength.

Fig. 5 presents the relationship between the modulus of elasticity and square root of compressive strength compared to the values suggested by ACI 318 (ACI Committee 2005a). Eq. (1) is used to predict modulus of elasticity values of recycled aggregate concretes. Results indicated that modulus of elasticity values of recycled aggregate concrete (with and without high fineness of fly ash) were about 5.9% lower than values predicted by ACI 318. However, note that the modulus of elasticity and compressive strength of all concrete specimens in this study were obtained from cylinder samples 100 mm in diameter and 200 mm in height

$$E_C = 4.450\sqrt{f_c'} \tag{1}$$

where E_C=modulus of elasticity (GPa) and f_c'=compressive strength (MPa).

Conclusions

The results of this experiment yielded the following conclusions:

1. Use of high fineness of fly ash to replace Portland cement type I in the amounts of 35 and 50% by weight of the binder resulted in 15 to 30 min slower slump loss of concrete than recycled aggregate concrete without fly ash. Moreover, the slump loss of recycled aggregate concretes (AF and BF concrete groups) containing 35% high fineness of fly ash by weight of the binder was equivalent to that of NAC.
2. Use of high fineness of fly ash in recycled aggregate concrete yielded greater compressive strength than recycled aggregate concrete without high fineness of fly ash. Concretes made from 100% RCA and river sand had compressive strengths equivalent to or greater than NAC at 28 days when Portland cement was replaced by high fineness of fly ash at 20 to 35% by weight of the binder. Additionally, concretes made from 100% RCA, 50% RFA, and 35% high fineness of fly ash as a cement replacement had a greater compressive strength at 90 days than NAC.
3. Use of high fineness of fly ash did not affect the splitting tensile strength of recycled aggregate concrete. Recycled aggregate concrete had an average splitting tensile strength of 8.2% of its compressive strength, slightly lower than that of NAC.
4. Modulus of elasticity of recycled aggregate concretes was still related to its compressive strength, i.e., it increased with the increase of compressive strength. Recycled aggregate concretes with and without high fineness of fly ash had lower modulus of elasticity values than NAC and were about 5.9% lower than the value predicted by ACI 318 (ACI Committee 2005a).

Acknowledgments

The writers gratefully acknowledge the financial supports from the Thailand Research Fund (TRF) under TRF Senior Research Scholar Contact No. RTA5080020 and the Commission on Higher Education, Ministry of Education, Thailand.

References

American Concrete Institute (ACI) Committee. (2005a). "Building code requirements for structural concrete (ACI 318-05) and commentary (ACI 318R-05)." *ACI 318*, Detroit, 430.

American Concrete Institute (ACI) Committee. (2005b). "Removal and reuse of hardened concrete." *ACI 555R-01*, Detroit, 26.

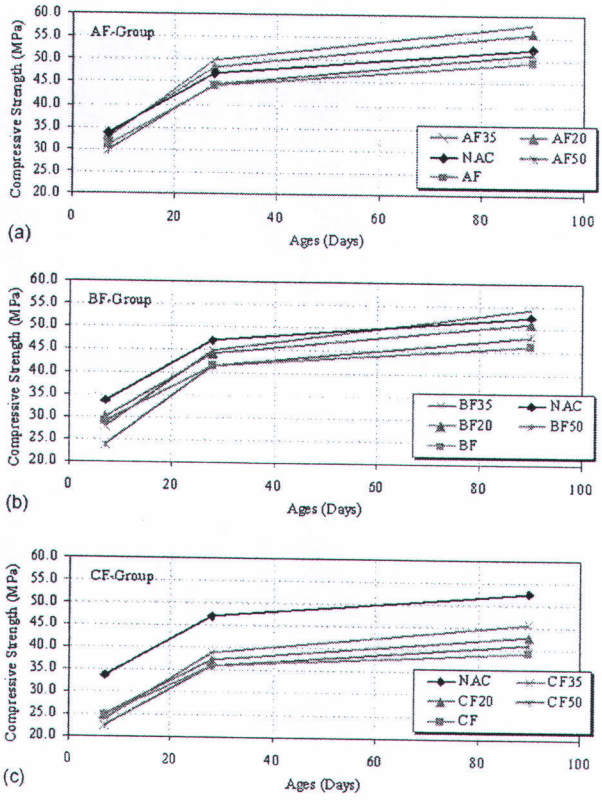

Fig. 3. Compressive strength of recycled aggregate concretes: (a) concrete containing 100% RCA and 0% of RFA (100% river sand); (b) concrete containing 100% RCA and 50% RFA; and (c) concrete containing 100% RCA and 100% RFA

recycled aggregate concrete. Hansen and Narud (1983) and Topçu and Guncan (1995) observed a similar relationship caused by the large quantities of concretes containing RFA, which resulted in lower compressive strength.

Fig. 3(a) presents the compressive strengths of concretes made from 100% RCA, 100% river sand, and those containing high fineness of fly ash. After 7 days, all recycled aggregate concretes mixed with fly ash had a lower compressive strength than NAC. However, at 28 days, the AF20 concrete had a compressive strength of 48.3 MPa, greater than AF and NAC. At 28 days, the AF35 concrete had the highest compressive strength of the AF group: 49.7 MPa or 106% of NAC; this value tended to increase as time passed. This finding indicates that incorporating high fineness of fly ash increased the compressive strength of recycled aggregate concrete. In addition, incorporating high fineness of fly ash at 50% by weight of the binder to replace Portland cement resulted in greater compressive strength than the AF concrete and a slightly lower compressive strength than NAC. At 28 and 90 days, the AF50 concrete had a compressive strength of 44.4 and 51.5 MPa (94 and 98% of NAC), respectively.

When concretes contained 100% RCA and 50% RFA [see Fig. 3(b)], BF, BF20, BF35, and BF50 concretes had respective compressive strengths of 41.3, 44.2, 45.0, and 41.4 MPa (88, 94, 96, and 88% of NAC) at 28 days. At 90 days, the compressive strength of the BF35 concrete increased to 54.4 MPa, or 104% of NAC. The high fineness of fly ash probably contributed compressive strength though a pozzolanic reaction as well as the packing

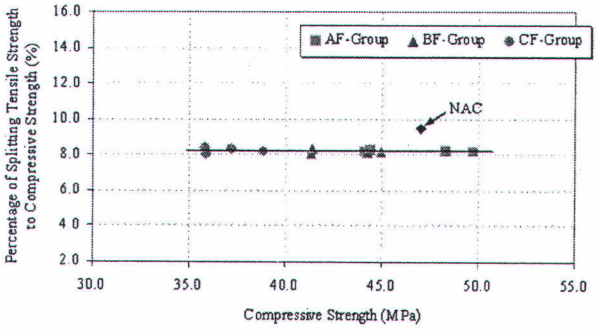

Fig. 4. Relationship between percentage of splitting tensile strength to compressive strength and the compressive strength of recycled aggregate concretes

effect provided by the small particles of fly ash (Isaia et al. 2003; Tangpagasit et al. 2005). When cement was replaced with 50% high fineness of fly ash (BF50 concrete), its compressive strength at 90 days was 48.3 MPa (92% of NAC), slightly lower than the BF concrete (46.2 MPa).

Fig. 3(c) presents the relationships between compressive strength and ages of concrete made from 100% RFA, 100% RCA, and cement replaced by high fineness of fly ash at 20, 35, and 50% by weight of the binder. At 28 days, CF20, CF35, and CF50 samples had respective compressive weights of 37.2, 38.8, and 35.8 MPa (79, 83, and 76% of NAC), and at 90 days these values had increased to 42.7, 45.6, and 41.2 MPa (81, 87, and 78% of NAC), respectively. When 35% of cement was replaced by high fineness of fly ash, this CF35 concrete had the highest compressive strength in the CF group; compressive strength decreased slightly when levels of high fineness of fly ash were increased to replace 50% of the cement by weight of binder.

These findings on the compressive strengths of recycled aggregate concrete indicated that high fineness of fly ash can be used to increase the overall compressive strength of recycled aggregate concretes. For concrete made from 100% RCA and river sand, 100% RCA, and 50% RFA, the best results occurred when high fineness of fly ash was used to replace about 35% of the concrete by weight of the binder. At 90 days, this mixture proportion appears to give recycled aggregate concrete a greater compressive strength than that of NAC. In addition, concrete made from 100% RCA and river sand, and containing high fineness of fly ash up to 50% by weight of the binder, can produce compressive strengths as high as that of NAC.

Splitting Tensile Strength

Fig. 4 shows the relationships between the percentage of splitting tensile strength to compressive strength and the compressive strength of recycled aggregate concrete. Recycled aggregate concretes with and without high fineness of fly ash had maximum and minimum values (percentage of splitting tensile strength) of 8.4 and 8.0%, respectively (average 8.2%). According to Mindess et al. (2003) the splitting test generally indicates that normal concrete (NAC) has a tensile strength about 8–14% of its compressive strength (Mindess et al. 2003). The splitting tensile strength of the NAC sample used in this study was 9.5% of its compressive strength, so the recycled aggregate concretes did not have a very different splitting tensile strength compared to concrete made from normal aggregates. Sagoe-Crentsil et al. (2001) reported that the tensile/compressive strength ratio of recycled ag-

ASTM. (2001a). "Standard specification for concrete aggregates." *ASTM C-33*, West Conshohocken, Pa., 10–17.
ASTM. (2001b). "Standard test method for compressive strength of cylinder concrete specimens." *ASTM C-39/C-39M-01*, West Conshohocken, Pa., 18–22.
Barra de Oliveira, M., and Vazquez, E. (1996). "The influence of retained moisture in aggregates from recycling on the properties of new hardened concrete." *Waste Manage.*, 16(1–3), 113–117.
Cetin, A., and Carrasquillo, R. L. (1998). "High-performance concrete: Influence of coarse aggregate on mechanical properties." *ACI Mater. J.*, 95(3), 252–261.
Chen, H. J., Ten, T., and Chen, K. U. (2003). "Use of building rubbles as recycled aggregates." *Cem. Concr. Res.*, 33(1), 125–132.
Gerardu, J. J. A., and Hendriks, C. F. (1985). "Recycled of road pavement materials in the Netherlands." *Rijkswaterstaat communications No. 38*, Road Engineering Division, Delft, The Netherlands.
Hansen, T. C., and Narud, H. (1983). "Strength of recycled concrete made from crushed concrete coarse aggregate." *Concr. Int.*, 5(1), 79–83.
Isaia, G. C., Gastaldini, A. L. G., and Moraes, R. (2003). "Physical and pozzolanic action of mineral additions on the mechanical strength of high-performance concrete." *Cem. Concr. Res.*, 25(1), 69–76.
Jaturapitakkul, C., Kiattikomol, K., Sata, V., and Leekeeratikul, T. (2004). "Use of ground coarse fly ash as a replacement of condensed silica fume in producing high-strength concrete." *Cem. Concr. Res.*, 34(4), 549–555.
Katz, A. (2003). "Properties of concrete made with recycled aggregate from partially hydrated old concrete." *Cem. Concr. Res.*, 33(5), 703–711.
Katz, A. (2004). "Treatment for the improvement of recycled aggregate." *J. Mater. Civ. Eng.*, 16(6), 597–603.
Kiattikomol, K., Jaturapitakkul, C., Singpiriyakij, S., and Chututim, S. (2001). "A study of ground coarse fly ashes with different finenesses from various sources as pozzolanic materials." *Cem. Concr. Compos.*, 23(4–5), 335–343.
Kou, S. C., Poon, C. S., and Chan, D. (2007). "Influence of fly ash as cement replacement on the properties of recycled aggregate concrete." *J. Mater. Civ. Eng.*, 19(9), 709–717.
Mehta, P. K. (1985). "Influence of fly ash characteristics on the strength of Portland-fly ash mixture." *Cem. Concr. Res.*, 15(4), 669–674.
Mindess, S., Young, J. F., and Darwin, D. (2003). *Concrete*, 2nd Ed., Pearson Education, Upper Saddle River, N.J., 317.
Montgomery, D. G. (1998). "Workability and compressive strength properties of concrete containing recycled concrete aggregate." *Proc., Sustainable Construction: Use of Recycled Concrete Aggregate*, R. K. Dhir, N. A. Henderson, and M. C. Limbachiya, eds., Thomas Telford, London, 289–296.
Naik, T. R., and Ramme, B. W. (1989). "High-strength concrete containing large quantities of fly ash." *ACI Mater. J.*, 86(2), 111–116.
Neville, A. M. (1997). "Aggregate bond and modulus of elasticity of concrete." *ACI Mater. J.*, 94(1), 71–74.
Otsuki, N., Miyazato, S., and Yodsudjai, W. (2003). "Influence of recycled aggregate on interfacial transition zone, strength, chloride penetration and carbonation of concrete." *J. Mater. Civ. Eng.*, 15(5), 443–451.
Poon, C. S., Shui, Z. H., Lam, L., Fok, H., and Kou, S. C. (2004). "Influence of moisture states of natural and recycled aggregate on the slump and compressive strength of concrete." *Cem. Concr. Res.*, 34(1), 31–36.
Ravina, D. (1984). "Slump loss of fly ash concrete." *Concr. Int.*, 6(4), 35–39.
Sagoe-Crentsil, K. K., Brown, T., and Taylor, A. H. (2001). "Performance of concrete made with commercially produced coarse recycled aggregate." *Cem. Concr. Res.*, 31(5), 707–712.
Shayan, A., and Xu, A. (2003). "Performance and properties of structural concrete made with recycled concrete aggregate." *ACI Mater. J.*, 100(5), 371–380.
Sri Ravindrarajah, R. S., and Tam, T. C. (1985). "Properties of concrete made with crushed concrete as coarse aggregate." *Mag. Concrete Res.*, 37(130), 29–38.
Tangchirapat, W., Buranasing, R., Jaturapitakkul, C., and Chindaprasirt, P. (2008). "Influence of rice husk-bark ash on mechanical properties of concrete containing high amount of recycled aggregates." *Constr. Build. Mater.*, 22(8), 1812–1819.
Tangpagasit, J., Cheerarot, R., Jaturapitakkul, C., and Kiattikomol, K. (2005). "Packing effect and pozzolanic reaction of fly ash in mortar." *Cem. Concr. Res.*, 35(6), 1145–1151.
Topçu, I. B., and Guncan, N. F. (1995). "Using waste concrete as aggregate." *Cem. Concr. Res.*, 25(7), 1385–1390.
Topçu, I. B., and Sengel, S. (2004). "Properties of concrete produced with waste concrete aggregate." *Cem. Concr. Res.*, 34(8), 1307–1312.

13. J. Wongpa, K. Kiattikomol, C. Jaturapitakkul, P. Chindaprasirt. Compressive strength, modulus of elasticity, and water permeability of inorganic polymer concrete, Materials & Design, 31 (2010), 4748-4754. (IF 1.107).

Materials and Design 31 (2010) 4748–4754

Contents lists available at ScienceDirect

Materials and Design

journal homepage: www.elsevier.com/locate/matdes

Compressive strength, modulus of elasticity, and water permeability of inorganic polymer concrete

J. Wongpa [a], K. Kiattikomol [a], C. Jaturapitakkul [a,*], P. Chindaprasirt [b]

[a] Department of Civil Engineering, Faculty of Engineering, King Mongkut's University of Technology Thonburi, Bangkok 10140, Thailand
[b] Department of Civil Engineering, Faculty of Engineering, Khon Kaen University, Khon Kaen 40002, Thailand

ARTICLE INFO

Article history:
Received 6 March 2010
Accepted 6 May 2010
Available online 11 May 2010

Keywords:
A. Composites
Polymer matrix
A. Concrete
E. Mechanical

ABSTRACT

Inorganic polymer concretes (IPCs) were produced from rice husk–bark ash (RHBA) combined with fly ash (FA) as a cementitious raw material. Six different mixtures were used to study the properties of IPC. Since RHBA is rich in silica material, varying the ratio of FA to RHBA results in differing SiO_2/Al_2O_3 ratios. To keep the SiO_2/Al_2O_3 ratio constant, the ratio of FA to RHBA was fixed at 80:20 by weight. High concentration sodium hydroxide solution and sodium silicate solution were used as a liquid component of the concrete mixture. The mixing and curing of these inorganic polymer concretes were performed under ambient conditions. Compressive strength, modulus of elasticity, and water permeability of the IPCs were investigated at specified intervals up to 90 days. The results showed that the compressive strength, modulus of elasticity, and water permeability of IPCs depend on the mix proportions, especially the solution to ash (*S/A*) ratio and the paste to aggregate (*P/Agg*) ratio. Moreover, the results showed that the water permeability and the elastic modulus of IPCs were significantly related to their compressive strength.

1. Introduction

Geopolymer is an inorganic material developed by Davidovits [1], a French scientist. The materials containing both silica and alumina can be used as a binder to produce geopolymer [2]. Various alkali activators also play a major role in producing geopolymers by dissolving silica and alumina from the raw material and forming aluminosilicate structures [3]. Geopolymer has been used for various works such as for sculpture, building, repairing, and restoration [4,5]. Numerous research publications relating to geopolymers have been released, with some reporting on chemical composition aspects or reaction processes [6–8] while others present results relating to mechanical properties and durability [9–12]. As already known, the compressive strength of an inorganic polymer depends on both the ratio of Si/Al and the types of raw material used [10,13,14]. Fly ash (FA) has recently been used as a source material to produce geopolymer because it has a suitable chemical composition along with its favorable size and shape [13,15].

Fly ash is a by-product of coal power plants. In Thailand, the total output of fly ash from power plants is about 4.0 million tons annually [13]. Reports in literature specify that fly ash is primarily composed of SiO_2, Al_2O_3 and Fe_2O_3 [13,16–19]. Since the quality of fly ash depends on the type and the quality of coal along with the performance of the power plant, it is sometimes difficult to control its chemical composition. In order to achieve a suitable chemical composition for the production of geopolymers, the preferred method is to blend fly ash with another high silica material.

Rice husk–bark ash (RHBA) is a solid waste generated by biomass power plants using rice husk and eucalyptus bark as fuel. The power plant company providing RHBA for this research reported that about 450 tons/day of RHBA are produced and discarded. The major chemical constituent of RHBA is SiO_2 (about 75%) as reported from previous investigations [20,21]. Therefore, blending FA and RHBA can adjust the ratio of Si/Al as required. It seems that no publication about the use of RHBA as a raw material in inorganic polymer concrete has been found based on our literature review. Moreover, only a few researchers have studied the effect of mix proportions on the properties of IPCs such as the effect of paste content, aggregate content, and the water to binder ratio (*W/B*) on the strength and durability of IPCs [22,23].

In this study, the effect of mix proportions on the properties of IPCs was studied and compared to that of conventional concrete. For conventional concrete, target compressive strength is the most important parameter specified in the mixed design of concrete recommended by ACI 211 [24]. The design process begins with specifying of cement content and *W/B* ratios to serve the desired target strength. This means that cement content and water content are the most important ingredients for controlling the compressive strength of the concrete. In other words, the paste content (composed of cement and water) is the parameter that controls the compressive strength of conventional Portland cement concrete.

* Corresponding author. Tel.: +66 2470 9131; fax: +66 2427 9063.
E-mail address: chai.jat@kmutt.ac.th (C. Jaturapitakkul).

0261-3069/$ - see front matter © 2010 Elsevier Ltd. All rights reserved.
doi:10.1016/j.matdes.2010.05.012

Rice husk–bark ash (RHBA) and fly ash (FA) were selected as the cementitious raw material for this research. The design of mix proportions follows the method of ACI 211 [24]. The ratio of FA to RHBA was fixed at 80:20 by weight to avoid the effect of differing Si/Al ratios. To relate conventional concrete with IPCs, the cement and water content of conventional concrete can be compared to the ash and solution content of IPCs, respectively. This research focuses on *P/Agg* ratio (paste content/aggregate content) and *S/A* ratio (solution content/ash content) to study their effects on the compressive strength, modulus of elasticity, and water permeability of IPCs.

2. Materials

Fly ash was collected from the Mae Moh power plant in Thailand, in which lignite is used as a fuel. Rice husk–bark ash (RHBA) was collected from a biomass power plant in the Chachoengsao province of Thailand, in which a fluidized-bed system is in use. Biomass combustion is performed at 800–900 °C for 5–10 s, thus generating RHBA with high uniformity. Fly ash and RHBA were mixed together in the ratio of 80:20 by weight and used as the cementitious raw material to create inorganic polymer concrete mixtures.

Sodium silicate solution or water glass (WG) and sodium hydroxide were used as the solution part of the mixture. Sodium silicate solution was used without any modification, but the sodium hydroxide was diluted to a concentration of 14 M before use.

Table 1 shows the chemical composition of RHBA, FA, and sodium silicate solution. RHBA contains about 85% SiO_2 but only 0.16% Al_2O_3. Fly ash is composed of both SiO_2 and Al_2O_3 at 36% and 21%, respectively. In other words, the SiO_2/Al_2O_3 ratio of RHBA is about 530 while that of fly ash is only 1.75. Thus, the ratio of FA to RHBA has an influence on the SiO_2/Al_2O_3 ratio of inorganic polymer concrete and also the amount and type of aluminosilicate structures [10]. Sodium silicate solution contains about 15% Na_2O, 33% SiO_2 and the rest is water.

Table 1
Chemical composition of raw materials (by weight).

Materials	SiO_2	Al_2O_3	Fe_2O_3	CaO	SO_3	Na_2O	LOI
RHBA[a]	84.75	0.16	–	2.78	0.6	–	3.72
FA[b]	36.02	20.58	15.91	18.75	2.24	–	0.07
WG[c]	33.28	–	–	–	–	15.36	–

[a] Rice husk–bark ash.
[b] Fly ash.
[c] Water glass or sodium silicate solution having specific gravity of 1.598 at 20 °C and density of 54.2 Baume'.

3. Experimental program

This experimental work focused on the effect of mix proportions on the properties of IPCs while attempting to keep the effect of chemical composition to a minimum. Therefore, the ratio of FA to RHBA was fixed at 80:20 by weight and the ratio of sodium silicate solution to sodium hydroxide solution was 2.5 by weight for all mixtures.

3.1. Material preparation

As-received RHBA has rough surfaces and high porosity as shown in Fig. 1a. Therefore, RHBA was ground using a ball mill in order to obtain smaller particle sizes and fewer pores. This results in a higher specific surface area and faster chemical reaction rate [25]. The RHBA particle retained on a 45 μm sieve was 2.2% by weight. Fig. 1b shows a SEM image of the ground RHBA indicating that grinding reduced the particle size of the RHBA and destroyed its voids.

As-received fly ash was used without any improvement because it had a smooth surface, round shape and low porosity. From the literatures [13,26], the fresh IPCs using raw FA as the binder had higher workability than non-FA mixtures. However, the workability of fresh IPC could not be compared to fresh concrete from Portland cement because the fresh IPC had a very high viscosity. Fly ash and RHBA were dry-mixed together before adding the solution as suggested by Teixeira-Pinto et al. [27]. The FA to RHBA ratio of 80:20 by weight was used for all mixtures and this material was called "ash" in this research.

Sodium hydroxide (flake type, 98% pure) was diluted by tap water to have a concentration of 14 M. The solution was left under ambient conditions until the excess heat had completely dissipated to avoid accelerating the setting of the IPCs.

The sodium silicate solution was used without preparation. It was mixed with the sodium hydroxide solution and the mixed solution was called "solution". The ratio between the sodium silicate solution and sodium hydroxide solution was 2.5 by weight for all mixtures because this ratio demonstrated the best properties for fly ash-based geopolymer [22,28].

3.2. Mixing and curing

The FA and RHBA were incorporated at the ratios indicated in Table 2. Because of the high viscosity of fresh inorganic polymeric paste, the sequence of mixing was important to homogenize the fresh IPCs. Coarse aggregate was added first to the concrete mixer

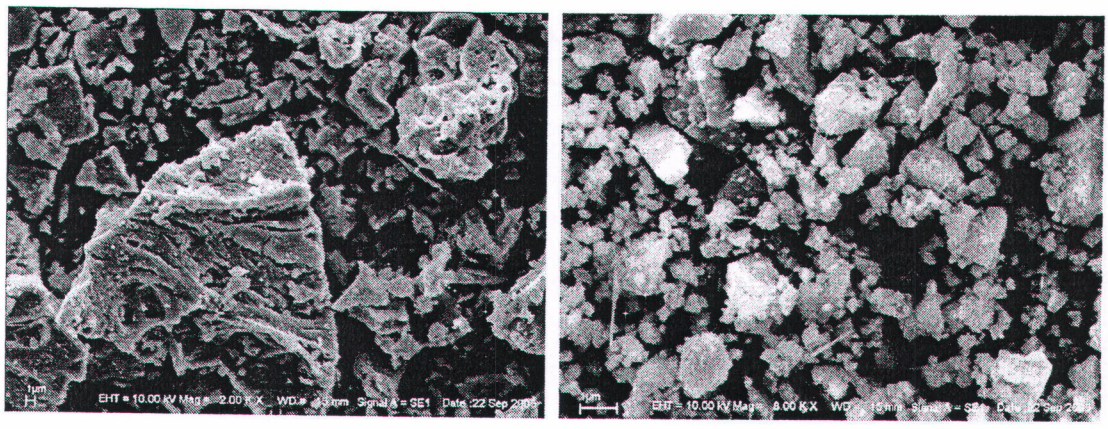

Fig. 1. Particle images of original and ground RHBA.

Table 2
Mix proportions of inorganic polymer concrete mixtures (kg/m³).

Sample	FA	RHBA	WG	NaOH	C.Agg	F.Agg	*P/Agg*	*S/A*
P3–6	320	80	180	72	956	751	0.38	0.63
P3–7	280	70	181	72	990	778	0.34	0.72
P4–7	320	80	207	83	920	722	0.42	0.73
P4–8	320	80	233	93	884	694	0.46	0.82
P5–7	360	90	232	93	850	667	0.51	0.72
P6–7	400	100	265	106	746	617	0.64	0.74

followed by fine aggregate. The blended ash and mixed solution were added gradually one by one and all of them were mixed together to obtain the uniform fresh mixture. The mixture was then cast into Ø5 × 10 cm steel molds. A tamping rod and vibration table were used to compact the fresh IPCs, which were then left in room temperature for 24 h before de-molding. Hardened IPCs were cured under ambient conditions without any further treatment. The properties of the samples were then examined at specified intervals.

The *P/Agg* ratio is the ratio between the paste content and the aggregate content as shown in:

$$P/Agg\ \text{ratio} = \frac{(\text{ash content} + \text{solution content})}{\text{aggregate content}} \quad (1)$$

where ash content is the amount of fly ash and RHBA (g), solution content is the combination of sodium silicate solution and sodium hydroxide solution (g) and aggregate content includes both the coarse and fine aggregates. The *S/A* ratio is the weight ratio between the solution content (*S*) and the ash content (*A*).

The symbols used in this investigation are defined by *PX–Y* where *P* represents the "*P/Agg* ratio", and *X* and *Y* are the round off values for *P/Agg* ratio and *S/A* ratio, respectively. The values of *X* of 3, 4, 5, and 6 specified the *P/Agg* ratios of 0.34 and 0.38; 0.42 and 0.46; 0.51; and 0.64, respectively. The values of *Y* of 6, 7, and 8 specified the *S/A* ratios of 0.63; 0.72, 0.73, and 0.74; and 0.82, respectively.

3.3. Preparation of samples, testing, and calculation

Compressive strengths of the IPCs were examined at 3, 7, 14, 28, 60, and 90 days to observe the development of the compressive strength. The elastic modulus of each sample was investigated at 7, 28, and 90 days. Water permeability was examined at 28 and 90 days.

To prepare the water permeability testing specimens, the top and bottom of ø5 × 10 cm samples from each mixture were removed to avoid any effects caused by surface paste. Then the samples were cut at the middle in order to make the two pieces of specimen having ø5 × 4 cm and to be used as representative specimens for each mixture. Non-shrinking epoxy resin was cast around all specimens with a thickness of 25 mm to prevent water leakage. These specimens were installed in housing cells to test their water permeability coefficient. The water pressure in the system (gauge pressure) was 0.2 MPa. The housing cell, water permeability apparatus and testing method followed the procedure used by Chusilp et al. [29] and Chindaprasirt et al. [30]. The water permeability coefficient was calculated using Darcy's law, as shown in the equation below.

$$K_f = \frac{\rho L g Q}{P_{\text{pressure}} A_{\text{area}}} \quad (2)$$

where K_f is the coefficient of water permeability of the specimen (m/s), ρ is the density of water (kg/m³), L is the length of specimen (m), g is the gravitational acceleration (m/s²), Q is the net flow rate (m³/s), A_{area} is the cross-sectional area of the specimen (m²) and P_{pressure} is the water pressure [(kg m s^{-2})/(m²) or MPa].

4. Results and discussion

4.1. Compressive strength

Fig. 2 shows the compressive strength development of the IPCs for various ages and different mix proportions. It is observed that the compressive strength of all mixtures tend to decrease after the age of 14 days or 28 days, depending on the mix proportions. Moreover, the compressive strengths of the P4–8, P5–7, and P6–7 mixtures decreased obviously while the others decreased slightly. It was observed that P4–8 has the highest *S/A* ratio while P6–7 has the highest *P/Agg* ratio followed by P5–7. So, it could be said that *S/A* ratio was the most important factor that controlled the rate of reduction in compressive strength of IPCs while *P/Agg* ratio had the less influence, however, in the same direction. In addition, both *S/A* ratio and *P/Agg* ratio also controlled the compressive strength of IPCs. The higher the *S/A* ratio, the lower the compressive strength. On the other hand, for the same *S/A* ratio, the mixtures containing higher *P/Agg* ratio produced lower compressive strength than that with lower *P/Agg* ratio and could be observed that P3–6 mixture which has *P/Agg* of 0.34 and *S/A* of 0.63 showed the highest compressive strength.

Normally, the compressive strength of concrete should not decrease with time. If the compressive strength drops at a specific age, it means that cracks were occurred from shrinkage due to the continuing reaction. The reduction in compressive strength of IPC depended on the rate of shrinking (or cracking), and this rate was controlled by the *P/Agg* ratio and *S/A* ratio of the mixture. Shrinkage might be occurred at later ages due to the lacking of solution which is necessary for IPCs to produce strength. If it was insufficient, shrinking will be started, then, resulted in cracks of IPCs. Other researchers have also found strength reduction of geopolymers in their investigations and reported a similar assumption. Zuhua et al. [31] reported that the use of high molarity NaOH (such as 12 M) and a high liquid/solid ratio could accelerate dissolution and hydrolysis but obstruct polycondensation. When the samples were cured in the air, geopolymers showed considerable shrinkage. In addition, they also reported that non-evaporable water was necessary to maintain the strength and volume stability of the geopolymer. Lee and Deventer [11] concluded that the nature and the amount of dissolved water in the gels of geopolymers could control their durability. Another assumption, by Pacheco-Torgal et al. [22], was that excess sodium ions reacted with carbon dioxide and formed sodium carbonate crystals that made the structure unstable. Duxon et al. [10] reported that compressive strength

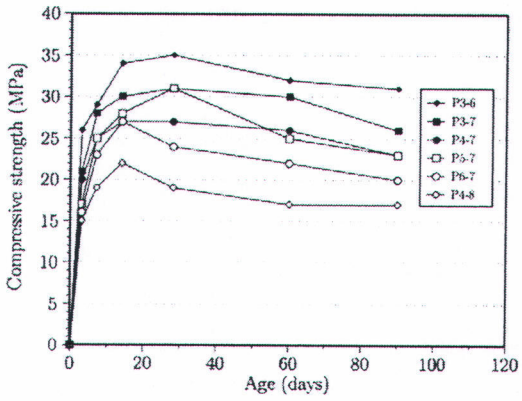

Fig. 2. Compressive strength development of IPCs and age.

decreased with time when a SiO_2/Al_2O_3 ratio of the mixture was higher than 3.8. This phenomenon appeared occasionally and depended on the mix proportions. However, some researchers have found that the compressive strength of geopolymers continuously increased during the testing period [9,32].

4.2. Modulus of elasticity

According to Table 3, the modulus of elasticity of IPCs decreased from 7 days to 90 days but the compressive strengths in Fig. 2 showed different results. The compressive strength of IPCs at the age of 28 days had the highest value compared to 7 days and 90 days, but the modulus of elasticity reached a maximum value after 7 days. Normally, the elastic modulus of concrete relates to its compressive strength as the simple equation (3),

$$E = \frac{\sigma}{\varepsilon} \tag{3}$$

where E is the modulus of elasticity (MPa), σ is the compressive stress (MPa), and ε is the strain value (dimensionless). Naturally, strain along the time of concrete-like materials would slightly decrease after hardened. This means that the elastic modulus of such materials do not decrease even though the compressive strength is stable. If not, then there are some unusual circumstances regarding the strain behavior of those materials.

Fig. 3a–c illustrates the assumption on strain variation of IPCs over time. To understand the varying in strain of IPCs, compressive strength development rate and crack growths must be considered. At early age, the compressive strength developed very fast as shown in Fig. 2 while cracks did not originate or developed very slowly as shown in Fig. 3a. At 28 days, for example, shown in Fig. 3b, the compressive strength of IPCs developed at very low rate but cracks grew very fast due to the solution consumption in the polycondensation process. So, the modulus of elasticity of IPCs at 28 days was lower than the earlier age such as 7 days, even though the compressive strength was slightly higher. The long-term results (90 days) show the lowest values for both modulus of elasticity and compressive strength because the compressive strength very slowly increased and cracks developed very fast due to insufficient solution as shown in Fig. 3c and d.

Table 3
Modulus of elasticity and water permeability of IPCs.

Sample	Modulus of elasticity (MPa)			Water permeability (m/s)	
	7 Days	28 Days	90 Days	28 Days	90 Days
P3–6	16922	14951	14397	1.03×10^{-10}	5.72×10^{-10}
P3–7	15250	12635	10432	2.43×10^{-10}	3.07×10^{-10}
P4–7	12522	9882	7971	6.88×10^{-10}	4.45×10^{-9}
P4–8	10406	8120	5613	2.63×10^{-9}	6.79×10^{-9}
P5–7	11412	9086	6972	6.13×10^{-10}	2.05×10^{-9}
P6–7	15473	13686	10744	1.56×10^{-10}	6.35×10^{-10}

4.3. Water permeability

Table 3 shows that the water permeability coefficients for all IPCs increase from 28 days to 90 days, which is opposite from their compressive strength, as shown in Fig. 2. The mixture of P4–8 yields the highest water permeability value since it has the highest *S/A* ratio and the lowest compressive strength. This suggested that there is a relationship between the compressive strength and the water permeability of IPCs and this relationship is inversely pro-

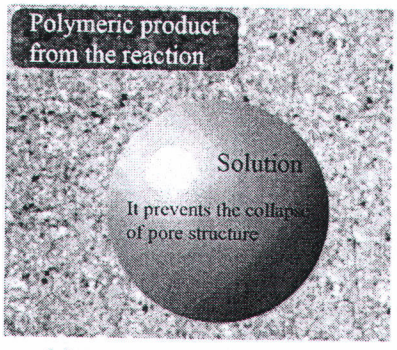

(a) Solution in a void at early age of polymerization (less than 7 days)

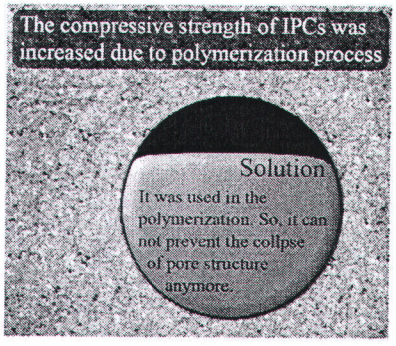

(b) Solution in a void was used during polymerization process (7 – 28 days)

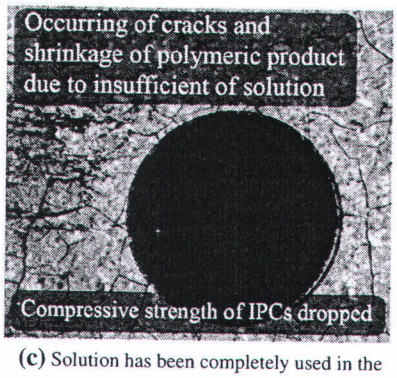

(c) Solution has been completely used in the polymerization process (over 28 days)

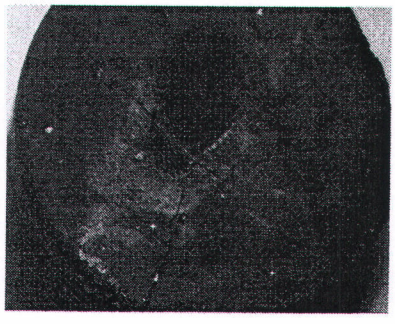

(d) A picture of cracks on the surface of an inorganic polymeric paste sample

Fig. 3. The occurring of cracks in IPCs illustrated from the assumption.

portional. On the other hand, both the compressive strength and water permeability of IPCs depend on the amount of pores and cracks inside the microstructures. This result confirms that the shrinkage of IPCs really occurs over the long term because all mixtures show the compressive strength decreases from the age of 28–90 days while the water permeability coefficient increases during the same period. Shrinkage was the cause of cracks and these cracks increased the water permeability of the samples and reduced the compressive strength at a time. Fig. 3a–c show the occurrence of cracks from the consumption of the solution during the polymerization process. Fig. 3d shows a picture of a hardened paste sample to represent the cracks on its surface. This picture confirms that cracks in IPCs occur at the later age due to the shrinkage of the inorganic polymeric paste.

4.4. Effect of P/Agg ratio and S/A ratio on compressive strength of IPCs

Fig. 4 shows the relationship between compressive strength and *P/Agg* ratio of IPCs. The concrete containing a lower *P/Agg* ratio tended to yield slightly higher compressive strength than the one with a higher *P/Agg* ratio. Since the chemical composition of all mixtures was similar, the difference in compressive strength between the mixtures was due to variations in the paste content of the mixture. Segregation was found in hardened IPCs mixtures with a high *P/Agg* ratio. Moreover, cracks were also observed in the segregation specimen at the low aggregate zone. Generally, paste is used to bind the aggregates together and the compressive strength of IPCs develops with the hardening of the paste. However, it should be noted that too much paste results in a reduction of compressive strength [33]. At the low aggregates zone of the segregated specimen, cracks occur easily due to insufficient aggregates. Pacheco-Torgal et al. [22] reported that the IPC mixtures using higher aggregate content showed higher compressive strength due to the dissolution of quartz and alumina in the presence of alkalis that enhanced the bonding between paste and aggregates. This explains why cracks might occur more readily in lower aggregate zones. Moreover, they found a reduction in compressive strength after 14 days. They reported an assumption that this phenomenon occurred due to shrinkage and cracks near the aggregates.

Fig. 5 shows the relationship between the compressive strength and the *S/A* ratio. It is obvious that lower *S/A* ratios give higher compressive strengths for IPCs. Since water in conventional concrete and solution in IPCs are both liquid while cement and ash are solid powder, the *S/A* ratio of IPCs could be used and compared to the *W/C* ratio of conventional concrete. Since the *W/C* ratio is the major parameter that controls the compressive strength of conventional concrete [34], then the *S/A* ratio can control the compressive strength of IPCs with the same reason. Similar to conventional concrete, excess solution in an IPC mixture would produce a lot of voids in the microstructure. Thus, higher solution content results in more voids and lower compressive strength for IPCs. Considering Figs. 4 and 5, the *S/A* ratio has a greater influence on the compressive strength of IPCs than the *P/Agg* ratio.

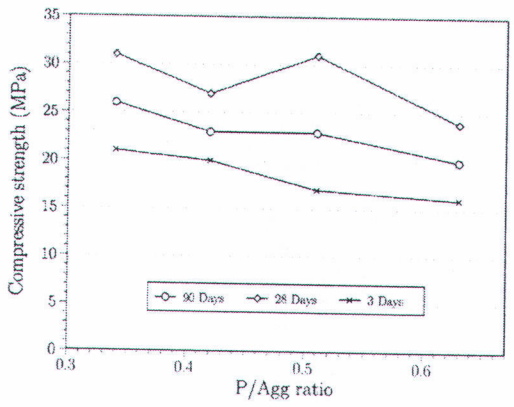

Fig. 4. Relationship between compressive strength and *P/Agg* ratio of IPCs.

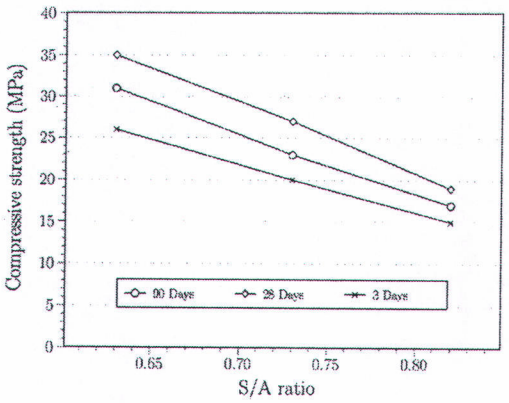

Fig. 5. Relationship between compressive strength and *S/A* ratio of IPCs.

4.5. Relationship between compressive strength and modulus of elasticity of IPCs

Fig. 6 shows the relationship between compressive strength and modulus of elasticity of all the samples and every age in this investigation. The Young's modulus of IPCs tends to increase linearly to the square root of the compressive strength. The modulus of elasticity of IPCs has a very high deviation because the elastic modulus of IPCs depends not only on the compressive strength but also on the strain, as described in the previous section. The linear relationship between the square root of the compressive strength and the modulus of elasticity, however, could be observed. The equation predicting the modulus of elasticity from the known compressive strength is shown in the following equation:

$$E = 1687\sqrt{f'_c} - 16078 \tag{4}$$

where E and f'_c are in MPa.

The modulus of elasticity of conventional concrete is calculated from the equation $E = 4700\sqrt{f'_c}$, recommended by ACI 318-08 [35] for normal weight concrete. Although IPC is not brittle like conventional concrete, the compressive strength is high enough to be used as a normal strength concrete. IPC has a low elastic modulus as compared to conventional concrete, then investigation of creep

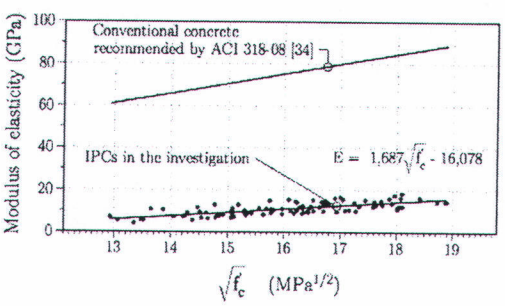

Fig. 6. Relationship between modulus of elasticity and compressive strength of IPCs.

and fatigue are needed to prevent the long-term damage. Duxson et al. [10] reported that the elastic modulus of an IPC depended on the SiO_2/Al_2O_3 ratio. Sofi et al. [9] found that the elastic modulus of IPC depended not only on SiO_2/Al_2O_3 ratio but also mix design and curing method. However, both Duxson and Sofi found that the elastic modulus of IPCs varied from 1000 to 55,000 MPa, which covers the values of 6000–17,000 MPa found in this research.

4.6. Relationship between compressive strength and water permeability of IPCs

Fig. 7 shows the relationship between compressive strength and water permeability of conventional concretes and IPCs. The relationship between the water permeability and compressive strength studied by Malhotra as shown in Fig. 7 were taken from Hearn [36]. The water permeability of both concretes depends on their compressive strengths. Both the conventional concrete and IPC show that the higher the compressive strength of concrete, the lower the water permeability. Also, for the same compressive strength, the water permeability coefficient of conventional concrete is much lower than that of IPC. Consequently, after 28 days and 90 days, which were the examination intervals for water permeability, the cracking of IPCs had already occurred. Therefore, the water permeability of IPCs is very high compared to conventional concrete.

Moreover, the difference in the water permeability coefficient between IPC and conventional concrete is lower when the compressive strengths of both concretes are higher. For example, the water permeability coefficient of conventional concrete predicted by equation in Fig. 7 is 5.36×10^{-13} m/s at the compressive strength of 20 MPa while that of the IPCs is 1.28×10^{-9} m/s. In other words, the water permeability of IPCs in this investigation was higher than that of conventional concrete obtained from Malhotra [36] by about 2390 times. In case of higher compressive strength, the difference in water permeability coefficient between the two concretes is smaller. The water permeability of IPC was 294 times higher than the data obtained from Malhotra [36] when the compressive strength was 30 MPa. The water permeability coefficient tends to decrease continuously as the compressive strength increases. A probable cause was that the lower compressive strength of IPCs mixtures contained a higher *S/A* ratio. It resulted in very sticky fresh polymeric paste which was more difficult to cast than the higher compressive strength IPCs. Including the occurrence of cracks and numerous of voids containing in the low strength IPCs, the higher water permeability coefficient was observed. However, the water permeability of conventional concrete reported by Malhotra [36] tended to be constant at the high values of compressive strength. Hence, the difference in water permeability coefficient between IPC and conventional concrete is higher at the lower compressive strength and lower at the higher compressive strength.

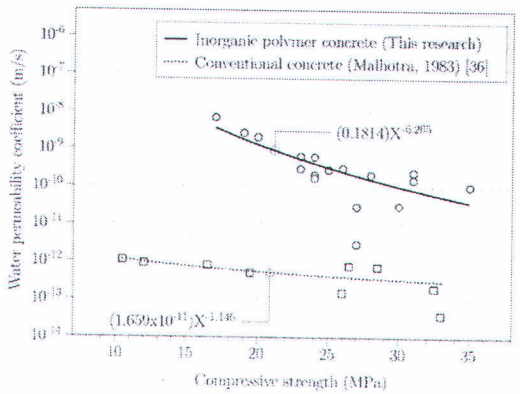

Fig. 7. Relationship between water permeability coefficient and compressive strength of conventional concrete and IPCs.

5. Conclusions

The *S/A* ratio is the major parameter controlling the compressive strength, modulus of elasticity, and water permeability of IPCs. *P/Agg* ratio also affects such properties of IPCs in the same direction of *S/A* ratio, however, with less influence. Higher *S/A* ratios and higher *P/Agg* ratios result in lower compressive strength and higher water permeability. P3–6 produces the highest compressive strength and also shows the best properties in modulus of elasticity and water permeability. At the same compressive strength, the water permeability coefficient of IPCs is much higher than that of conventional concrete. The differences in water permeability become smaller when the compressive strength is higher. In addition, the compressive strength has an influence on the modulus of elasticity of IPCs. The square root of compressive strength linearly affects the elastic modulus of IPCs the same as Portland cement concrete but the slope of the relation of IPCs is lower than that of conventional concrete by about three times.

Acknowledgements

We would like to thank the Office of the Higher Education Commission, Thailand and the Thailand Research Fund (TRF) for financial support under the Royal Golden Jubilee (RGJ) Ph.D. program Contract No. PHD/0161/2547 and TRF Senior Research Scholar Contract No. RTA5080020.

References

[1] Davidovits J. Geopolymers: inorganic polymeric new materials. J Therm Anal 1991;37:1633–56.
[2] Davidovits J. Mineral polymers and methods of making them. US patent no. 4349,386; 1982.
[3] MacKenzie KJD, Komphanchai S, Vagana R. Formation of inorganic polymers (geopolymers) from 2:1 layer lattice aluminosilicates. J Eur Ceram Soc 2008;28(1):177–81.
[4] Davidovits J. 30 Years of successes and failures in geopolymer applications. Market trends and potential breakthroughs. In: Geopolymer conference. Melbourne, Australia; 2002.
[5] Hanzlíček T, Steinerová M, Straka P, Perná I, Siegl P, Švarcová T. Reinforcement of the terracotta sculpture by geopolymer composite. Mater Des 2009;30(8):3229–34.
[6] Lee WKW, van Deventer JSJ. Chemical interactions between siliceous aggregates and low-Ca alkali-activated cements. Compos Concr Res 2007;27(6):844–55.
[7] MacKenzie KJD, O'Leary B. Inorganic polymers (geopolymers) containing acid–base indicators as possible colour-change humidity indicators. Mater Lett 2009;63(2):230–2.
[8] Mozgawa W, Deja J. Spectroscopic studies of alkaline activated slag geopolymers. J Mol Struct 2009;924–926:434–41.
[9] Sofi M, van Deventer JSJ, Mendis PA, Lukey GC. Engineering properties of inorganic polymer concrete (IPCs). Compos Concr Res 2007;37(2):251–7.
[10] Duxson P, Mallicoat SW, Lukey GC, Kriven WM, van Deventer JSJ. The effect of alkali and Si/Al ratio on the development of mechanical properties of metakaolin-based geopolymers. Colloids Surf A 2007;292(1):8–20.
[11] Lee WKW, van Deventer JSJ. The effects of inorganic salt contamination on the strength and durability of geopolymers. Colloids Surf A 2002;211(2–3):115–26.
[12] Yang KH, Song JK, Ashour AF, Lee ET. Properties of cementless mortars activated by sodium silicate. Constr Build Mater 2008;22(2):1981–9.
[13] Chindaprasirt P, Jaturapitakkul C, Chalee W, Rattanasak U. Comparative study on the characteristics of fly ash and bottom ash geopolymers. Waste Manag 2009;29(2):539–43.
[14] Duxson P, Provis JL, Lukey GC, Mallicoat SW, Kriven WM, van Deventer JSJ. Understanding the relationship between geopolymer composition, microstructure and mechanical properties. Colloids Surf A 2005;269(1–3):47–58.

[15] Andini S, Cioffi R, Colangelo F, Grieco T, Montagnaro F, Santoro L. Coal fly ash as raw material for the manufacture of geopolymer-based products. Waste Manag 2008;28(2):416–23.
[16] Kiattikomol K, Jaturapitakkul C, Songpiriyakij S, Chutubtim S. A study of ground coarse fly ashes with different finenesses from various sources as pozzolanic materials. Cem Concr Compos 2001;23(4–5):335–43.
[17] Cheerarot R, Jaturapitakkul C. A study of disposed fly ash from landfill to replace Portland cement. Waste Manag 2004;24(7):701–9.
[18] Jaturapitakkul C, Kiattikomol K, Sata V, Leekeeratikul T. Use of ground coarse fly ash as a replacement of condensed silica fume in producing high-strength concrete. Cem Concr Res 2004;34(4):549–55.
[19] Tangpagasit J, Cheerarot R, Jaturapitakkul C, Kiattikomol K. Packing effect and pozzolanic reaction of fly ash in mortar. Cem Concr Res 2005;35(6):1145–51.
[20] Sata V, Jaturapitakkul C, Kiattikomol K. Influence of pozzolan from various by-product materials on mechanical properties of high-strength concrete. Constr Build Mater 2007;21(7):1589–98.
[21] Tangchirapat W, Buranasing R, Jaturapitakkul C, Chindaprasirt P. Influence of rice husk – bark ash on mechanical properties of concrete containing high amount of recycled aggregates. Constr Build Mater 2008;22(8):1812–9.
[22] Pacheco-Togal F, Castro-Gomes J, Jalali S. Investigation about the effect of aggregates on strength and microstructure of geopolymeric mine waste mud binders. Cem Concr Res 2007;37(6):933–41.
[23] Sathonsaowaphak A, Chindaprasirt P, Pimraksa K. Workability and strength of lignite bottom ash geopolymer mortar. J Hazard Mater 2009;168(1):44–50.
[24] ACI Commitee 211.1-91. Standard practice for selecting proportions for normal, heavyweight, and mass concrete. ACI manual of concrete practice, Part 1. Michigan (USA): American Concrete Institute; 2000. p. 38.
[25] Chindaprasirt P, Jaturapitakkul C, Sinsiri T. Effect of fly ash fineness on compressive strength and pore size of blended cement paste. Cem Concr Compos 2005;27(4):425–8.
[26] van Jaarsveld JGS, van Deventer JSJ, Lukey GC. The characterisation of source materials in fly ash-based geopolymers. Mater Lett 2003;57(7):1272–80.
[27] Teixeira-Pinto A, Pacheco-Torgal F, Jalali S. Geopolymer manufacture and applications – main problems when using concrete technology. In: Geopolymer conference, Melbourne, Australia; 2002.
[28] Pacheco-Torgal F, Castro-Gomes JP, Jalali S. Studies about mix composition of alkali-activated mortars using waste mud from Panasqueira. In: Proceedings of the engineering conference, University of Beira Interior, Covilhã, Portugal; 2005.
[29] Chusilp N, Jaturapitakkul C, Kiattikomol K. Utilization of bagasse ash as a pozzolanic material in concrete. Constr Build Mater 2009;23(11):3352–8.
[30] Chindaprasirt P, Homwuttiwong S, Jaturapitakkul C. Strength and water permeability of concrete containing palm oil fuel ash and rice husk–bark ash. Constr Build Mater 2007;21(7):1492–9.
[31] Zuhua Z, Xiao Y, Huajun Z, Yue C. Role of water in the synthesis of calcined kaolin-based geopolymer. Appl Clay Sci 2009;43(2):218–23.
[32] De Silva P, Sagoe-Crenstil K, Sirivivatnanon V. Kinetics of geopolymerization: role of Al_2O_3 and SiO_2. Cem Concr Res 2007;37(4):512–8.
[33] Kolias S, Georgiou C. The effect of paste volume and of water content on the strength and water absorption of concrete. Cem Concr Com 2005;27(2):211–6.
[34] Yaşar E, Erdoğan Y, Kılıç A. Effect of limestone aggregate type and water–cement ratio on concrete strength. Mater Lett 2004;58(5):772–7.
[35] ACI Commitee 318-08. Building Code Requirements for Structural Concrete (ACI 318-08) and Commentary. An ACI Standard. Michigan (USA): American Concrete Institute; 2008. p. 465.
[36] Hearn N. Saturated permeability of concrete as influenced by cracking and self-sealing. PhD thesis. University of Cambridge, Cambridge, UK; 1993.

14. Vanchai Sata, Chai Jaturapitakkul, Chaiyanunt Rattanashotinunt. Compressive Strength and heat evolution of concrete containing palm oil fuel ash, Journal of Materials in Civil Engineering ASCE. (accepted) (IF 0.526).

Journal of Materials in Civil Engineering. Submitted May 21, 2009; accepted March 17, 2010; posted ahead of print March 22, 2010. doi:10.1061/(ASCE)MT.1943-5533.0000104

Compressive Strength and Heat Evolution of Concretes Containing Palm Oil Fuel Ash

Vanchai Sata [1]; Chai Jaturapitakkul [2]; and Chaiyanunt Rattanashotinunt [3]

Abstract

The study of using palm oil fuel ash (POFA) in concrete work is just a beginning and obtained data are very little as compared to fly ash and silica fume. In order to collect experimental data, the effects of ground palm oil fuel ash (GPOFA) replacement rates up to 30%wt and Water/Binder (W/B) ratios of 0.50, 0.55, and 0.60 on normal concrete properties were studied. GPOFA with high fineness was found to be a possible pozzolanic material in concrete. Cement replacement of GPOFA at rates of 10 and 20% yielded higher compressive strength than that of control concrete after 28 days of curing. In addition, heat evolution in term of temperature rise of fresh concrete decreased with an increased of GPOFA replacement. For concrete with a W/B ratio of 0.50, the use of 30% GPOFA as a cement replacement exhibited the lowest peak temperature rise. However, a decrease compressive strength at early age might be considered if a high replacement rate of GPOFA was used.

Keywords: Palm oil fuel ash; Pozzolan; Biomass ash; Concrete; Heat evolution; Thailand

---

[1]Corresponding author, Lecturer, Dept. of Civil Engineering, Khon Kaen University (KKU), Khon Kaen 40002, Thailand. E-mail: vancsa@kku.ac.th

[2]Professor, Dept. of Civil Engineering, King Mongkut's University of Technology Thonburi (KMUTT), Bangkok 10140, Thailand. E-mail: chai.jat@kmutt.ac.th

[3]Ph.D. Student, Dept. of Civil Engineering, King Mongkut's University of Technology Thonburi (KMUTT), Bangkok 10140, Thailand. E-mail: mengt_t@hotmail.com

Journal of Materials in Civil Engineering. Submitted May 21, 2009; accepted March 17, 2010;
posted ahead of print March 22, 2010. doi:10.1061/(ASCE)MT.1943-5533.0000104

Introduction

It is known that there are several causes for global warming including CO_2 from cement. Approximately 5% of total CO_2 emission is released to atmosphere, with about 0.7-1.1 ton of CO_2 being emitted for every ton of cement production. Carbon dioxide emission by cement industry 50% result from the calcination of limestone, 40% from combustion of fuel in the kiln, and 10% from transportation and manufacturing operations (Bosaoga et al. 2009). In order to reduce the amount of CO_2 emission, cement manufactures can help by improving production process. For concrete production, the reducing cement content in concrete by utilization of supplementary cementitious materials such as fly ash, blast-furnace slag, silica fume, metakaolin, natural pozzolans, and biomass ash to replace cement is one of the solutions.

Palm oil is extracted from the fruit and copra of the palm oil tree. After the extraction process, waste products such as palm oil fibers, shells, and empty fruit brunches are burnt as biomass fuel to boil water, which generates steam for electricity and the extraction process in palm oil mills. The result is palm oil fuel ash (POFA), which is about 5%, by weight, of solid waste product. In Thailand, a total of 5.4 million tons of fresh fruit brunches was produced in 2005, resulting in high amount of solids waste and biomass ash, which tends to increase every year (Rangsan and Titida 2007). This biomass ash is not utilized, and most of it has to be deposited in landfills, creating environmental problems. However, many researchers (Tay 1990, Hussin and Awal 1996, Awal and Hussin 1997, Sukuntapree et al. 2000, and Sata et al. 2004) have found that POFA can be used in the construction industry, specifically as a supplementary cementitious material in concrete. In 1990, Tay (1990) investigated the use of ash derived from oil-palm waste incineration in making blended cement; the results showed that replacing 10-50% ash by weight of cementitious material in blended cement had no significant effect on segregation, shrinkage, water absorption, density, or soundness of concrete. Within the 20-50% replacement rate range, the decrease in the compressive strength of concrete at various ages was almost proportional to the amount of ash in the blended cement, with the exception of 10% replacement. A few years later, Hussin and Awal (1996) studied the compressive strength of concrete containing POFA. The results revealed that it was possible to replace at a level of 40% palm oil fuel ash without affecting compressive strength. The maximum compressive strength gain occurred at a replacement level of 30% by weight of binder. In addition, Awal and Hussin (1997) revealed that POFA has good potential for suppressing expansion due to alkali-silica reactions.

In Thailand, Sukantapree et al. (2002) revealed that the compressive strength of mortar containing

Journal of Materials in Civil Engineering. Submitted May 21, 2009; accepted March 17, 2010;
posted ahead of print March 22, 2010. doi:10.1061/(ASCE)MT.1943-5533.0000104

original POFA was low due to the large particle size and high porosity of palm oil fuel ash. However, mortar containing ground palm oil fuel ash with particles retained on a 45-μm sieve (No. 325) of 4.3% gave a compressive strength higher than 100% of control mortar at the curing ages of 7 and 28 days. Furthermore, a previous investigation (Sata et al. 2004) indicated that POFA with high fineness has a highly pozzolanic reaction and can be used as a supplementary cementitious material for producing high strength concrete.

However, study of POFA is just beginning, and the obtained data are scarce compared to studies of fly ash and silica fume. In order to obtain experimental data for publication and utilize of POFA effectively which lead to reduce cement consumption and environmental problems, concretes containing POFA are studied. The aim of this research is to study the compressive strength of concrete containing GPOFA at various replacement levels (0, 10, 20, and 30%) and different W/B ratios (0.50, 0.55, and 0.60). It is well established that the use of Portland cement in concrete releases a lot of heat during the hydration process. Under controlled condition, this spontaneous heating can be beneficial; with, for example, concrete in cold weather areas. On the other hand, heating may cause cracking from temperature differences and lead to a reduction in the quality and durability of concrete (Hansen and Jensen 1998, and Schutter 1999). Therefore, the evolution of heat in term of temperature rise of fresh concrete containing GPOFA was investigated in concrete mixtures with a W/B ratio of 0.50.

Experimental programs

Materials

The materials used in this study consisted of Type I Portland cement, palm oil fuel ash from the southern part of Thailand, coarse and fine aggregates, type F superplasticizer, and tap water.

Cement

Type I Portland cement was used in this study. The physical properties and chemical composition are summarized in Tables 1 and 2, respectively. The major oxides of Type I Portland cement were CaO (65.4%), SiO_2 (20.9%), Al_2O_3 (4.8%), and Fe_2O_3 (3.4%). SO_3 and LOI were 2.7%, and 1.0%, respectively. The specific gravity of cement was 3.15, with a mean particle size (d_{50}) of 14.7 μm.

Journal of Materials in Civil Engineering. Submitted May 21, 2009; accepted March 17, 2010;
posted ahead of print March 22, 2010. doi:10.1061/(ASCE)MT.1943-5533.0000104

Palm oil fuel ash (POFA)

The original POFA was collected from a mill in Surathanee province in the southern part of Thailand. Original POFA was not suitable for use as a pozzolanic material in concrete due to large particle size and high porosity (Sukantapree et al. 2002, and Tangchirapat et al. 2006). In addition, Vazquez et al. (2004) and Cordeiro et al. (2008) also showed that pozzolanic activity and the filler effect of industrial ash depends on its particle size and fineness; thus, original POFA was ground by ball mill to a required level of fineness until the retained particles on a No. 325 sieve were less than 2% by weight and respected as ground palm oil fuel ash (GPOFA). Particle size distribution of GPOFA is shown in Fig. 1, and particle shape, ascertained by Scanning Electron Microscopy (SEM), is presented in Fig. 2. As presented in Table 1, the mean particle size (d_{50}) of GPOFA is 9.2 μm, which is less than that of Type I Portland cement (14.7 μm). The specific gravity of GPOFA is 2.50, and the amount retained on a No. 325 sieve for GPOFA is 1.2% (less than 2.0%).

Chemical compositions analyzed by X-ray fluorescence spectrometer (XRF) of Type I Portland cement and GPOFA are shown in Table 2. GPOFA is found to have SiO_2, Al_2O_3, Fe_2O_3, CaO, SO_3, and LOI compositions of 42.5 %, 0.9%, 2.4%, 11.0%, 2.2%, and 20.9%, respectively. The high value of LOI in GPOFA is due to the burning condition (fluidized bed combustion), under which the burning temperature is about 800-900°C. Abdullah et al. (2006) found that the chemical composition of POFA consists of SiO_2, Al_2O_3, Fe_2O_3, CaO, SO_3, and LOI at levels of 52.2%, 4.5%, 5.4%, 4.1%, 2.2%, and 13.9%, respectively; they concluded that differences in the operating systems of the palm oil mills are the major cause of differences in the chemical composition of POFA.

Aggregates

The coarse aggregate used in this study was crushed limestone with a maximum size of 20 mm, specific gravity of 2.7, fineness modulus of 7.3, and water absorption of 0.5%. The fine aggregate was local river sand, with a fineness modulus of 2.6, specific gravity of 2.6, and water absorption of 1.0%.

Mixture proportions and testing

Based on the high water requirement of POFA concrete (Sukantapree et al. 2002), mixture proportions were approximated, followed by modification of trial mixes to obtain homogeneous and workable fresh concrete. All concretes had the same binder content of 350 kg/m^3; the ratio of fine-to-coarse aggregate was kept constant at

Journal of Materials in Civil Engineering. Submitted May 21, 2009; accepted March 17, 2010;
posted ahead of print March 22, 2010. doi:10.1061/(ASCE)MT.1943-5533.0000104

45:55 by volume, and a superplasticizer was employed in order to maintain the slump of fresh concrete between 50 and 100 mm. The W/B ratios of the concrete were varied as 0.50, 0.55, and 0.60.

CT0.50, CT0.55, and CT0.60 were control concretes in which Type I Portland cement was used as a binder with W/B ratios of 0.50, 0.55, and 0.60, respectively. For all W/B ratios, Type I Portland cement was replaced by GPOFA at rates of 10, 20, and 30% by weight of binder. Concrete mixture proportions are summarized in Table 3. For example, GPOFA-0.55-30 concrete indicates that the concrete has a W/B ratio of 0.55, and the Type I Portland cement is replaced by GPOFA at the rate of 30% by weight of binder.

The fresh concretes were prepared using a rotating drum mixer. The cylindrical concrete specimens with 100 mm in diameter and 200 mm in height were cast and covered with a plastic sheet to prevent excessive evaporation of water from the fresh concrete. After casting for 24 h, the concrete samples were removed from the moulds and transferred into a room temperature water tank until testing. The compressive strengths of concretes were determined at 3, 7, 14, 28, 60, and 90 days according to ASTM C39 (2001).

In addition, the concretes with a W/B ratio of 0.50 were selected for testing the heat evolution of fresh concrete in term of temperature rise under semi-adiabatic conditions. Four mixtures of fresh concrete (CT0.50, GPOFA-0.50-10, GPOFA-0.50-20, and GPOFA-0.50-30) were placed in a 450-mm cube with a lining insulator of 50 mm on each side (concrete specimen of 350x350x350 mm^3). A thermocouple was embedded in the center of the specimen. The temperature rise was measured immediately after casting for a period of 168 hours. Figure 3 shows the testing for heat evolution in term of temperature rise of fresh concrete.

Results and discussion

Compressive strength

The compressive strengths of concretes in this study were the average values of three specimens and the relationships between the compressive strength of control concretes and the curing ages are shown in Fig. 4. For all W/B ratios, the compressive strength of control concretes increased with curing age. At 28 days, the compressive strengths of CT0.50, CT0.55, and CT0.60 concretes were 39.6, 36.5, and 32.0 MPa, respectively; they increased to 49.4, 43.4, and 38.1 MPa, respectively, at 90 days. The compressive strength was also found to decrease as the W/B ratio of concrete increased according to Abrams's Law (Abrams 1918).

Fig. 5 shows the relationship between the compressive strength of GPOFA concretes at a W/B ratio of 0.50 and replacement of GPOFA. At early ages, the strength development of concretes containing GPOFA as a

Journal of Materials in Civil Engineering. Submitted May 21, 2009; accepted March 17, 2010;
posted ahead of print March 22, 2010. doi:10.1061/(ASCE)MT.1943-5533.0000104

cement replacement of 10, 20, and 30% was lower than that of CT concrete. At 3 days, the compressive strengths of GPOFA-0.50-10, GPOFA-0.50-20 and GPOFA-0.50-30 concretes were 29.3, 28.6, and 26.5 MPa, or about 95, 93, and 86% of CT concrete, respectively. The compressive strength of GPOFA concretes, which was over 75% of that of CT concrete, at early ages may be due to the packing effect of the small particle of GPOFA (Tangpagasit et al. 2005). Afterward, the compressive strength tended to increase with curing age. The compressive strengths of GPOFA-0.50-10, GPOFA-0.50-20, and GPOFA-0.50-30 concretes at 28 days were 39.6, 40.0, and 36.8 MPa, or about 101, 100, and 93% of CT0.50 concrete, respectively. This can be explained by the very high fineness of the particles and the silicon dioxide (SiO_2) content in GPOFA, which reacts with calcium hydroxide ($Ca(OH)_2$) to produce an addition calcium silicate hydrated (C-S-H). These characteristics tend to improve the compressive strength of concrete at later ages. This result agrees with Chindaprasirt et al. (2004), who found that the high fineness of fly ash was a major factor affecting the compressive strength and improved sulfate resistance of blended cement mortar. In addition, Saccani et al. (2005) studied the pozzolanic property of municipal solid waste incineration bottom ashes (MSWI BA) and found that with sufficiently long curing times, the modified mortar containing up to 30% by weight of ground MSWI BA exhibited higher mechanical strength and lower porosity than unmodified mortar.

After 28 days of curing, 10 and 20% GPOFA cement replacement resulted in higher compressive strength than CT0.50 concrete; the replacement rate of 10% produced the highest compressive strength. With replacement of GPOFA at 30% by weight of binder, concrete exhibited compressive strength lower than the control concrete at all testing ages. For example, the compressive strength of GPOFA-0.50-30 concrete at 90 days was 46.2 MPa, or about 94% of CT0.50 concrete. This is due in part to the low Type I Portland cement content (70%) in 30% GPOFA replacement, which induces lower $Ca(OH)_2$ from hydration reactions than 10 and 20% GPOFA replacement.

The relationship between compressive strength of GPOFA concretes at a W/B ratio of 0.55 and GPOFA replacement level is shown in Fig. 6. At 3 and 7 days, GPOFA-0.55-10, GPOFA-0.55-20, and GPOFA-0.55-30 concretes had compressive strengths lower than CT0.55 concrete. At later ages, GPOFA-0.55-10 and GPOFA-0.55-20 had compressive strengths higher than CT0.55 concrete. For example, the compressive strengths of GPOFA-0.55-10 and GPOFA-0.55-20 concretes at 28 days were 37.6 and 36.9 MPa, or about 103 and 101% of CT0.55 concrete (36.5 MPa), respectively. At 30% GPOFA cement replacement with a W/B ratio of 0.55, the concrete exhibited lower compressive strength than that of CT0.55 concrete at all ages.

Fig. 7 shows the strength development and effect of GPOFA replacement on compressive strength of

Journal of Materials in Civil Engineering. Submitted May 21, 2009; accepted March 17, 2010;
posted ahead of print March 22, 2010. doi:10.1061/(ASCE)MT.1943-5533.0000104

concretes with a W/B ratio of 0.60. The results tended to be in the same direction as concretes with W/B ratios of 0.50 and 0.55. The compressive strength testing results of GPOFA concretes at W/B ratios of 0.50, 0.55 and 0.60 indicate that ground palm oil fuel ash with high fineness is a reactive pozzolanic material that can be used in making concrete with compressive strength on the order of 87-105% of the control concrete. A replacement rate of 10% resulted in the optimum compressive strength and yielded higher strength than all CT concretes after 14 days of curing.

Heat Evolution

The results of each concrete mix proportion of heat evolution in term of temperature rise of fresh concrete are shown in Table 4. Control concrete (CT0.50) was observed to reach a peak temperature rise of 30.3°C about 12 h after casting. Concrete containing a high fineness of palm oil fuel ash 10% (GPOFA-0.50-10) had a peak temperature rise of 30.0°C at 14 h after casting. This temperature increase was close to that of CT0.50 concrete (as seen in Fig. 8) and was due to the high Portland cement content of GPOFA-0.50-10 concrete (90%). The peak temperature rises of GPOFA-0.50-20 and GPOFA-0.50-30 concretes were 27.3 and 24.3°C, respectively, lower than those of CT0.50 and GPOFA-0.50-10 concretes. GPOFA-0.50-20 and GPOFA-0.50-30 concretes showed reductions in temperature of 3.0 and 6.0°C, or about 90.1 and 80.2% of CT0.50 concrete, respectively. The reduced temperature rise of fresh concretes containing 20 and 30% GPOFA is due to the high replacement of cement by GPOFA, which reduces the amount of cement in concrete, causing a reduction of heat due to the hydration process (Rojas et al. 1993). In addition, the decrease of cement in concrete resulted in a prolonging of the time to peak temperature. The peak temperature rises for GPOFA-0.50-20 and GPOFA-0.50-30 concretes occurred about 15 and 16 hours after casting, respectively. In the above results, the temperature rise of fresh concrete was found to decrease as GPOFA content increased; the use of 30% GPOFA as a cement replacement yielded the lowest peak temperature rise.

Table 5 shows the compressive strength, normalized compressive strength, and peak temperature rise of GPOFA concretes with a W/B ratio of 0.50. At 3 days, control concrete was found to have the highest compressive strength. However, at 90 days, GPOFA-0.50-10 concrete exhibited the highest normalized compressive strength at 102% of CT0.50 concrete and the peak temperature rise of fresh concrete was 30.0°C. High rate cement replacement by GPOFA in concrete decreased compressive strength at early ages. However, long-term strength tended to increase with curing age. For example, the normalized compressive strength of

Journal of Materials in Civil Engineering. Submitted May 21, 2009; accepted March 17, 2010; posted ahead of print March 22, 2010. doi:10.1061/(ASCE)MT.1943-5533.0000104

GPOFA-0.50-30 concrete at 3 days was 86%; this increased to 94% at 90 days. In addition, increase in replacement of GPOFA in concrete mixture can reduce the temperature rise of fresh concrete. For this study, the lowest peak temperature rise, 24.3°C, was observed in GPOFA-0.50-30 concrete.

Conclusions

The following conclusions can be drawn from the use of 10-30% of ground palm oil fuel ash with high fineness in concrete:

1. The strength development of GPOFA concretes with W/B ratios of 0.50, 0.55, and 0.60 tended to be in the same direction. At early ages, concretes containing GPOFA as a cement replacement of 10, 20, and 30% had lower strength development than control concretes while at later age (>28 days), the replacement at rates of 10 and 20% yielded higher strength development.
2. Ground palm oil fuel ash with high fineness can be used as a pozzolanic material in concrete. A replacement of GPOFA at rate of 10% resulted in the optimum compressive strength and yielded higher strength than control concrete after 14 days of curing.
3. The temperature rise of fresh concrete decreased as GPOFA content increased. For concrete with a W/B ratio of 0.50, the use of 30% GPOFA as a cement replacement had the lowest peak temperature rise. However, the decrease in compressive strength at early age due to high replacement GPOFA (30%) should be considered.

Acknowledgements

The authors gratefully acknowledge the financial supports from the Thailand Research Fund (TRF) under TRF Senior Research Scholar Contact No. RTA5080020 and the Commission on Higher Education, Ministry of Education, Thailand.

Journal of Materials in Civil Engineering. Submitted May 21, 2009; accepted March 17, 2010; posted ahead of print March 22, 2010. doi:10.1061/(ASCE)MT.1943-5533.0000104

References

Abdullah, K., Hussin, M. W., Zakaria, F., Muhamud, R., and Hamid, Z. A. (2006) "POFA : A potential partial cement replacement material in aerated concrete." *Proceedings of the 6th Asia-Pacific Structural Engineering and Construction Conference, Kuala Lumpur, Malaysia.*, 132-140.

Abrams, A. D. (1918). "Design of concrete mixtures." *Structure Materials Research Laboratory*, Bulletin 1, Levis Institute, Chicaco.

ASTM. (2001). "Standard test method for compressive strength of cylindrical concrete specimens." C39, *Annual Book of ASTM Standards*, West Conshohocken, Pa.

Awal, A. S. M. A., and Hussin, M. W. (1997). "The effectiveness of palm oil fuel ash in preventing expansion due to alkali-silica reaction." *Cem. Concr. Compos.*, 19, 367-372.

Bosoaga, A., Masek, O., and Oakey, J. E. (2009). "CO_2 capture technologies for cement industry." Energy Procedia., 1, 133-40.

Chindraprasirt, P., Homwuttiwong, S., and Sirivivatnanon, V. (2004). "Influence of fly ash fineness on strength, drying shrinkage and sulfate resistance of blended cement mortar." *Cem. Concr. Res.*, 34, 1087-1092.

Cordeiro, G. C., Filho, R. D. T., Tavares, L. M., and Fairbairn, E. M. R. (2008). "Pozzolanic activity and filler effect of sugar cane bagasse ash in Portland cement and lime mortar." *Cem. Concr Compos.*, 30, 410-418.

Hansen, P. F., and Jensen, O. P. (1998). "A sample holder for the study of isothermal heat of Hydration of cement." *Mater. Struct.*, 31, 133-136.

Hussin, M. W., and Awal A. S. M. A. (1996). "Palm oil fuel ash-a potential pozzolanic material in concrete construction." *Proceedings International Conference on Urban Engineering in Asia Cities in the 21st Century, Bangkok, Thailand.*, D361-366.

Rangsan, N., and Titida N. (2007). "Price transmission in Thai palm oil industry." *International Business Academics Consortium 2007,* 2007bai7336.pdf.

Rojas, M. I. S. D., Luxan, M. P., Frias, M., and Garcia, N. (1993). "The influence of difference additions on portland cement hydration heat." *Cem. Concr. Res.*, 23, 46-54.

Saccani, A., Sandrolini, F., Andreola, F., Barbieri, L., Corradi, A., and Lancellotti, I. (2005). "Influence of the pozzolanic fraction obtained from vitrified bottom-ashes from MSWI on properties of cementitious composites." *Mater. Struct.*, 38, 367-371.

Journal of Materials in Civil Engineering. Submitted May 21, 2009; accepted March 17, 2010;
posted ahead of print March 22, 2010. doi:10.1061/(ASCE)MT.1943-5533.0000104

Sata, V., Jaturapitakkul, C., and Kiattikomol, K. (2004). "Utilization of palm oil fuel ash in high-strength concrete." *J. Mater. Civ. Eng.*, 16, 623-628.

Schutter, G. D. (1999). "Hydration and temperature development of concrete made with blast-furnace slag cement" *Cem. Concr. Res.*, 29, 143-149.

Sukantapree, S., Namarak, C., and Jaturapitakkul, C. (2002). "Use of calcium carbide residue and palm oil fuel ash in concrete." *Proceedings of the 2002 Annual Conference of the Engineering, Bangkok Thailand, 2002.*, 191-199. (in Thai)

Tangchirapat, W., Seating, T., Jaturapitakkul, C., Kiattikomol, K., and Siripanichagorn, A. (2006). "Use of waste ash from palm oil industry in concrete." *Waste Management.*, 27, 81-88.

Tangpagasit, J., Cheerarot, R., Jaturapitakkul, C., and Kiattikomol, K. (2005). "Packing effect and pozzolanic reaction of fly ash in mortar." *Cem. Concr. Res.*, 35, 1145-1151.

Tay, J. K. (1990) "Ash from oil-palm waste as a concrete material." *J. Mat. Civ. Eng.*, 2(2), 94-105.

Vazquez, E., Hendriks, C. F., and Janssen, G. M. T. (2004). "Influence of mechanical grinding on the pozzolanic activity of residual sugarcane bagasse ash." *International RILEM Conference on the Use of Recycled Materials in Building and Structures.*, 731-740.

Figure Caption List

Journal of Materials in Civil Engineering. Submitted May 21, 2009; accepted March 17, 2010;
posted ahead of print March 22, 2010. doi:10.1061/(ASCE)MT.1943-5533.0000104

Fig. 1. Particle size distribution of cement and ground palm oil fuel ash (GPOFA)

2(a) Type I Portland cement 2(b) Ground palm oil fuel ash (GPOFA)

Fig. 2. Scanning electron microscopy of materials

Fig. 3. Testing of heat evolution in term of temperature rise of fresh concrete

Fig. 4. Relationship between compressive strength of control concretes and curing age

Fig. 5. Comparison of compressive strength of concretes mixed with ground palm oil fuel ash (W/B = 0.50)

Fig. 6. Comparison of compressive strength of concretes mixed with ground palm oil fuel ash (W/B = 0.55)

Fig. 7. Comparison of compressive strength of concretes mixed with ground palm oil fuel ash (W/B = 0.60)

Fig. 8. Temperature rise of fresh concretes containing GPOFA

Figure 1

Journal of Materials in Civil Engineering. Submitted May 21, 2009; accepted March 17, 2010;
posted ahead of print March 22, 2010. doi:10.1061/(ASCE)MT.1943-5533.0000104

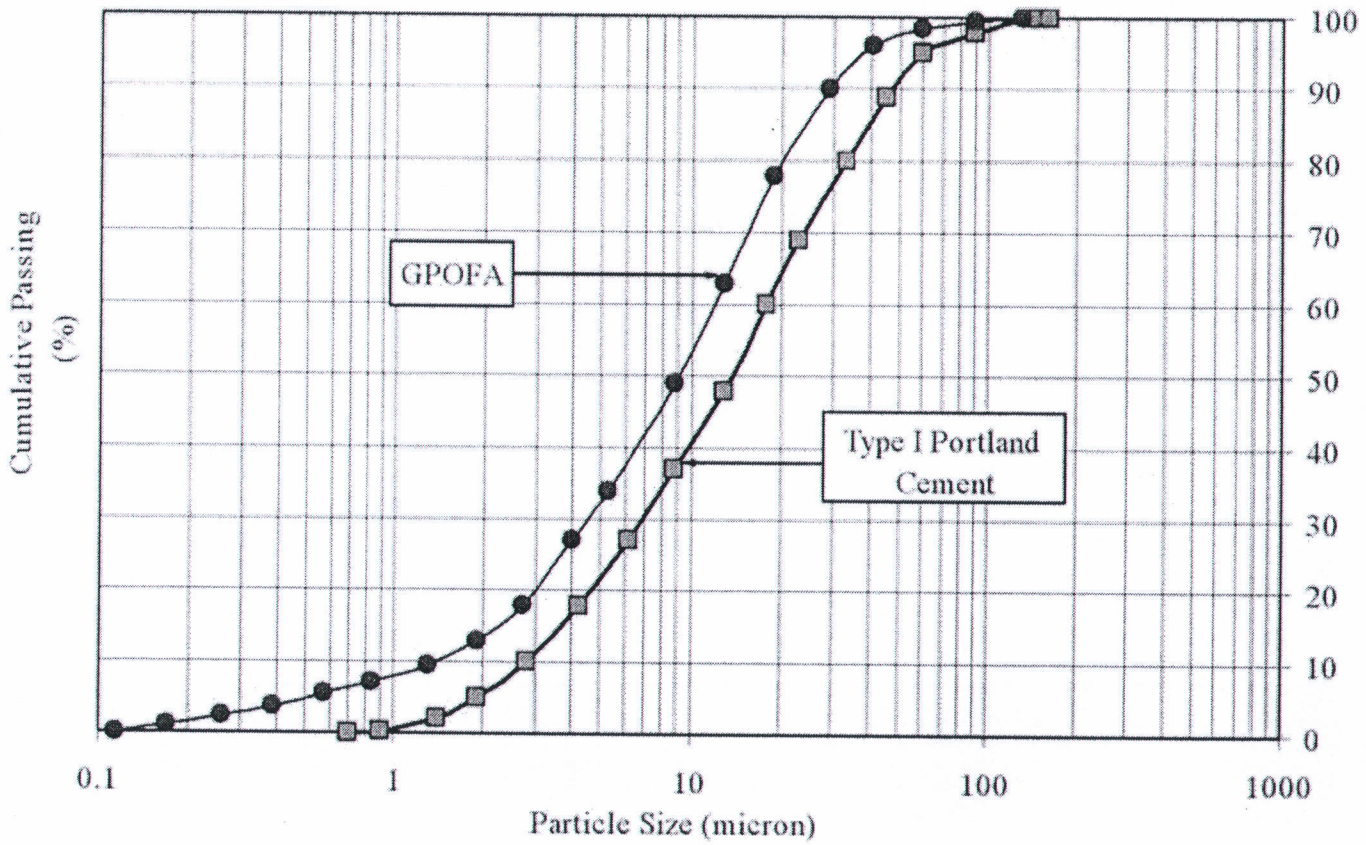

Figure 2(a)

Journal of Materials in Civil Engineering. Submitted May 21, 2009; accepted March 17, 2010;
posted ahead of print March 22, 2010. doi:10.1061/(ASCE)MT.1943-5533.0000104

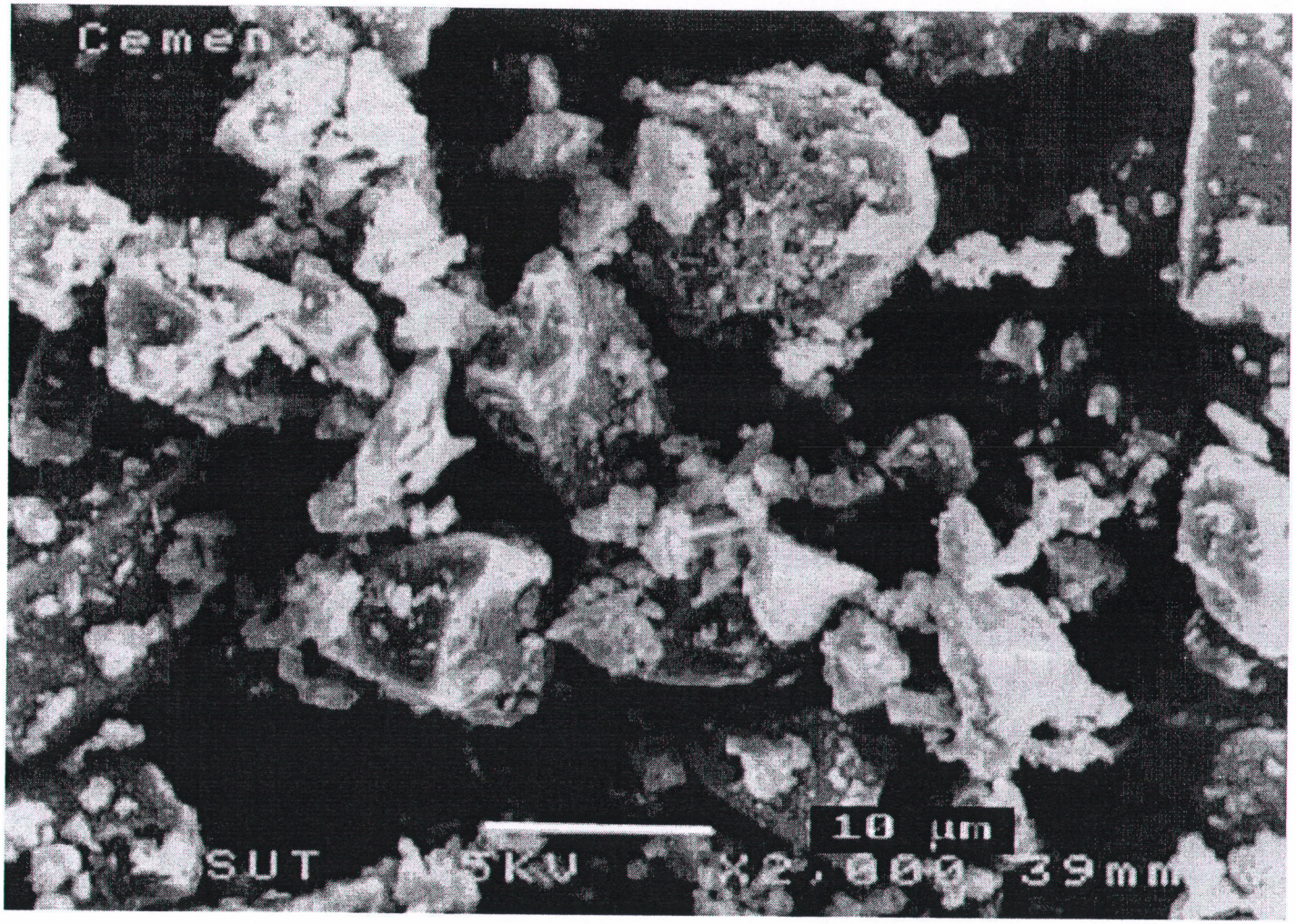

Figure 2(b)

Journal of Materials in Civil Engineering. Submitted May 21, 2009; accepted March 17, 2010;
posted ahead of print March 22, 2010. doi:10.1061/(ASCE)MT.1943-5533.0000104

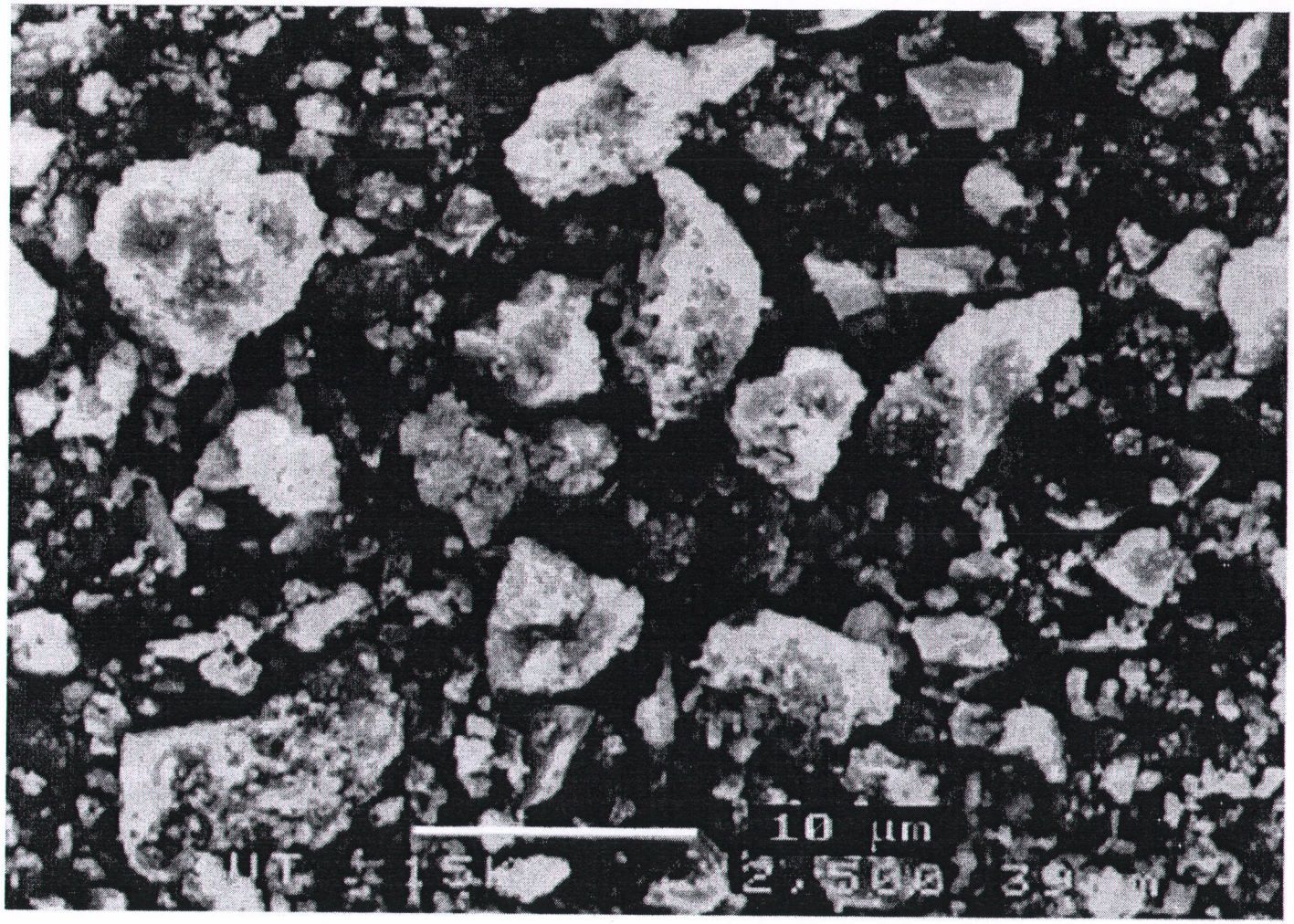

Figure 3

Journal of Materials in Civil Engineering. Submitted May 21, 2009; accepted March 17, 2010;
posted ahead of print March 22, 2010. doi:10.1061/(ASCE)MT.1943-5533.0000104

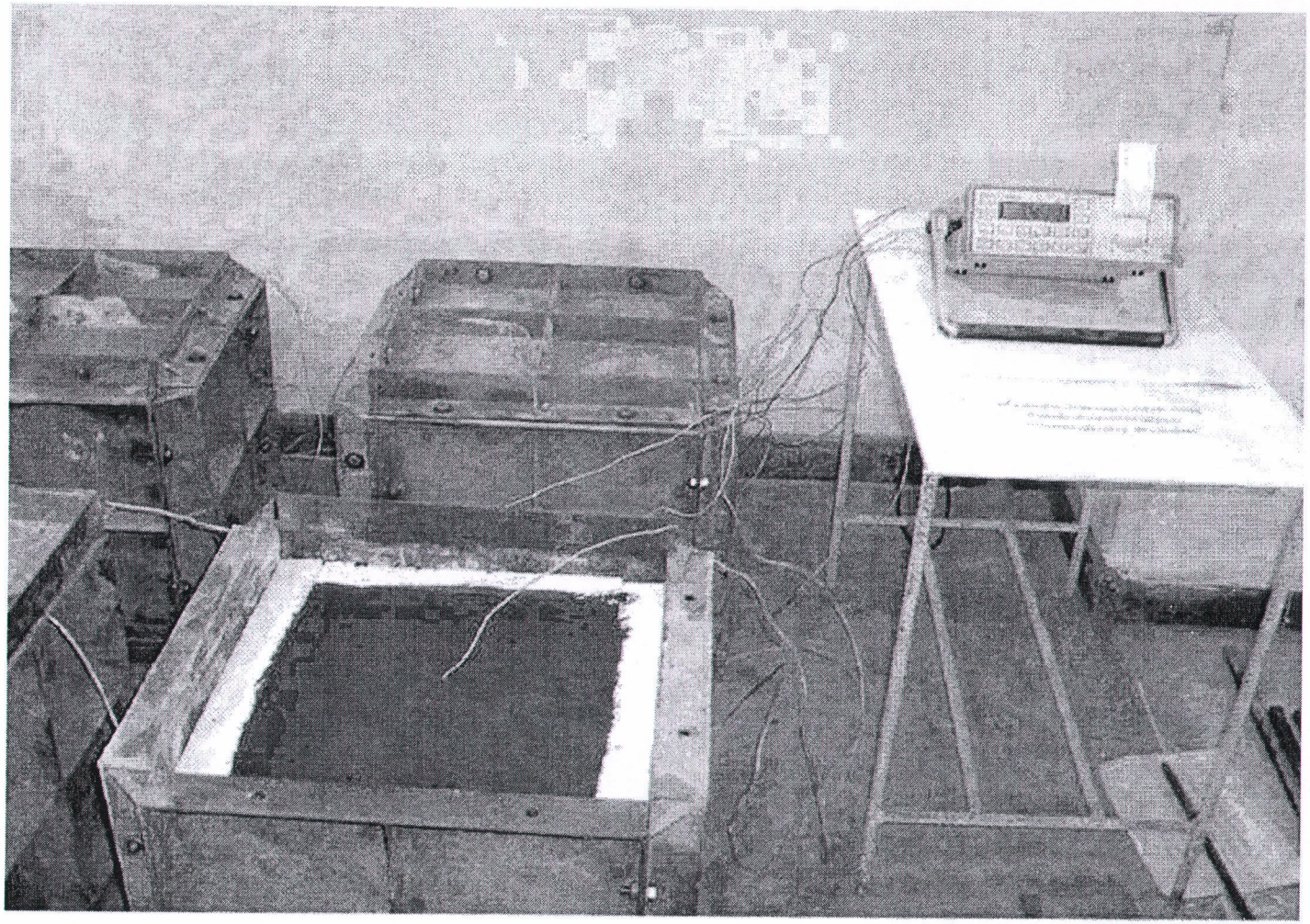

Figure 4

Journal of Materials in Civil Engineering. Submitted May 21, 2009; accepted March 17, 2010;
posted ahead of print March 22, 2010. doi:10.1061/(ASCE)MT.1943-5533.0000104

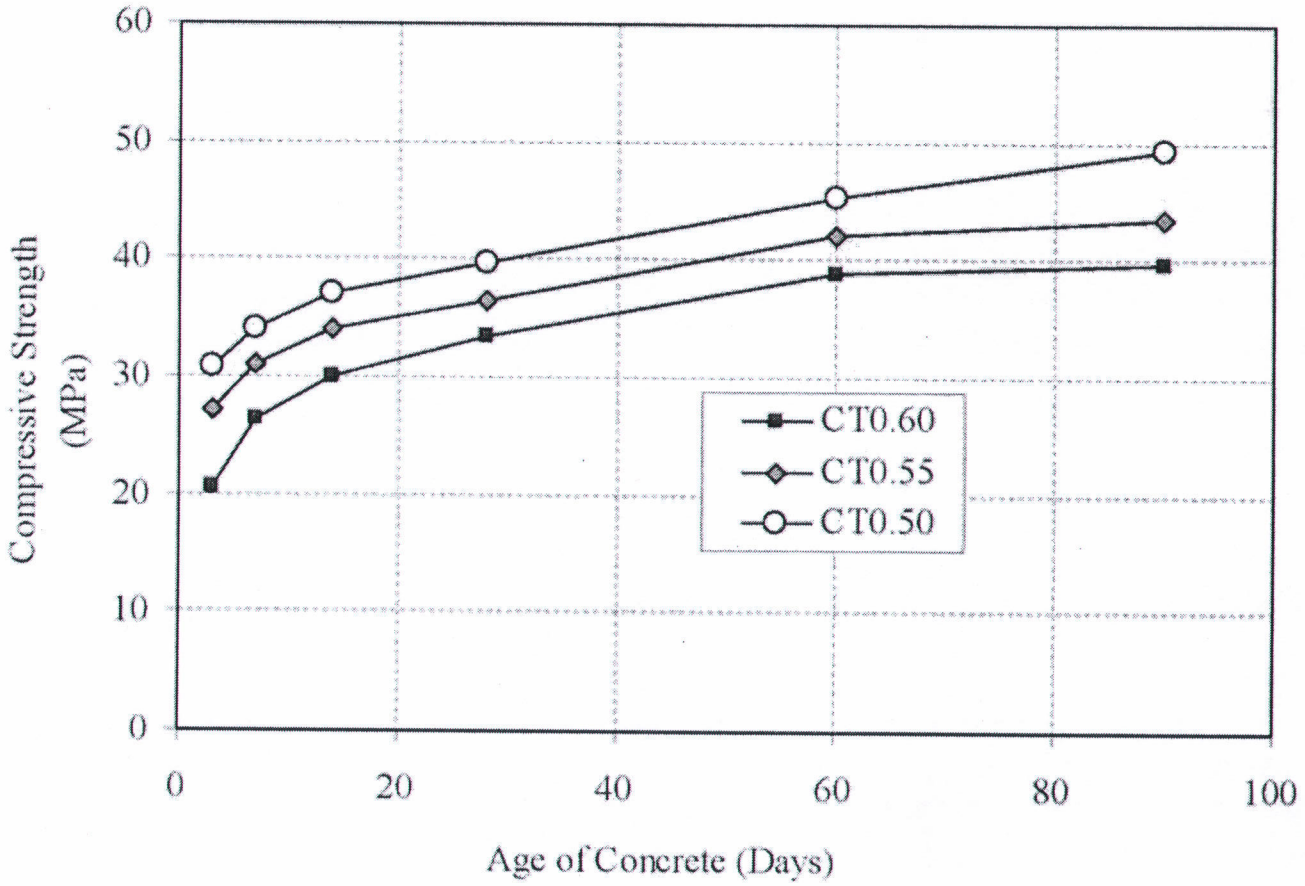

Figure 5

Journal of Materials in Civil Engineering. Submitted May 21, 2009; accepted March 17, 2010;
posted ahead of print March 22, 2010. doi:10.1061/(ASCE)MT.1943-5533.0000104

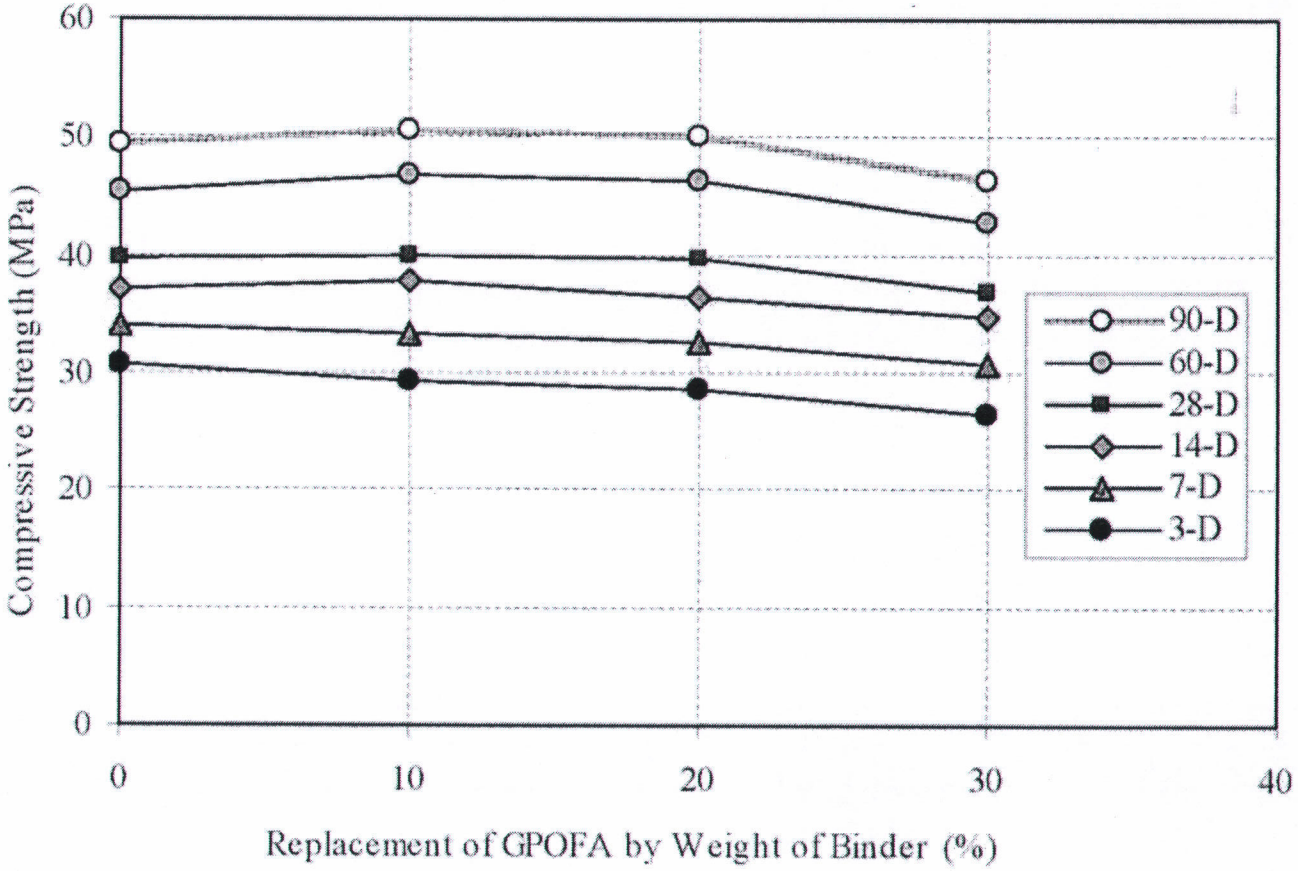

Figure 6

Journal of Materials in Civil Engineering. Submitted May 21, 2009; accepted March 17, 2010;
posted ahead of print March 22, 2010. doi:10.1061/(ASCE)MT.1943-5533.0000104

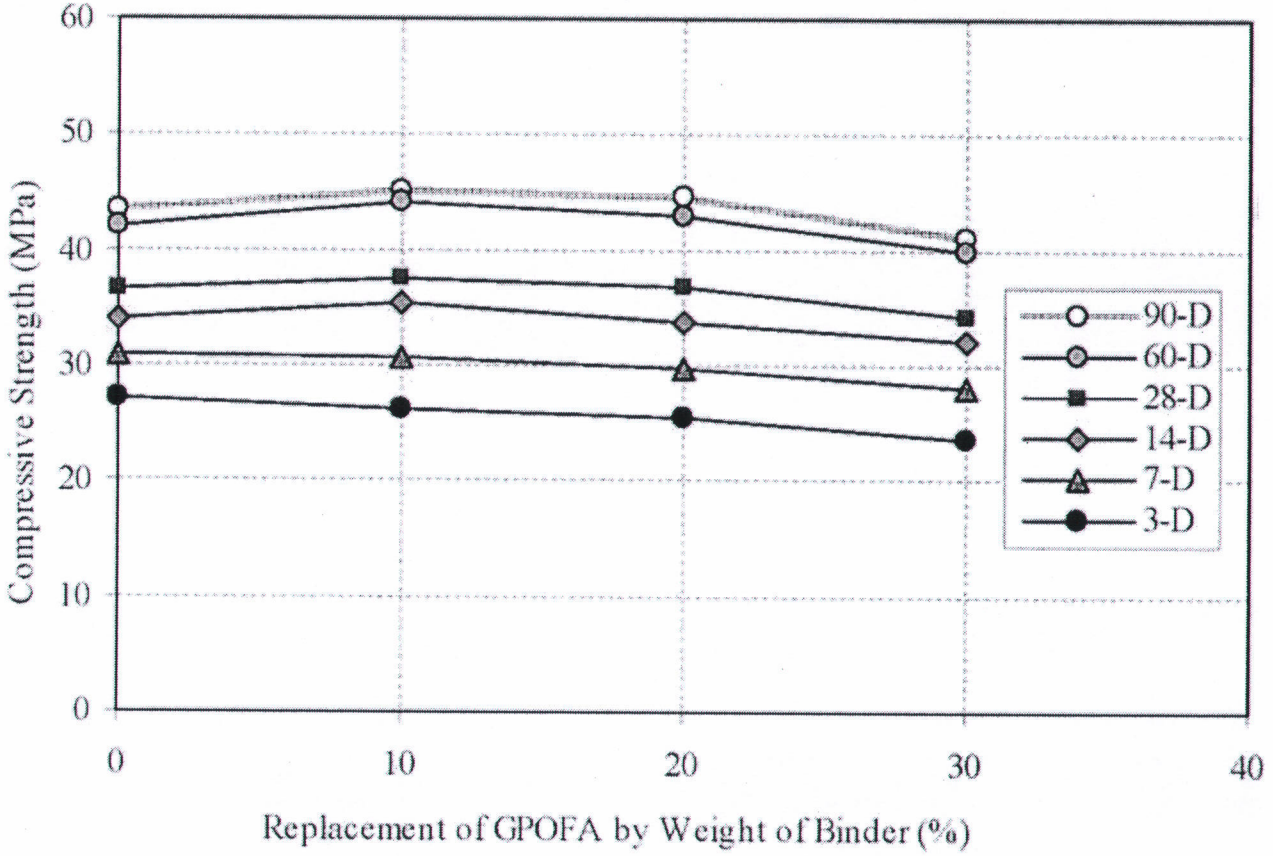

Figure 7

Journal of Materials in Civil Engineering. Submitted May 21, 2009; accepted March 17, 2010;
posted ahead of print March 22, 2010. doi:10.1061/(ASCE)MT.1943-5533.0000104

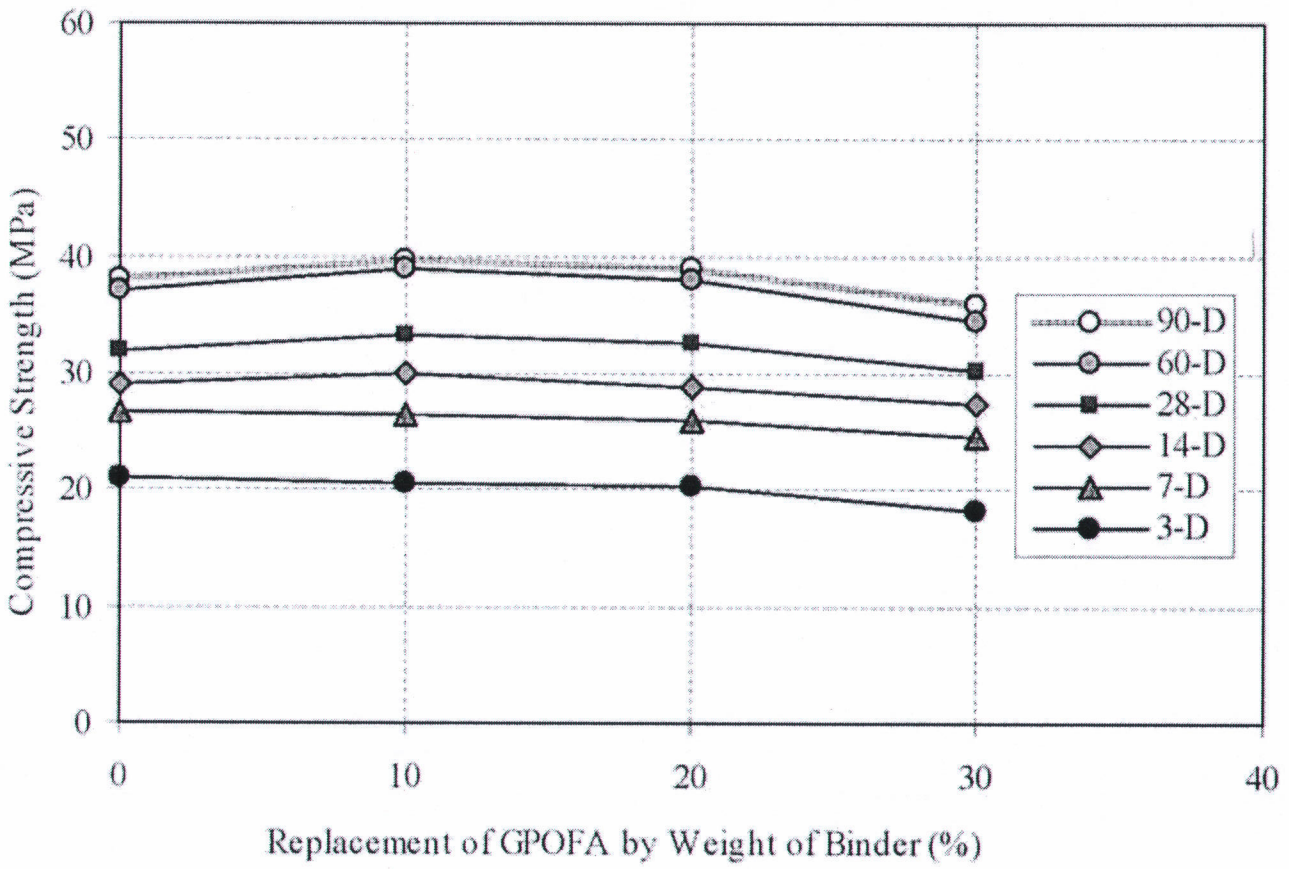

Figure 8

Journal of Materials in Civil Engineering. Submitted May 21, 2009; accepted March 17, 2010;
posted ahead of print March 22, 2010. doi:10.1061/(ASCE)MT.1943-5533.0000104

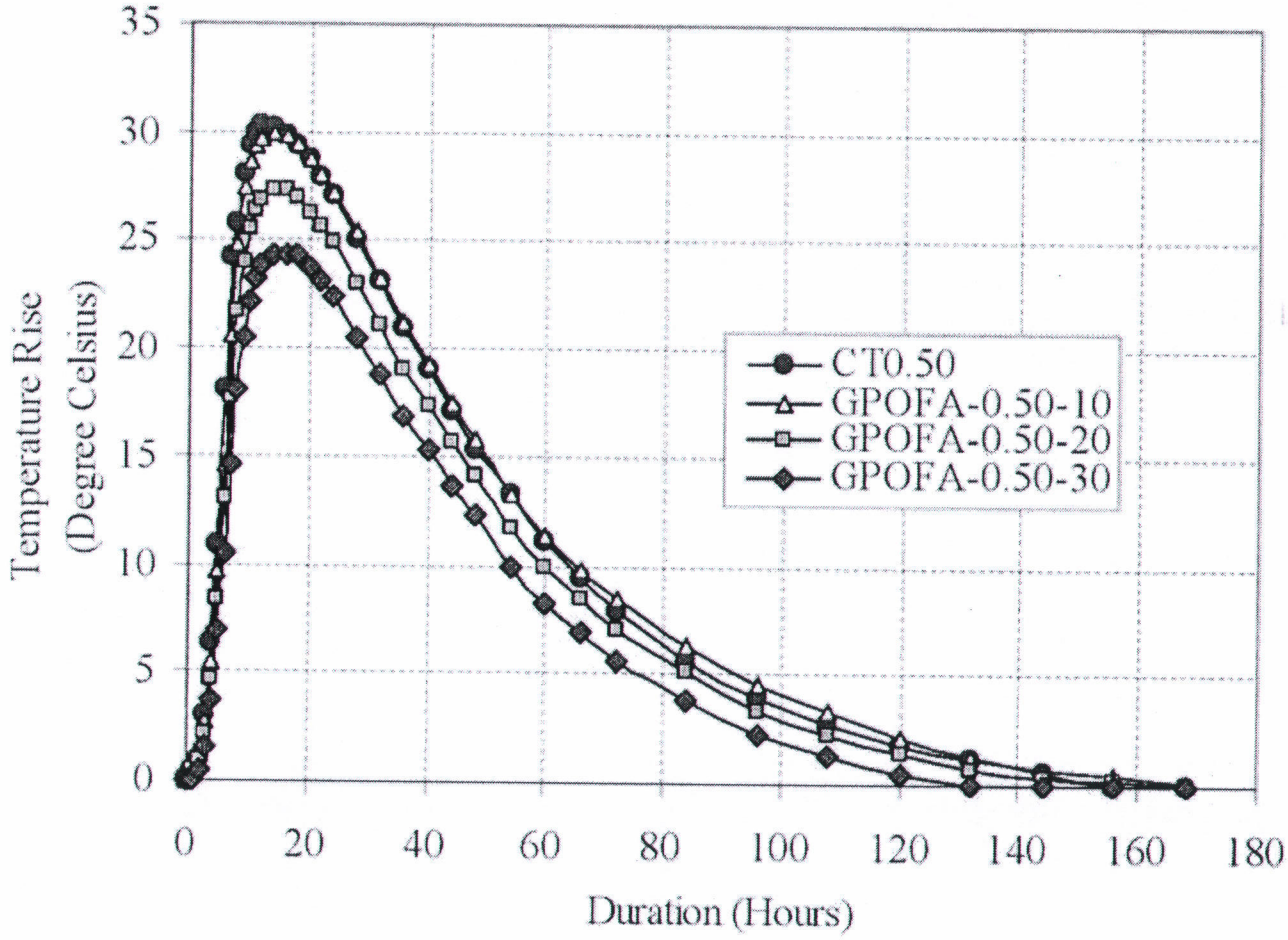

Journal of Materials in Civil Engineering. Submitted May 21, 2009; accepted March 17, 2010;
posted ahead of print March 22, 2010. doi:10.1061/(ASCE)MT.1943-5533.0000104

Table 1. Physical Properties of Type I Portland Cement and Ground Palm Oil Fuel Ash (GPOFA)

Materials	Specific gravity	Retained on a No. 325 sieve	Mean particle size, d_{50} (μm)
Cement	3.15	N/A	14.7
GPOFA	2.50	1.2	9.2

Journal of Materials in Civil Engineering. Submitted May 21, 2009; accepted March 17, 2010;
posted ahead of print March 22, 2010. doi:10.1061/(ASCE)MT.1943-5533.0000104

Table 2. Chemical Composition of Type I Portland Cement and Ground Palm Oil Fuel Ash (GPOFA)

Chemical composition (%)	Type I Portland Cement	GPOFA
Silicon dioxide (SiO_2)	20.9	42.5
Aluminium oxide (Al_2O_3)	4.8	0.9
Iron oxide (Fe_2O_3)	3.4	2.4
Calcium oxide (CaO)	65.4	11.0
Magnesium oxide (MgO)	1.2	7.1
Potassium oxide (K_2O)	0.4	7.0
Sodium oxide (Na_2O)	0.2	0.4
Sulfur trioxide (SO_3)	2.7	2.2
Phosphorus pentoxide (P_2O_5)	0.0	5.7
Loss on ignition (LOI)	1.0	20.9
$SiO_2 + Al_2O_3 + Fe_2O_3$	29.1	45.8

Journal of Materials in Civil Engineering. Submitted May 21, 2009; accepted March 17, 2010;
posted ahead of print March 22, 2010. doi:10.1061/(ASCE)MT.1943-5533.0000104

Table 3. Concrete Mixture Proportions

Mix. No.	Symbol	Mix Proportion (kg/m^3)						W/B	Slump (mm)
		OPC	GPOFA	F-Agg	C-Agg	Water	Super P		
1	CT0.50	350	-	808	1049	175.0	1.7	0.50	60
2	CT0.55	350	-	788	1023	192.5	0.7	0.55	70
3	CT0.60	350	-	768	997	210.0	-	0.60	95
4	GPOFA-0.50-10	315	35	804	1045	175.0	3.2	0.50	60
5	GPOFA-0.50-20	280	70	801	1041	175.0	4.2	0.50	70
6	GPOFA-0.50-30	245	105	798	1037	175.0	5.3	0.50	60
7	GPOFA-0.55-10	315	35	784	1019	192.5	1.4	0.55	70
8	GPOFA-0.55-20	280	70	781	1015	192.5	2.1	0.55	60
9	GPOFA-0.55-30	245	105	777	1011	192.5	2.8	0.55	70
10	GPOFA-0.60-10	315	35	764	993	210.0	-	0.60	85
11	GPOFA-0.60-20	280	70	761	989	210.0	-	0.60	75
12	GPOFA-0.60-30	245	105	757	984	210.0	-	0.60	70

Note: OPC = type I Portland cement; F-Agg = fine aggregate; C-Agg = coarse aggregate; and Super P = type F superplasticizer.

Journal of Materials in Civil Engineering. Submitted May 21, 2009; accepted March 17, 2010;
posted ahead of print March 22, 2010. doi:10.1061/(ASCE)MT.1943-5533.0000104

Table 4. Temperature Rise of Fresh Concretes

Mix No.	Concrete	Initial Temp. (°C)	Max. Temp. (°C)	Peak Temp. Rise (°C)	Reduce from Control (°C)	Reduce of Peak Temperature Rise (%)	Peak Time (Hours)
1	CT0.50	30.7	61.0	30.3	-	100.0	12
2	GPOFA-0.50-10	30.4	60.4	30.0	0.3	99.0	14
3	GPOFA-0.50-20	30.4	57.7	27.3	3.0	90.1	15
4	GPOFA-0.50-30	30.6	54.9	24.3	6.0	80.2	16

Journal of Materials in Civil Engineering. Submitted May 21, 2009; accepted March 17, 2010;
posted ahead of print March 22, 2010. doi:10.1061/(ASCE)MT.1943-5533.0000104

Table 5. Compressive Strength and Peak Temperature Rise of Fresh Concretes

Mix No.	Concrete	Compressive Strength, MPa.-(Normalized Comp. Strength (%))				Peak Temp. Rise (°C)
		3-Day	7-Day	28-Day	90-Day	
1	CT0.50	30.8-(100)	34.0-(100)	39.6-(100)	49.4-(100)	30.3
2	GPOFA-0.50-10	29.3-(95)	33.3-(98)	40.0-(101)	50.5-(102)	30.0
3	GPOFA-0.50-20	28.6-(93)	32.6-(96)	39.6-(100)	50.1-(101)	27.3
4	GPOFA-0.50-30	26.5-(86)	30.6-(90)	36.8-(93)	46.2-(94)	24.3

15. Nattapong Makaratat, Chai Jaturapitakkul, Thanapol Laosamathikul. Effects of calcium carbide residue-fly ash binder on mechanical properties of concrete, Journal of Materials in Civil Engineering ASCE. (accepted) (IF 0.526).

Journal of Materials in Civil Engineering. Submitted July 21, 2009; accepted May 7, 2010;
posted ahead of print May 13, 2010. doi:10.1061/(ASCE)MT.1943-5533.0000127

Effects of Calcium Carbide Residue-Fly Ash Binder on Mechanical Properties of Concrete

Nattapong Makaratat [1], Chai Jaturapitakkul [2], and Thanapol Laosamathikul [3]

Abstract

This study investigated the use of two kinds of waste from landfills, calcium carbide residue and fly ash, as a low CO_2 emission concrete binder. Calcium carbide residue is a by-product of an acetylene gas production process, and fly ash is a by-product of a thermal power plant. Ground calcium carbide residue (CR) was mixed with original fly ash (OF) or ground fly ash (GF) at a ratio of 30:70 by weight and was used as a binder to cast concrete without Portland cement. The effects of fly ash finenesses and water to binder (W/B) ratios of CR-OF and CR-GF concretes on setting times, compressive strength, modulus of elasticity, and splitting tensile strength were investigated. The results indicated that CR-OF and CR-GF mixtures could not only be used as a new binder in concrete, but could also help reduce environmental problems associated with CO_2 emissions. Without the use of Portland cement, CR-GF concrete yielded compressive strengths of 28.4 and 33.5 MPa at 28 and 90 days, respectively. In addition, lower W/B ratio and high fineness of fly ash produced higher compressive strength of the concrete. The hardened concretes produced from CR-OF and CR-GF mixtures had mechanical properties similar to those of control samples made from normal Portland cement concrete.

Keywords: Calcium carbide residue; Concrete; Fly ash; Setting times; Modulus of elasticity; Thailand

Journal of Materials in Civil Engineering. Submitted July 21, 2009; accepted May 7, 2010;
posted ahead of print May 13, 2010. doi:10.1061/(ASCE)MT.1943-5533.0000127

[1] Ph.D. Candidate of Civil Engineering, Department of Civil Engineering, Faculty of Engineering, King Mongkut's University of Technology Thonburi, Bangmod, Bangkok 10140, Thailand E-mail: natmakaratat@gmail.com
[2] Professor of Civil Engineering, Department of Civil Engineering, Faculty of Engineering, King Mongkut's University of Technology Thonburi, Bangmod, Bangkok 10140, Thailand (Corresponding author) Tel.: +66-2-470-9131; fax: +66-2-427-9063. E-mail address: chai.jat@kmutt.ac.th
[3] Graduate student of Civil Engineering, Department of Civil Engineering, Faculty of Engineering, King Mongkut's University of Technology Thonburi, Bangmod, Bangkok 10140, Thailand E-mail: thanutlao@hotmail.com

Introduction

Portland cement is an important cementitious material and is commonly used to produce concrete. Due to rapid expansion in the construction industry, especially as a result of rapid economic growth in countries such as China and India, large amounts of concrete have been required to make various kinds of structures (Price 1999). In 2005, the worldwide cement demand was approximately 2.2 billion tons, and by 2010, the demand is estimated to reach 2.8 billion tons.

Climate change has become an important worldwide problem due to increasing quantities of greenhouse gases in the atmosphere namely carbon dioxide (CO_2), methane (CH_4), and nitrous oxide (N_2O) (Marmo 2008). The clinker manufacturing process in the cement industry is known to contribute to the greenhouse effect, through the release of CO_2 gas into the atmosphere: about 0.9 tons of CO_2 is released during the production of every ton of clinker (Mehta 2009). In 2010, the production of cement will release as much as 2.07 billion tons of CO_2 into the atmosphere. To address this issue, cement manufacturers have tried to reduce Portland cement consumption by using supplementary cementitious materials, such as fly ash and natural pozzolan in producing cement binder (Gartner 2004; Damtoft et al. 2008). In addition, many studies have investigated the properties of concrete, which consumed less cement by incorporating large amount of fly ash or natural pozzolan (Jiang et al. 1999;

Journal of Materials in Civil Engineering. Submitted July 21, 2009; accepted May 7, 2010;
posted ahead of print May 13, 2010. doi:10.1061/(ASCE)MT.1943-5533.0000127

Malhotra et al. 2000; Uzal et al. 2007). These studies also showed that the concrete containing large amount of pozzolans yielded good mechanical properties and high durability. However, reducing the problem of climate change will require not only cement manufacturers, but also concrete producers and researchers to focus on these environmental issues.

Calcium carbide residue is a by-product from the acetylene gas production. This gas is used around the world for lighting, welding, metal cutting, and to ripen fruit. The calcium carbide residue is produced by a simple process, which is obtained from a reaction between calcium carbide (CaC_2) and water (H_2O) to form acetylene gas (C_2H_2) and calcium hydroxide ($Ca(OH)_2$), as shown by the following equation:

$$CaC_2 + 2H_2O \rightarrow C_2H_2 + Ca(OH)_2 \quad (1)$$

Calcium carbide residue mainly consists of calcium hydroxide, ($Ca(OH)_2$), in a slurry form. Thailand has a large amount of calcium carbide residue resulting from acetylene gas factories, and the residue has accumulated over time. From 2002-2007, an acetylene gas factory produced approximately 1,000 tons/month or about 12,000 tons/year of calcium carbide residue, and very little of this residue has been used. Thus, most of the residue has been sent to landfills, causing many environmental problems such as dust and high alkalinity of the disposal area (see Fig. 1). Krammart et al. (1996) found that calcium carbide residue and fly ash mixture can produce a pozzolanic reaction, resulting in products similar to those obtained from the cement hydration process. They found that the optimal ratio of calcium carbide residue and fly ash mixture to achieve the highest compressive strength of mortar was 30:70 by weight. At 90 days, mortar made from a calcium carbide residue-fly ash mixture had a compressive strength of 20.9 MPa.

Journal of Materials in Civil Engineering. Submitted July 21, 2009; accepted May 7, 2010;
posted ahead of print May 13, 2010. doi:10.1061/(ASCE)MT.1943-5533.0000127

Fly ash obtained from the pulverized coal process is widely used as a pozzolan in many countries and also in Thailand (Kiattikomol et al. 2001; Jaturapitakkul et al. 2004). However, the thermal power plant that produces fly ash is located in the northern part of Thailand, far from Bangkok, where most construction sites are located. This shows that the major constraint for the unused pulverized coal fly ash is the transportation cost. Thus, fluidized bed fly ash produced in the central part of Thailand, near Bangkok, was used in this study. The coal was burned at temperatures of 800 – 900 °C to generate fluidized bed fly ash. This power plant can produce approximately 500 tons/days of fly ash, but this fly ash has been rarely used due to its large particle and high porosity. Therefore, the fly ash is disposed of in landfills every day, creating environment problems such as dust and groundwater pollution (Sinthaworn and Nimityongskul 2009). Sata et al. (2007) found that high fineness fly ash from fluidized bed combustion can be used to partially replace Portland cement 40% by weight of binder to make high-strength concrete, producing compressive strengths ranging from 85.0 to 91.4 MPa at 28 days.

This research focuses on use of a new binder material, consisting of a mixture of two kinds of waste, calcium carbide residue and fly ash, for casting concrete. The effects of fly ash fineness and water to binder (W/B) ratios on the setting times, compressive strength, modulus of elasticity, and splitting tensile strength of calcium carbide residue-fly ash concretes were investigated. The present paper should encourage concrete researchers and users to utilize the mixture of the two wastes as a new binder material as alternate to Portland cement in concrete.

Experimental Program

Materials

Journal of Materials in Civil Engineering. Submitted July 21, 2009; accepted May 7, 2010;
posted ahead of print May 13, 2010. doi:10.1061/(ASCE)MT.1943-5533.0000127

The materials used in this research were ground calcium carbide residue (CR), original fly ash (fly ash as received from the power plant, OF), ground fly ash (GF), river sand, crushed limestone, water, and naphthalene formaldehyde superplasticizer (Type A&F) conforming to ASTM C 494 (2001d). The particle morphologies and the particle size distributions of materials are shown in Figs. 2 and 3, respectively. Table 1 shows the physical properties of CR, OF and GF. Table 2 shows the chemical compositions of each material, determined by X-Ray Fluorescence analysis.

Local river sand with a fineness modulus of 3.20 and a specific gravity of 2.61 was used as a fine aggregate. Crushed limestone was used as a coarse aggregate; it had a maximum size of 19 mm, a fineness modulus of 6.90, and a specific gravity of 2.73. The water absorptions of fine and coarse aggregates were 0.69% and 0.45%, respectively.

Calcium carbide residue was collected from a disposal area (see Fig. 1). Because this calcium carbide residue had a high water content (approximately 52%), it was sun-dried for approximately 3 - 4 days to reduce the moisture content to approximately 2 - 4%. Next, it was ground by ball mill until less than 3% of particles by weight were retained on a 45-μm sieve (CR). After grinding, CR had an irregular shape (see Fig. 2(a)) and a specific gravity of 2.41, higher than those reported in previous research by Jaturapitakkul and Roongreung (2003) and Krammart and Tangtermsirikul (2004) of 2.21 and 2.26, respectively. The mean particle size (d_{50}) of CR was 4.4 μm, and 2.3% of CR particles by weight were retained on a 45-μm sieve. The major chemical composition of CR was 56.5% CaO, with a high degree of loss on ignition (LOI): 36.1%. This LOI was particularly high because it was measured at temperatures of 950 – 1000 °C, whereas material mainly consisting of $Ca(OH)_2$ decomposes into CaO and H_2O (gas) at approximately 550 °C (Jaturapitakkul and Roongreung 2003). This high LOI value is similar to that reported by Krammart and Tangtermsirikul (2004):

Journal of Materials in Civil Engineering. Submitted July 21, 2009; accepted May 7, 2010;
posted ahead of print May 13, 2010. doi:10.1061/(ASCE)MT.1943-5533.0000127

31.7%. It should be noted that the CaO content of CR was 56.5% or about half of the total chemical composition.

Original fly ash (OF) was obtained from a thermal power plant in the central part of Thailand where sub-bituminous coal was burnt at controlled temperatures of 800 – 900 °C in a fluidized bed burning process. The original fly ash was ground to increase fineness until less than 3% of particles by weight were retained on a 45-μm sieve and was assigned as GF. Figs. 2(b) and (c) show that both OF and GF had irregular shape. OF contained large particles with high porosity while GF was composed of crushed particles with less porosity. OF and GF had specific gravities of 2.34 and 2.39, respectively, suggesting that when the fly ash was ground, the specific gravity increased. This is consistent with results of Paya et al. (1995), Cheerarot and Jaturapitakkul (2004), and Jaturapitakkul et al. (2004) and for other pozzolans, namely palm oil fuel ash (Tangchirapat et al. 2007) and rice husk-bark ash (Makaratat et al. 2004). The mean particle sizes (d_{50}) of OF and GF were 28.9 and 5.4 μm, and 48.6 and 2.3% of OF and GF particles by weight were retained on a 45-μm sieve, respectively. These results showed that the grinding process increased not only the fineness of the material, but also the specific gravity, which was likely caused by the crushing of porous particles into smaller sizes with lower porosity.

The original and ground fly ashes were tested for chemical composition. The oxide content (SiO_2, Fe_2O_3, and Al_2O_3) of OF and GF was 74 and 71.7%, respectively higher than the minimum requirement of 70.0% specified by ASTM C 618 (2001e) for fly ash Class F. In addition, the CaO, SO_3, and LOI values of OF were 17.2, 2.6, and 0.3% while GF were 21.9, 4.1, and 5.2%, respectively. Therefore, both original and ground fly ashes used in this study can be classified as Class F fly ash, according to ASTM C 618 (2001e). This is consistent

Journal of Materials in Civil Engineering. Submitted July 21, 2009; accepted May 7, 2010;
posted ahead of print May 13, 2010. doi:10.1061/(ASCE)MT.1943-5533.0000127

with previous result of Jaturapitakkul et al. (2004) who reported that the grinding process did not have much effect on the chemical composition of fly ash.

Mix Proportions and Test Specimens

Six mixture proportions of concrete were assessed to evaluate the effects of fly ash fineness and W/B ratios on properties of CR-fly ash concretes as shown in Table 3. For CR-OF and CR-GF concretes, a ratio by weight of 30:70 (CR:OF or CR:GF) was used as a binder because this ratio was shown to yield the highest compressive strength (Krammart et al. 1996). A normal strength concrete (NC30), in which 300 kg/m^3 of Portland cement was used as a binder with a target compressive strength at 28 days of 30 MPa was prepared for comparison purposes. Fresh concrete properties such as superplasticizer requirements and setting times were measured. The amount of superplasticizer required to maintain the same degree of slump (50 and 100 mm) was measured in all concrete mixtures according to ASTM C 143 (2001a). Initial and final setting times of the fresh concrete were determined using ASTM C 403 (2001b) procedures.

Cylindrical concrete specimens (100 mm in diameter and 200 mm in height) were cast and tested to evaluate the mechanical properties of the hardened concrete. The compressive strength was determined at 7, 28, 60, 90, and 180 days; the modulus of elasticity was determined at 28 and 90 days; and the splitting tensile strength was determined at 28, 60, and 90 days.

Results and Discussion

Requirement of Superplasticizer

Table 3 shows the superplasticizer requirements to maintain a slump of fresh concrete between 50 - 100 mm. It was found that 0.45OF, 0.53OF, and 0.65OF concretes required

Journal of Materials in Civil Engineering. Submitted July 21, 2009; accepted May 7, 2010;
posted ahead of print May 13, 2010. doi:10.1061/(ASCE)MT.1943-5533.0000127

superplasticizer of 18.0, 10.3, and 3.0 kg/m^3, respectively. This is due to the fact that OF had large particles with high porosity, which increased the water requirement of the concrete mixture. As a result the superplasticizer dosage in the mixture needed to be increased to maintain the same slump of concrete. 0.45GF, 0.53GF, and 0.65GF concretes required 9.0, 6.6, and 0.8 kg/m^3 of superplasticizer to maintain the slump of fresh concrete within the controlled range, respectively. This demonstrated that a concrete mixture with ground fly ash (GF) needed less superplasticizer than a concrete mixture with unground or original fly ash (OF) to achieve the same slump of concrete. This result supports the finding of Sata et al. (2007), who reported that grinding fly ash from a fluidized bed power plant into smaller particles, helped the fly ash to reduce its porosity and the friction between binder and aggregates, resulting in improved workability of fresh concrete.

Setting Times of Concrete

Table 4 shows the results from the evaluation of concrete setting times of all mixtures. The results indicated that the initial and final setting times were much longer for CR-OF and CR-GF concretes than for normal concrete NC30. The NC30 concrete had an initial setting time of 4 h : 10 min and a final setting time of 6 h : 30 min. The initial setting times of 0.65OF, 0.53OF, and 0.45OF concretes were 26 h : 10 min, 18 h : 20 min, and 14 h : 10 min, and the final setting times were 50 h, 48 h, and 47 h : 5 min, respectively. Since the CR-OF mixtures did not have the hydration reaction from Portland cement, the long delay in setting times of CR-OF concretes was expected. 0.65OF concrete had the longest setting times because it contained more free water present in mixture than 0.53OF and 0.45OF concretes (Andrade et al. 2009).

After the fly ash was ground into high fineness, the initial and final setting times were shorter in CR-GF concretes than in CR-OF concretes. The initial setting times of 0.65GF, 0.53GF,

Journal of Materials in Civil Engineering. Submitted July 21, 2009; accepted May 7, 2010;
posted ahead of print May 13, 2010. doi:10.1061/(ASCE)MT.1943-5533.0000127

and 0.45GF concretes were 15 h : 10 min, 13 h : 50 min, and 11 h : 40 min, and the final setting times were 33 h : 5 min, 32 h : 5 min, and 29 h : 40 min, respectively. Although 0.45GF concrete had the shortest setting times, its initial and final setting times were still about 2.8 and 4.5 times longer than those of normal concrete (NC30). This finding suggests that the use of CR-OF or CR-GF mixtures as a binder in concretes considerably increases both initial and final setting times. This results from the fact that the reaction between CR and fly ash is a pozzolanic reaction which is much slower than the hydration reaction of Portland cement (Safwan and Mohamed Nagib 1994). Therefore, one possible application where longer setting times may be desirable is in mass concrete. However, if the long delay in setting times of the CR-OF and CR-GF concretes is an issue, $CaCl_2$ or Portland cement may be used as an admixture to accelerate the setting times as well as the early compressive strength of the concrete.

Compressive Strength of Concrete

At each testing date, the average compressive strength of three concrete specimens was measured and the results are tabulated in Table 5. The results showed that the compressive strengths of CR-OF and CR-GF concretes ranged from 6.1 to 28.4 MPa at 28 days and increased to 7.9 to 34.5 MPa at 180 days depending on the W/B ratio and the fineness of fly ash, while normal concrete NC30 had compressive strengths of 23.5, 31.9, 36.2, 37.1, and 38.9 MPa at 7, 28, 60, 90, and 180 days, respectively. The compressive strength of CR-OF concretes increased with curing age. For example, 0.65OF and 0.53OF concretes had compressive strengths of 4.4 and 6.3 MPa at 7 days and 6.1 and 16.4 MPa at 28 days, respectively. At the later ages of 60, 90 and 180 days, 0.65OF and 0.53OF concretes had compressive strengths of 6.5, 7.0, 7.9 and 18.0, 19.9, and 20.5 MPa, respectively. These results indicated that most of the compressive strength of CR-OF concretes developed within 28 days and then increased moderately afterwards.

Journal of Materials in Civil Engineering. Submitted July 21, 2009; accepted May 7, 2010;
posted ahead of print May 13, 2010. doi:10.1061/(ASCE)MT.1943-5533.0000127

CR-GF concretes developed compressive strength in a way similar to CR-OF concretes, but their compressive strengths were higher than those of CR-OF concretes when the same W/B ratio was used. At 7 days, 0.65GF and 0.53GF concretes had compressive strengths of 8.2 and 10.0 MPa, which increased to 10.2 and 18.2 MPa at 28 days, respectively. After 28 days, the compressive strengths of CR-GF concretes increased gradually. At 60 and 180 days, 0.65GF and 0.53GF concretes had compressive strengths of 13.3, 25.7 and 13.9, 26.9 MPa, respectively. The result is consistent with Portland cement concrete containing fly ash since it indicated that the compressive strength of concrete could be improved by grinding the fly ash to have high fineness (Jaturapitakkul et al. 2004; Sata et al. 2007).

Figs. 4 and 5 present the relationships between compressive strength and the W/B ratio in CR-OF and CR-GF concretes, respectively. It was found that the W/B ratio had a pronounced effect on the compressive strength of CR-OF and CR-GF concretes: lower W/B ratios corresponded to higher compressive strength development. At 7, 28, 60, 90, and 180 days, 0.45OF concrete had compressive strengths of 8.4, 19.0, 23.4, 24.7, and 25.5 MPa, respectively. These values were higher than those of other CR-OF concretes at higher W/B ratios (0.53 or 0.65). This result confirms the reported results for plain concretes using Portland cement as a binder (Beshr et al. 2003; Behnood and Ziari 2008; Khatib 2008), which indicated that the increased W/B ratios increased the porosity in concrete, resulting in lowering concrete strength. It was also noted that at 7 days, 0.45OF concrete had compressive strength of 8.4 MPa, about 2 times greater than that of 0.65OF concrete (4.4 MPa), and the compressive strength of 0.45OF concrete increased to about 3 times and 3.5 times that of 0.65OF concrete at 28 and 90 days, respectively.

The highest compressive strength was observed in 0.45GF concrete which had compressive strengths of 10.7 and 28.4 MPa at 7 and 28 days, respectively. At 90 days, this concrete had a

Journal of Materials in Civil Engineering. Submitted July 21, 2009; accepted May 7, 2010;
posted ahead of print May 13, 2010. doi:10.1061/(ASCE)MT.1943-5533.0000127

compressive strength of 33.5 MPa (about 2.5 times greater than that of 0.65GF concrete, 13.5 MPa), and then it gradually increased to 34.5 MPa at 180 days or about 24 MPa gain from its compressive strength at 7 days, although the mixture did not contain any Portland cement.

Modulus of Elasticity of Concrete

The elastic modulus of cylindrical 100 x 200 mm concrete specimens was measured in accordance with ASTM C 469 (2001c) procedures. Table 5 shows the average test results for each of the three concrete specimens. It was found that the elastic modulus of CR-OF and CR-GF concretes increased with age and ranged from 18.6 to 33.6 GPa, while normal concrete NC30 had elastic modulus of 29.4 and 36.9 GPa at 28 and 90 days, respectively. Moreover, the elastic modulus values of CR-GF concretes were higher than those of CR-OF concretes which followed the same trend as the compressive strength. These results indicated that in CR-OF or CR-GF concretes, the modulus of elasticity was related to the compressive strength. The results support those for the plain concrete researches reported by Cetin and Carrasquillo (1998), Abdelgader and Gorski (2003), and Nassif et al. (2005). For example, at 28 days 0.65GF, 0.53GF, and 0.45GF concretes had modulus of elasticity values of 18.6, 22.6, and 27.7 GPa, and their compressive strengths were 10.2, 18.2, and 28.4 MPa, respectively.

Fig. 6 shows the modulus of elasticity values predicted by ACI 318 (2005) and the data obtained from this experiment. Most experimental data revealed that elastic modulus values of CR-OF and CR-GF concretes were higher than those predicted by ACI 318 (2005), probably because the specimens used in this experiment (cylinders sized 100 x 200 mm) were smaller than the standard specimen (cylinders sized 150 x 300 mm) (Rashid et al. 2002). Moreover, differences in the coarse aggregates used in the concrete may also affect the elastic modulus of concrete, as well as the compressive strength (Huo et al. 2001; Beshr et al. 2003).

Journal of Materials in Civil Engineering. Submitted July 21, 2009; accepted May 7, 2010;
posted ahead of print May 13, 2010. doi:10.1061/(ASCE)MT.1943-5533.0000127

Splitting Tensile Strength of Concrete

Table 6 shows the splitting tensile strengths of concretes and the ratios of splitting tensile strength to compressive strength. The splitting tensile strengths of CR-OF and CR-GF concretes tended to increase with increased compressive strength. This reveals that the splitting tensile strength is related to its compressive strength (Swamy 1990; Abdelgader and Elgalhud 2008). At 28 days, 0.53OF and 0.45OF concretes had splitting tensile strengths of 1.89 and 2.33 MPa, and their compressive strengths were 16.4 and 19.0 MPa, respectively. Furthermore, the splitting tensile strength tended to increase with age. For example at 60 and 90 days, 0.65OF, 0.53OF, and 0.45OF concretes had splitting tensile strengths of 1.03, 2.45, 2.64 and 1.14, 2.53, 3.10 MPa, respectively.

The use of ground fly ash in CR-GF concretes can increase the splitting tensile strength as well as the compressive strength of concrete. 0.65GF, 0.53GF, and 0.45GF had the splitting tensile strengths of 1.62, 2.45, 3.43 and 2.08, 2.94, 4.08 MPa, at 28 and 90 days, respectively. The splitting tensile strengths of CR-OF and CR-GF concretes ranged from 11% to 16% of their compressive strengths, which were close to the splitting tensile strength ratios of normal concrete NC30 (11% to 14%). This result supports previous researches, which indicated that the splitting tensile strength of plain concrete is about 10% of its compressive strength (Yazici 2008; Siddique et al. 2009).

Conclusions

Based on the experimental results, the following conclusions can be drawn:

1. The use of ground fly ash (GF) could reduce the amount of superplasticizer required in the concrete mixture compared to the use of original fly ash (OF) when the same slump of fresh concrete was maintained.

Journal of Materials in Civil Engineering. Submitted July 21, 2009; accepted May 7, 2010;
posted ahead of print May 13, 2010. doi:10.1061/(ASCE)MT.1943-5533.0000127

2. Because the initial and final setting times of CR-OF and CR-GF concretes were much longer than those of normal concrete, CR-OF or CR-GF concretes should be considered carefully for use in construction work.
3. The 0.45GF concrete had the highest compressive strength, 28.4 and 33.5 MPa at 28 and 90 days, respectively. This compressive strength could be achieved without the use of Portland cement. Fly ash with high fineness was more reactive with CR, and thus gave higher compressive strength of the concrete. In addition, lower W/B ratios produced higher compressive strengths in both CR-OF and CR-GF concretes.
4. Both CR-OF and CR-GF concretes had hardened concrete properties similar to normal concrete: the compressive strength increased with age, the modulus of elasticity increased with the increased compressive strength, and the splitting tensile strength increased with the increased compressive strength and was about 11 - 16% of the compressive strength.
5. The mixture of calcium carbide residue and fly ash could not only be used as a new binder in concrete, but could also help reduce the environmental problems due to reduce the production of Portland cement and disposal of calcium carbide residue and fly ash.

Acknowledgements

The writers gratefully acknowledge the financial supports from the Thailand Research Fund (TRF) under TRF Senior Research Scholar, Contact No. RTA5080020 and the Commission on Higher Education, Ministry of Education, Thailand. Thank is also extend to the National Research Council of Thailand.

References

Journal of Materials in Civil Engineering. Submitted July 21, 2009; accepted May 7, 2010;
posted ahead of print May 13, 2010. doi:10.1061/(ASCE)MT.1943-5533.0000127

Abdelgader, H. S., and Gorski, J. (2003). "Stress-strain relations and modulus of elasticity of two-stage concrete." *J. Mater. Civ. Eng.*, 15(4), 329-334.

Abdelgader, H. S., and Elgalhud, A. A. (2008). "Effect of grout proportions on strength of two-stage concrete." *Str. Concr.*, 9(3), 163-170.

American Concrete Institute (ACI). (2005). "Building code requirements for structural concrete and commentary." *ACI 318/318R*, Detroit.

Andrade, L. B., Rocha, J. C., and Cheriaf, M. (2009). "Infuence of coal bottom ash as fine aggregate on fresh properties of concrete." *Constr. Build. Mater.*, 23(2), 609-614.

ASTM. (2001a). "Standard test method for slump of hydraulic-cement concrete." C 143, *Annual Book of ASTM Standards*, West Conshohocken, Pa.

ASTM. (2001b). "Standard test method for time of setting of concrete mixtures by penetration resistance. C 403, *Annual Book of ASTM Standards*, West Conshohocken, Pa.

ASTM. (2001c). "Standard test method for static modulus of elasticity and poison's ratio of concrete in compression." C 469, *Annual Book of ASTM Standards*, West Conshohocken, Pa.

ASTM. (2001d). "Standard specification for chemical admixtures for concrete." C 494, *Annual Book of ASTM Standards*, West Conshohocken, Pa.

ASTM. (2001e). "Standard specification for coal fly ash and raw or calcined natural pozzolan for use as a mineral admixture in concrete." C 618, *Annual Book of ASTM Standards*, West Conshohocken, Pa.

Behnood, A., and Ziari, H. (2008). "Effects of silica fume addition and water to cement ratio on the properties of high-strength concrete after exposure to high temperatures." *Cem. Concr. Compos.*, 30(2), 106-112.

Journal of Materials in Civil Engineering. Submitted July 21, 2009; accepted May 7, 2010;
posted ahead of print May 13, 2010. doi:10.1061/(ASCE)MT.1943-5533.0000127

Beshr, H., Almusallam, A. A., and Maslehuddin, M. (2003). "Effect of coarse aggregate quality on the mechanical properties of high strength concrete." *Constr. Build. Mater.*, 17(2), 97-103.

Cetin, A., and Carrasquillo, R. L. (1998). "High-performance concrete: influence of coarse aggregates on mechanical properties." *ACI Mater. J.*, 95(3), 252-261.

Cheerarot, R., and Jaturapitakkul, C. (2004). "A study of disposed fly ash from landfill to replace Portland cement." *Waste Manage.*, 24(7), 701-709.

Damtoft, J. S., Lukasik, J., Herfort, D., Sorrentino, D., and Gartner, E. M. (2008). "Sustainable development and climate change initiatives." *Cem. Concr. Res.*, 38(2), 115-127.

Gartner, E. (2004). "Industrially interesting approaches to "low-CO_2" cements." *Cem. Concr. Res.*, 34(9), 1489-1498.

Huo, X. S., Al-Omaishi, N., and Tadros, M. K. (2001). "Creep, shrinkage and modulus of elasticity of high-performance concrete." *ACI Mater. J.*, 98(6), 440-449.

Jaturapitakkul, C., and Roongreung, B. (2003). "Cementing material from calcium carbide residue-rice husk ash." *J. Mater. Civ. Eng.*, 15(5), 470-475.

Jaturapitakkul, C., Kiattikomol, K., Sata, V., and Leekeeratikul, T. (2004). "Use of ground coarse fly ash as a replacement of condensed silica fume in producing high-strength concrete." *Cem. Concr. Res.*, 34(4), 549-555.

Jiang, L., Lin, B., and Cai Y. (1999). "Studies on hydration in high-volume fly ash concrete binders." *ACI Mater. J.*, 96(6), 703-706.

Khatib, J. M. (2008). "Metakaolin concrete at a low water to binder ratio." *Constr. Build. Mater.*, 22(8), 1691-1700.

Kiattikomol, K., Jaturapitakkul, C., Songpiriyakij, S., and Chutubtim S. (2001). "A study of ground coarse fly ashes with different finenesses from various sources as pozzolanic materials." *Cem. Concr. Compos.*, 23(4-5), 335-343.

Journal of Materials in Civil Engineering. Submitted July 21, 2009; accepted May 7, 2010;
posted ahead of print May 13, 2010. doi:10.1061/(ASCE)MT.1943-5533.0000127

Krammart, P., Martputhorn, S., Jaturapitakkul, C., and Ngaopisadarn, V. (1996). "A study of compressive strength of mortar made from calcium carbide residue and fly ash." *Res. Devel., J., The Engineering Institute of Thailand*, 7(2), 65-75 (in Thai).

Krammart, P., and Tangtermsirikul, S. (2004). "Properties of cement made by partially replacing cement raw materials with municipal solid waste ashes and calcium carbide waste." *Constr. Build. Mater.*, 18(8), 579-583.

Makaratat, N., Tangchirapat, W., Jaturapitakkul, C., Kiattikomol, K., and Siripanichgorn, A. (2004). "Utilization of rice husk-bark ash as a cement replacement." *Proc., the First International Conference of Asian Concrete Federation*, Chiang Mai, Thailand, 650-659.

Malhotra, V. M., Zhang, M. H., and Learman, G. H. (2000). "Long-term performance of steel reinforcing bars in Portland cement concrete and concrete incorporating moderate and high volumes of ASTM Class F fly ash." *ACI Mater. J.*, 97(4), 409-417.

Marmo, L. (2008). "EU strategies and policies on soil and waste management to offset greenhouse gas emissions." *Waste Manage.*, 28(4), 685-689.

Mehta, P. K. (2009). "Global concrete industry sustainability." *Concr. Int.*, 31(2), 45-48.

Nassif, H. H., Najm, H., and Suksawang, N. (2005). "Effect of pozzolanic materials and curing methods on the elastic modulus of HPC." *Cem. Concr. Compos.*, 27(6), 661-670.

Paya, J., Monzo, J., Borrachero, M. V., and Peris-Mora, E. (1995). "Mechanical treatments of fly ashes. Part I: Physico-chemical characterization of ground fly ashes." *Cem. Concr. Res.*, 25(7), 1469-1479.

Price, L., Worrell, E., and Phylipsen, D. (1999). "Energy use and carbon dioxide emissions in energy-intensive industries in key developing countries." *Proc., the 1999 Earth Technologies Forum*, Washington DC, Sept. 27-29.

Rashid, M. A., Mansur, M. A., and Paramasivam, P. (2002). "Correlations between mechanical properties of high-strength concrete." *J. Mater. Civ. Eng.*, 14(3), 230-238.

Journal of Materials in Civil Engineering. Submitted July 21, 2009; accepted May 7, 2010;
posted ahead of print May 13, 2010. doi:10.1061/(ASCE)MT.1943-5533.0000127

Safwan, A. K. and Mohamed Nagib, A. Z. (1994). "Characteristics of silica-fume concrete." *J. Mater. Civ. Eng.*, 6(3), 357-375.

Sata, V., Jaturapitakkul, C., and Kiattikomol, K. (2007). "Influence of pozzolan from various by-product materials on mechanical properties of high-strength concrete." *Constr. Build. Mater.*, 21(7), 1589-1598.

Siddique, R., Schutter, G. D., and Noumowe, A. (2009). "Effect of used-foundry sand on the mechanical properties of concrete." *Constr. Build. Mater.*, 23(2), 976-980.

Sinthaworn, S., and Nimityongskul, P. (2009). "Quick monitoring of pozzolanic reactivity of waste ashes." *Waste Manage.*, 29(5), 1526-1531.

Swamy, R. N. (1990). "Fly ash concrete-potential without misuse." *Mater. Struct.*, 23(6), 397-411.

Tangchirapat, W., Saeting, T., Jaturapitakkul, C., Kiattikomol, K., and Siripanichgorn, A. (2007). "Use of waste ash from palm oil industry in concrete." *Waste Manage.*, 27(1), 81-88.

Uzal, B., Turanli, L., and Mehta, P. K. (2007). "High-volume natural pozzolan concrete for structural applications." *ACI Mater. J.*, 104(5), 535-538.

Yazici, H. (2008). "The effect of silica fume and high-volume Class C fly ash on mechanical properties, chloride penetration and freeze-thaw resistance of self-compacting concrete." *Constr. Build. Mater.*, 22(4), 456-462.

Journal of Materials in Civil Engineering. Submitted July 21, 2009; accepted May 7, 2010;
posted ahead of print May 13, 2010. doi:10.1061/(ASCE)MT.1943-5533.0000127

Table 1

Physical properties of ground calcium carbide residue (CR), original fly ash (OF), and ground fly ash (GF).

Physical properties	Ground CaC_2 residue (CR)	Original fly ash (OF)	Ground fly ash (GF)
Specific gravity	2.41	2.34	2.39
Retained on a 45-μm sieve (%)	2.3	48.6	2.3
Mean particle size, d_{50} (micron)	4.4	28.9	5.4

Journal of Materials in Civil Engineering. Submitted July 21, 2009; accepted May 7, 2010;
posted ahead of print May 13, 2010. doi:10.1061/(ASCE)MT.1943-5533.0000127

Table 2

Chemical compositions of ground calcium carbide residue (CR), original fly ash (OF), and ground fly ash (GF).

Chemical composition (%)	CR	OF	GF
SiO_2	4.3	37.3	47.8
Fe_2O_3	0.9	15.3	6.2
Al_2O_3	0.4	21.4	17.7
CaO	56.5	17.2	21.9
MgO	1.7	3.1	1.3
SO_3	0.06	2.6	4.1
Loss on ignition	36.1	0.3	5.2

Journal of Materials in Civil Engineering. Submitted July 21, 2009; accepted May 7, 2010;
posted ahead of print May 13, 2010. doi:10.1061/(ASCE)MT.1943-5533.0000127

Table 3

Concrete mixture proportions.

Concretes	Mixture proportions (kg/m^3)								W/B	Slump (mm)
	Cement	CR	OF	GF	Water	Sand	Coarse Agg.	Super P.		
0.65OF	-	90	210	-	194	770	985	3.0	0.65	90
0.65GF	-	90	-	210	195	780	1000	0.8	0.65	55
0.53OF	-	112.5	262.5	-	194	750	960	10.3	0.53	70
0.53GF	-	112.5	-	262.5	195	750	960	6.6	0.53	65
0.45OF	-	135	315	-	194	700	895	18.0	0.45	60
0.45GF	-	135	-	315	198	710	910	9.0	0.45	65
NC30	300	-	-	-	195	825	1055	-	0.65	70

Notes: CR: ground calcium carbide residue; OF: original fly ash; GF: ground fly ash. The numbers 0.65, 0.53, and 0.45 in front of OF and GF indicate the water to binder (W/B) ratio of the concrete mixture. For example, 0.45GF means concrete containing ground calcium carbide residue and ground fly ash mixture with a W/B ratio of 0.45. NC30 is a normal concrete using Portland cement as a binder.

Journal of Materials in Civil Engineering. Submitted July 21, 2009; accepted May 7, 2010;
posted ahead of print May 13, 2010. doi:10.1061/(ASCE)MT.1943-5533.0000127

Table 4

Setting times of CR-OF, CR-GF, and normal concretes.

Concretes	Initial setting times h:min	Final setting times h:min
0.65OF	26:10	50:00
0.65GF	15:10	33:05
0.53OF	18:20	48:00
0.53GF	13:50	32:05
0.45OF	14:10	47:05
0.45GF	11:40	29:40
NC30	4:10	6:30

Journal of Materials in Civil Engineering. Submitted July 21, 2009; accepted May 7, 2010;
posted ahead of print May 13, 2010. doi:10.1061/(ASCE)MT.1943-5533.0000127

Table 5

Compressive strength and elastic modulus of concretes.

Concretes	Compressive strength (MPa)					Elastic modulus (GPa)	
	7 days	28 days	60 days	90 days	180 days	28 days	90 days
0.65OF	4.4	6.1	6.5	7.0	7.9	*	*
0.65GF	8.2	10.2	13.3	13.5	13.9	18.6	21.9
0.53OF	6.3	16.4	18.0	19.9	20.5	21.1	25.5
0.53GF	10.0	18.2	25.7	26.5	26.9	22.6	28.7
0.45OF	8.4	19.0	23.4	24.7	25.5	22.1	29.3
0.45GF	10.7	28.4	31.7	33.5	34.5	27.7	33.6
NC30	23.5	31.9	36.2	37.1	38.9	29.4	36.9

* Note: The compressive strengths of 0.65OF concrete at 28 and 90 days were too low to obtain the elastic modulus of concrete.

Journal of Materials in Civil Engineering. Submitted July 21, 2009; accepted May 7, 2010;
posted ahead of print May 13, 2010. doi:10.1061/(ASCE)MT.1943-5533.0000127

Table 6

Splitting tensile strength of concretes.

Concretes	Splitting tensile strength (MPa)			*Ratio of splitting tensile strength to compressive strength (%)*		
	28 days	60 days	90 days	28 days	60 days	90 days
0.65OF	*	1.03	1.14	*	*16*	*16*
0.65GF	1.62	1.83	2.08	*16*	*14*	*15*
0.53OF	1.89	2.45	2.53	*12*	*14*	*13*
0.53GF	2.45	2.80	2.94	*13*	*11*	*11*
0.45OF	2.33	2.64	3.10	*12*	*11*	*13*
0.45GF	3.43	3.79	4.08	*12*	*12*	*12*
NC30	3.54	4.43	5.06	*11*	*12*	*14*

* Note: The splitting tensile strength of 0.65OF concrete at 28 days was too low to measure.

Journal of Materials in Civil Engineering. Submitted July 21, 2009; accepted May 7, 2010;
posted ahead of print May 13, 2010. doi:10.1061/(ASCE)MT.1943-5533.0000127

List of Figures caption

Fig. 1. Disposal area of calcium carbide residue.

Fig. 2. Scanning electron microscope images of CR, OF, and GF.

(a) Ground calcium carbide residue (CR).

(b) Original fly ash (OF).

(c) Ground fly ash (GF).

Fig. 3. Particle size distributions of materials.

Fig. 4. Relationship between the compressive strength and water to binder (W/B) ratio of CR-OF concrete.

Fig. 5. Relationship between the compressive strength and water to binder (W/B) ratio of CR-GF concrete.

Fig. 6. Relationships between the modulus of elasticity and square root of the compressive strength of concretes.

Fig1.eps

Journal of Materials in Civil Engineering. Submitted July 21, 2009; accepted May 7, 2010;
posted ahead of print May 13, 2010. doi:10.1061/(ASCE)MT.1943-5533.0000127

Fig2a.eps

Journal of Materials in Civil Engineering. Submitted July 21, 2009; accepted May 7, 2010;
posted ahead of print May 13, 2010. doi:10.1061/(ASCE)MT.1943-5533.0000127

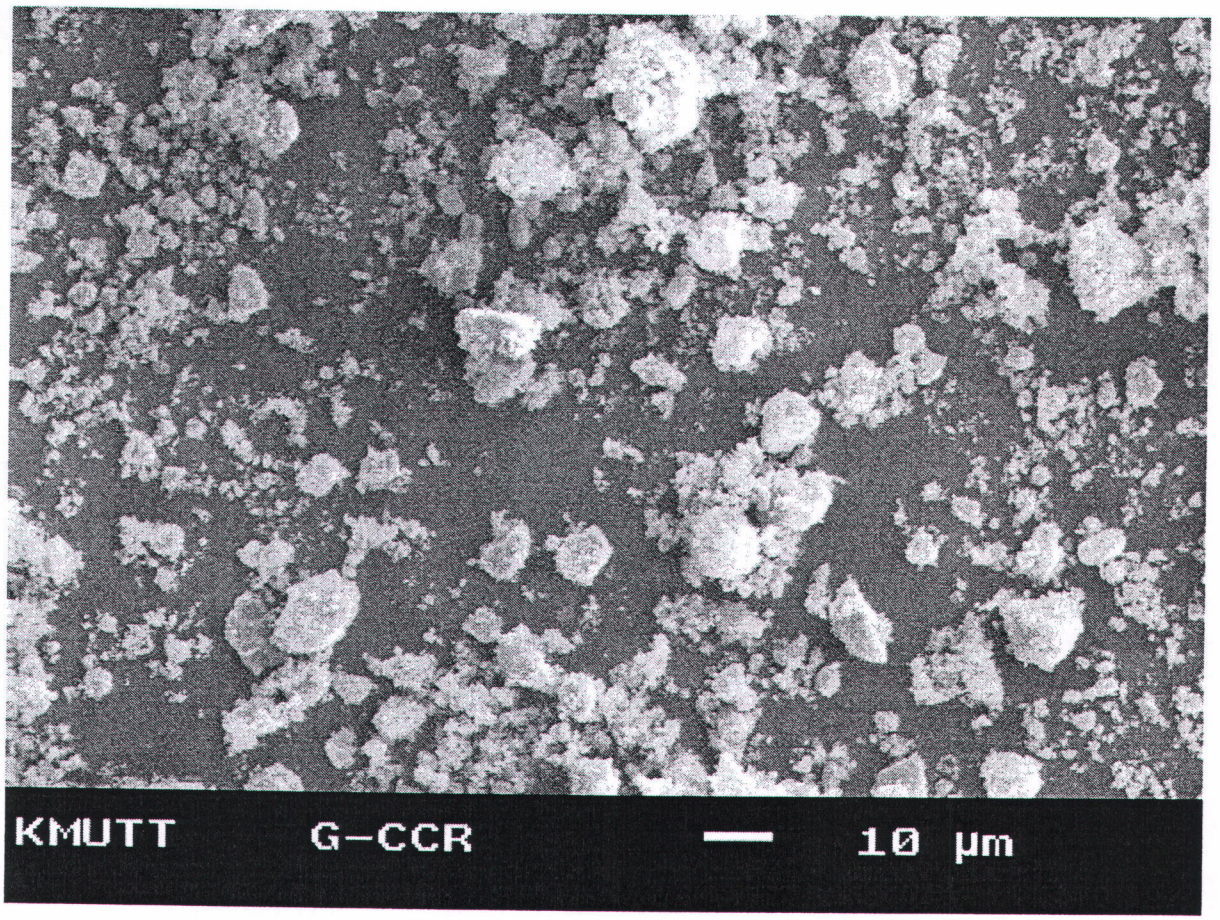

Fig2b.eps

Journal of Materials in Civil Engineering. Submitted July 21, 2009; accepted May 7, 2010;
posted ahead of print May 13, 2010. doi:10.1061/(ASCE)MT.1943-5533.0000127

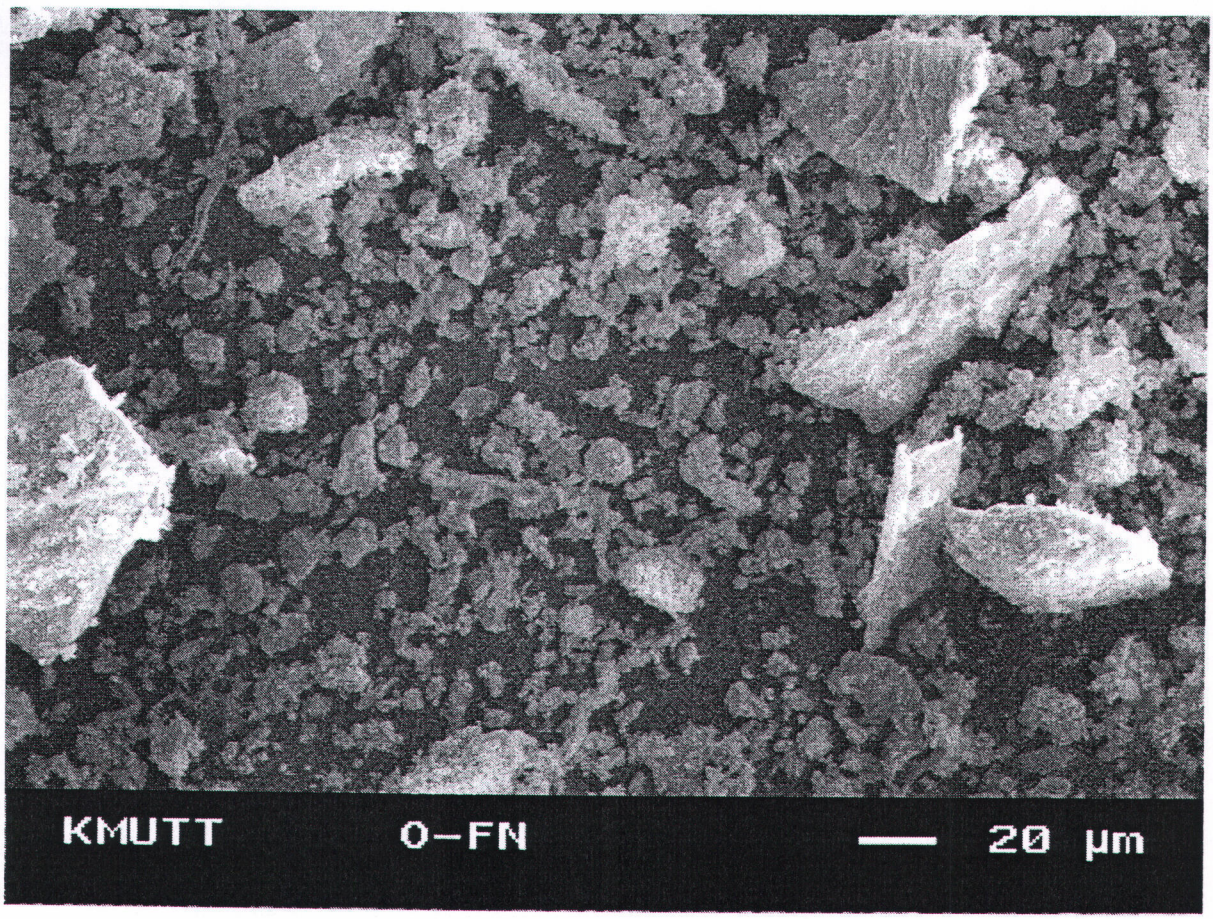

Fig2c.eps

Journal of Materials in Civil Engineering. Submitted July 21, 2009; accepted May 7, 2010;
posted ahead of print May 13, 2010. doi:10.1061/(ASCE)MT.1943-5533.0000127

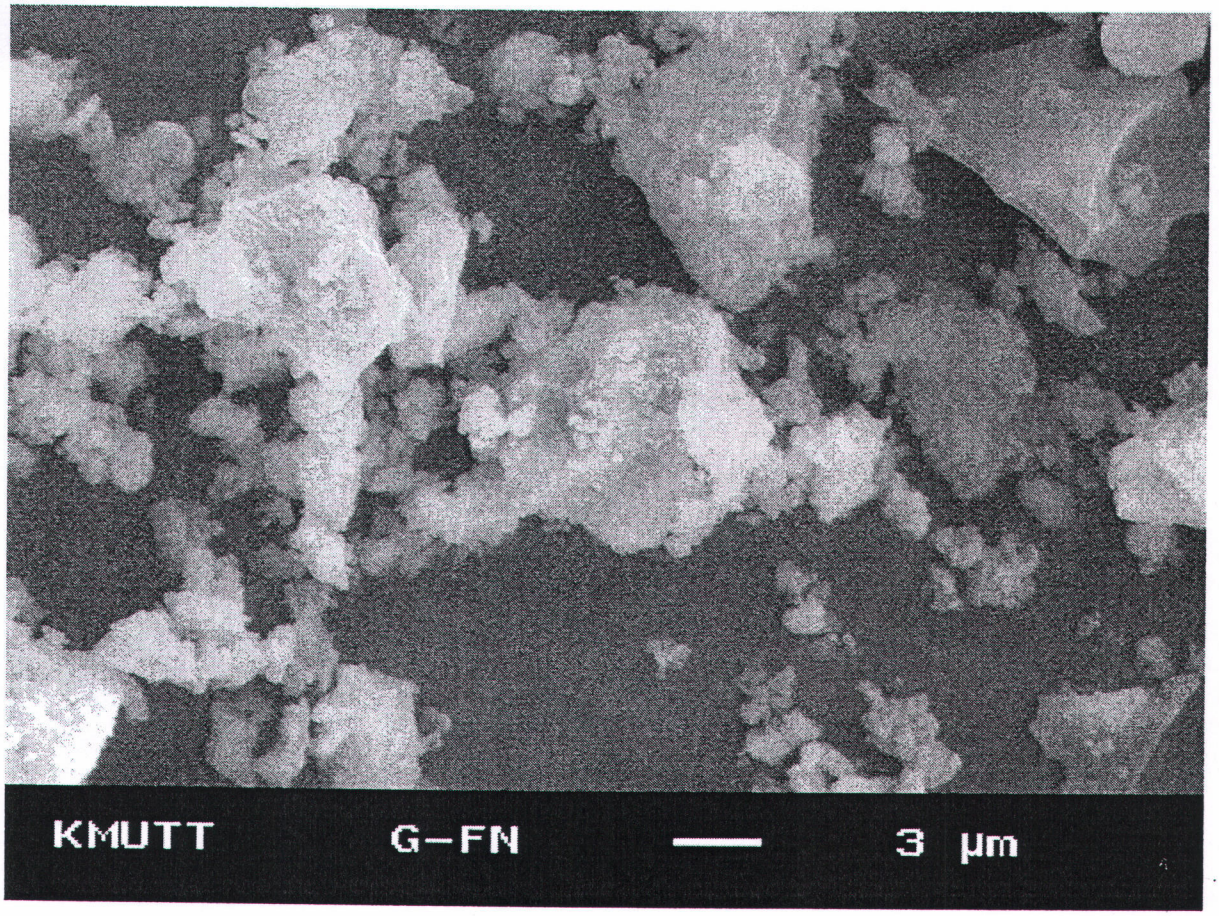

Fig3.eps

Journal of Materials in Civil Engineering. Submitted July 21, 2009; accepted May 7, 2010;
posted ahead of print May 13, 2010. doi:10.1061/(ASCE)MT.1943-5533.0000127

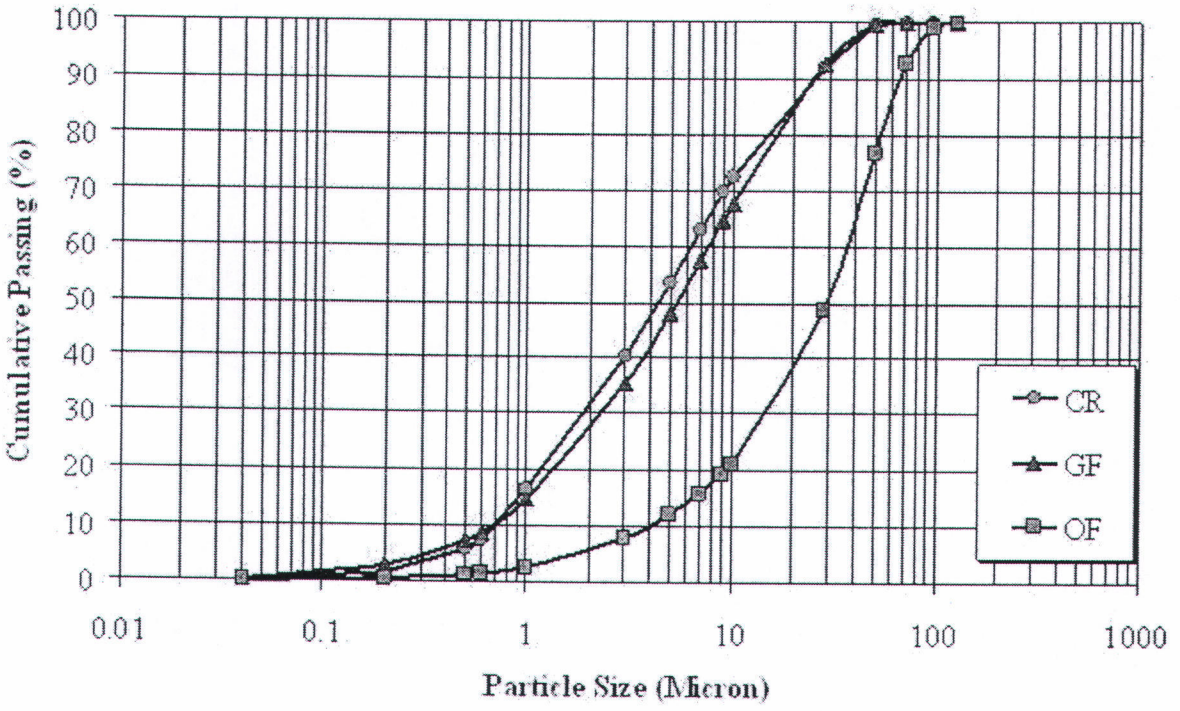

Fig4.eps

Journal of Materials in Civil Engineering. Submitted July 21, 2009; accepted May 7, 2010;
posted ahead of print May 13, 2010. doi:10.1061/(ASCE)MT.1943-5533.0000127

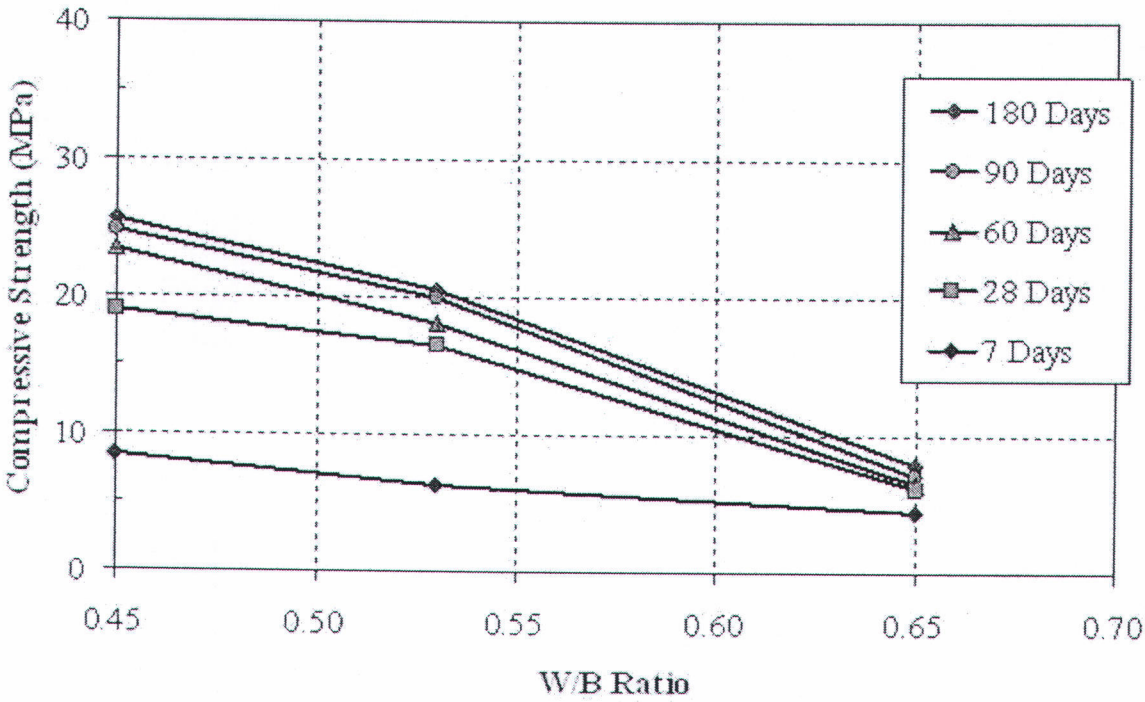

Fig5.eps

Journal of Materials in Civil Engineering. Submitted July 21, 2009; accepted May 7, 2010;
posted ahead of print May 13, 2010. doi:10.1061/(ASCE)MT.1943-5533.0000127

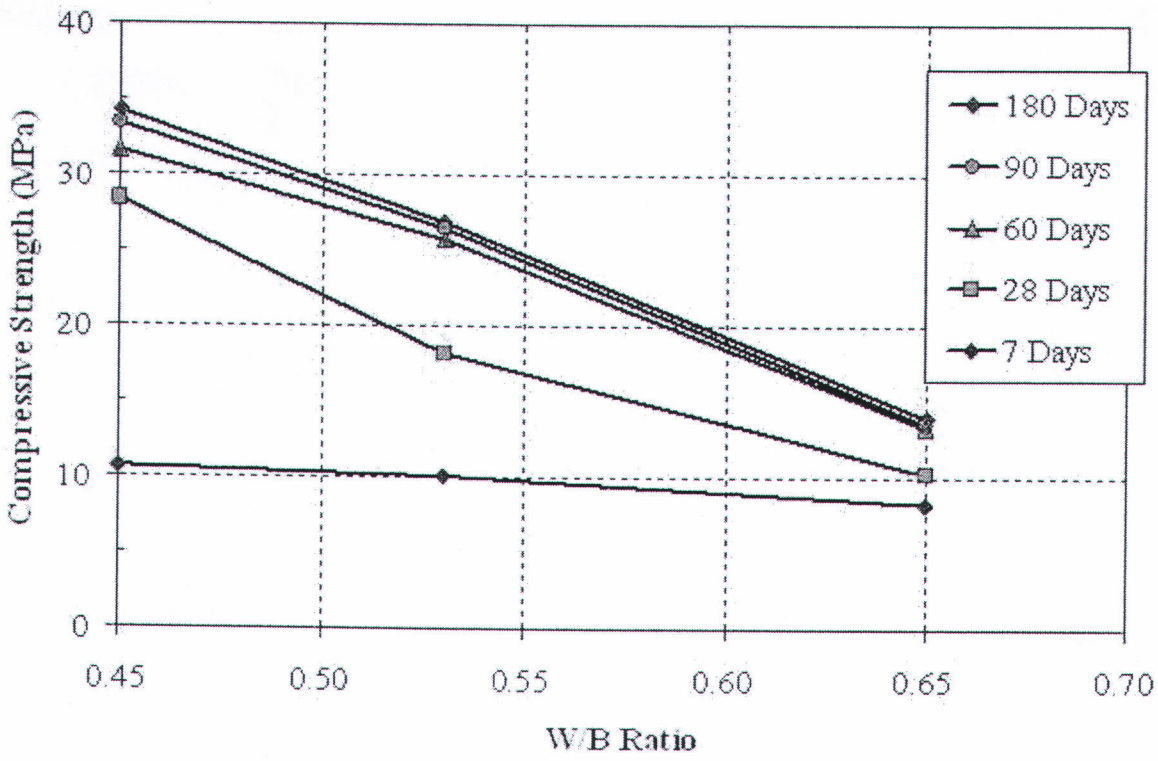

Fig6.eps

Journal of Materials in Civil Engineering. Submitted July 21, 2009; accepted May 7, 2010;
posted ahead of print May 13, 2010. doi:10.1061/(ASCE)MT.1943-5533.0000127

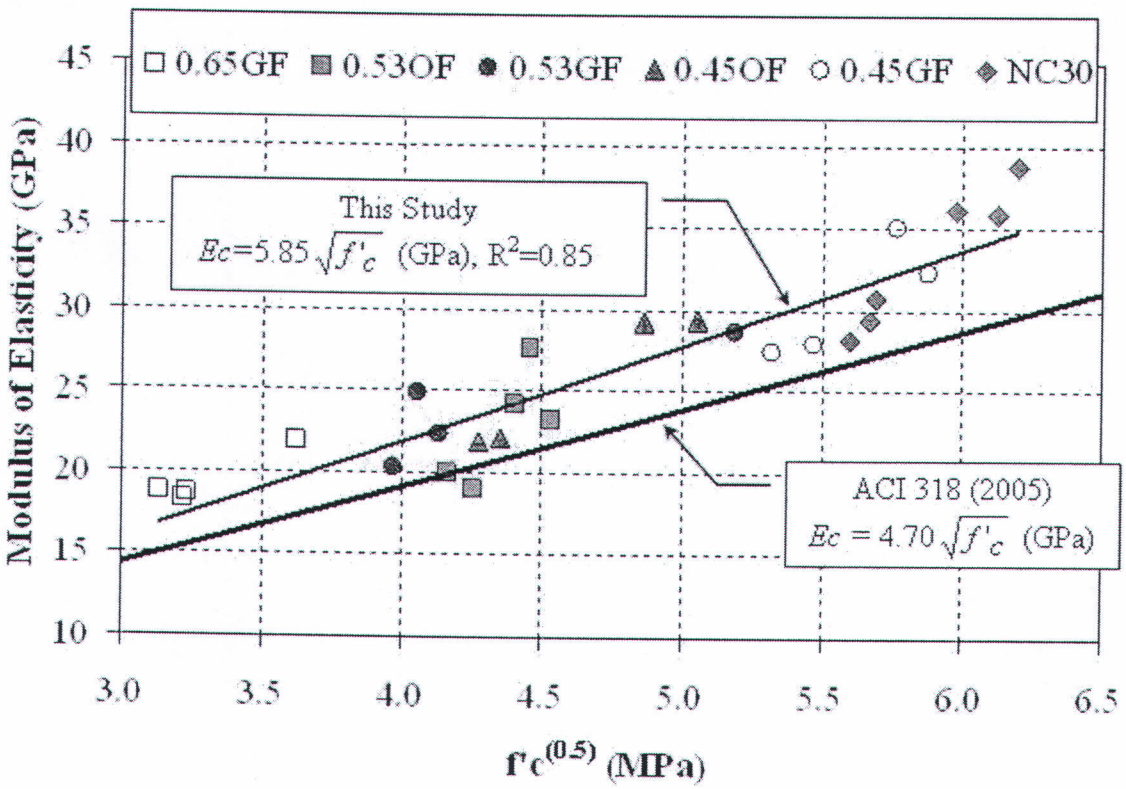

เอกสารคำขอจดสิทธิบัตร ที่ 100100038 เรื่อง **"กรรมวิธีการผลิตวัสดุประสานสำหรับผลิตคอนกรีตซึ่งมีกำลังสูง มีความร้อนต่ำ และมีความทนทานสูง"**

คำขอรับสิทธิบัตร/อนุสิทธิบัตร

☐ การประดิษฐ์
☐ การออกแบบผลิตภัณฑ์
☐ อนุสิทธิบัตร

ข้าพเจ้าผู้ลงลายมือชื่อในคำขอรับสิทธิบัตร/อนุสิทธิบัตรนี้ขอรับสิทธิบัตร/อนุสิทธิบัตร ตามพระราชบัญญัติสิทธิบัตร พ.ศ. 2522 แก้ไขเพิ่มเติมโดยพระราชบัญญัติสิทธิบัตร (ฉบับที่ 2) พ.ศ. 2535 และพระราชบัญญัติสิทธิบัตร (ฉบับที่ 3) พ.ศ. 2542

สำหรับเจ้าหน้าที่	
วันรับคำขอ - 14 มี.ค. 2555 วันยื่นคำขอ	เลขที่คำขอ 1001000038
สัญลักษณ์จำแนกการประดิษฐ์ระหว่างประเทศ	
ใช้กับแบบผลิตภัณฑ์ ประเภทผลิตภัณฑ์	
วันประกาศโฆษณา	เลขที่ประกาศโฆษณา
วันออกสิทธิบัตร/อนุสิทธิบัตร	เลขที่สิทธิบัตร/อนุสิทธิบัตร
ลายมือชื่อเจ้าหน้าที่	

1. ชื่อที่แสดงถึงการประดิษฐ์/~~การออกแบบผลิตภัณฑ์~~

"กรรมวิธีการผลิตวัสดุประสานสำหรับผลิตคอนกรีตซึ่งมีกำลังสูง มีความร้อนต่ำ และมีความทนทานสูง"

2. คำขอรับสิทธิบัตรการออกแบบผลิตภัณฑ์นี้เป็นคำขอสำหรับแบบผลิตภัณฑ์อย่างเดียวกันและเป็นคำขอลำดับที่
ในจำนวน คำขอ ที่ยื่นในคราวเดียวกัน

3. ผู้ขอรับสิทธิบัตร/อนุสิทธิบัตร และที่อยู่ (เลขที่ ถนน จังหวัด ประเทศ)

มหาวิทยาลัยเทคโนโลยีพระจอมเกล้าธนบุรี
126 ถ.ประชาอุทิศ แขวงบางมด เขตทุ่งครุ กรุงเทพฯ 10140 และ
สำนักงานกองทุนสนับสนุนการวิจัย ตั้งอยู่ที่ชั้น 14 อาคาร เอส เอ็ม ทาวเวอร์ เลขที่ 979/17-21 ถนนพหลโยธิน แขวงสามเสนใน เขตพญาไท กรุงเทพฯ 10400

3.1 สัญชาติ **ไทย**
3.2 โทรศัพท์ 0-2470-9685-8
3.3 โทรสาร 0-2872-9083
3.4 อีเมล์ research@kmutt.ac.th

4. สิทธิในการขอรับสิทธิบัตร/อนุสิทธิบัตร
☐ ผู้ประดิษฐ์/ผู้ออกแบบ ☐ ผู้รับโอน ☐ ผู้ขอรับสิทธิโดยเหตุอื่น

5. ตัวแทน (ถ้ามี)/ ที่อยู่ (เลขที่ ถนน จังหวัด ประเทศ, รหัสไปรษณีย์)

นางสาวผ่องศรี เวสารัช และ/หรือ นางสาวเชิญจันทร์ สนธิธรรม
ศูนย์ส่งเสริมงานวิจัยและทรัพย์สินทางปัญญา
มหาวิทยาลัยเทคโนโลยีพระจอมเกล้าธนบุรี
126 ถ.ประชาอุทิศ แขวงบางมด เขตทุ่งครุ กรุงเทพฯ 10140

5.1 ตัวแทนเลขที่ 1745,1739
5.2 โทรศัพท์ 0-2470-9685-8
5.3 โทรสาร 0-2872-9083
5.4 อีเมล์ research@kmutt.ac.th

6. ผู้ประดิษฐ์/~~ผู้ออกแบบผลิตภัณฑ์~~ และที่อยู่ (เลขที่ ถนน จังหวัด ประเทศ)

1.นายชัย จาตุรพิทักษ์กุล บ้านเลขที่ 71/51 ซอยวุฒากาศ 53 แขวงบางค้อ เขตจอมทอง กรุงเทพฯ 10150 2. นายณัฐพงศ์ มกระธัช อยู่บ้านเลขที่ 710/155 ซอยแก้วทอง 2 ถนนวัดแก้ว-ฉิมพลี แขวงคลองชักพระ เขตตลิ่งชัน กรุงเทพฯ 10170 3.นายกิตติพงศ์ อำนาจเหนือ อยู่บ้านเลขที่ 89 หมู่ 5 แขวงเวินพระบาท เขตสามพราน นครปฐม 73110

7. คำขอรับสิทธิบัตร/อนุสิทธิบัตรนี้แยกจากหรือเกี่ยวข้องกับคำขอเดิม

ผู้ขอรับสิทธิบัตร/อนุสิทธิบัตรขอให้ถือว่าได้ยื่นคำขอรับสิทธิบัตร/อนุสิทธิบัตรนี้ไว้ในวันเดียวกับคำขอรับสิทธิบัตรเลขที่ วันยื่น เพราะคำขอรับสิทธิบัตร/อนุสิทธิบัตรนี้แยกจากหรือเกี่ยวข้องกับคำขอเดิมเพราะ

☐ คำขอเดิมมีการประดิษฐ์หลายอย่าง ☐ ถูกคัดค้านเนื่องจากผู้ขอไม่มีสิทธิ ☐ ขอเปลี่ยนแปลงประเภทของสิทธิ

หมายเหตุ ในกรณีที่ไม่อาจระบุรายละเอียดได้ครบถ้วน ให้จัดทำเป็นเอกสารแนบท้ายแบบพิมพ์นี้โดยระบุหมายเลขกำกับข้อและหัวข้อที่แสดง

รายละเอียดการประดิษฐ์

ชื่อที่แสดงถึงการประดิษฐ์

กรรมวิธีการผลิตวัสดุประสานสำหรับผลิตคอนกรีตซึ่งมีกำลังสูง มีความร้อนต่ำ และมีความทนทานสูง

สาขาวิทยาการที่เกี่ยวข้องกับการประดิษฐ์

วิทยาการด้านวิศวกรรมในส่วนที่เกี่ยวกับวัสดุประสานชนิดใหม่สำหรับผลิตคอนกรีตซึ่งมีกำลังสูง มีความร้อนต่ำ และมีความทนทานสูง ทำจากส่วนผสมระหว่างกากแคลเซียมคาร์ไบด์และเถ้าถ่านหิน

ภูมิหลังของศิลปะหรือวิทยาการที่เกี่ยวข้อง

กากแคลเซียมคาร์ไบด์เป็นส่วนที่เหลือจากการทำปฏิกิริยาเคมีระหว่างแคลเซียมคาร์ไบด์กับน้ำในกระบวนการผลิตก๊าซอะเซทิลีน ซึ่งเป็นก๊าซที่ใช้กันมากในอุตสาหกรรมเชื่อมประสาน โดยปกติกากแคลเซียมคาร์ไบด์ที่ปล่อยทิ้งจากโรงงานอยู่ในรูปของแคลเซียมไฮดรอกไซด์ ($Ca(OH)_2$) ซึ่งแสดงในสมการที่ 1 ในสถานะของเหลว เป็นโคลนเหลวสีเทาอมขาว มีสภาพความเป็นด่างสูง เมื่อปล่อยให้ตกตะกอนและแห้งตามธรรมชาติจะจับตัวเป็นก้อนและมีสีขาวเพิ่มขึ้นเมื่อความชื้นมีปริมาณลดลง

$$CaC_2 + 2H_2O \rightarrow C_2H_2 + Ca(OH)_2 \qquad \text{(สมการที่ 1)}$$

วัสดุปอซโซลาน (Pozzolan) ตามคำจำกัดความของมาตรฐาน ASTM C 618 (2001) หมายถึง วัสดุที่ประกอบด้วยออกไซด์ของซิลิกา (Siliceous) หรือ ซิลิกาและอลูมินา (Siliceous and Aluminous) เป็นองค์ประกอบหลัก วัสดุปอซโซลานโดยทั่วไปมีคุณสมบัติของวัสดุประสานน้อยมากหรือไม่มีเลย แต่เมื่อวัสดุปอซโซลานมีความละเอียดสูงและมีความชื้นที่เพียงพอสามารถทำปฏิกิริยากับด่างหรือแคลเซียมไฮดรอกไซด์ ($Ca(OH)_2$) ทำให้ได้สารประกอบที่มีคุณสมบัติในการยึดประสานได้ดีคล้ายกับปูนซีเมนต์ เรียกปฏิกิริยาที่เกิดขึ้นนี้ว่าปฏิกิริยาปอซโซลาน (Pozzolanic reaction)

เถ้าถ่านหินได้จากการเผาถ่านหินซึ่งใช้เป็นเชื้อเพลิงในการผลิตกระแสไฟฟ้าหรืออุตสาหกรรมอื่นที่ใช้ถ่านหินเป็นเชื้อเพลิง มีลักษณะเป็นผงละเอียด ขนาดอนุภาคตั้งแต่ 1-150 ไมโครเมตร มีสีเทา เทาดำ หรือสีน้ำตาล ในกระบวนการเผาถ่านหินจะได้เถ้าถ่านหินลอยขึ้นไปด้านบนเนื่องจากอนุภาคของเถ้าถ่านหินมีน้ำหนักเบาจึงถูกพัดออกมาตามปล่องควันพร้อมไอร้อนจากการเผาไหม้ และดักจับเถ้าถ่านหินด้วยเครื่องดักจับแบบไฟฟ้าสถิต (Electrostatic precipitator) จากนั้นลำเลียงไปเก็บไว้ในไซโลเพื่อรวบรวมและนำไปทิ้งหรือนำไปใช้ต่อไป

เถ้าถ่านหินจัดเป็นวัสดุปอซโซลานชนิดหนึ่ง ซึ่งประกอบด้วยออกไซด์ของแร่ธาตุต่าง ๆ หลายชนิด โดยมีซิลิกาออกไซด์ (SiO_2) อลูมินาออกไซด์ (Al_2O_3) และเฟอร์ริกออกไซด์ (Fe_2O_3) เป็นองค์ประกอบหลัก ตามมาตรฐาน ASTM C 618 (2001) ได้แบ่งเถ้าถ่านหินตามองค์ประกอบทาง

เคมีเป็น 2 ประเภท คือ Class F และ Class C โดยพิจารณาจากผลรวมของ $SiO_2+Al_2O_3+Fe_2O_3$ กล่าวคือ เถ้าถ่านหิน Class F ต้องมีผลรวมของ $SiO_2+Al_2O_3+Fe_2O_3$ รวมกันมากกว่าร้อยละ 70 โดยน้ำหนัก ส่วนใหญ่มักได้จากการเผาถ่านหินประเภทแอนทราไซต์ หรือบิทูมินัส ส่วนเถ้าถ่านหิน Class C ต้องมีผลรวมของ $SiO_2+Al_2O_3+Fe_2O_3$ อยู่ระหว่าง 50-70 โดยน้ำหนัก และส่วนใหญ่ได้จากการเผาถ่านหินประเภทลิกไนต์ หรือซับบิทูมินัส โดยทั่วไปเถ้าถ่านหิน Class F มีปริมาณแคลเซียมออกไซด์ค่อนข้างต่ำ คือ น้อยกว่าร้อยละ 5 ซึ่งบางครั้งเรียกว่า Low-Calcium Fly Ash ส่วนเถ้าถ่านหิน Class C มีปริมาณแคลเซียมออกไซด์ มากกว่าร้อยละ 10 และเรียกว่า High-Calcium Fly Ash ซึ่งมีคุณสมบัติของซีเมนต์ร่วมกับคุณสมบัติปอซโซลานในตัวเอง

สถาบันคอนกรีตอเมริกัน (American Concrete Institute, ACI 363 (2008)) กำหนดให้คอนกรีตทรงกระบอกเส้นผ่านศูนย์กลาง 15 ซม สูง 30 ซม ที่มีกำลังอัดที่อายุ 28 วัน มากกว่า 410 กก/ซม^2 ถือว่าเป็นคอนกรีตกำลังสูง ข้อดีของคอนกรีตกำลังสูงคือ สามารถลดขนาดและน้ำหนักของโครงสร้างได้ โดยเฉพาะการก่อสร้างอาคารสูงหรือสะพานที่มีช่วงความยาวมาก ๆ ซึ่งทำให้ขนาดของโครงสร้าง เช่น เสา หรือ คาน ลดลง โดยทั่วไปการทำคอนกรีตกำลังสูงนิยมใส่สารเคมีผสมเพิ่มประเภทสารลดน้ำพิเศษเพื่อลดอัตราส่วนน้ำต่อปูนซีเมนต์ให้ต่ำลง และใส่สารผสมเพิ่มประเภทวัสดุปอซโซลานเพื่อเพิ่มกำลังอัดประลัยเมื่อคอนกรีตมีอายุมากขึ้น จากการศึกษาที่ผ่านมาพบว่าเถ้าถ่านหินที่นำมาใช้ในงานคอนกรีตกำลังสูงมักใช้เถ้าถ่านหินที่มีความละเอียดสูง และในประเทศไทยมีเถ้าถ่านหินที่มีความละเอียดสูงซึ่งได้จากการบดหรือแยกขนาดของเถ้าถ่านหินจากโรงงานให้ละเอียดมากขึ้น

งานโครงสร้างคอนกรีตขนาดใหญ่และต้องรับน้ำหนักบรรทุกสูงมาก ๆ เช่น ฐานราก เขื่อน ตอม่อ ทำให้การเทคอนกรีตในบางครั้งต้องทำการเทครั้งเดียวอย่างต่อเนื่องในปริมาณมาก ๆ ซึ่งเรียกว่า คอนกรีตหลา และส่วนใหญ่จะเกิดปัญหาในขณะที่คอนกรีตเริ่มแข็งตัวคือ อุณหภูมิที่ผิวภายนอกกับอุณหภูมิภายในเนื้อคอนกรีตมีค่าแตกต่างกันมากจนทำให้เกิดการหดตัวที่ไม่เท่ากันและเกิดการแตกร้าวที่ผิวของคอนกรีตขึ้นได้ ทำให้การรับกำลังของคอนกรีตลดลงและนำมาซึ่งปัญหาการกัดกร่อนต่อเหล็กเสริมภายในเมื่อใช้งานเป็นระยะเวลานาน ๆ จากปัญหาดังกล่าวผู้ใช้คอนกรีตในงานโครงสร้างขนาดใหญ่จึงได้พยายามลดผลต่างของอุณหภูมิภายในและที่ผิวภายนอกของคอนกรีตด้วยวิธีการต่าง ๆ เช่น การลดปริมาณคอนกรีตที่เทโดยแบ่งเป็นส่วน ๆ การฝังท่อน้ำในคอนกรีตเพื่อระบายความร้อน และการใช้น้ำแข็งในการผสมคอนกรีต เป็นต้น ซึ่งเทคนิคดังกล่าวเป็นการแก้ปัญหาทางอ้อม แต่มีอีกวิธีหนึ่งซึ่งเป็นการแก้ปัญหาโดยตรง คือ การลดปริมาณปูนซีเมนต์ที่ใช้ในส่วนผสมคอนกรีตให้น้อยลง เพราะปูนซีเมนต์เมื่อทำปฏิกิริยากับน้ำจะคายความร้อนออกมา หรือใช้วัสดุประสานที่มีการคายความร้อนต่ำในส่วนผสมคอนกรีต

การนำคอนกรีตไปใช้ในงานก่อสร้างต้องคำนึงถึงความทนทานต่อสภาพอากาศและสิ่งแวดล้อมด้วยนอกเหนือจากการพิจารณาด้านกำลังอัด โดยเฉพาะความทนทานต่อการซึมของน้ำหรือของเหลวที่ผ่านเข้าไปในเนื้อของคอนกรีต โดยทั่วไปคอนกรีตไม่ได้เป็นวัสดุที่ทึบน้ำแต่เป็นวัสดุที่น้ำซึมผ่านได้ในอัตราที่ช้า เมื่อน้ำหรือของเหลวไม่สามารถซึมผ่านเข้าไปในเนื้อคอนกรีตได้หรือซึมผ่านได้ช้าลง สารละลายต่าง ๆ ที่จะซึมเข้าไปทำลายในเนื้อคอนกรีตย่อมลดลง ส่งผลให้คอนกรีตมีอายุการใช้งานที่ยาวมากขึ้น

จากปัญหามลภาวะต่อสิ่งแวดล้อมเนื่องจากการกองเก็บและการทิ้งกากแคลเซียมคาร์ไบด์รวมถึงเถ้าถ่านหินในปัจจุบัน การประดิษฐ์นี้จึงมุ่งเน้นนำกากแคลเซียมคาร์ไบด์มาผสมกับเถ้าถ่านหินเพื่อใช้เป็นวัสดุประสานสำหรับผลิตคอนกรีตกำลังธรรมดา คอนกรีตกำลังสูง รวมถึงคอนกรีตขนาดใหญ่ที่มีความร้อนต่ำและความทนทานสูง โดยอาศัยปฏิกิริยาปอซโซลานระหว่างวัสดุทั้งสอง ซึ่งเป็นการลดพลังงานที่ใช้ในการผลิตปูนซีเมนต์ และยังเป็นการลดมลภาวะต่อสิ่งแวดล้อมที่เกิดจากการเผาปูนซีเมนต์ ปี ค.ศ. 2003 งานวิจัยของ Jaturapitakkul และ Roongreung (2003) รายงานว่ากากแคลเซียมคาร์ไบด์ประกอบไปด้วยแคลเซียมไฮดรอกไซด์ ($Ca(OH)_2$) ในปริมาณที่สูง สามารถทำปฏิกิริยาปอซโซลานกับเถ้าแกลบที่เผาในเตาเฟอร์โรซีเมนต์ กำลังอัดของมอร์ต้าร์ที่ได้จากส่วนผสมระหว่างกากแคลเซียมคาร์ไบด์และเถ้าแกลบในอัตราส่วนร้อยละ 50:50 โดยน้ำหนัก มีศักยภาพสูงพอที่จะนำมาใช้เป็นวัสดุประสานแทนปูนซีเมนต์ได้ ปี พ.ศ. 2539 ปิติศานต์ กร้ำมาตร และคณะ (2539) ได้นำส่วนผสมของกากแคลเซียมคาร์ไบด์กับเถ้าถ่านหินมาใช้เป็นวัสดุประสานแทนปูนซีเมนต์ โดยพบว่าอัตราส่วนผสมระหว่างกากแคลเซียมคาร์ไบด์กับเถ้าถ่านหิน ในอัตราร้อยละ 30:70 โดยน้ำหนัก ให้กำลังอัดของมอร์ต้าร์ที่อายุ 90 วัน สูงถึง 209 กก/ซม^2 และยังแนะนำว่าส่วนผสมของวัสดุทั้งสองชนิดนี้มีความเป็นไปได้ที่จะพัฒนาให้เป็นประโยชน์ในการก่อสร้างโดยควรมีการวิจัยเพิ่มเติม

งานวิจัยที่ผ่านมาเห็นได้ชัดว่ากากแคลเซียมคาร์ไบด์และเถ้าถ่านหินมีศักยภาพที่จะนำมาประดิษฐ์เป็นวัสดุประสานสำหรับผลิตคอนกรีต ดังนั้นหากมีการพัฒนาวัสดุประสานจากส่วนผสมระหว่างกากแคลเซียมคาร์ไบด์และเถ้าถ่านหินให้มีประสิทธิภาพสูงขึ้นเพื่อใช้เป็นวัสดุประสานในการประดิษฐ์คอนกรีตซึ่งมีกำลังสูง มีความร้อนต่ำ และมีความทนทานสูงได้ ก็จะเป็นประโยชน์ต่อภาคอุตสาหกรรมการผลิตคอนกรีต โดยการนำวัสดุประสานชนิดใหม่นี้มาใช้แทนปูนซีเมนต์ปอร์ตแลนด์

ลักษณะและความมุ่งหมายการประดิษฐ์โดยย่อ

การประดิษฐ์นี้ใช้กากแคลเซียมคาร์ไบด์จากโรงงานผลิตก๊าซอะเซทิลีนมาทำการปรับปรุงคุณภาพด้วยการบดให้มีความละเอียดมากขึ้น นอกจากนี้ทำการบดเถ้าถ่านหินด้วยเครื่องบดวัสดุเช่นกัน โดยให้มีปริมาณอนุภาคค้างบนตะแกรงมาตรฐานเบอร์ 325 ไม่เกินร้อยละ 3 จากนั้นนำกากแคลเซียม

คาร์ไบด์ผสมกับเถ้าถ่านหินในอัตราส่วน 30:70 โดยน้ำหนัก เพื่อใช้เป็นวัสดุประสานในการหล่อคอนกรีตทรงกระบอกขนาดเส้นผ่านศูนย์กลาง 10 เซนติเมตร สูง 20 เซนติเมตร ทำการทดสอบหาระยะเวลาในการก่อตัวของคอนกรีต ทดสอบกำลังอัดของคอนกรีตที่อายุ 7, 28, 60 และ 90 วัน ทดสอบหาความร้อนที่เกิดจากคอนกรีตสดในทุกอัตราส่วนผสม นอกจากนี้ยังทำการทดสอบหาค่าอัตราการซึมของน้ำผ่านคอนกรีตที่อายุ 90 วัน

ความมุ่งหมายของการประดิษฐ์นี้เพื่อพัฒนาวัสดุประสานที่ทำจากส่วนผสมระหว่างกากแคลเซียมคาร์ไบด์และเถ้าถ่านหิน สำหรับนำมาใช้ในงานคอนกรีตกำลังธรรมดา หรือคอนกรีตกำลังสูงซึ่งมีความร้อนต่ำ และมีความทนทานสูง โดยกำลังอัดของคอนกรีตมีค่ามากกว่า 200 กก/ซม^2 ที่อายุ 7 วันขึ้นไป ความร้อนที่วัดได้จากคอนกรีตสดต้องไม่แตกต่างจากอุณหภูมิสภาวะแวดล้อมมากนัก และคอนกรีตมีความทนทานสูงเนื่องจากน้ำซึมผ่านคอนกรีตได้ยาก การประดิษฐ์วัสดุประสานชนิดใหม่นี้จะเป็นการกระตุ้นให้ลดปริมาณการใช้ปูนซีเมนต์ลง ซึ่งการลดการใช้ปูนซีเมนต์ลงย่อมทำให้การผลิตปูนซีเมนต์ลดลง เป็นผลให้เป็นการลดพลังงานที่ใช้ในการผลิตปูนซีเมนต์ได้ และลดมลภาวะที่เกิดจากการปล่อยก๊าซคาร์บอนไดออกไซด์ออกสู่ชั้นบรรยากาศ รวมทั้งการกองเก็บกากแคลเซียมคาร์ไบด์และเถ้าถ่านหินได้อีกด้วย

คำอธิบายรูปเขียนโดยย่อ

ตารางที่ 1 แสดงอัตราส่วนผสมของคอนกรีตที่ใช้ในการประดิษฐ์นี้

ตารางที่ 2 แสดงระยะเวลาการก่อตัวของคอนกรีตที่ใช้กากแคลเซียมคาร์ไบด์-เถ้าถ่านหินและคอนกรีตทั่วไปที่ใช้ปูนซีเมนต์ปอร์ตแลนด์เป็นวัสดุประสาน

ตารางที่ 3 แสดงค่ากำลังอัดของคอนกรีตที่ใช้กากแคลเซียมคาร์ไบด์-เถ้าถ่านหินเป็นวัสดุประสานและคอนกรีตทั่วไปที่ใช้ปูนซีเมนต์ปอร์ตแลนด์เป็นวัสดุประสานที่อายุต่าง ๆ

รูปที่ 1 แสดงความสัมพันธ์ระหว่างกำลังอัดของคอนกรีตที่ใช้กากแคลเซียมคาร์ไบด์-เถ้าถ่านหินเป็นวัสดุประสาน โดยมีปูนซีเมนต์เป็นตัวเร่งกำลังในอัตราการแทนที่ร้อยละ 0, 5, 10, 15 และ 20 โดยน้ำหนักวัสดุประสาน กับอายุในการบ่ม

ตารางที่ 4 แสดงความร้อนที่วัดได้จากคอนกรีตสด

รูปที่ 2 แสดงความสัมพันธ์ระหว่างอุณหภูมิที่เพิ่มขึ้นของคอนกรีตสด ที่ใช้กากแคลเซียมคาร์ไบด์-เถ้าถ่านหินเป็นวัสดุประสาน โดยมีปูนซีเมนต์เป็นตัวเร่งกำลังในอัตราการแทนที่ร้อยละ 0, 5, 10, 15 และ 20 โดยน้ำหนักวัสดุประสาน กับระยะเวลาหลังทำการหล่อคอนกรีต

ตารางที่ 5 แสดงค่าสัมประสิทธิ์การซึมของน้ำผ่านคอนกรีต ที่อายุ 90 วัน

ความหมายของสัญลักษณ์ย่อ โดยสังเขป CR คือ กากแคลเซียมคาร์ไบด์ FM คือ เถ้าถ่านหิน ตัวเลข 5, 10, 15 และ 20 หลังอักษร FM หมายถึง ร้อยละของปูนซีเมนต์ปอร์ตแลนด์ที่ใช้แทนที่วัสดุประสานโดยน้ำหนักเพื่อใช้เป็นตัวเร่งกำลังในระยะต้น สำหรับ NC70 หมายถึง คอนกรีตทั่วไป

ที่ใช้ปูนซีเมนต์ปอร์ตแลนด์เป็นวัสดุประสาน โดยมีค่าอัตราส่วนระหว่างน้ำต่อวัสดุประสาน เท่ากับ 0.25

การเปิดเผยการประดิษฐ์โดยสมบูรณ์

กรรมวิธีการผลิตวัสดุประสานสำหรับผลิตคอนกรีตซึ่งมีกำลังสูง มีความร้อนต่ำ และมีความทนทานสูง มีวัสดุที่เป็นส่วนผสมดังนี้

-กากแคลเซียมคาร์ไบด์ ร้อยละ 30 โดยน้ำหนัก
-เถ้าถ่านหิน ร้อยละ 70 โดยน้ำหนัก
-ปูนซีเมนต์ปอร์ตแลนด์ ประเภทที่ 1
-น้ำสะอาด
-ทรายแม่น้ำ หรือทรายประดิษฐ์ (Manufactured sand)
-หินย่อยจากธรรมชาติ
-สารลดน้ำพิเศษ (Superplasticizer Type F)

กรรมวิธีการผลิตวัสดุประสานสำหรับผลิตคอนกรีตซึ่งมีกำลังสูง มีความร้อนต่ำ และมีความทนทานสูง ประกอบไปด้วยขั้นตอนดังต่อไปนี้

1. นำกากแคลเซียมคาร์ไบด์และเถ้าถ่านหินมาบดจนมีปริมาณอนุภาคค้างบนตะแกรงมาตรฐานเบอร์ 325 น้อยกว่าร้อยละ 3 โดยน้ำหนัก
2. นำกากแคลเซียมคาร์ไบด์มาผสมกับเถ้าถ่านหินในอัตราส่วน 30:70 โดยน้ำหนัก เพื่อใช้เป็นวัสดุประสานในการหล่อตัวอย่างคอนกรีต
3. ทำการแทนที่วัสดุประสานในอัตราร้อยละ 0, 5, 10, 15 และ 20 โดยน้ำหนัก ด้วยปูนซีเมนต์ปอร์ตแลนด์ เพื่อใช้เป็นตัวเร่งกำลังอัดของคอนกรีต จากนั้นทำการผสมคอนกรีตโดยใช้อัตราส่วนผสมดังแสดงในตารางที่ 1
4. ทำการถอดแบบหล่อหลังจาก 24 ชั่วโมง จากนั้นนำไปบ่มในน้ำสะอาดเพื่อรอการทดสอบ

ตารางที่ 1 อัตราส่วนผสมของคอนกรีต

Concretes	Mixture proportions (kg/m^3)							W/B	Slump
	Cement	CR	FM	Water	Sand	Coarse Agg.	Super P.		(mm)
FM	-	165.0	385	135.55	765	980	3.9	0.25	185
FM5	27.5	156.8	365.8	135.40	765	980	4.2	0.25	190
FM10	55.0	148.5	346.5	135.30	770	985	4.4	0.25	185
FM15	82.5	140.3	327.3	135.70	770	985	3.6	0.25	170
FM20	110.0	132.0	308.0	135.80	770	990	3.4	0.25	165
NC70	550	-	-	135.45	800	1020	4.1	0.25	180

ตารางที่ 2 แสดงระยะเวลาในการก่อตัวของคอนกรีต พบว่าคอนกรีตที่ใช้กากแคลเซียมคาร์ไบด์-เถ้าถ่านหินเป็นวัสดุประสานโดยมีปูนซีเมนต์เป็นตัวเร่งกำลังมีระยะเวลาการก่อตัวทั้งระยะต้นและระยะปลายสั้นกว่าคอนกรีตทั่วไปที่ใช้ปูนซีเมนต์ปอร์ตแลนด์เป็นวัสดุประสาน นอกจากนี้ยังพบว่าเมื่อเพิ่มปริมาณปูนซีเมนต์เป็นตัวเร่งกำลังในอัตราส่วนที่สูงขึ้นส่งผลให้ระยะเวลาในการก่อตัวเร็วยิ่งขึ้น ทั้งนี้การเพิ่มปูนซีเมนต์เป็นการเพิ่ม C_3S และ C_3A ในส่วนผสม สำหรับคอนกรีต FM มีระยะเวลาในการก่อตัวทั้งระยะต้นและระยะปลายที่ใกล้เคียงกับคอนกรีตทั่วไป (NC70) เป็นที่น่าสังเกตว่าคอนกรีต FM20 มีระยะเวลาในการก่อตัวระยะต้นและระยะปลายเท่ากับ 2 ชั่วโมง 40 นาที และ 4 ชั่วโมง 30 นาที ในขณะที่คอนกรีต NC70 มีระยะเวลาในการก่อตัวระยะต้นและระยะปลาย เท่ากับ 5 ชั่วโมง 15 นาที และ 6 ชั่วโมง 35 นาที ตามลำดับ

ตารางที่ 2 ระยะเวลาการก่อตัวของคอนกรีต

Concretes	Initial setting times h:min	Final setting times h:min
FM	4:20	6:50
FM5	3:35	6:35
FM10	3:00	5:10
FM15	2:50	4:50
FM20	2:40	4:30
NC70	5:15	6:35

ค่ากำลังอัดของคอนกรีตได้แสดงในตารางที่ 3 นอกจากนี้รูปที่ 1 แสดงความสัมพันธ์ระหว่างกำลังอัดกับอายุการบ่มของคอนกรีตที่ใช้กากแคลเซียมคาร์ไบด์-เถ้าถ่านหินเป็นวัสดุประสาน โดยมีปูนซีเมนต์เป็นตัวเร่งกำลัง เพื่อแทนที่วัสดุประสานในอัตราส่วนร้อยละ 0, 5, 10, 15 และ 20 โดยน้ำหนัก ชี้ให้เห็นว่าคอนกรีตที่ใช้กากแคลเซียมคาร์ไบด์-เถ้าถ่านหินเป็นวัสดุประสานให้ค่ากำลังอัดสูงขึ้นตามอายุการบ่มที่เพิ่มขึ้น ซึ่งคล้ายกับคอนกรีตทั่วไปที่ใช้ปูนซีเมนต์ปอร์ตแลนด์เป็นวัสดุประสาน คอนกรีต FM5 (ใช้ปูนซีเมนต์ร้อยละ 5 เป็นตัวเร่งกำลัง) ให้ค่ากำลังอัดสูงถึง 475 กก/ซม^2 ที่อายุ 28 วัน ซึ่งถือได้ว่าคอนกรีตส่วนผสมนี้เป็นคอนกรีตกำลังสูงตามมาตรฐาน ACI 363 (2008) ที่ได้กำหนดไว้ นอกจากนี้เมื่อเพิ่มปริมาณการแทนที่ปูนซีเมนต์ให้สูงขึ้นส่งผลให้การพัฒนากำลังอัดของคอนกรีตที่ใช้กากแคลเซียมคาร์ไบด์-เถ้าถ่านหินเป็นวัสดุประสานมีค่าเพิ่มขึ้นตามไปด้วย สังเกตได้จากคอนกรีต FM20 เป็นคอนกรีตที่ให้ค่ากำลังอัดสูงที่สุดเมื่อเปรียบเทียบกับคอนกรีตที่ใช้กากแคลเซียมคาร์ไบด์-เถ้าถ่านหินเป็นวัสดุประสานส่วนผสมอื่น ๆ โดยคอนกรีต FM20 ให้ค่ากำลังอัด เท่ากับ 456, 678, 693 และ 727 กก/ซม^2 ที่อายุ 7, 28, 60 และ 90 วัน ตามลำดับ อย่างไรก็ตามกำลังอัดของคอนกรีต FM20 ต่ำกว่าคอนกรีตทั่วไปที่ใช้ปูนซีเมนต์ปอร์ตแลนด์เป็นวัสดุประสานเล็กน้อย โดยให้ค่ากำลังอัดคิดเป็นร้อยละ 77, 97, 94 และ 89 เมื่อเปรียบเทียบกับกำลังอัดของคอนกรีตทั่วไป (NC70) ที่อายุ 7, 28, 60 และ 90 วัน ตามลำดับ

ตารางที่ 3 กำลังอัดของคอนกรีต

Concretes	Compressive strength (ksc) – *Normalized Compressive Strength (%)*			
	7 days	28 days	60 days	90 days
FM	227-***38***	379-***54***	430-***58***	512-***63***
FM5	307-***52***	475-***68***	536-***72***	568-***70***
FM10	385-***65***	558-***80***	571-***77***	618-***76***
FM15	427-***72***	607-***87***	615-***83***	645-***80***
FM20	456-***77***	678-***97***	693-***94***	727-***89***
NC70	590-***100***	696-***100***	738-***100***	809-***100***

ค่าความร้อนของคอนกรีตสดที่เกิดขึ้นจากการทำปฏิกิริยา ได้แสดงในตารางที่ 4 และรูปที่ 2 แสดงความสัมพันธ์ของอุณหภูมิที่เพิ่มขึ้นของคอนกรีตสด ที่ใช้กากแคลเซียมคาร์ไบด์-เถ้าถ่านหินเป็นวัสดุประสาน โดยมีปูนซีเมนต์เป็นตัวเร่งกำลังในอัตราการแทนที่ร้อยละ 0, 5, 10, 15 และ 20 โดยน้ำหนักวัสดุประสาน โดยการวัดอุณหภูมิที่แกนกลางของคอนกรีต พบว่าคอนกรีตทั่วไป (NC70) ซึ่งใช้ปูนซีเมนต์ปอร์ตแลนด์เป็นวัสดุประสาน มีอุณหภูมิเพิ่มขึ้นสูงสุดที่ 42 องศาเซลเซียส หลังจากหล่อคอนกรีตแล้วเป็นเวลา 18 ชั่วโมง ในขณะที่คอนกรีตที่ใช้กากแคลเซียมคาร์ไบด์-เถ้าถ่านหินเป็นวัสดุประสานโดยมีปูนซีเมนต์เป็นตัวเร่งกำลังมีอุณหภูมิเพิ่มขึ้นที่ต่ำกว่าคอนกรีตทั่วไป (NC70) มาก นอกจากนี้ยังพบว่าการใช้ปูนซีเมนต์เป็นตัวเร่งกำลังในอัตราที่สูงขึ้นส่งผลให้อุณหภูมิสูงสุดเพิ่มขึ้นตามไปด้วย อย่างไรก็ตามอุณหภูมิสูงสุดที่วัดได้จากคอนกรีตสดที่ใช้กากแคลเซียมคาร์ไบด์-เถ้าถ่านหินเป็นวัสดุประสานโดยใช้ปูนซีเมนต์เป็นตัวเร่งกำลังยังต่ำกว่าคอนกรีตทั่วไปที่ใช้ปูนซีเมนต์ปอร์ตแลนด์ โดยคอนกรีต FM, FM5, FM10, FM15 และ FM20 มีอุณหภูมิที่เพิ่มขึ้นสูงสุดต่ำกว่าคอนกรีตทั่วไป (NC70) เท่ากับ 31, 28, 27, 25 และ 24 องศาเซลเซียส หรือคิดเป็นร้อยละ 26, 33, 35, 40 และ 43 ของอุณหภูมิของคอนกรีตทั่วไป (NC70) ตามลำดับ นอกจากนี้คอนกรีต FM, FM5, FM10, FM15 และ FM20 มีเวลาที่เกิดอุณหภูมิสูงสุด เท่ากับ 16, 22, 20, 18 และ 18 ชั่วโมง ภายหลังจากหล่อคอนกรีตตามลำดับ ชี้ให้เห็นว่าการใช้ปูนซีเมนต์เพื่อเร่งการเกิดปฏิกิริยาส่งผลให้เวลาในการเกิดอุณหภูมิสูงสุดเปลี่ยนแปลงน้อยมากหรืออาจสรุปได้ว่าไม่มีผลต่อเวลาในการเกิดอุณหภูมิสูงสุด ทั้งนี้อาจเป็นเพราะปริมาณการใช้สารลดน้ำพิเศษในส่วนผสมไม่แตกต่างกันมากนักจึงส่งผลให้เวลาการเกิดอุณหภูมิสูงสุดเปลี่ยนแปลงน้อย ดังนั้นคอนกรีตที่มีกำลังสูงและมีความร้อนต่ำที่ได้จากวัสดุประสานซึ่งเป็นสิ่งประดิษฐ์นี้ สามารถทำได้จากคอนกรีต FM20 ซึ่งให้ค่ากำลังอัดสูงถึง 727 กก/ซม^2 ที่อายุ 90 วัน และมีการเพิ่มขึ้นของอุณหภูมิสูงสุดที่วัดได้จากคอนกรีตสดต่ำกว่าคอนกรีตทั่วไปที่ใช้ปูนซีเมนต์ปอร์ตแลนด์ ถึง 2.3 เท่า

ตารางที่ 4 ความร้อนที่วัดได้จากคอนกรีตสด

Concretes	Initial Temp. (°C)	Max. Temp. (°C)	Peak Temp. (°C)	Reduce from NC70 (°C)	Reduce Temp. (%)	Peak time after casting (Hours)
FM	29	40	11	31	26	16
FM5	29	43	14	28	33	22
FM10	29	44	15	27	35	20
FM15	29	46	17	25	40	18
FM20	29	47	18	24	43	18
NC70	29	71	42	-	100	18

ตารางที่ 5 แสดงค่าสัมประสิทธิ์การซึมของน้ำและร้อยละการซึมของน้ำผ่านคอนกรีตที่อายุ 90 วัน เห็นได้ชัดว่าเมื่อเพิ่มปูนซีเมนต์ให้สูงขึ้นส่งผลให้ค่าสัมประสิทธิ์การซึมของน้ำผ่านคอนกรีตที่ใช้กากแคลเซียมคาร์ไบด์-เถ้าถ่านหินเป็นวัสดุประสานมีค่าต่ำลง ทั้งนี้เป็นเพราะค่าสัมประสิทธิ์การซึมของน้ำผ่านคอนกรีตมีค่าต่ำลงตามกำลังอัดที่เพิ่มขึ้น โดยคอนกรีต FM20 มีค่าสัมประสิทธิ์การซึมของน้ำผ่านคอนกรีตต่ำที่สุดเมื่อเปรียบเทียบกับคอนกรีตส่วนผสมอื่น ๆ ที่ใช้กากแคลเซียมคาร์ไบด์-เถ้าถ่านหินเป็นวัสดุประสาน ซึ่งมีค่าเท่ากับ 0.85×10^{-13} เมตร/วินาที นอกจากนี้คอนกรีต FM20 ยังให้ค่ากำลังอัดสูงที่สุดอีกด้วยเมื่อเปรียบเทียบกับคอนกรีตส่วนผสมอื่น ๆ ที่ใช้กากแคลเซียมคาร์ไบด์-เถ้าถ่านหินเป็นวัสดุประสาน เป็นที่น่าสังเกตว่าค่าสัมประสิทธิ์การซึมของน้ำผ่านคอนกรีตของคอนกรีต FM10 มีค่าใกล้เคียงกับคอนกรีตทั่วไป ในขณะที่คอนกรีต FM15 และ FM20 มีค่าสัมประสิทธิ์การซึมของน้ำผ่านคอนกรีตต่ำกว่าคอนกรีตทั่วไป แม้ว่าคอนกรีต FM10, FM15 และ FM20 มีกำลังอัดที่ต่ำกว่าคอนกรีตทั่วไป (NC70) ดังนั้นสามารถสรุปได้ว่าวัสดุประสานที่ใช้ทำคอนกรีต FM10, FM15 และ FM20 ที่ได้จากสิ่งประดิษฐ์นี้สามารถทำให้คอนกรีตมีกำลังสูง มีความร้อนต่ำ และมีความทนทานสูงอีกด้วย

ตารางที่ 5 ค่าสัมประสิทธิ์การซึมของน้ำผ่านคอนกรีตที่อายุ 90 วัน

Concretes	W/B	Coefficient of water permeability at 90 days, $K \times 10^{-13}$ (m/sec)	K/K_{NC70}
FM	0.25	2.53	2.78
FM5	0.25	2.28	2.51
FM10	0.25	0.94	1.03
FM15	0.25	0.89	0.98
FM20	0.25	0.85	0.93
NC70	0.25	0.91	1.00

วิธีการในการประดิษฐ์ที่ดีที่สุด

เหมือนกับที่กล่าวไว้แล้วในหัวข้อการเปิดเผยการประดิษฐ์โดยสมบูรณ์

การประยุกต์ใช้ในทางอุตสาหกรรม

วัสดุประสานสำหรับผลิตคอนกรีตที่ทำจากกากแคลเซียมคาร์ไบด์ผสมเถ้าถ่านหิน โดยใช้ปูนซีเมนต์เป็นสารเร่งกำลัง สามารถให้กำลังอัดสูงถึง 727 กก/ซม^2 ที่อายุ 90 วัน และยังให้ความร้อนของคอนกรีตสดต่ำกว่าคอนกรีตทั่วไปที่ใช้ปูนซีเมนต์ปอร์ตแลนด์เป็นวัสดุประสาน ถึง 2.3 เท่า จึงเหมาะสำหรับนำวัสดุประสานชนิดนี้มาใช้ในการก่อสร้างอาคารคอนกรีตทั่วไป อาคารคอนกรีตขนาดใหญ่หรือคอนกรีตที่ต้องรับกำลังสูงๆ เช่น อาคารสูง เขื่อน สะพาน ฐานราก หรือ ตอม่อขนาดใหญ่ ได้เป็นอย่างดี นอกจากนี้วัสดุประสานที่ทำจากกากแคลเซียมคาร์ไบด์ผสมเถ้าถ่านหินโดยใช้ปูนซีเมนต์เป็นสารเร่งกำลังสามารถผลิตคอนกรีตที่ให้กำลังอัดสูงและมีความร้อนต่ำแล้ว ยังทำให้คอนกรีตมีความทนทานสูงอีกด้วย เนื่องจากมีค่าอัตราการซึมของน้ำผ่านคอนกรีตต่ำกว่าคอนกรีตทั่วไป อีกทั้งกรรมวิธีการผลิตวัสดุประสานชนิดใหม่นี้ไม่ยุ่งยากสามารถนำไปประยุกต์ใช้แทนปูนซีเมนต์ปอร์ตแลนด์ในการผลิตคอนกรีตได้

เอกสารอ้างอิง

ACI Committee 363, 2005, "State-of-the-Art Report on High-Strength Concrete", ACI 363R-92, **ACI Manual of Concrete Practice Part I**, American Concrete Institute, Detroit, 55 p.

American Society for Testing and Materials, 2001, "ASTM C 618: Standard Specification for Coal Fly Ash and Raw or Calcined Natural Pozzolan for Use Mineral Admixture in Portland Cement Concrete", In **Annual Book of ASTM Standard**, Vol. 04.02, Philadelphia, ASTM, pp. 310-313.

Jaturapitakkul, C., and Roongreung, B., 2003, "Cementing Material from Calcium Carbide Residue-Rice Husk Ash", **Journal of Materials in Civil Engineering**, Vol. 15, No. 5, pp. 470-475.

ปิติศานต์ กร้ำมาตร, สุภิชาติ มาตย์ภูธร, ชัย จาตุรพิทักษ์กุล และ วิมล เงาพิสดาร, 2539, "การศึกษากำลังอัดของมอร์ต้าร์ที่ได้จากกากแคลเซียมคาร์ไบด์ผสมกับเถ้าถ่านหิน", วิศวกรรมสาร ฉบับวิจัยและพัฒนา, ปีที่ 7, ฉบับที่ 2, หน้า 65-75.

ข้อถือสิทธิ

1. กรรมวิธีการผลิตวัสดุประสานสำหรับผลิตคอนกรีตซึ่งมีกำลังสูง มีความร้อนต่ำ และมีความทนทานสูง มีลักษณะพิเศษ คือ อัตราส่วนระหว่างกากแคลเซียมคาร์ไบด์และเถ้าถ่านหินในอัตราส่วน 30:70 โดยน้ำหนัก เป็นส่วนผสมที่เหมาะสมที่สุดในการทำปฏิกิริยา เพื่อใช้เป็นวัสดุประสานในการผลิตคอนกรีต

2. กรรมวิธีการผลิตวัสดุประสานสำหรับผลิตคอนกรีตจากส่วนผสมระหว่างกากแคลเซียมคาร์ไบด์และเถ้าถ่านหินตามข้อถือสิทธิที่ 1 ซึ่งให้กำลังอัดของคอนกรีตที่สูง มีความร้อนต่ำ และมีความทนทานสูง ทำได้โดยการบดวัสดุทั้งสองจนมีปริมาณอนุภาคค้างบนตะแกรงมาตรฐานเบอร์ 325 น้อยกว่าร้อยละ 3 โดยน้ำหนัก ทำให้กากแคลเซียมคาร์ไบด์ทำปฏิกิริยากับเถ้าถ่านหินได้รวดเร็ว

3. กรรมวิธีการผลิตวัสดุประสานสำหรับผลิตคอนกรีตจากส่วนผสมระหว่างกากแคลเซียมคาร์ไบด์และเถ้าถ่านหินตามข้อถือสิทธิที่ 1 และ/หรือ 2 ซึ่งให้กำลังอัดของคอนกรีตที่สูง มีความร้อนต่ำ และมีความทนทานสูง โดยใช้ปริมาณวัสดุประสานระหว่าง 300 ถึง 550 กก/$ม^3$, ใช้ปูนซีเมนต์ปอร์ตแลนด์เป็นสารเร่งกำลังให้น้อยที่สุด และ/หรือ ไม่ใช้ปูนซีเมนต์ปอร์ตแลนด์เลยในส่วนผสม, ใช้สารลดน้ำพิเศษ, และใช้อัตราส่วนระหว่างน้ำต่อวัสดุประสานต่ำ ส่งผลให้คอนกรีตมีกำลังสูง มีความร้อนต่ำ และมีความทนทานสูงเนื่องจากน้ำซึมผ่านคอนกรีตได้ยาก

4. กรรมวิธีการผลิตวัสดุประสานสำหรับผลิตคอนกรีตจากส่วนผสมระหว่างกากแคลเซียมคาร์ไบด์และเถ้าถ่านหินตามข้อถือสิทธิ 1 และ/หรือ 2 และ/หรือ 3 ซึ่งให้กำลังอัดของคอนกรีตที่สูง มีความร้อนต่ำ และมีความทนทานสูง โดยใช้ปริมาณปูนซีเมนต์ให้น้อยที่สุด และ/หรือไม่ใช้ปูนซีเมนต์ปอร์ตแลนด์เลยในส่วนผสม เพื่อลดความร้อนของคอนกรีตสดที่เกิดขึ้น จึงส่งผลให้คอนกรีตที่ได้จากการประดิษฐ์นี้มีความร้อนที่ต่ำกว่าคอนกรีตทั่วไปมาก

บทสรุปการประดิษฐ์

จากกระบวนการผลิตวัสดุประสานสำหรับผลิตคอนกรีตซึ่งมีกำลังสูง มีความร้อนต่ำ และมีความทนทานสูง จากส่วนผสมระหว่างกากแคลเซียมคาร์ไบด์และเถ้าถ่านหินโดยมีหรือไม่มีปูนซีเมนต์เป็นสารเร่งกำลัง ในการประดิษฐ์นี้พบว่าคอนกรีตที่ใช้กากแคลเซียมคาร์ไบด์-เถ้าถ่านหินเป็นวัสดุประสานโดยมีปูนซีเมนต์เป็นสารเร่งกำลังมีเวลาการก่อตัวทั้งระยะต้นและระยะปลายสั้นกว่าคอนกรีตทั่วไปที่ใช้ปูนซีเมนต์ปอร์ตแลนด์เป็นวัสดุประสาน นอกจากนี้เมื่อเพิ่มปริมาณปูนซีเมนต์เพื่อใช้เป็นสารเร่งกำลังในอัตราส่วนที่สูงขึ้นส่งผลให้เวลาในการก่อตัวเร็วยิ่งขึ้น คอนกรีตที่ใช้กากแคลเซียมคาร์ไบด์-เถ้าถ่านหินเป็นวัสดุประสานให้ค่ากำลังอัดสูงขึ้นตามอายุการบ่ม ซึ่งคล้ายกับคอนกรีตทั่วไป นอกจากนี้เมื่อเพิ่มปริมาณการแทนที่วัสดุประสานด้วยปูนซีเมนต์ให้สูงขึ้นส่งผลให้การพัฒนากำลังอัดของคอนกรีตที่ใช้กากแคลเซียมคาร์ไบด์-เถ้าถ่านหินเป็นวัสดุประสานมีค่าเพิ่มขึ้นตามไปด้วย

การประดิษฐ์วัสดุประสานสำหรับผลิตคอนกรีต FM5 ให้คอนกรีตที่มีกำลังอัดสูงและมีความร้อนต่ำ ส่วนการประดิษฐ์วัสดุประสานสำหรับคอนกรีต FM10, FM15 และ FM20 ให้คอนกรีตที่มีกำลังอัดสูง มีความร้อนต่ำและมีความทนทานสูง โดยคอนกรีต FM20 เป็นคอนกรีตกำลังสูงที่ให้ค่ากำลังอัดสูงที่สุดเมื่อเปรียบเทียบกับคอนกรีตส่วนผสมอื่น ๆ ที่ใช้กากแคลเซียมคาร์ไบด์-เถ้าถ่านหินเป็นวัสดุประสาน โดยคอนกรีต FM20 ให้ค่ากำลังอัดเท่ากับ 456, 678, 693 และ 727 กก/ซม^2 ที่อายุ 7, 28, 60 และ 90 วัน ตามลำดับ ซึ่งคอนกรีตกำลังสูง FM20 มีความร้อนที่เกิดขึ้นสูงสุดต่ำกว่าคอนกรีตทั่วไปที่ใช้ปูนซีเมนต์ปอร์ตแลนด์เป็นวัสดุประสาน ถึง 2.3 เท่า และมีความทนทานสูงกว่าคอนกรีตทั่วไปเนื่องจากมีค่าอัตราการซึมของน้ำผ่านคอนกรีตต่ำกว่าคอนกรีตทั่วไป

หน้า 1 ของจำนวน 1 หน้า

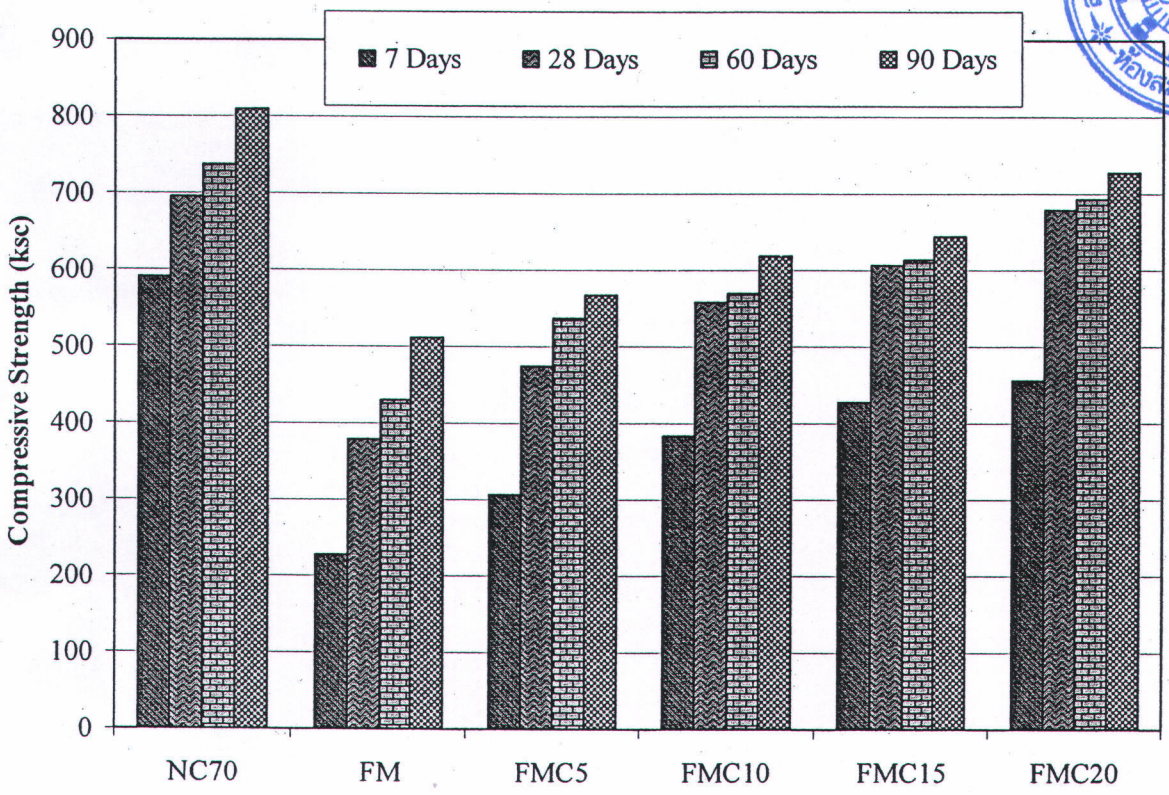

รูปที่ 1 แสดงความสัมพันธ์ระหว่างกำลังอัดของคอนกรีตกับอายุในการบ่ม

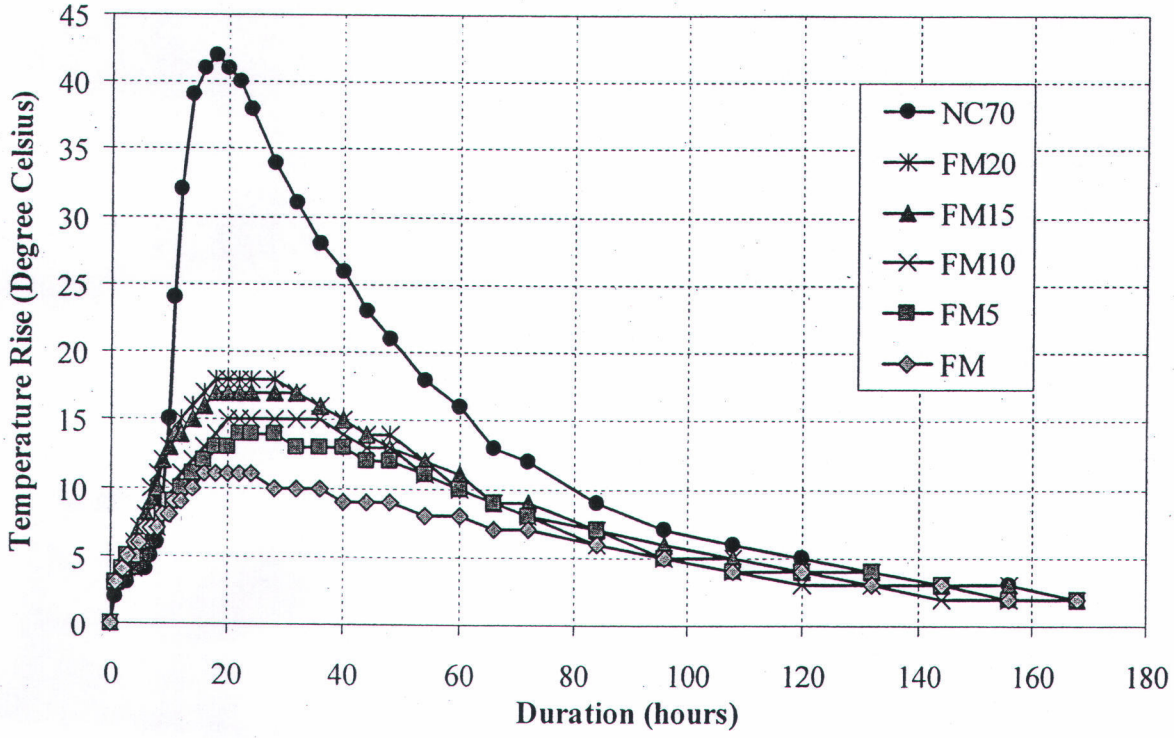

รูปที่ 2 แสดงความสัมพันธ์ระหว่างอุณหภูมิที่เพิ่มขึ้นของคอนกรีตสดกับเวลาหลังทำการหล่อคอนกรีต